In-Space Transportation with Tethers

NASA Grant NAG8-1303

Final Report

For the period 1 September 1996 through 15 March 1999

Principal Investigator

Enrico C. Lorenzini

September 1999

Prepared for

National Aeronautics and Space Administration

Marshall Space Flight Center, Alabama 35812

Smithsonian Institution

Astrophysical Observatory

Cambridge, Massachusetts 02138

The Smithsonian Astrophysical Observatory
is a member of the
Harvard-Smithsonian Center for Astrophysics

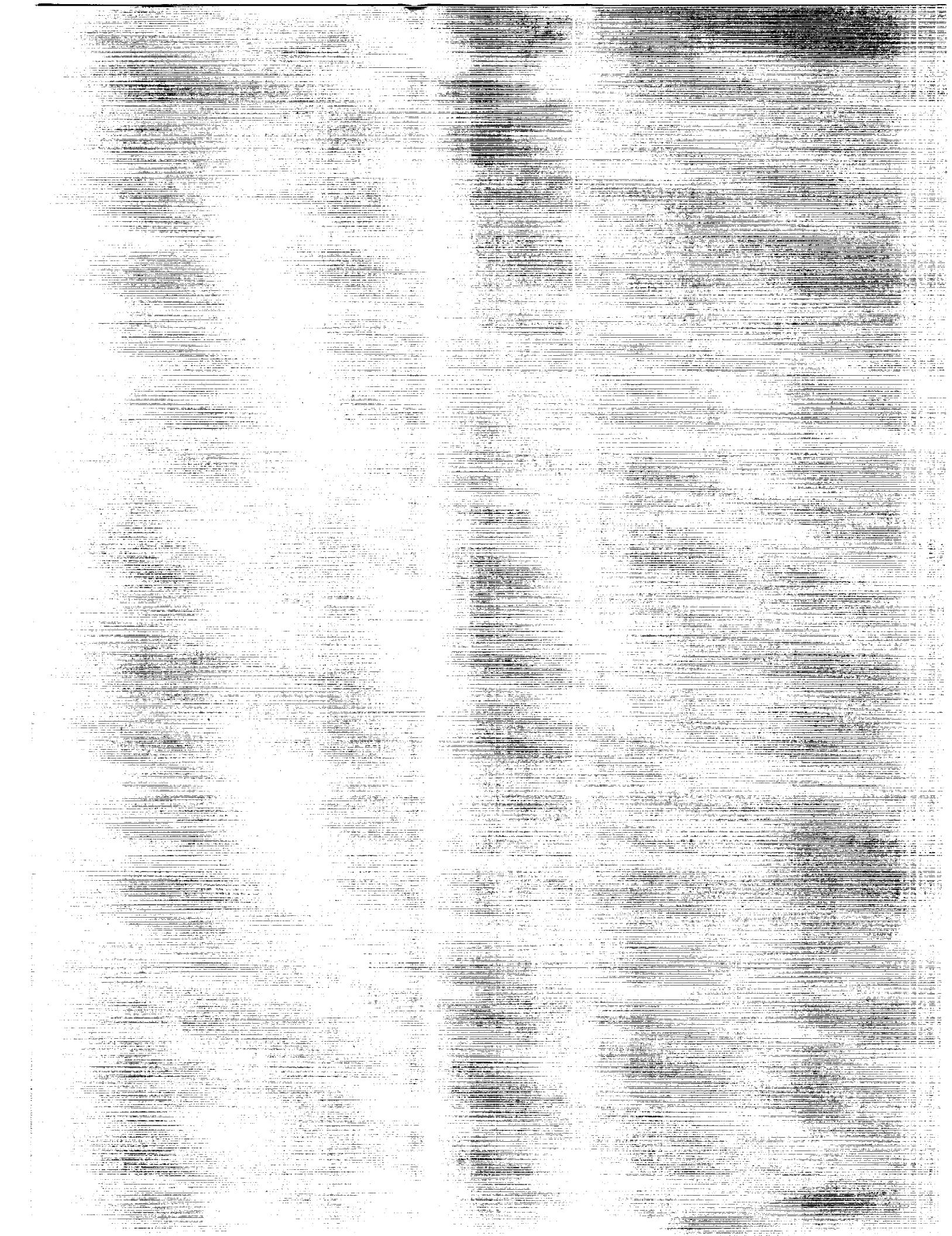

In-Space Transportation with Tethers

NASA Grant NAG8-1303

Final Report

For the period 1 September 1996 through 15 March 1999

Principal Investigator

Enrico C. Lorenzini

Co-Investigators

Robert D. Estes

Mario L. Cosmo

Robert L. Forward

Robert P. Hoyt

Collaborators

Juan Sanmartin

Jesus Peláez

Marcus Kaiser

September 1999

Prepared for

National Aeronautics and Space Administration

Marshall Space Flight Center, Alabama 35812

Smithsonian Institution

Astrophysical Observatory

Cambridge, Massachusetts 02138

TABLE OF CONTENTS

SCOPE

This is the Final Report for Grant NAG8-1303 entitled "In-Space Transportation with Tethers" prepared by the Smithsonian Astrophysical Observatory for NASA Marshall Space Flight Center. The technical monitor for this grant is Les Johnson. This report covers the period of activity from 1 September 1996 through 15 March 1999.

SUMMARY

This Final Report covers the research conducted on the following topics related to the use of spaceborne tethers for in-space transportation:

1. Electrodynamic (ED) tethers for the International Space Station

Electrodynamic tether for ISS Power

Electrodynamic tether for ISS Reboost

2. Electrodynamic tethers for transportation in LEO

Electrodynamic tether tug

Upper stage demo

3. Electrodynamic tethers for spacecraft reentry

Propulsive Small Expendable Deployment System (ProSEDS) overview

ProSEDS electrodynamics

ProSEDS dynamics

ProSEDS deployment

ProSEDS deboost performance

4. Stationary tethers for position control of large platforms

Position control of a solar power station in GEO

5. Spinning tethers for Earth and planetary transportation

LEO to GEO tether transport system study

LEO-Lunar Tether Transport System Study

1.0 Electrodynamic tethers for the International Space Station

1.1 Introduction

The need for high currents and the difficulty in achieving them

Any analysis of electrodynamic tethers for Space Station applications will soon arrive at the conclusion that currents on the order of 10 A are required. For power generation, we have to foresee needs of several kilowatts even for an emergency backup system. For reboost, we need thrust forces on the order of a Newton, due to the large aerodynamic drag of the Station. In addition, we are restricted by the need to keep perturbations to the Station environment to a minimum. Very long tethers are ruled out by this condition, as they would move the system's center of gravity too much and pose additional operational problems when the Station is docking with other spacecraft.

It is easy to show that "standard" tether systems, such as TSS-1, which rely on a large spherical surface to collect electron current from the ionosphere, are unsuitable for ISS applications. A study conducted by MSFC into the possible use of the TSS-1/R system on the Space Station came to the conclusion that it did not make sense. A quick calculation, using the 10 A benchmark, shows why. TSS-1R collected 1 A, while the satellite was biased to 1.5 kV. This was twice what had been predicted. Even so, the current collected by the satellite was observed to increase only as the square root of the bias voltage. Thus, to achieve 10 A with the TSS-1 system under the same (daytime) conditions would require a bias voltage of 150 kV, or a tether length of over 850 km! Going to a larger surface would help some, but there is a strong law of diminishing returns for that route. Even if very large spheres were to be allowed (say of 8 m radius), which might achieve useful power levels during optimal conditions of daytime plasma densities with a tether 10 km long, they would suffer from the other Achilles heel of passive spherical collectors: a strong drop in the current (and power goes as the square of the current), as the low plasma densities are encountered during the third of the orbit which is in the Earth's shadow.

The alternative of using hollow cathode type plasma contactors is not attractive at the current state of the technology either. The only space experiment to attempt electron collection by this means, PMG, was limited to small currents and the results can not be scaled to 10 A systems. Such systems, even if they could be made to work, would require additional power, gas, and electronics, all at the end of the tether several km away from the Station. The complexity and likelihood of failure alone argue strongly against such a system.

Bare tethers for high currents

Fortunately, there is another alternative way of collecting electrons. A thin wire (radius less than Debye length and electron gyroradius) is a very efficient collector of plasma current, able to collect many times the current per surface area that a large sphere equally biased with respect to the surrounding plasma can. And this efficient collection is independent of the wire's length. This is the basic idea of the bare tether: use the uninsulated portion of the tether itself to collect current. The collecting area is large by virtue of the tether's length, which is of necessity several kilometers long just to get sufficient voltage.

Bare tethers have another attractive feature, which might be decisive. They are much less susceptible to having the current drop as the plasma density goes down. This is accomplished automatically, as both the collecting area and the maximum bias voltage increase when the current drops, thus largely offsetting a drop in available plasma. This means that nighttime operation is feasible. In the case of power generation it also means that the need for leveling batteries could be greatly reduced if a constant power delivery is required from the system.

The Smithsonain Astrophysical Observatory (SAO) circulated a white paper [1] advocating the use of a bare tether for ISS power generation in late 1995 and then joined in

a 1996 proposal effort with MSFC for a program to test and develop bare-tether-based systems for ISS power and reboost.

While these proposals were still being evaluated, the Advanced Concepts Office of NASA expressed interest in further study of the use of electrodynamic tethers, especially the bare tether system, for ISS applications. SAO was one of the institutions participating in this study. Our main role was in determining system performance and performing tradeoffs relative to performance. We helped with preparing and delivering the oral presentations of the study to the NASA HQ representative. Summaries of our contributions to this study of ISS power and reboost follow.

1.2 Electrodynamic Tethers for ISS Power

A basic power generating system

A bare-tether-based power generation system for the ISS is shown schematically in Figure 1.2.1. The tether is deployed upward, which biases the top portion of the wire positively with respect to the surrounding plasma. Along this positively biased portion electrons are collected, which are ejected at the Station by a hollow cathode. The baselined hollow cathodes for the Station are rated at 10 A. Contactors of this design might be adequate for use with the ED tether system, but we feel that a dedicated contactor, or pair of contactors would be required. Useful power is extracted by a load placed in series with the tether. The details of the power conversion system were worked out by engineers at MSFC with input from SAO.

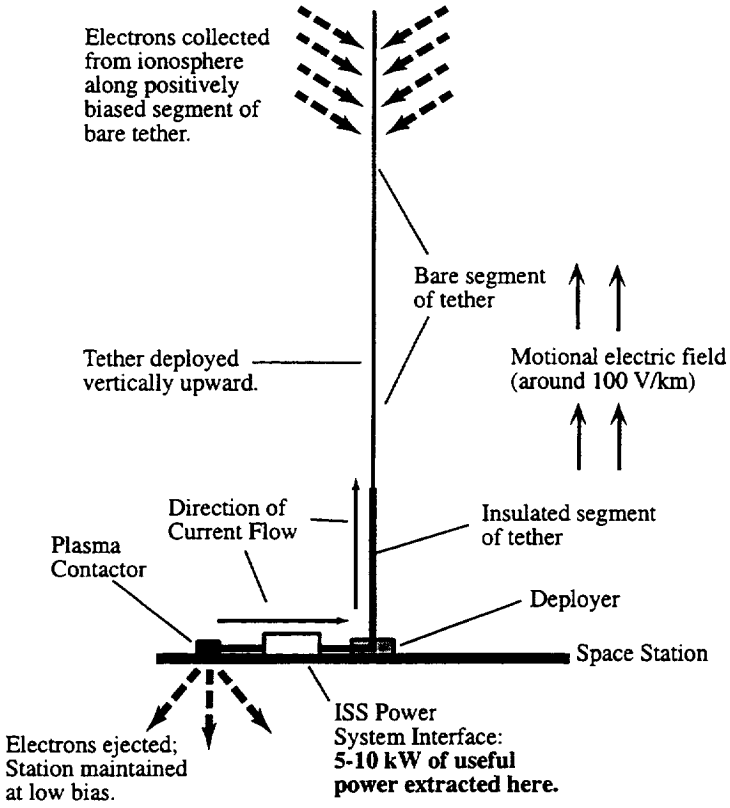

Figure 1.2.1. Schematic of an EDT power generator

The self-adjustment of the tether to a decrease in electron density is shown in Figure 1.2.2. As indicated there, the point of zero bias moves down the tether as the ohmic drop due to current through the load and tether decreases.

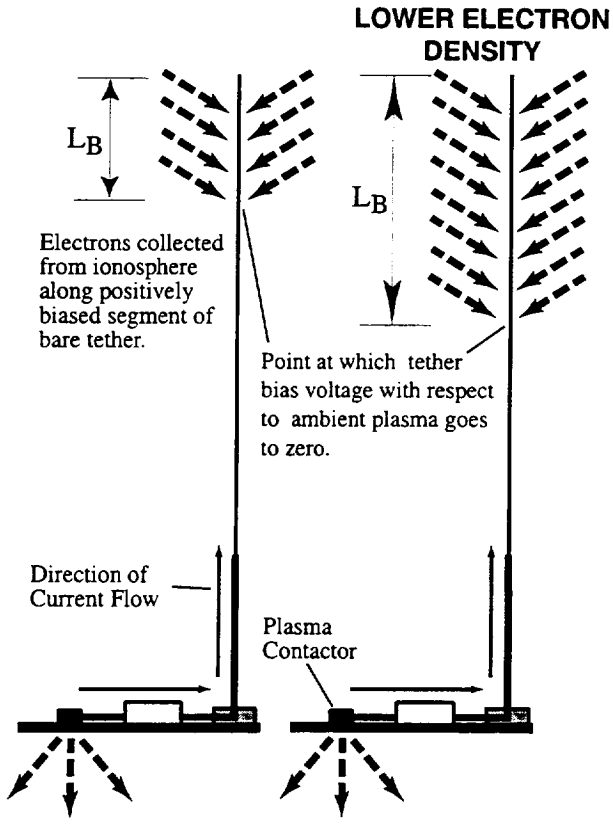

Figure 1.2.2. The bare tether adjusts to lower electron density

Orbital variations that affect performance

An orbiting system such as the Space Station encounters a constantly changing environment as it moves through the ionosphere and the Earth's magnetic field. The plasma density encountered in a typical twenty-four hour period is seen in Figure 1.2.3. Even though the bare tether adjusts to these variations and suffers much less than a passive sphere would, it does experience a decrease in power generation at night.

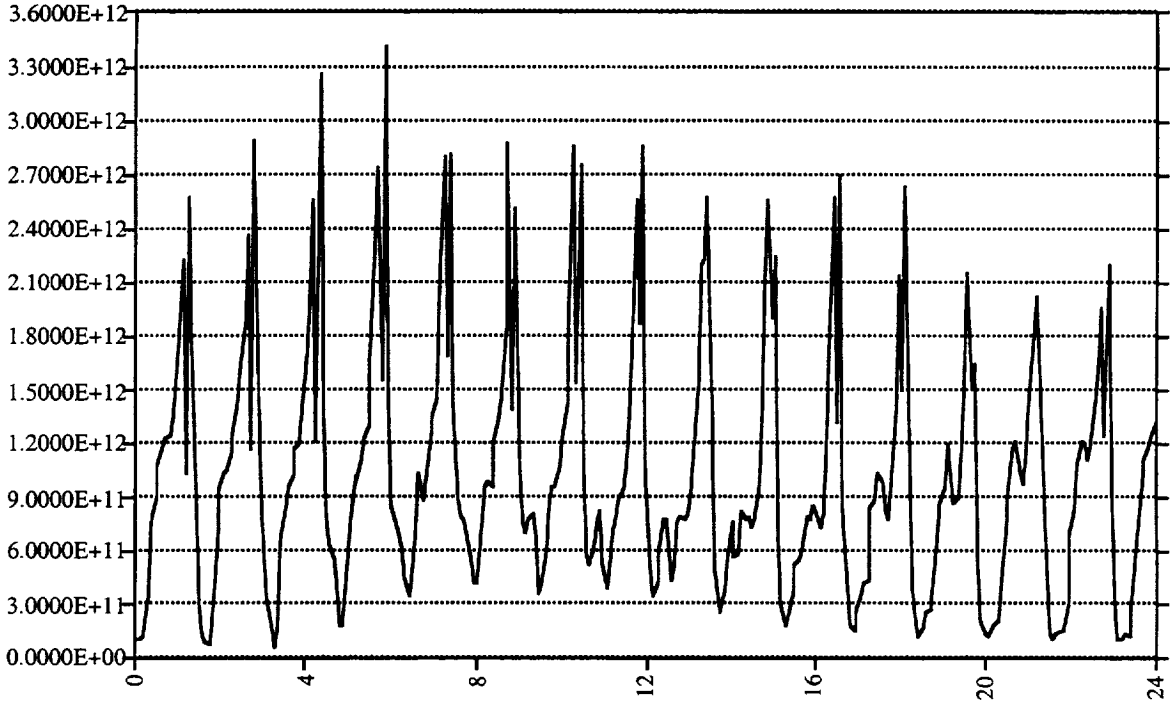

Figure 1.2.3. Electron density (m^{-3}) variations around an ISS orbit (hrs). Data supplied by Kai Hwang, MSFC

More important than the density variations are variations in the component of the motional electric field along the tether, since this is what drives the current. The end-to-end EMF for an 18 km-long tether in ISS orbit is shown in Figure 1.2.4, for a twenty-four hour period. The range covers 500-3000 V, corresponding to an electric field of 0.027 to 0.17 V/m. The bare tether system maintains its efficiency under changes in the motional electric field, but that only says that the ratio of the power out to that of the power in is steady.

The problem is that the power available from the orbital energy varies as both the magnitude of the Earth's magnetic field and the orientation of the field vector with respect to the Station's velocity vector change. The induced end-to-end EMF is a good measure of how the input power varies, as the input (orbital) power is the product of the EMF and the

average current in the tether, which for efficient operation is close to the value of the current through the load at the Station.

The way we have chosen to deal with this problem is to design the system to perform well at some typical "good" value of EMF and to get the maximum power possible during troughs of the EMF by choosing an optimal load impedance. These low points in power will still be low points, just not as marked as they would otherwise be.

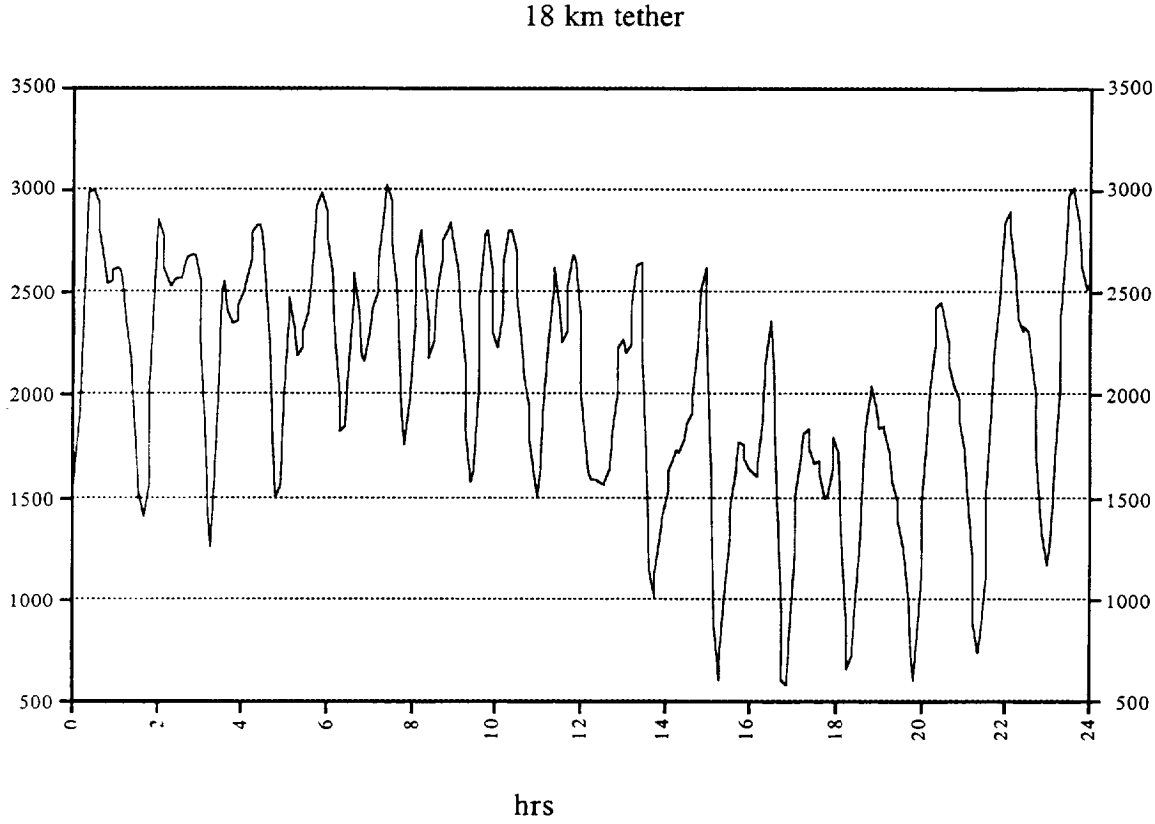

Figure 1.2.4. Variations in end-to-end EMF (Volts) around a typical ISS orbit. Data supplied by Kai Hwang, MSFC

A candidate system used for analysis

Time did not permit the design of an optimal power system, but we chose the following system as a first cut at what a bare tether system for ISS power generation might look like.

It has been used in all of the following analysis of power generation.

- Material: Aluminum braided with Spectra
- Length: 18 kilometers (11.25 miles)
- Width: 1.1 cm (0.43 in)
- Thickness: 0.6 mm (0.024 in)
- Weight: 300 kg (660 lbs.)
- Coating (insulation) along lower section: a few hundreds of meters

It utilizes a tape geometry for the tether, which gives increased collecting surface per unit mass. Mass reduction was a primary concern, due to ISS restrictions on CG displacement. The same system could be operated in different modes, depending on the desires of the user.

Figure 1.2.5 illustrates the self-adjustment of the system to changes in electron density. A load impedance of 300 Ohm and a 120 V/km motional electric field are assumed. The maximum useful power in the example is around 9 kW. A factor of 20 decrease in the electron density is seen to cause only a 17% decrease in current. The reason is clear: the collecting length has increased from less than 1 km to 4.5 km.

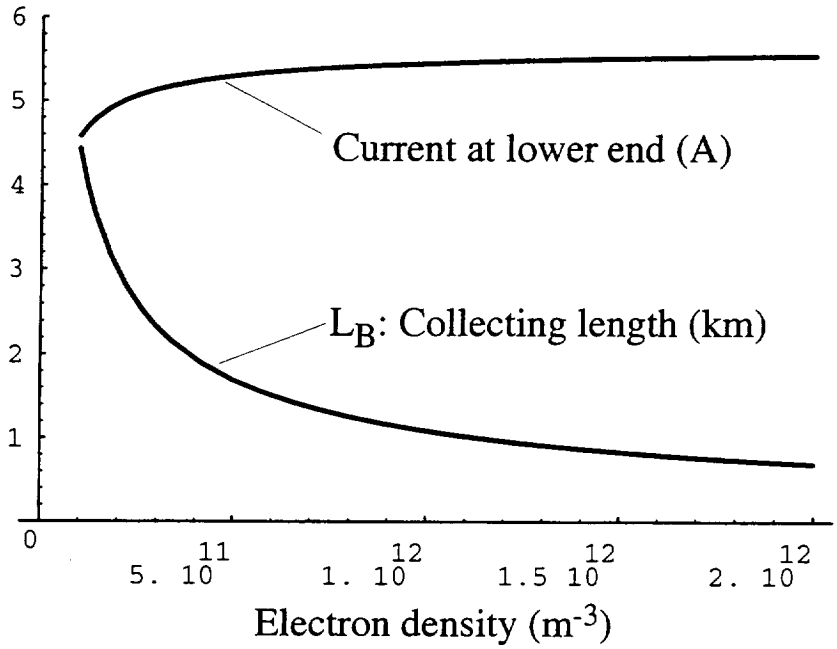

Figure 1.2.5. Variable collecting length of an 18 km bare tether

Operating Mode A (High Power):

- power output from the tether before conversion
  - 9 kW orbital average
  - 12 kW peak (regulated by variable impedance)
- maximum current
  - 12 Amperes (above rating for single ISS contactor)
- average drag force
  - 2.0 Newton
- average efficiency of orbital to electrical energy conversion
  - 55%

Mode A gives higher average power at lower efficiency. The power is kept below 12 kW by controlling the impedance of the power converter. The average drag force would be more than twice that of the normal aerodynamic drag on the Station. Thus, it would not be desirable for continual use, unless required to make up for a defect in the solar power

system, in which case immediate power needs might outweigh reboost concerns. The system is actually capable of generating higher power, if higher currents can be handled by the plasma contactor, just by lowering the load impedance at favorable points on the orbit to allow power greater than 12 kW to be generated.

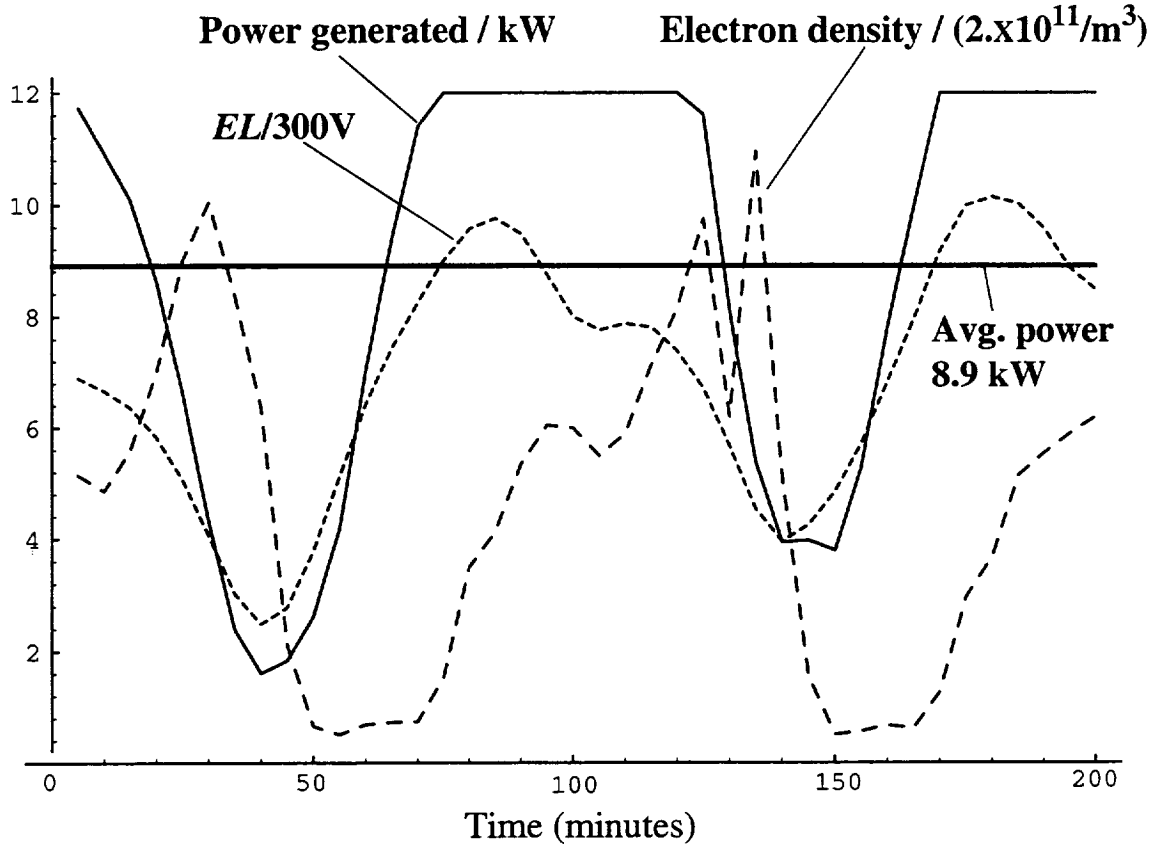

Figure 1.2.6. Variations of system parameters around two orbits. Operating in Mode A.

Figure 1.2.6 shows how generated power depends on motional EMF and electron density around two revolutions of the ISS orbit with our system operating in the "high power" Mode A. The troughs in power around 40 secs and 140 secs are obviously due to the dips in EMF encountered at those points in the orbit. Power over 10 kW is seen to be generated during the nighttime troughs in electron density during times when there is adequate motional EMF. The case in Figure 1.2.6 might well be considered near worst

case, since we have both EMF and density dipping together. It is clear, however, that EMF drops dominate.

For the future, we recommend that a shorter tethered system that does not attempt to generate much power during the EMF low points be evaluated. Should steady power output not be an ISS requirement, and we have some indication that it would not, the benefits of having a shorter tether might outweigh those of maintaining to a greater degree the power levels at the worst times.

Operating Mode B (Steady Power):

- power output from the tether before conversion
  - 5.3 kW orbital average
  - 6 kW peak power (regulated by variable impedance)
  - 6 kW continual power needs 700 W average power from leveling batteries
- maximum current
  - 8 Amperes
- average drag force
  - 1.0 Newton
- average efficiency of orbital to electrical energy conversion
  - 66%

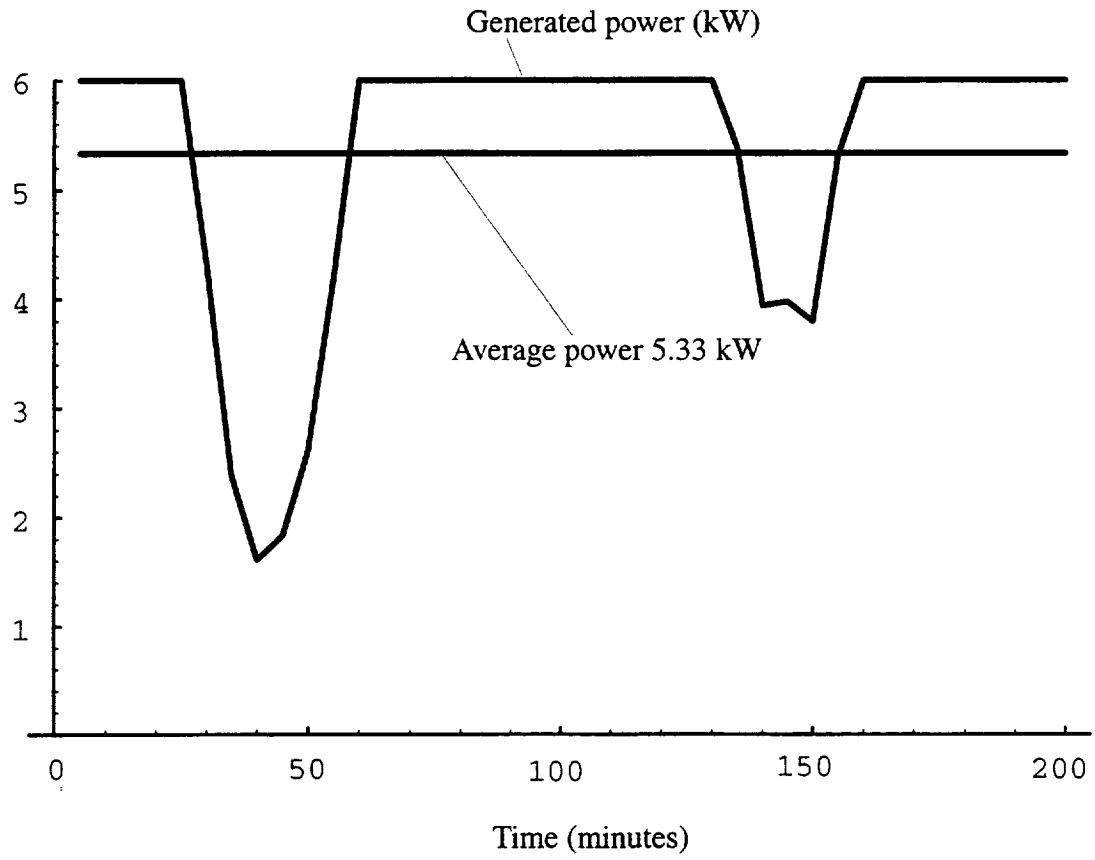

Fig. 1.2.7. Variations of power generated around two orbits. Operating in Mode B.

Mode B is envisioned as a constant power mode, though it would not have to be used that way. It gives higher average efficiency at lower power. The power is kept below 6 kW, and only 700 W would have to be made up, on the average, to maintain a steady power output. This is clear from Figure 1.2.7, which shows the power variation around two revolutions of the orbit for Mode B. The average power output would be 5.3 kW.

1.3 Electrodynamic Tethers for ISS Reboost

A basic reboost system

Any wire carrying a current in a magnetic field experiences a force proportional to the product of the current, the component of the magnetic field perpendicular to the wire, and the length of the wire. This well-known phenomenon is the source of the boost force. In addition to the boost, there is usually also a force component perpendicular to the direction of motion.

In the case of a reboost system, the tether is deployed downward, and the tether is biased positively by a power supply, which drives a positive current down the tether. This is actually accomplished, of course, by collecting electrons from the ionosphere with part of the exposed length of the tether. In order to bias at least a portion of the bare tether positively, an input voltage greater than the motion-induced voltage of the end of the insulation with respect to the Station is required. A plasma contactor can handle electron ejection at Station. A schematic diagram of a reboost system for ISS is shown in Fig.1.3.1.

The maximum bias voltage occurs right at the end of the insulation and decreases linearly as we move down from there. Below the zero bias point, an ion current is collected. Thrust is maximized for maximum average current in the tether, since the magnetic field exerts a force on the tether all along its length proportional to the (local) current. This leads us to insulate part of the tether. Generally speaking, the longer the tether is, the greater the thrust for a given input power. Current through the tether depends on the applied voltage, the motional potential to be overcome, and the efficiency with which the system can exchange charge with the plasma.

We have considered systems based on constant input power, which were deemed feasible by MSFC power experts. This seems a reasonable way to proceed, since we are

basically limited by the power available to us. Of course, the same tethered system could operate with different input power to take advantage of surplus power situations.

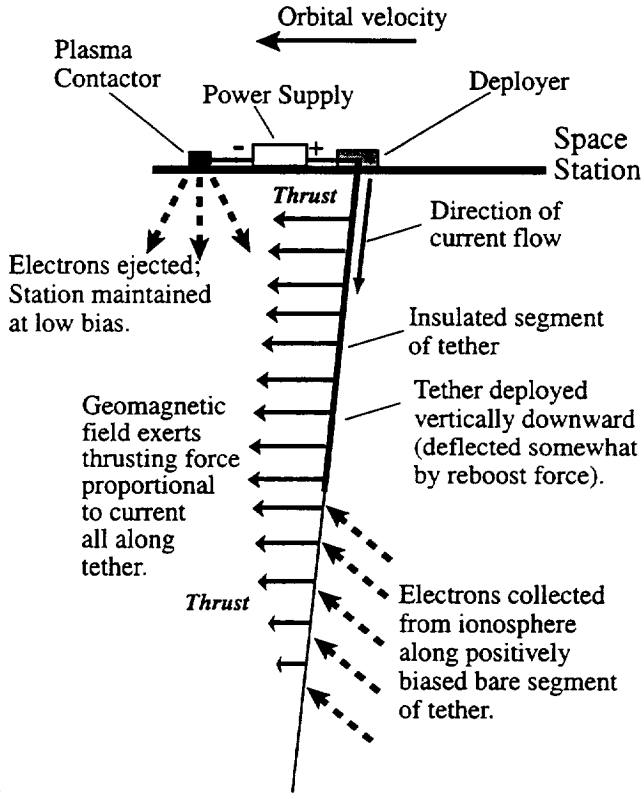

Figure 1.3.1. Schematic diagram of a bare tether reboost system for the ISS.

The tether can be designed with some "head room", so that there is more bare tether than necessary during periods of high plasma density. That is, current collection occurs on only the portion near the end of the insulation, when there is plenty of plasma. The extra segment of bare tether is available to provide greater collecting surface for lower density (night) operation, thus minimizing thrust fluctuations. The zero bias point works its way down the tether in much the same way as it works its way down from the tip in the case of a power generator. This is illustrated in Figure 1.3.2. As in the case of the bare tether power generator, nighttime operation was found to be feasible.

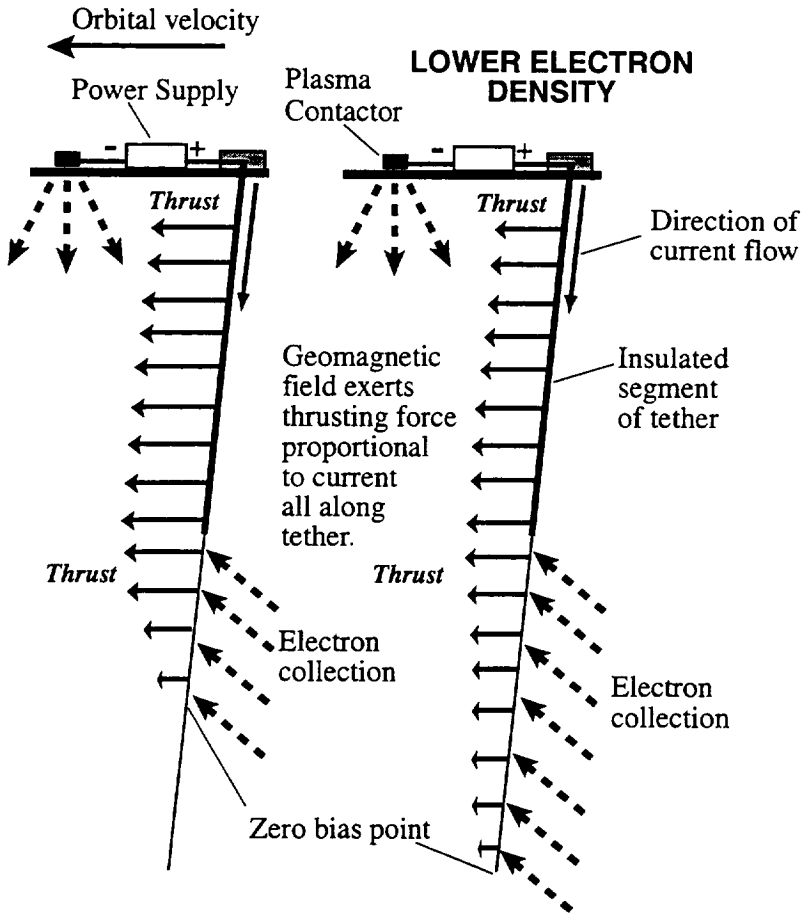

Figure 1.3.2. The adjustment of a bare tether reboost system to lower electron density

A candidate system used for analysis

Time did not permit the design of an optimal reboost system, but we chose the following system as a first cut at what a bare tether system for ISS reboost might look like.

- Material – Aluminum braided with Spectra
- Length – 7 kilometers (4.4 miles)
- Width – 1.0 cm (0.39 in)
- Thickness – 0.6 mm (0.024 in)
- Weight – 106 kg (233 lbs.)
- Insulation over 5 km – 50%-80%

This system has been used in all of the following analysis of reboost. As in the case of the ISS power generator, a tape geometry was chosen to increase the collecting area to mass ratio of the tether. An input power of 5 kW was generally assumed, but some analysis with 10 kW was also done. For 5 kW, the system delivers an orbital average thrust of around 0.4 N at an efficiency of 65%.

Other systems with different tether lengths, insulated portions, and input power were also considered. These are summarized in the Table 1.3.1.

Table 1.3.1. Parameters of different systems for ISS reboost.

	5 kW input					10 kW input					15 kW input					
	Thrust (N)	Max Amps	eff.	kW/kg	bare km	Thrust (N)	Max Amps	eff.	kW/kg	bare km	Thrust (N)	Max Amps	eff.	kW/kg	bare km	
5 km	0.36	11.8	0.55	0.034	2.0	0.59	17.5	0.45	0.056	2.0	0.78	21.9	0.40	0.074	2.0	5 km
81 kg	0.36	9.8	0.55	0.034	1.0	0.57	14.3	0.44	0.054	1.0						81 kg
7 km						0.69	15.7	0.53	0.047	3.0	0.92	19.8	0.47	0.062	3.0	7 km
113 kg	0.43	9.4	0.66	0.029	2.0											113 kg
						0.78	14.3	0.60	0.037	5.0						
10 km						0.81	13.1	0.62	0.038	4.0	1.09	16.6	0.56	0.052	4.0	10 km
162 kg	0.46	7.8	0.70	0.022	3.0	0.83	12.1	0.64	0.039	3.0						162 kg
						0.83	11.3	0.64	0.039	2.0						
						0.84	12.6	0.64	0.031	6.5	1.14	16.0	0.58	0.041	6.5	
13 km	0.51	5.5	0.78	0.019	4.0	0.90	10.6	0.69	0.033	4.0	1.19	14.5	0.61	0.043	5.5	13 km
211 kg											1.24	12.8	0.63	0.045	3.0	211 kg

Influence of environmental and system parameters on performance

The thrust generated depends on the average current in the tether, the tether length, and the magnetic field vector (which by determining motional EMF to be overcome, also influences current). In the following figures can be discerned the interplay of environmental and system parameters in determining system performance. We assume the nominal system outlined above.

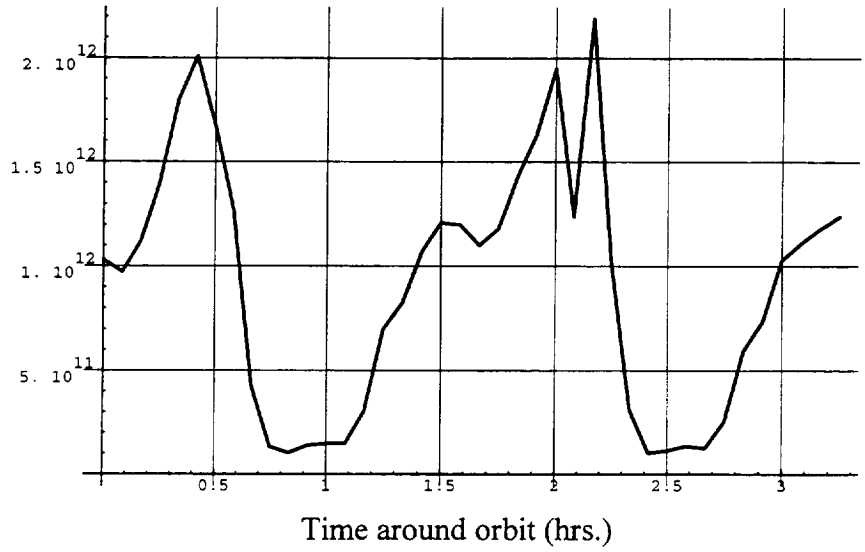

Figure 1.3.3. Electron density encountered in a typical three hour period of ISS orbit.

The current collected depends to a certain extent on the density of electrons available for collection. Figure 1.3.3 displays the electron density encountered by the ISS in two typical revolutions. The density clearly drops by a factor of around twenty as it goes from day to night.

Motion-induced voltage variation results from the changing angle between the ISS velocity vector and the Earth's magnetic field and from field magnitude variations. In general, applied voltage need not overcome the entire end-to-end motional voltage, just something more than 5/7 of that for 5 km of insulation out of a 7 km tether. Motional voltage is also a measure of how effective the magnetic field will be in generating thrust at a given average tether current. As in the case of the power generator, the motion-induced voltage is far and away the most important factor in determining system performance. Figure 1.3.4 shows how it varies for a 7 km long tether over the same period as that shown in Figure 1.3.3. It is seen to vary by more than a factor of four.

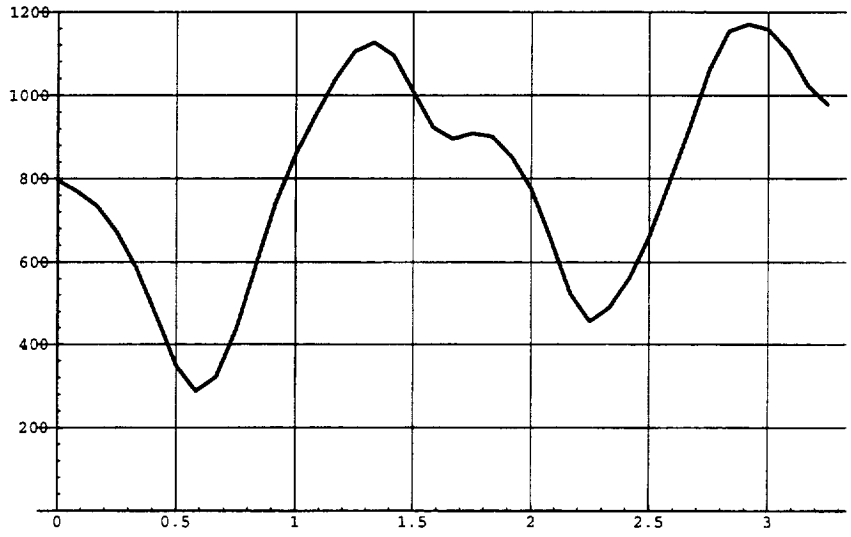

Figure 1.3.4. End-to-end motional EMF (Volts) of our nominal 7-km / 5 kW reboost system for the same three hour period of ISS orbit as in Figure 1.3.3.

How the density and EMF variations translate into collected current is quite different from what we saw in the case of the power generator. The current is inversely proportional to the input voltage for the case of constant power. Since the input voltage must increase when the motional voltage increases, in order to maintain a positively biased bare tether segment, we actually see the current increasing as motional EMF decreases. Compare Figures 1.3.4 and 1.3.5.

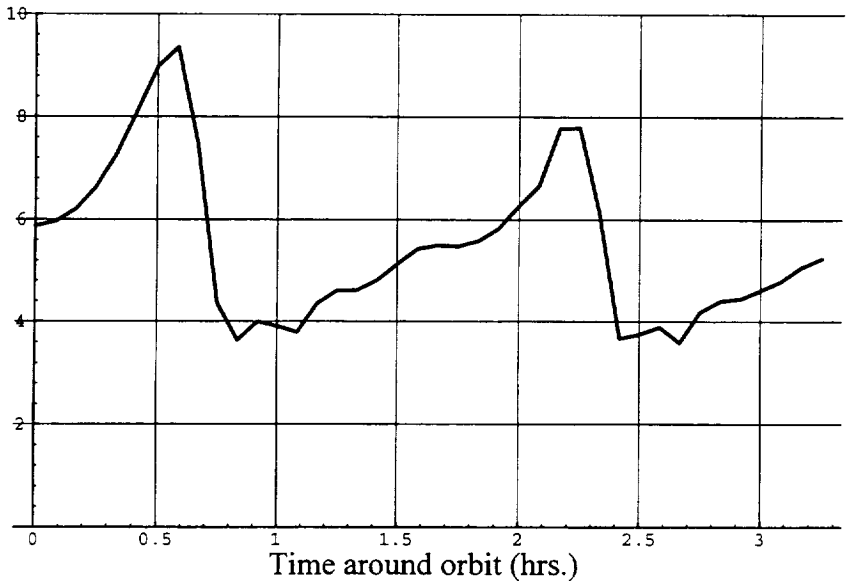

Figure 1.3.5. Tether current delivered to the Station (Amperes) by our nominal 7-km / 5 kW reboost system for the same three hour period of ISS orbit as in Figure 1.3.3.

Thrust, however, is, in the final analysis, determined by the motional EMF. Figure 1.3.6 shows how thrust varies. The thrust force is just the product of the end-to-end motional voltage times the average current in the tether divided by the orbital velocity.

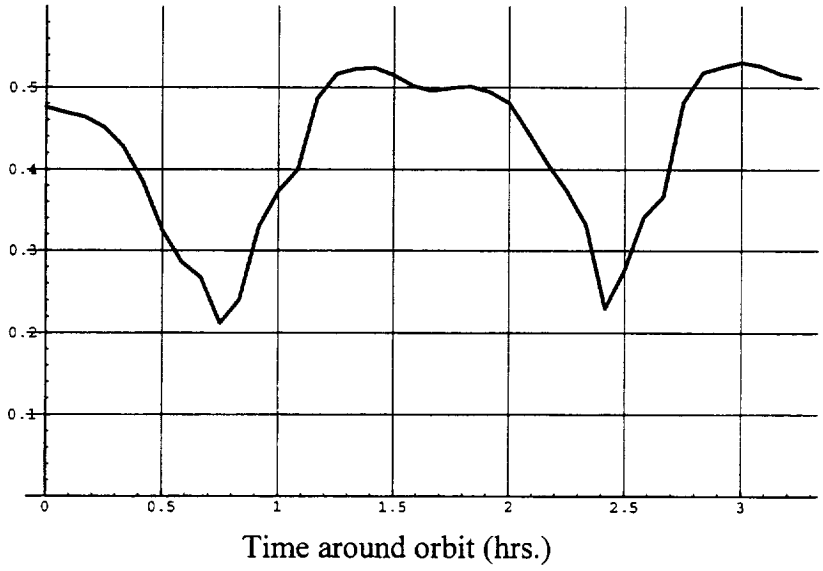

Figure 1.3.6. Thrust force (Newtons) of our nominal 7-km / 5 kW reboost system for the same three hour period of ISS orbit as in Figure 1.3.3.

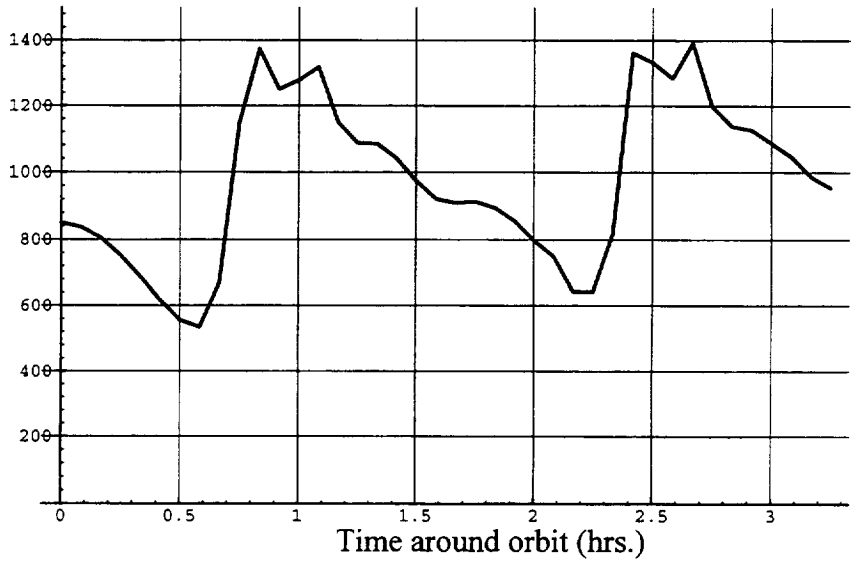

Figure 1.3.7. Input voltage required at the Station (Volts) by our nominal 7-km / 5 kW reboost system for the same three hour period of ISS orbit as in Fig. 1.3.3.

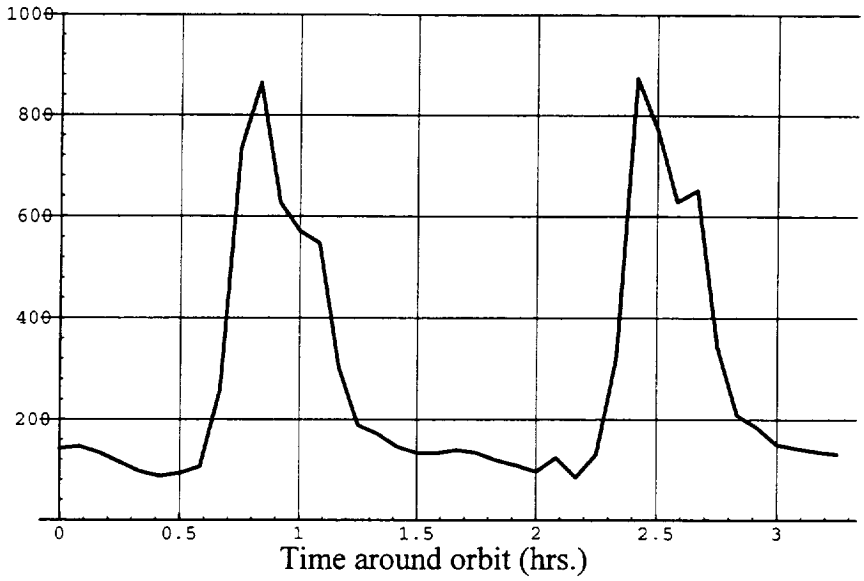

Figure 1.3.8. Bias voltage at the end of the 5 km insulation (Volts) for our nominal 7-km / 5 kW reboost system in the same three hour period of ISS orbit as in Fig. 1.3.3.

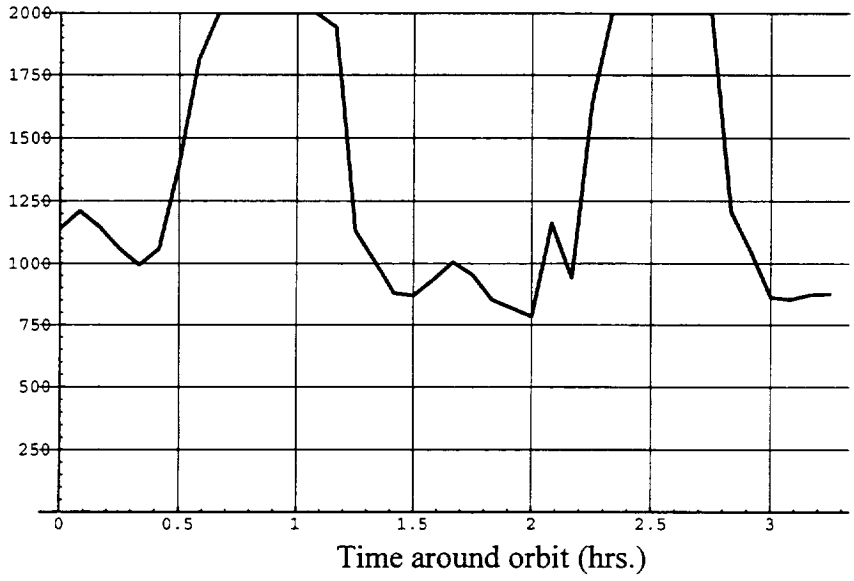

Figure 1.3.9. Current-collecting length (meters) for our nominal 7-km / 5 kW reboost system in the same three hour period of ISS orbit as in Fig. 1.3.3.

The input voltage required to operate the system during the same period at 5 kW is shown in Figure 1.3.7. It never exceeds 1.4 kV.

The bias voltage at the end of the insulation, seen if Figure 1.3.8, is seen to be greatly dependent on the plasma density. Density troughs correspond to voltage peaks.

The expansion of the collecting surface during periods of low electron density is strikingly demonstrated in Figure 1.3.9.

Propellant Savings Estimates

The obvious advantage of an electrodynamic tether reboost system is its freedom from propellant and utilization of "free" surplus solar energy. Since propellant is one of the biggest expenses involved in Space Station operation, the chances for significant savings are obvious [10]. SAO compiled the following tables illustrating possible annual savings under different assumptions.

For a 5-kW bare tether system operating 50% of the time (i.e, 182 days per year), the propellant saved per year is shown in Fig. 1.3.10 and compared to the propellant required for reboost (i.e., without RCS propellant). The total propellant saved over a 10-year operating life of the station is shown in Fig. 1.3.11. In summary, 22 tons can be saved out of the 77 tons required for the station reboost by tapping only 7% of the power available on the station.

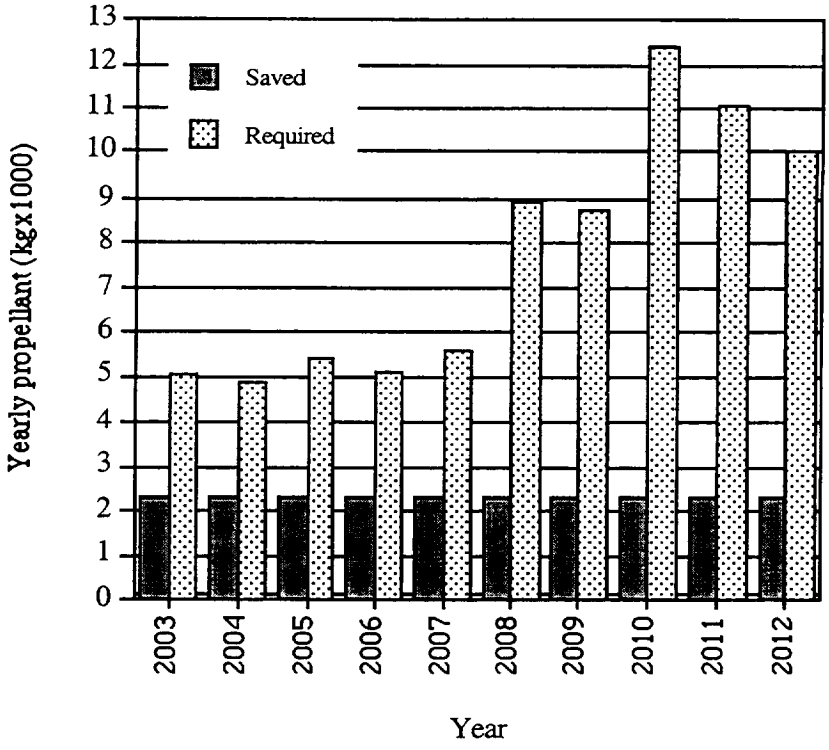

Fig. 1.3.10. Yearly propellant required and propellant saved with a 5-kW bare tether operating 50% of the time

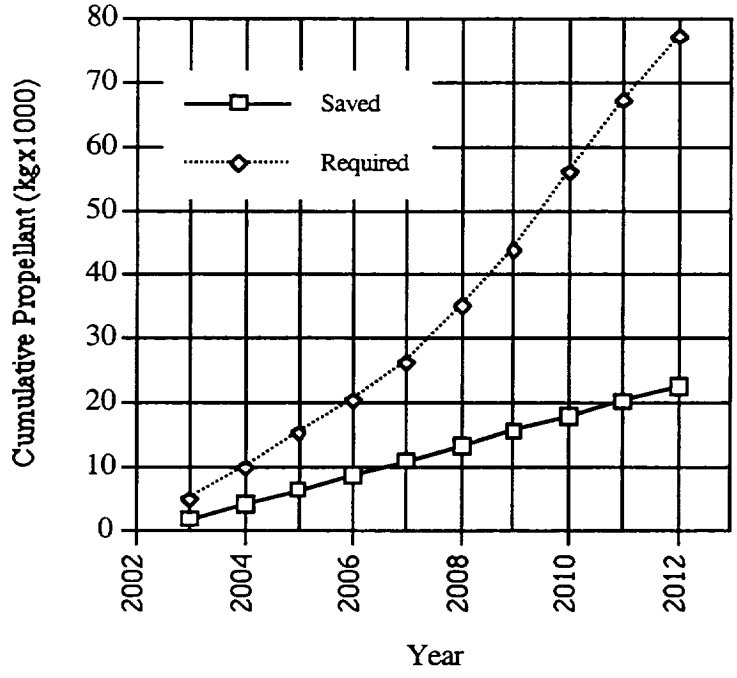

Fig. 1.3.11. Propellant saved in 10 years with 5-kW system operating 50% of the time: 22 tons out of 77 tons

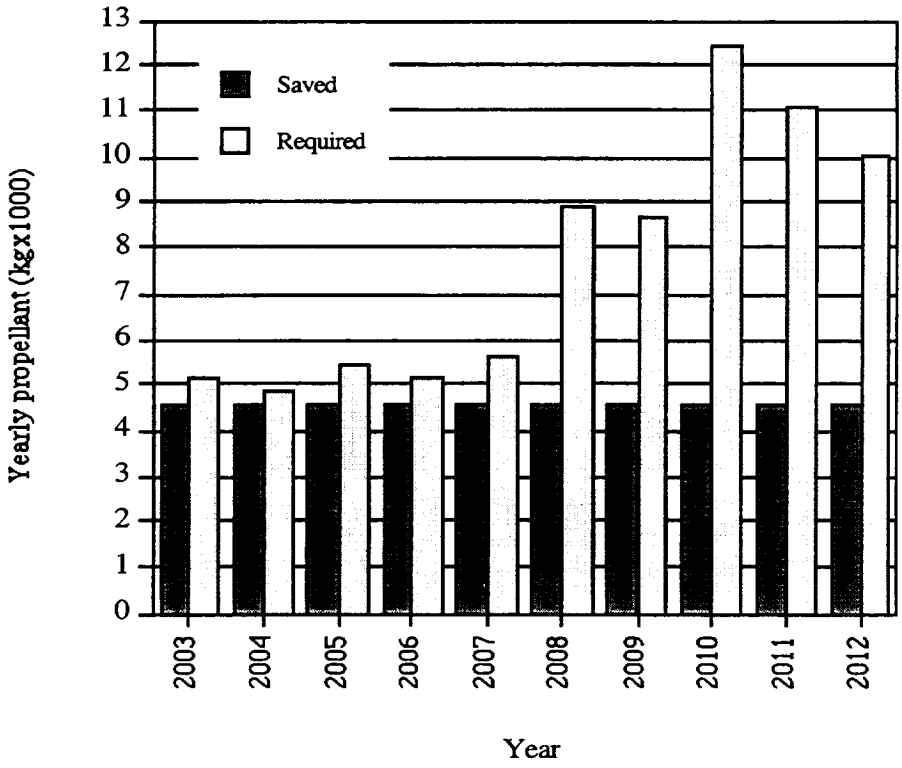

Fig. 1.3.12. Yearly propellant required and propellant saved with a 10-kW bare tether operating 50% of the time

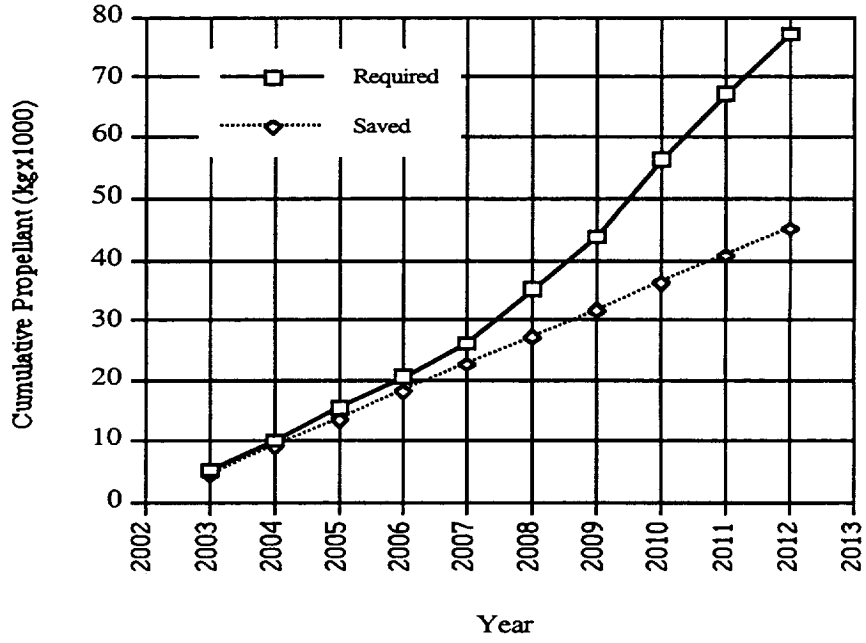

Fig. 1.3.13. Propellant saved in 10 years with 10-kW system operating 50% of the time: 45 tons out of 77 tons

If we assume a 10-kW, 10-km bare tether system operating 50% of the time (see Figs. 1.3.12 and 1.3.13), then the total savings over 10 years are 45 tons out of 77 tons required by tapping only 15% of the station power. A tether system, moreover, can help reduce dramatically the additional 11 tons of propellant required for the RCS system to mantain the attitude of the station because the tether stabilizes passively the attitude about the pitch and roll axes.

Cost Savings

Engineers at the Boeing Company in Huntsville, Alabama have computed the cost savings for station operations brought about by the ED bare tether for reboost. Since every 1000 kg of propellant delivered to the station requires the launch of a Progress-M, the number of Progress-M flights and the cost per flight directly translate into a total cost saved. Boeing engineers have estimated an overall cost saving over the 10 year station lifetime of 1 B$ for the 5 kW and 2 B$ for the 10 kW bare tether systems operating 50% of the time.

Conclusions

A bare tether system of a length short enough not to upset the microgravity requirements on board the space station can save a large portion of the propellant required for the station reboost at the expense of only 7%-15% (consistent with 5 kW and 10 kW delivered to the bare tether) of the station power for only 50% of the time.
The number of Progress-M launches saved per year ranges between 2 and 4 depending on the bare tether power level. Consequently, the expected cost savings (estimated by Boeing) over a 10 year station lifetime ranges between 1-2 B$.

References to Section 1.0

1. Estes, R.D., E.C. Lorenzini, J.R. Sanmartin, M. Martinez-Sanchez and N.A. Savich, "New High-Current Tethers: A Viable Power Source for the Space Station?," Smithsonian Astrophysical Observatory, White Paper, December 1995.

2. Parker, L. W. and Murphy, B. L., "Potential buildup on an electron-emitting ionospheric satellite," *Journal of Geophysical Research,* Vol. 72, No. 5, 1967, pp. 1631-1636.

3. Thompson, D. C., Bonifazi, C. Gilchrist, B. E., Williams, S.D., Raitt, W. J., Lebreton, J. P., Burke, W.J., Stone, N. H., and Wright, Jr., K. H., "The current-voltage characteristics of a large probe in low Earth orbit: TSS-1R results," *Geophysical Research Letters,* Vol. 25, No. 4, 1998, pp. 413-416.

4. Gilchrist, B. E., Bonifazi, C., Bilen, S. G., Raitt, W.J., Burke, W. J., Stone, N. H., and Lebreton, J.P., "Enhanced electrodynamic tether currents due to electron emission from a neutral gas discharge: Results from the TSS-1R mission, *Geophysical Research Letters,* Vol. 25, No. 4, 1998, pp. 437-440.

5. Laframboise, J. G., "Current collection by a positively charged spacecraft: Effects of its magnetic presheath," *Journal of Geophysical Research,* Vol. 102, No. A2, Feb. 1, 1997, pp. 2417-2432.

6. Cooke, D. L. and Katz, I., "TSS-1R electron currents: Magnetic limited collection from a heated presheath," *Geophysical Research Letters,* Vol. 25, No. 5, 1998, pp. 753-756.

7. Lam, S. H., "Unified theory for the Langmuir probe in a collisionless plasma," *Physics of Fluids,* Vol. 8, No. 1, Jan., 1965, pp.73-87.

8. Alpert, Y. L., Gurevitch, A. V., and Pitaevskii, L. P., *Space Physics with Artificial Satellites,* ch. VIII-X , Consultants Bureau, New York, 1965.

9. Vannaroni, G., Dobrowolny, M., Lebreton, J. P., Melchioni, E., De Venuto, F., Harvey, C. C., Iess, L., Guidoni U., Bonifazi, C., and Mariani, F., "Current-voltage characteristics of the TSS-1R satellite: Comparison with isotropic and anisotropic models," *Geophysical Research Letters,* Vol. 25, No. 5, 1998, pp. 749-752.

10. R.D. Estes, E.C. Lorenzini, J. Sanmartin, M. Martinez-Sanchez, J. Pelaez, L. Johnson, and I. Vas, "Bare Tethers for Electrodynamic Spacecraft Propulsion." Journal of Spacecraft and Rockets, Vol. 36, No. 6 (in press), Nov-Dec 1999.

2.0 ELECTRODYNAMIC TETHERS FOR TRANSPORTATION IN LEO

2.1 Electrodynamic Tether Tug

Orbital changes via an electrodynamic tether

An electrodynamic (ED) tether circulates a current I along the tether length L and the current interacts with the Earth's magnetic field B to produce an ED force F_D as follows:

$$\mathbf{F}_D = \mathbf{I'xBL} \tag{2.1}$$

where I' is the average current along the tether. Unlike an insulated tether, a bare tether has a variable current distribution along the tether and its average current along the tether does not coincide with the current measured at its ends. From eqn. (2.1), the ED force clearly depends on the relative position of the tether and the magnetic field and, hence, upon the orbital characteristics.

The ED force can be used to change the orbital characteristics of the initial orbit. All the orbital elements can be changed through electrodynamic forces [Carroll, 1984] but in practice some orbital elements change much more rapidly than others for a given tether current. Moreover, since the orbital inclination determines the orientation of the tether with respect to the magnetic field, the orbital inclination plays a major role in the effectiveness of orbital changes. In this study, we are particularly interested in altitude (or equivalently semimajor axis) and orbital inclination changes.

The expressions which relate the force to the rate of change of the semimajor axis a and the orbital inclination i for small orbital eccentricity are as follows:

$$\frac{da}{dt} = \frac{2F_x}{\Omega M} \tag{2.2}$$

$$\frac{di}{dt} = \frac{F_y}{a\Omega M}\cos(t\Omega) \tag{2.3}$$

where F_x and F_y are the components of the force along the flight direction and orthogonal to the orbital plane, Ω is the orbital rate, a is the semimajor axis and M is the system mass.

The force components F_x and F_y can be computed from eqn. (2.1). The complexity of their expressions depends upon the complexity of the magnetic field adopted.

For the only purpose of pointing out functional dependencies, we show here the relevant expressions of the changes over a time Δt in semimajor axis and inclination for a dipole magnetic field aligned with the Earth's spin axis:

$$\Delta a = 2\bar{B}\frac{L}{\Omega M}\int I\cos(i)dt \tag{2.4}$$

$$\Delta i = -\bar{B}\frac{L}{a\Omega M}\int I\cos^2(\phi)\sin(i)dt \tag{2.5}$$

where $\bar{B}$ is the magnetic field strength and ϕ is the argument of latitude (i.e., the angular position of the satellite with respect to the ascending node). More complicated expressions are obtained for more accurate magnetic field models. Even if simplified, eqns. (2.4) and (2.5) are useful to point out the following key features:

a) altitude changes can be obtained with a dc current (I = constant). Moreover, an altitude change involves an inclination change of opposite sign;

b) pure (without an associated altitude change) inclination changes are obtained by modulating the tether current as follows $I = -\cos(2\phi)$; this control strategy is strictly valid for a dipole magnetic field model;

c) inclination changes are of order 1/a slower than altitude changes;

d) the altitude rate of change is maximum for equatorial orbits and (consistently with a more accurate magnetic model) nearly zero for polar orbits;

e) the inclination rate of change is maximum for polar orbits and (consistently with a more accurate magnetic field) nearly zero for equatorial orbits.

Orbital changes with a bare tether

In this application bare tethers are used as effective anodes for obtaining relatively high currents with comparatively short tether lengths. A system with bare tether(s) can be used as a space tug to propel spacecraft, left in low altitude orbits by launch vehicles, to higher orbits and/or to change the orbital inclination.

It is important to remind that bare tethers are (passive) anodes, i.e., they can only collect electrons. Consequently, a bare-tether system capable of changing the altitude in both directions (up and down) and/or the orbital inclination requires two tethers: one upward deployed and the other downward deployed.

The following analysis is based on the following top-level system characteristics for the space tether tug:

Supplied power	= 10 kW
Tether	= 10-mm x 0.6-mm x 10 km (flat tether)
Bare tether section	= 50%
Tether material	= aluminum
Tether mass	= 162 kg (for one tether)

Based on the electron collection model of a bare tether in the orbital motion limited (OML) regime, a standard plasma density model and a tilted-dipole Earth's magnetic field, the orbital changes (per unit mass of payload) attainable vs. altitude are shown in the following plots for various initial orbital inclinations.

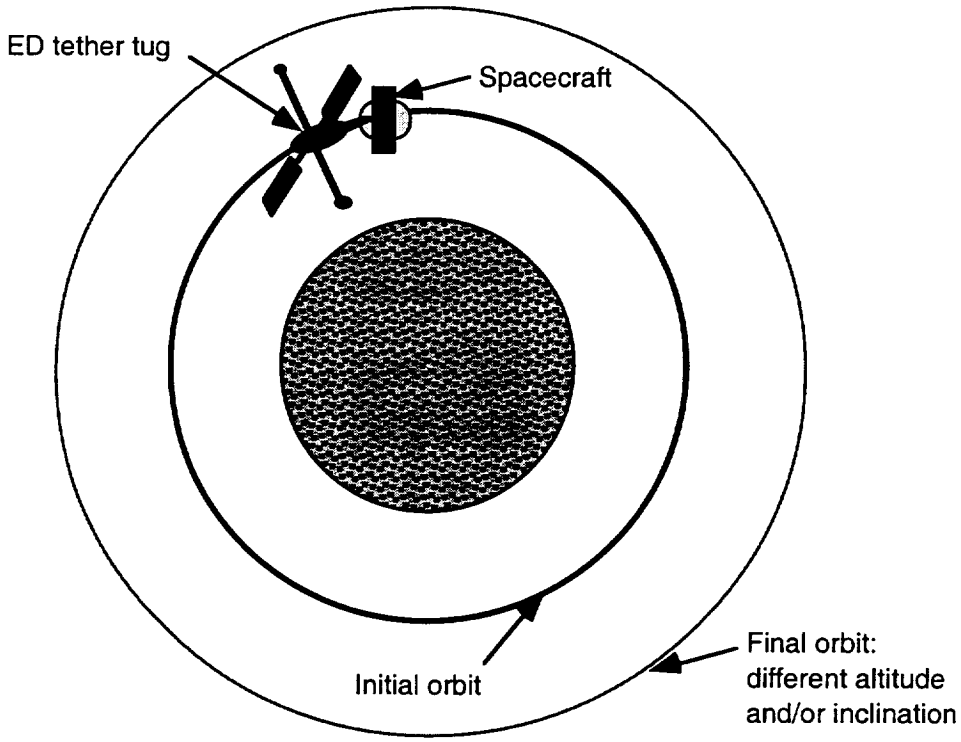

Fig. 2.1.1. Schematic of electrodynamic tether tug.

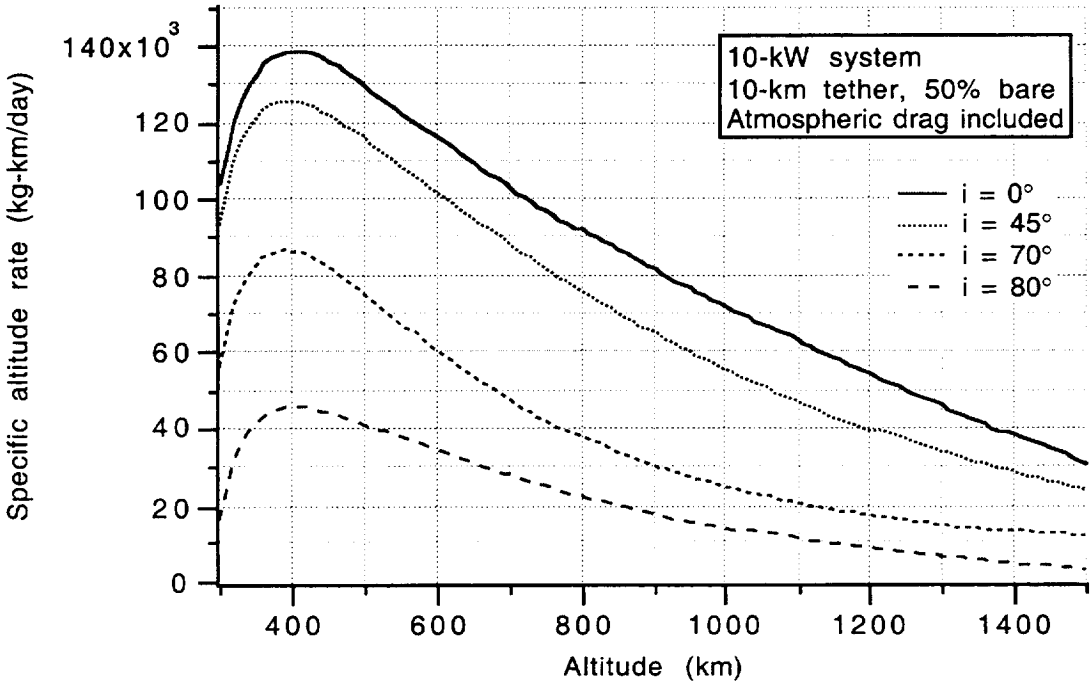

Fig. 2.1.2. Specific (per unit mass) altitude rate of change vs. altitude for various orbital inclinations.

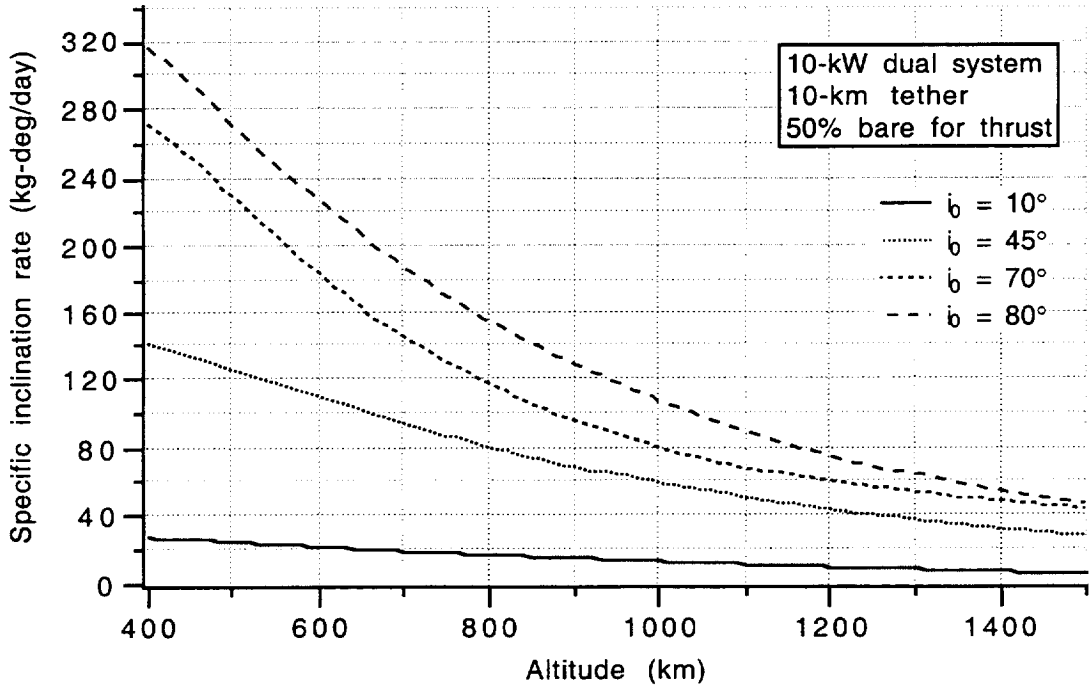

Fig. 2.1.3. Specific inclination rate vs. altitude for various initial orbital inclinations.

Figure 2.1.2 shows the specific (per unit mass) altitude rate vs. altitude for various orbital inclinations and Fig. 2.1.3 shows the specific orbital inclination rate vs. altitude for different initial inclinations. Rates for a given system mass M are readily obtained by dividing the specific rates by M. The system performance is heavily influenced by the plasma density which decreases as the altitude increases. A contributing factor to the decreasing performance with altitude is also the strength of the magnetic field even though it plays a lesser role than the plasma density.

For completeness, the modulus of the ED thrust vs. altitude is depicted in Fig. 2.1.4. Figure 2.1.5 shows the aerodynamic drag acting on the system under average solar activity inclusive of the drag acting on solar panels capable of delivering the required power to the tether tug.

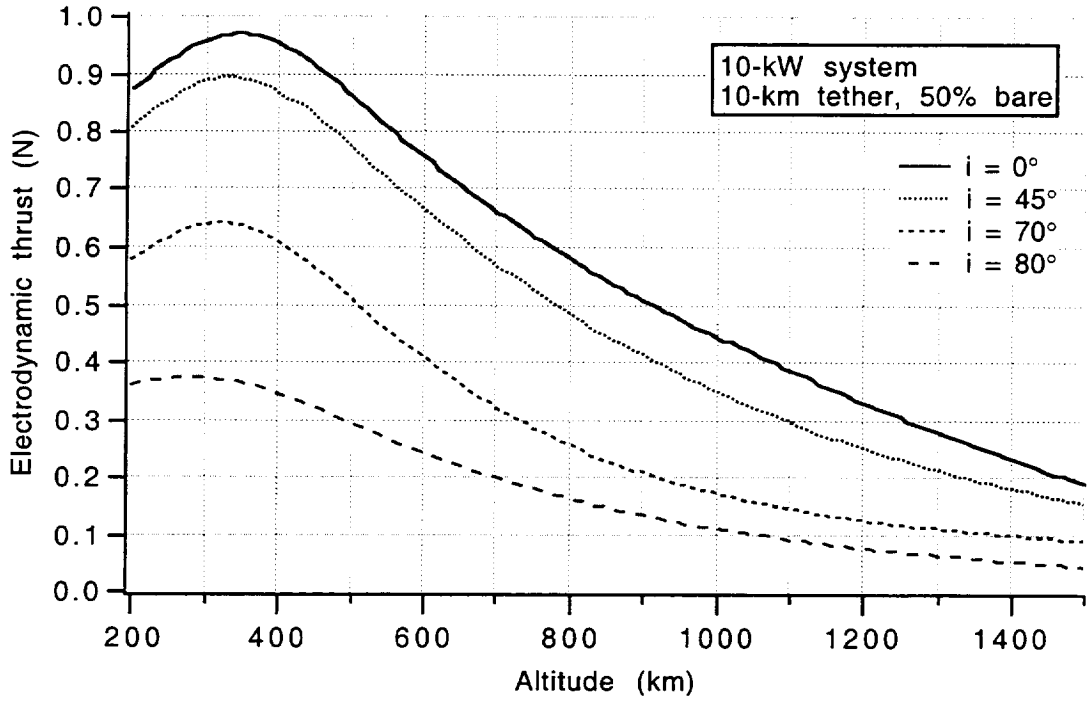

Fig. 2.1.4. Electrodynamic thrust vs. altitude for various orbital inclinations.

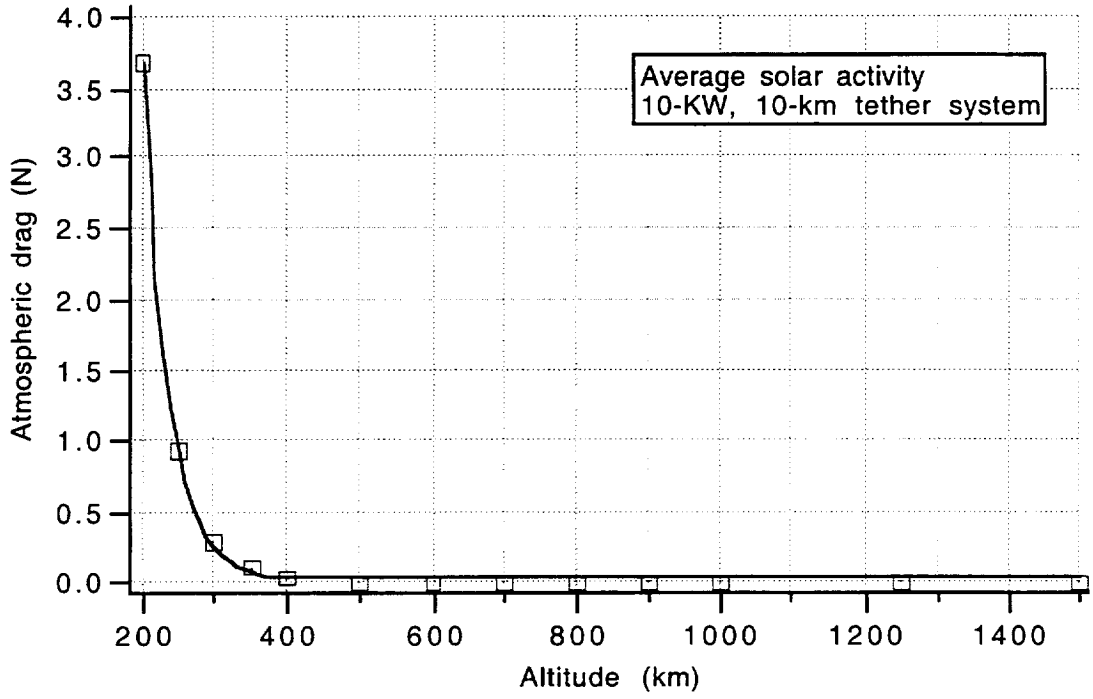

Fig. 2.1.5. Aerodynamic drag acting on tether and solar panels vs. altitude.

The aerodynamic drag is comparable to the ED thrust at about 250 km of altitude for a system in low-inclination orbit under average solar activity and it becomes rapidly smaller than the ED thrust at higher altitudes.

Concluding Remarks

In summary, a 10-kW tether tug would be capable of producing quite rapid altitude increases at low orbital inclinations (best condition) and rather slow inclination changes at high orbital inclinations (best condition). Key results are shown in Tables 2.1.1 and 2.1.2 for a 10-kW system with a reference mass of 1000 kg. It is worth reminding that the rates shown in the tables scale with inverse proportion to the system mass.

Table 2.1.1. Orbital altitude rate of change (km/day) for a 10-kW, 1000-kg tether tug.

Altitude rate (km/day)	Initial altitude 400 km	Initial altitude 1500 km
Equatorial orbit	**140**	**30**
Near polar orbit ($i_0 = 80°$)	**46**	**3**

Table 2.1.2. Orbital inclination rate of change (deg/day) for 10-kW, 1000-kg tether tug.

Inclination rate (deg/day)	Altitude 400 km	Altitude 1500 km
Near equatorial orbit ($i_0 = 10°$)	**0.027**	**0.006**
Near polar orbit ($i_0 = 80°$)	**0.3**	**0.046**

2.2 ED Upper Stage Demonstration Mission

Introductory Remarks

A smaller version of the tether tug could be developed as an upper stage demo to fly as a secondary payload on a future launch opportunity. Several secondary opportunities are available on the Pegasus rocket with an allowable total mass of 225 kg, i.e., half of the full payload capacity of Pegasus. The power considered for the scaled down demo is in the range 0.5kW - 1kW as better illustrated in the next chapters which deal with the preliminary system design of such a demo.

Preliminary Definition of the Upper Stage Demo

We first consider two bare-tether systems: (A) a 10-km x 10-mm x 0.6-mm aluminum tether 50% bare and (B) a 5-km x 7-mm x 0.5-mm aluminum tether 40% bare. System A is representative of a 1-kW system that is able to maintain its performance down to a plasma density of 10^{10} e/m^3. System B is representative of a 0.5-kW system whose performance decreases significantly as the plasma density is reduced to 10^{10} e/m^3. Tables 2.2.1 and 2.2.2 show the key characteristics of tether systems A and B, respectively, for two different values of plasma density and typical values of EMF encountered around the orbit.

Table 2.2.1. Characteristics of system A (10 km, 1-kW of supplied power)

Plasma density (e/m^3)	EMF (Volt)	Current at platform (A)	Average current along tether (A)	Thrust (N)	Collecting length (m)
10^{12}	1500	1.19	0.62	0.12	372
10^{10}	1500	0.62	0.44	0.086	5000

Table 2.2.2. Characteristics of system B (5 km, 0.5-kW of supplied power)

Plasma density (e/m^3)	EMF (Volt)	Current at platform (A)	Average current along tether (A)	Thrust (N)	Collecting length (m)
10^{12}	750	0.94	0.59	0.06	397
10^{10}	750	0.30	0.24	0.023	2000

The mass of a (single) aluminum tether is 162 kg for system A and 47 kg for system B. The tether mass of system A is clearly too high to meet the limit of 225 kg for half of the payload capacity of Pegasus. We are, therefore, bound to consider system B as a potential candidate for the electrodynamic upper stage.

In the following, we compute a preliminary mass budget for system B.

Solar Arrays

Table 2.2.3 shows the eclipse duration for the minimum and maximum altitude expected during the operation of the ED upper stage.

Table 2.2.3. Eclipses duration at inclination i = 30°

Altitude (km)	Min. Eclipse (min)	Max. Eclipse (min)	Orbit. Period (min)	% Min. Eclipse	% Max. Eclipse
220	31	37	90	34%	41%
800	21	35	101	21%	35%

The solar constant in Earth orbit is equal to 1353 W/m^2 ±3.5% (i.e., 1305-1400 W/m^2). Moreover, from the current literature on space systems engineering:

Solar arrays specific power = 26-100 W/kg --> specific mass = 38-10 kg/kW

The power to be delivered by solar arrays P_{sa} is given by the following formula:

$$P_{sa} = P_{load} (T_e/X_e + T_d/X_d)/T_d \quad (2.6)$$

where P_{load} is the power to payload, T_e and T_d are the eclipse and daylight times respectively, X_e and X_d are the conversion factors for the direct power transfer from the solar array to the payload and through the batteries, respectively.

For the worst case of low altitude (H = 220 km), maximum-duration eclipses and a power to the load P_{load} = 500 W, the power to be delivered by the solar arrays is:

$$P_{sa} = 500\ (37/0.65 + 53/0.85)/53 = 500\ (1.07 + 1.18) = 1125\ W$$

We assume an average value for the specific power of 60 W/kg, to obtain

$$M_{sa} = 1125/60 \approx 19\ kg$$

The power per unit surface from the arrays at beginning of life (BOL) is:

$$P_{BOL} = p_{sun}\ \nu\ I_d \cos(\beta) \quad (2.7)$$

where p_{sun} is the solar constant, ν is the efficiency of the solar array, β is the worst-condition illumination angle and I_d is the degradation coefficient of the arrays (due to shadowing, thermal conditions and assembly losses).

After assuming that the Sun is at solstice, ν = 0.14 (silicon solar arrays) and a typical value of the degradation factor of 0.75, we obtain:

$$p_{BOL} = 1305 \times 0.14 \times 0.75 \times \cos(23.5°) = 126\ W/m^2$$

The power per unit area at the end of life (EOL) is:

$$p_{EOL} = p_{BOL} \times L_d \quad (2.8)$$

where L_d is a degradation factor of the array due primarily to radiation but also to thermal cycling and other time-dependent degradation factors. The time degradation of a solar array performance in LEO is typically about 3.5% per year.

For a 1-year mission lifetime, we obtain:

$$p_{EOL} = 126 \times 0.965 = 122\ W/m^2$$

The areas of solar arrays of different configurations for system B are, then, as follows:

$A_{sa} = P_{sa}/p_{EOL} = 1125/122 = 9.2\ m^2$ pivoted arrays

$A_{sa} \approx 9.2x\pi = 29\ m^2$ body-mounted cylindrical arrays

$A_{sa} \approx 9.2x4 = 37\ m^2$ body-mounted cubic arrays

Batteries

The energy to be delivered during one eclipse period is:

$$E_d = P_{load}\, T_e/\eta \qquad (2.9)$$

where η is the battery-to-payload conversion factor. In our case, we obtain:

$E_d = 500x37x60/0.85/3600 = 363$ W-hr

If we assume a mission duration of 1 year, we will have about 6000 recharge cycles which imply the following depth of discharge (DOD) for the batteries:

DOD Nickel-Cadmium $\approx 35\%$

DOD Nickel-Hydrogen $\approx 57\%$

The energy capacity required of the batteries to operate the ED tether is then:

$$E_{cap} = E_d/DOD \qquad (2.10)$$

that is

$E_{cap} = 1037$ W-hr Nickel-Cadmium

$E_{cap} = 637$ W-hr Nickel-Hydrogen

From the current literature, the secondary (rechargeable) batteries energy densities are:

$E_{den} =$ 25-30 W-hr/kg Nickel-Cadmium

$E_{den} =$ 25-40 W-hr/kg Nickel-Hydrogen

After assuming average values of the energy densities, the batteries masses are estimated as follows:

M_{batt} = 1037/27.5 = 38 kg Nickel-Cadmium

M_{batt} = 637/32.5 = 20 kg Nickel-Hydrogen

System Mass Budget

It is worth reminding that a bare-tether system capable of changing the altitude and the inclination requires two tethers: one upward deployed and the other downward deployed. A bare-tether upper stage which is expected to raise the orbital altitude of its payload only requires one downward-deployed tether.

Table 2.2.4. Preliminary mass budget for 5-km, 0.5 kW systems.

System B1: Altitude + Inclination		System B2: Altitude only	
Item	Mass (kg)	Item	Mass (kg)
2 ED Tethers	94	1 ED Tether	47
2 Deployers	60	1 Deployer	30
Solar arrays	19	Solar arrays	19
Leveling batteries	20	Leveling batteries	20
Plasma contactor	12	Plasma contactor	12
Gas supply	2	Gas supply	2
End mass	25	End mass	25
Partial Tot	232	Partial Tot	155
Remainder	-7	Remainder	70
Tot Available	225	Tot Available	225

Table 2.2.4 shows the preliminary mass budget for the key elements of the ED upper stage for two separate systems: (B1) a dual-tether system for changing the orbital altitude and the inclination and (B2) a single-tether system for raising the orbital altitude.

Clearly, system B1 exceeds the mass limitation and the option of having a dual-system to perform orbital inclination changes must be dropped. This is has a positive consequence also on the mission lifetime because the altitude changes are much faster than inclination changes. The mission lifetime of an upper stage demo for raising the orbital altitude can be drastically shorten from the presently-specified one year as shown in the following.

Preliminary Mass Budget of Demo for Raising Altitude

We consider a single bare-tether 5-km x 7-mm x 0.5-mm made of aluminum and 40% bare. Moreover, we assume a constant power delivered to the tether of 0.5 kW for system C1 and 1 kW for system C2. Tables 2.2.5 and 2.2.6 show the key characteristics of systems C1 and C2 for the peak values of plasma density and EMF encountered around the orbit. The last column in the tables shows the altitude rate of change in km/day for a 1-kg-mass system. The altitude rate of change for a system of mass m is simply obtained by dividing the numbers in the last column by m.

Table 2.2.5. Characteristics of system C1 (5 km, 0.5-kW of supplied power)

Plasma density (e/m^3)	EMF (Volt)	Current at platform (A)	Average current along tether (A)	Collecting length (m)	Thrust (N)	$\partial H/\partial t$ (kg-km/ day)
10^{12}	1000	0.74	0.46	307	0.060	8968
10^{12}	500	1.28	0.83	559	0.054	8072
10^{10}	1000	0.28	0.22	2000	0.029	4335
10^{10}	500	0.31	0.25	2000	0.016	2392

Table 2.2.6. Characteristics of system C2 (5 km, 1-kW of supplied power)

Plasma density (e/m^3)	EMF (Volt)	Current at platform (A)	Average current along tether (A)	Collecting length (m)	Thrust (N)	$\partial H/\partial t$ (kg-km/ day)
10^{12}	1000	1.37	0.87	466	0.114	17040
10^{12}	500	2.26	1.50	812	0.098	14650
10^{10}	1000	0.38	0.31	2000	0.040	5980
10^{10}	500	0.41	0.33	2000	0.021	3140

After considering the thrust levels for different plasma and EMF values, we conclude that system C2 can change the altitude almost twice as fast as system C1 at high plasma densities and about 30% faster than system C1 at low plasma densities.

Table 2.2.7. Comparison between 2-mm cylindrical tether and a 7mmx0.5mm flat tether.

Tether type	Plasma density (e/m^3)	EMF (Volt)	Current at platform (A)	Average current along tether (A)	Collecting length (m)	Thrust (N)	$\partial H/\partial t$ (kg-km/ day)
Flat	10^{12}	750	0.94	0.59	397	0.058	8670
Cyl.	10^{12}	750	0.87	0.57	674	0.056	8370
Flat	10^{10}	750	0.30	0.24	2000	0.023	3438
Cyl.	10^{10}	750	0.18	0.14	2000	0.014	2093

We also compute the characteristics, for an average EMF of 750 V, of a cylindrical tether of 2-mm diameter (5-km-length and 0.5-kW of supplied power) and an almost-equal-mass flat tether. Results are shown in Table 2.2.7.

The mass of the ED flat tether is 47 kg with a volume of 0.018 m^3 while the mass of the cylindrical ED tether is 41 kg with a volume of 0.016 m^3 (i.e., twice the volume of the SEDS-II tether).

The performance of the flat and cylindrical tether of almost-equal masses are similar at high plasma densities while the flat tether performance is superior at low plasma densities.

In the following we estimate the mass of the major items associated with the ED tether for the systems C1/D1 and C2 where we call D1 the 0.5-kW-power, cylindrical tether system.

Size of Solar Arrays

The power to be delivered by the solar arrays is given by eqn. (2.6).

For the worst case of low altitude (220 km) and a maximum-duration eclipse of 37 min, we obtain for the two systems:

$P_{sa} = 1125$ W system C1/D1

$P_{sa} = 2250$ W system C2

Consequently, after assuming an average value for the specific power of solar arrays of 60 W/kg, we obtain

$M_{sa} \approx 19$ kg system C1/D1

$M_{sa} \approx 38$ kg system C2

We recall that the specific power of the array is 126 W/m^2 at the beginning of life (BOL) and 122 W/m^2 at the end of life (EOL) after one year lifetime. Since we are considering a demo for raising the orbit only, we can shorten the mission duration to 2 months or less. The BOL value of the specific power is, therefore, more pertinent to our mission. Moreover, if we assume that the solar arrays are body-mounted on a cylindrical body, the required area of the arrays is as follows:

$A_{sa} \approx 28\ m^2$ for system C1/D1; $A_{sa} \approx 56\ m^2$ for system C2.

These areas are too large to fit in the volume available on board Pegasus. Pivoted arrays must be considered with areas as follows:

$A_{sa} \approx 9\ m^2$ for system C1/D1; $A_{sa} \approx 18\ m^2$ for system C2.

Batteries Characteristics

We also refine the estimate of the mass of the leveling batteries by reducing the expected mission lifetime from 1 year (that was required for the orbital inclination changes) to 2 months which is a conservative time for carrying out a very significant altitude change.

In our two cases the energy to be delivered by the leveling batteries during an eclipse is:

$E_d = 363$ W-hr system C1/D1

$E_d = 726$ W-hr system C2.

Having reduced the mission lifetime from 1 year to 2 months, the number of recharge cycles will also be reduced from 6000 to 1000 and, consequently, the new depth of discharge (DOD) for the batteries is:

DOD Nickel-Cadmium $\approx 60\%$

DOD Nickel-Hydrogen $\approx 82\%$

The new energy capacity required of the leveling batteries for system C1 is:

$E_{cap} = 605$ W-hr Nickel-Cadmium (system C1/D1)

$E_{cap} = 443$ W-hr Nickel-Hydrogen (system C1/D1)

Twice this amount is required for the batteries of system C2.

After assuming average values of the energy densities for the two types of batteries, the battery mass is estimated as follows:

$M_{batt} = 605/27.5 = 22$ kg Nickel-Cadmium (system C1/D1)

$M_{batt} = 443/32.5 = 14$ kg Nickel-Hydrogen (system C1/D1)

Twice this amount is required for the leveling batteries of system C2.

New Systems Mass Budget

Table 2.2.8 shows the preliminary mass budget for the key elements of the ED upper stage for the following systems: C1 (0.5-kW of supplied power, flat tether); C2 (1-kW of supplied power, flat tether) and D1 (0.5-kW of supplied power, cylindrical tether). In estimating the deployer mass, we have taken the mass of the SEDS deployer (≈10 kg) and assumed that the mass increment is proportional to the volume of the tether spool. In the computation of the total tether volume we have also included an additional 10-km x 0.7-mm non-conductive tether segment for improving dynamic stability.

Table 2.2.8. Mass budgets for systems C1 (0.5-kW, flat tether), C2 (1-kW, flat tether) and D1 (0.5-kW, cylindrical tether).

Item	System C1 Mass (kg)	System C2 Mass (kg)	System D1 Mass (kg)
ED Tether	47	47	41
Deployer	30	30	25
Solar arrays	19	38	19
Plasma contactor	12	12	12
Gas supply (2-mo.)	2	4	2
Leveling batteries	14	28	14
Partial Total	124	159	113
End mass	20	35	20
Remainder	81	31	92
Total Allowed	225	225	225

In summary, the performance of the 1-kW system is superior to the performance of the two 0.5-kW systems (the flat and the cylindrical tether), especially at high plasma densities. The performance of the cylindrical tether (system D1) is comparable to the performance of the equal-power flat tether (system C1) at high plasma densities and inferior at low plasma densities. The mass left over for subsystems other than those listed in the table above is only 31 kg for the 1-kW system C2, 81 kg for the 0.5-kW system C1, and 92 kg for the 0.5-kW system with cylindrical tether D1. The 0.5-kW systems, therefore, have much more comfortable mass margins to fit within the 225-kg mass limit allowed on the Pegasus rocket as secondary payload.

Transfer Time

We compute the time for transferring an ED Upper Stage from 200 km to 800 km at an inclination of 30°. We assume an all-aluminum cylindrical tether 5-km x 2-mm with a bare portion covering 40% of the total length. The transfer time per unit mass is shown in Figure 2.2.1 for three different values of power delivered to the tether (day and night) under the assumption of average solar activity and average eclipse duration.

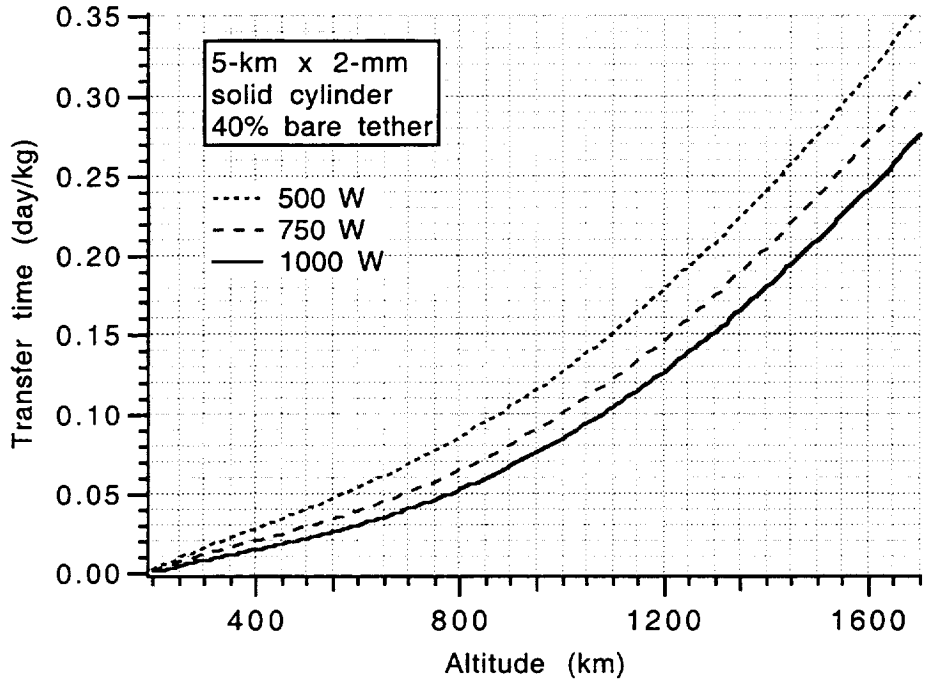

Fig. 2.2.1. Transfer time per unit of system mass for 500 W, 750 W and 1000 W of power delivered to the tether.

The preliminary mass budget for the three systems is shown in Table 2.2.9. We assume that the systems are detached from the Pegasus last stage. We also assume (based on SEDS end mass) that the mass for instrumentation and other ancillary equipment of 50 kg. We can now compute the transfer time for each system according to its estimated mass. Results are shown in Figure 2.2.2.

Table 2.2.9. Preliminary mass budgets for the 500-W, 750-W and 1000-W systems.

Item	500 W Mass (kg)	750 W Mass (kg)	1000 W Mass (kg)
ED Tether	41	41	41
Deployer	25	25	25
Solar arrays	19	28	38
Plasma contactor	12	12	12
Gas supply (2-mo.)	2	3	4
Leveling batteries	14	21	28
Regulator/converter	12	20	25
Stabilization mass	20	20	20
Instrum./Other	50	50	50
Total Mass	195	220	243*

*Total mass exceeds the mass limitation

The intermediate power level of 750 W appears to be preferable from a transfer time viewpoint. The system fits within the mass constraint of a secondary payload on Pegasus and its performance, in terms of orbital altitude rate of change, is close to the performance of the 1000-W system. The present estimate for transferring the upper stage from 200 km to 800 km (having assumed average solar activity and average eclipses) is about 14 days.

If this system were to be attached to the Pegasus last stage, the performance would decrease because of the additional ballast mass. Since the Pegasus last stage is about 180 kg, the ED tether upper stage transfer time would increase from 14 days to 25 days. We do not see any advantage, at this point, in staying attached to the Pegasus stage once the ED tether is deployed because the lifetime of rocket stages is generally very short because it is limited to the delivery of the payload to orbit.

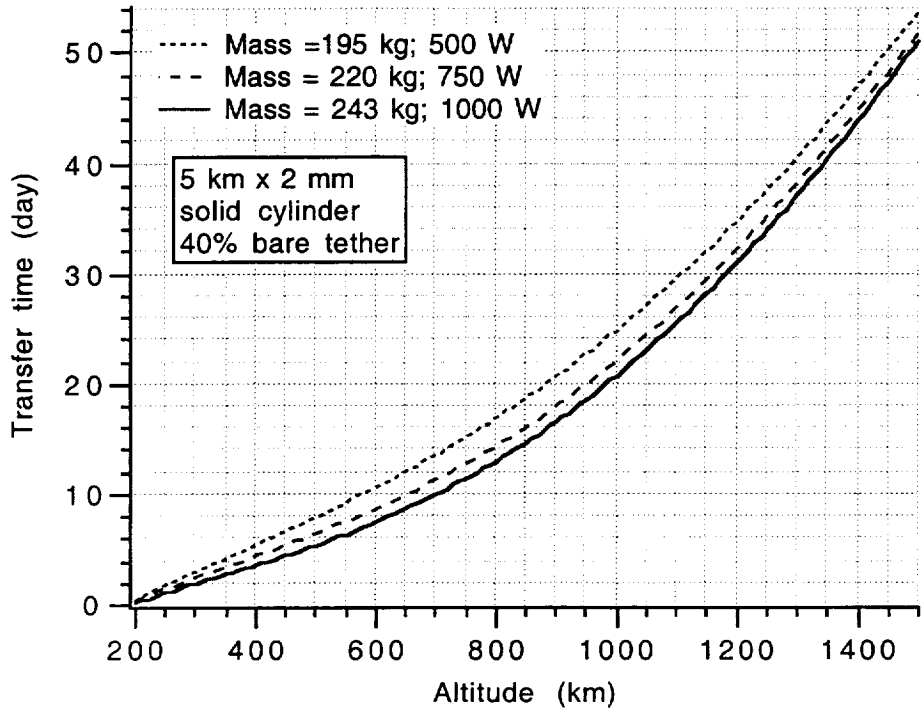

Fig. 2.2.2. Transfer time for the three tether systems considered according to their present total mass estimates.

There is also the possibility of reducing further the mass of the ED tether by utilizing a hollow cylinder as opposed to the all-aluminum tether. The former would have the same external diameter of 2 mm but the internal diameter of the conductor would be 1.5 mm. If the tether core is filled with a material with a density 10% of the aluminum density, the total mass of the tether would be 21 kg as opposed to 41 kg. The electrodynamic performance of the hollow tether (with the same outer diameter) is only slightly inferior to the performance of the all-aluminum tether.

Concluding Remarks

An upper stage demo can be designed to fit within the mass limitations of half a Pegasus rocket. A power of about 750 W delivered to the tether appears to be attainable at this preliminary stage of the design. The most challenging component of the demo is the power subsystem because the solar panels required are too large to be body mounted and more costly configurations must be pursued.

A 750-W tether upper stage would be capable of raising the orbit from 200 km to 800 km at an orbital inclination of 30 deg in about 2 weeks.

References to Section 2.0

1. Carroll, J.A., "Guidebook for Analysis of Tether Applications." NASA CR-178904, March 1985.

2. Wertz, J.R. and W.J. Larson, "Space Mission Analysis and Design." Kluwer Academic Publishers, 1991.

3. Lorenzini, E.C. and J.A. Carroll, "In-orbit experimentation with the Small Expendable-tether Deployment System." ESA Journal, Vol. 15, No. 1, pp. 27-33, 1991.

3.0 ELECTRODYNAMIC TETHERS FOR SPACECRAFT REENTRY

3.1 Propulsive Small Expendable Deployment System (ProSEDS) Overview

ProSEDS may be viewed as an outgrowth of the other studies SAO has been engaged in with MSFC under this grant. Much of the experience gained and the software developed for the other tasks involving bare tethers is directly applicable to ProSEDS. ProSEDS resembles the precursor experiments proposed quite a bit earlier to demonstrate bare tether operation in space and magnetic thrust or drag [1]. Our group at SAO has contributed to the ProSEDS project in the primary areas of electrodynamics, system dynamics, tether design and mission planning and testing.

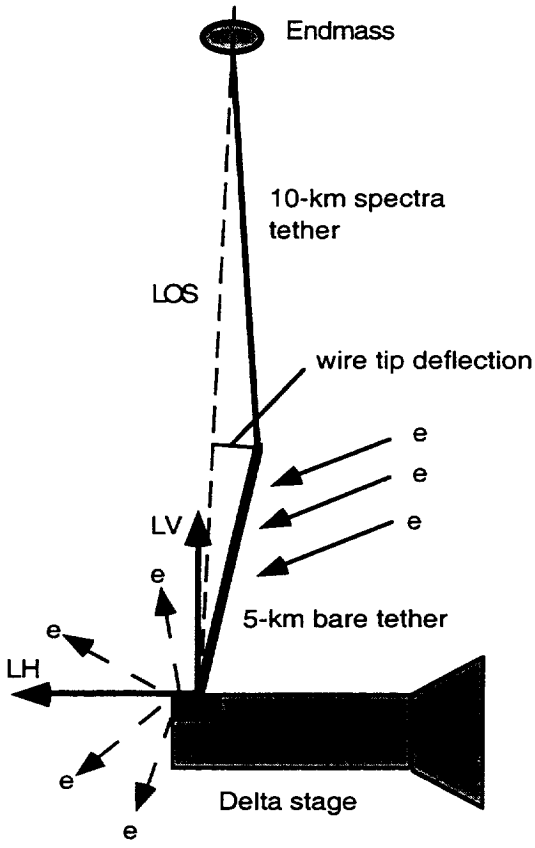

Fig. 3.1.1. Schematic of ProSEDS

As presently planned, ProSEDS will be carried into a 400 km orbit as a Delta-II secondary payload. It will use a SEDS deployer to deploy upward a tether made up of two parts (see Fig. 3.1.1). First a 10 km nonconductive ballast tether with an end mass will be deployed. This will serve to pull off the remaining 5 km segment of bare metallic tether, which will be used to collect electrons. A hollow cathode will maintain electrical connection

with the plasma at the Delta platform. The goals are to demonstrate high current collection by a bare tether and significantly accelerated orbital decay, due to the magnetic drag. ProSEDS is being funded by the Advanced Space Transportation Program (ASTP) at MSFC, which has an interest in electrodynamic tethers both for a tether upper stage type application and for rapid re-entry of dead spacecraft. This is an ongoing project, and we will summarize our work in this section of the report.

3.2 ProSEDS electrodynamics

Current collection

The success of ProSEDS will mainly be judged on whether or not it sets new standards in current collection by an electrodynamic tethered system. It is not necessary that the experiment attain current levels that would directly be useful in the ultimate applications, but it should attain current levels closely approaching the theoretical predictions of orbital motion limited current collection by a thin wire. Or, if there are deviations from the predictions, there should be sufficient data on plasma and magnetic conditions to determine where modifications to the theory need to be made, so that reasonable estimates for system performance for useful applications can be made. There must in the end be a convincing case for proceeding to the next level of development, or the bare tether concept will not be pursued further. Figure 3.2.1 shows our calculated current for a copper wire of 0.7 mm diameter and 5 km length.

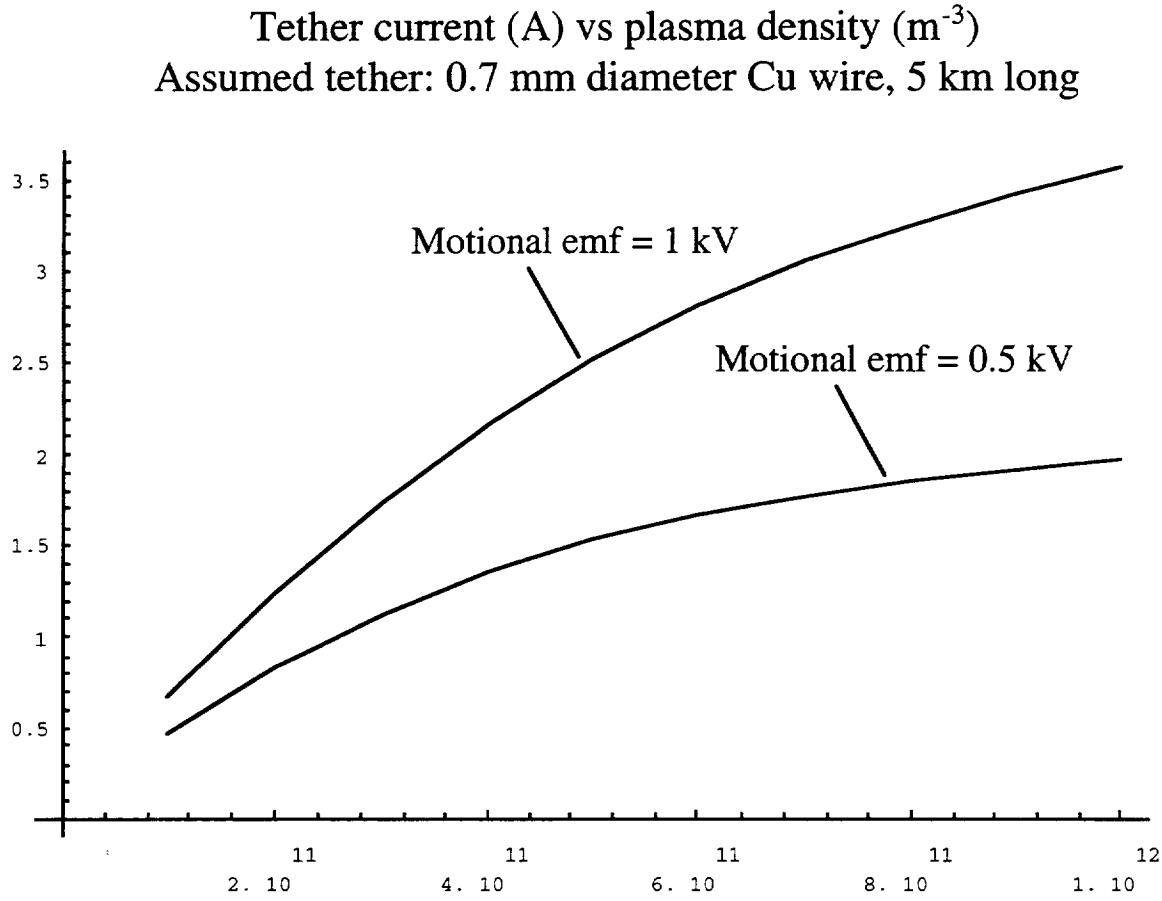

Fig. 3.2.1. Tether current predicted for ProSEDS under different orbital conditions.

If we are to obtain valuable data for more than the three orbits that the primary and secondary batteries can sustain, we must be able to recharge the batteries using the tether current. The current levels required depend on the power usage and the amount of time devoted to battery charging. Our calculations have been an indispensable aid to decisions on the operating cycle, battery choice, etc. Figures 3.2.2 and 3.2.3 show how the tether current at the Delta is reduced under the assumption of 50 V or 200 V of the motional EMF being used for battery charging. In each case the assumed tether is 5 km long with circular cross-section with 0.7 mm diameter. It is made of copper. A 10 Ohm impedance is assumed to be in series with the tether in addition to the charging device. The top curves are with no battery charging. Figure 3.2.2 is for a motional EMF of 1 kV, and Fig. 3.2.3 is for 500 V.

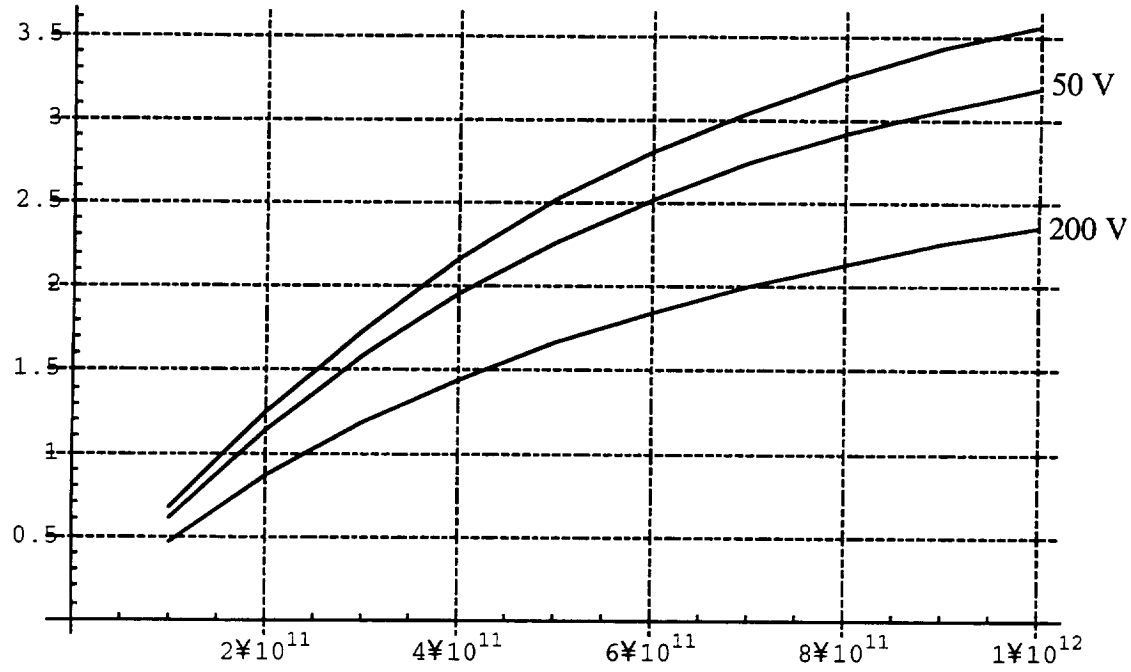

Fig. 3.2.2. Current available for battery charging under two assumptions of operating voltage. Tether current (A) shown vs plasma density (m^{-3}) for motional EMF of 1 kV.

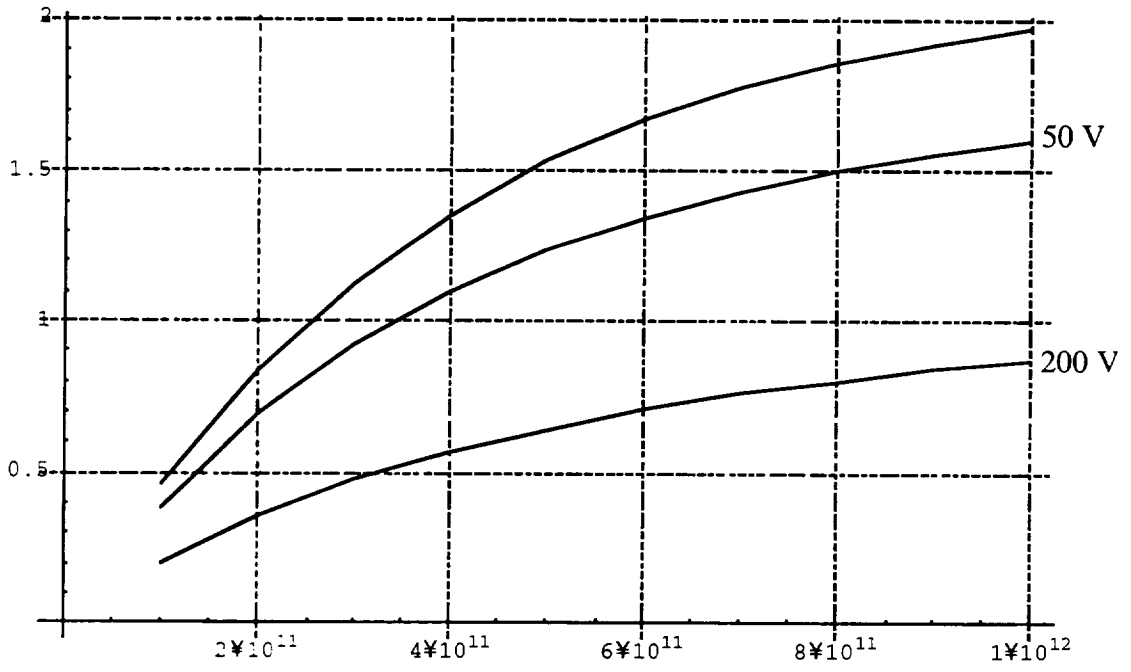

Fig. 3.2.3. Current available for battery charging under two assumptions of operating voltage. Tether current (A) shown vs plasma density (m^{-3}) for motional EMF of 500 V.

One of the primary concerns in mission planning is that mass restrictions be met. One way of reducing the mass would be to use a shorter tether. In order to see the effect on system performance of using a shorter tether, we made calculations for tether lengths of 3 km, 4 km, and 5 km over a range of plasma density values and for two different motional electric field values. These results are displayed in Figures 3.2.4 and 3.2.5. The same tether used in previous calculations was assumed. A 10 Ohm impedance was assumed to be in series with the tether in addition to a 50 V constant voltage between the Delta platform and the local plasma. Figure 3.2.4 is for a motional electric field along the tether of 0.2 V/km, which corresponds to 1 kV for the 5 km tether. Figure 3.2.5 is for a motional electric field along the tether of 0.1 V/km, which corresponds to 500 V for the 5 km tether.

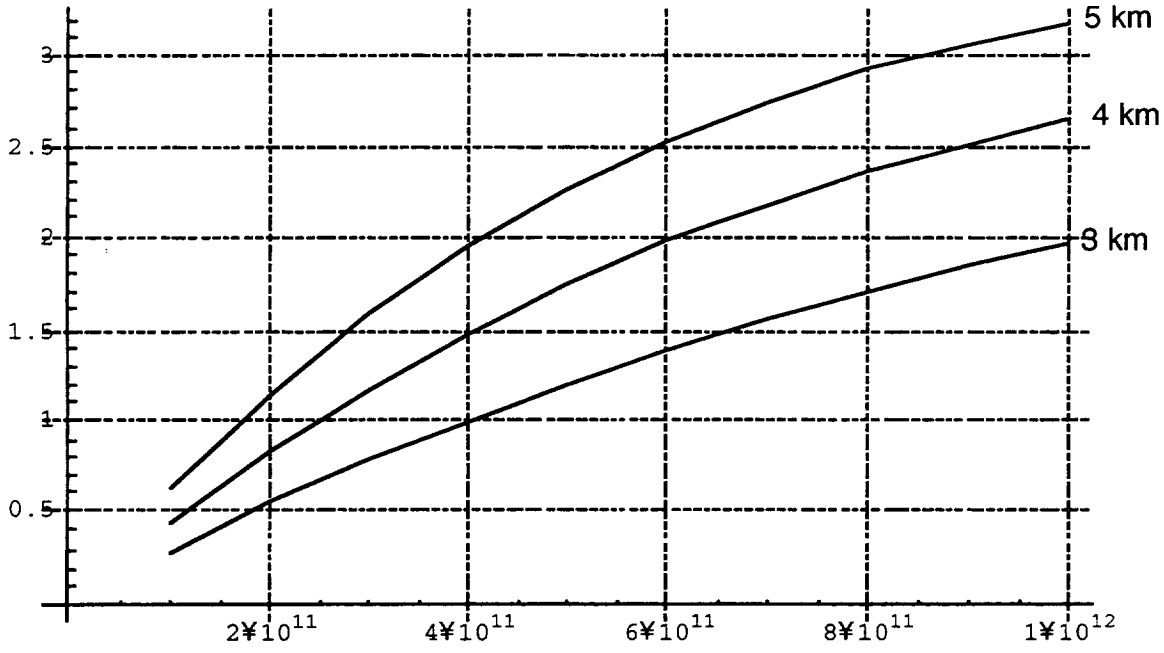

Fig. 3.2.4. Current collected for three different tether lengths. Tether current (A) shown vs plasma density (m^{-3}) for motional electric field of 0.2 V/km.

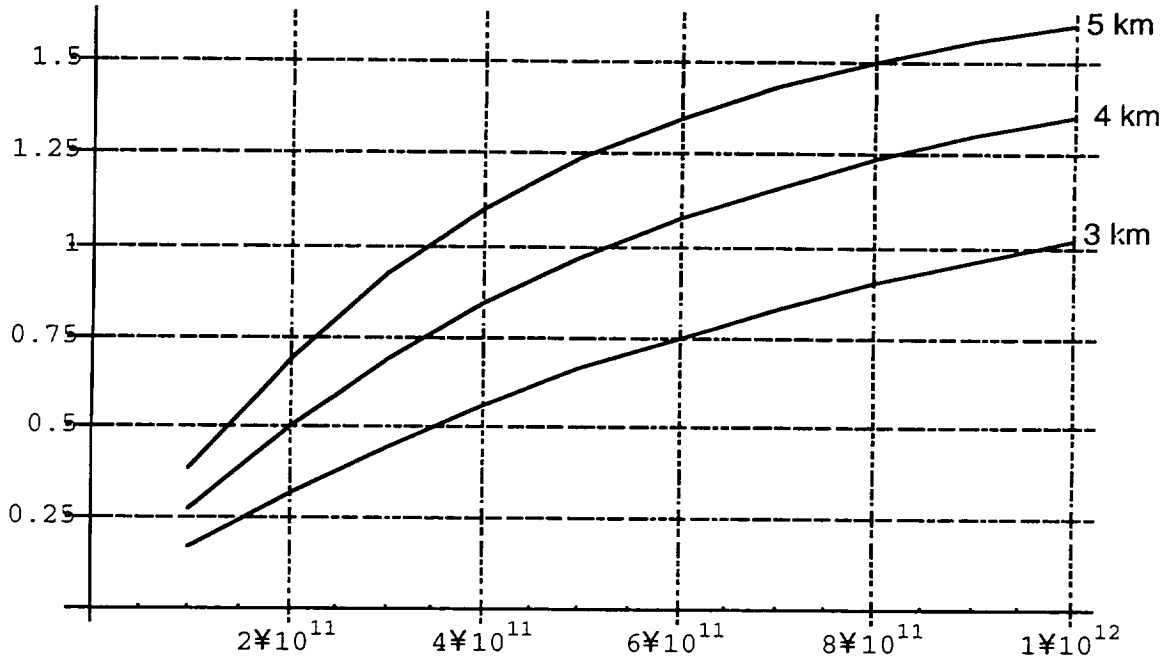

Fig. 3.2.5. Current collected for three different tether lengths. Tether current (A) shown vs plasma density (m^{-3}) for motional electric field of 0.1 V/km.

One of the proposed operating modes for ProSEDS places a 1000-Ω resistance in series with the tether. Figure 3.2.6 shows current collected with different series resistances. A 20 Volt negative bias with respect to the plasma is assumed at the Delta end.

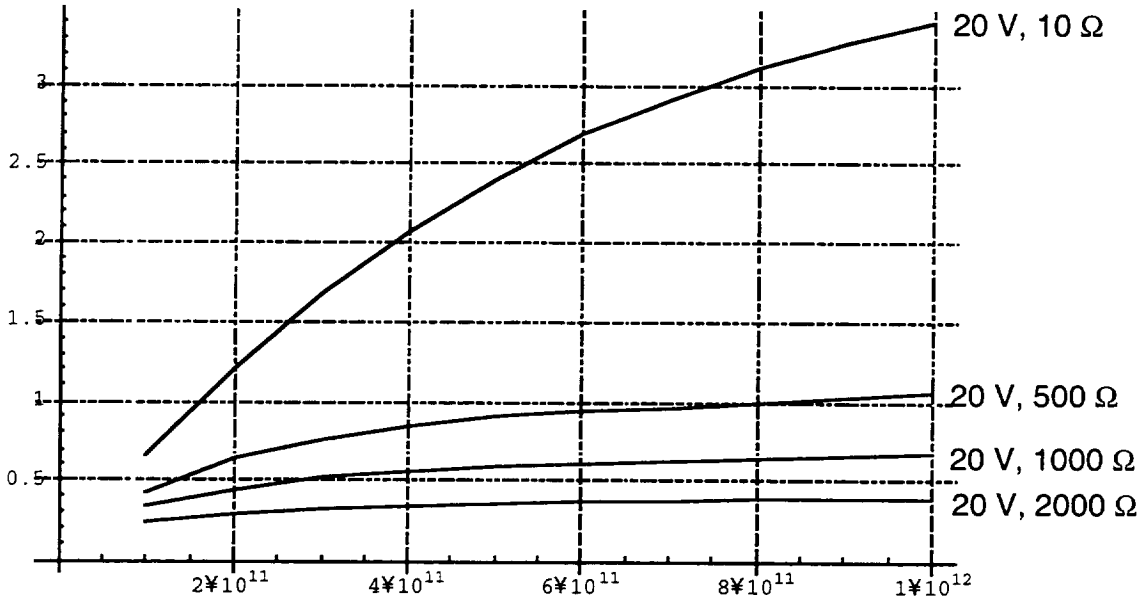

Fig. 3.2.6. Current collected for four values of series resistance. Tether current (A) shown vs plasma density (m^{-3}) for motional electric field of 0.2 V/km.

The current collected at the Delta is not the true measure of what the magnetic drag on the system will be, since this depends on the integral of the current along the tether, and is hence dependent on the average tether current. In order to estimate how long the system will stay in orbit we need the average tether current under various conditions.

Figures 3.2.7 and 3.2.8 display the average current compared to the current collected (measured) at the Delta over a range of plasma densities. The usual 5 km copper tether is assumed. A 10 Ohm impedance is assumed to be in series with the tether, and a 10 Volt negative bias with respect to plasma is assumed at Delta end. Figure 3.2.7 is for a 1 kV motional EMF, and Figure 3.2.8 is for a 500 V EMF. To obtain roughly the force in Newtons, divide the average current by 8 in Figure 3.2.7 and divide the average by 15 in Figure 3.2.8. The average current is seen to be roughly 30% less than the measured current. This is important because any limitations placed on current due to dynamics concerns must rely on measured current, when the primary dynamics effects are due to the average.

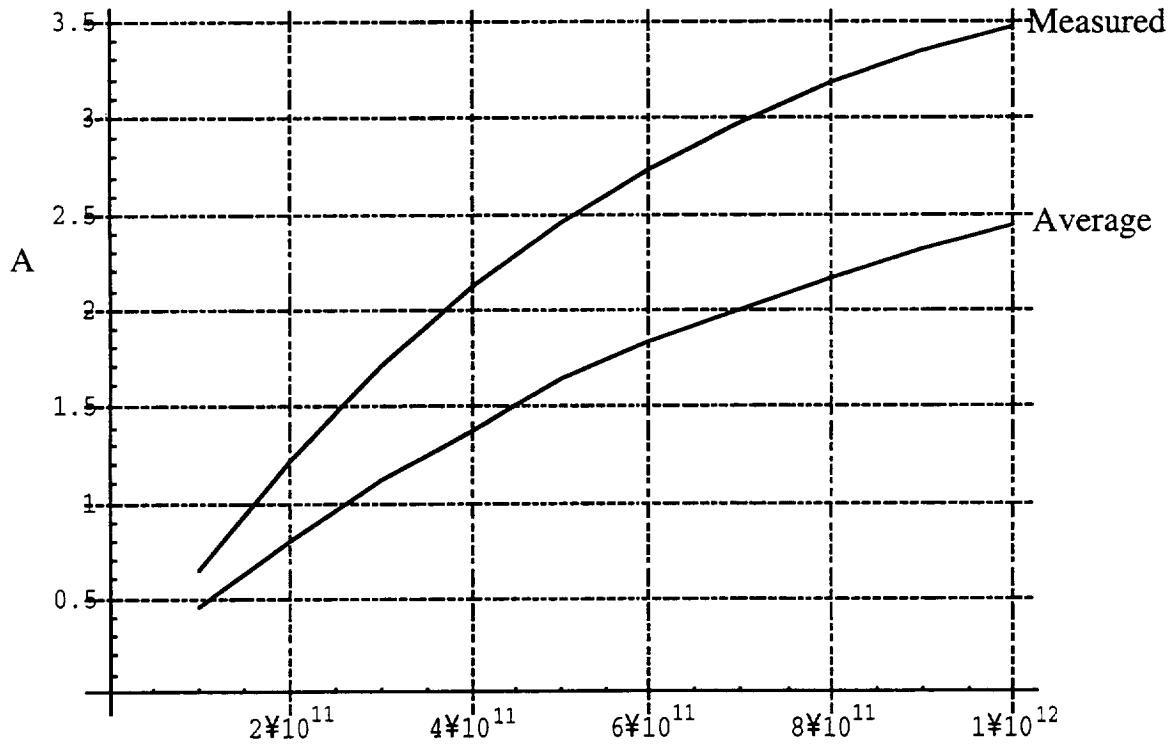

Fig. 3.2.7. Current measured at the Delta compared to average current along the tether. Tether current (A) shown vs plasma density (m^{-3}) for motional electric field of 0.2 V/km.

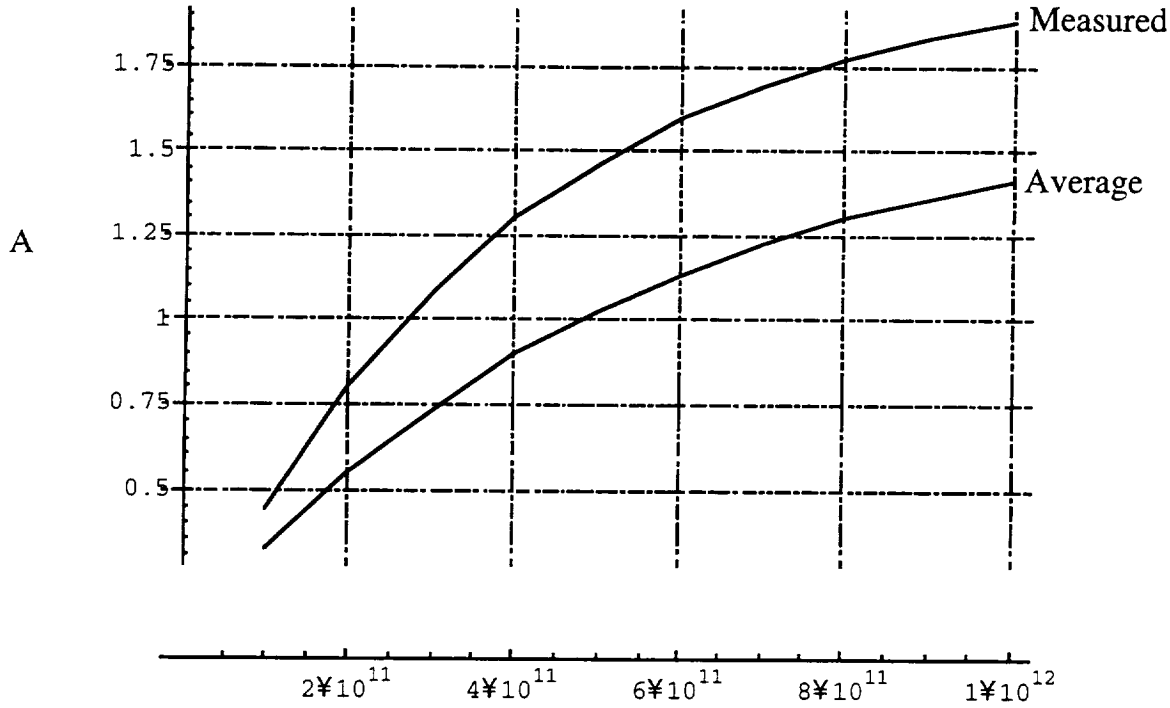

Fig. 3.2.8. Current measured at the Delta compared to average current along the tether. Tether current (A) shown vs plasma density (m^{-3}) for motional electric field of 0.1 V/km.

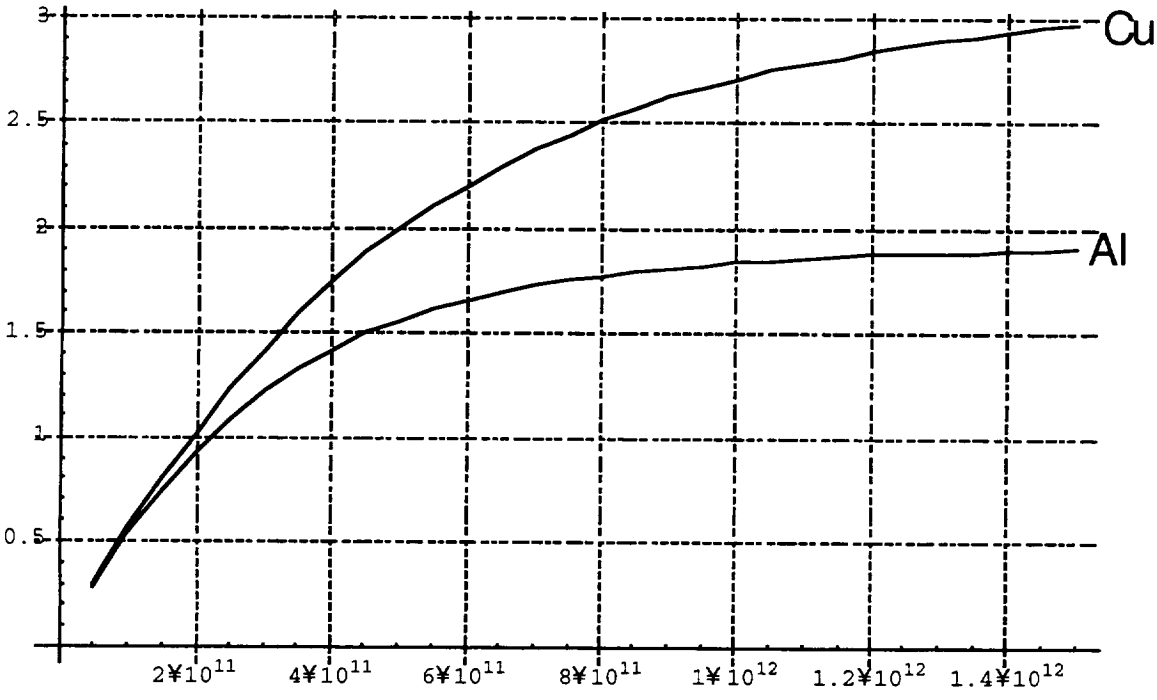

Fig. 3.2.9. Current collected for copper and aluminum tethers of equal size. Tether current (A) shown vs plasma density (m^{-3}) for 0.15-V/km motional EMF.

Another way to reduce system mass and possibly enhance deployability would be to use an aluminum tether instead of a copper one. Figure 3.2.9 shows calculations comparing the current collected by tethers made of the two materials. The size is the same as those for previously shown standard calculations. The increased resistance of the aluminum tether puts it in the constant current regime for higher plasma densities.

SAO has provided MSFC with current collection data to be used in dynamics simulations. A parallel effort to verify the coupling between dynamics and electrodynamics has been carried out using SAO and NASA/MSFC computer codes.

ProSEDS Tether Modeling

One of the ways to quantify the advantage a bare tether collector has over a TSS-1 "ball and chain" type collector, in which the wire is insulated and all collection is done by a large conductive sphere, is to compare the current collected for equal surface areas by the two types. Various figures were floating around, so SAO undertook to calculate the current for a range of electron densities. These results are shown in Figure 3.2.10. The figure reveals that the advantage of the bare tether becomes greater as the density becomes lower (and this would increase further at nighttime values). Boosting the current collected by the sphere by a factor of three (maximum factor observed in TSS-1R) over the plotted results, we still see the bare wires of equal area collecting from 6-8 times greater in the case of a 2 mm diameter and 3-5 times greater in the case of the smaller diameter of 0.7 mm. These diameters were chosen to fall within the range of those under consideration for the ProSEDS tether. They are smaller than what is envisioned for an operational system however, for which non circular cross-sections for the tether would also be likely. The trend is clearly for higher and higher differentials as the diameter of the wire increases.

The first results on bare wire collection seen in plasma chamber tests carried out at MSFC showed currents roughly 64% of Orbital-Motion-Limited (OML) current. Conditions in the plasma chamber deviate in certain significant ways from those in space. Juan Sanmartín of the Polytechnic University of Madrid and R. Estes of SAO have investigated how the maximum wire radius for which OML collection will apply varies with the ratio of electron to ion temperature. Some of their results are shown in Figure 3.2.11 where the maximum radius (in units of electron Debye length) is plotted versus the bias voltage, normalized to the electron thermal energy. For the MSFC test results, the wire radius exceeded the maximum for which OML current could have been expected by a large

factor due to the high electron to ion temperature ratio. Thus, the results are actually encouraging. The ProSEDS tether radius is well below that for which OML collection applies.

Choice of the tether conductive tether material has proved to be one of the most difficult tasks for ProSEDS. One of the earliest comparisons between Al and Cu wires made for ProSEDS is shown in Figure 3.2.12. It is clear from the figure that the Al wire, while weighing 20 lbs. less than the Cu wire can collect as much current (at the expense of some volume, however).

As tether development and analysis proceeded, it became apparent that heating might be a significant problem. While this first arose as an issue of whether the hot Al would be able to withstand periodic relatively large tension spikes that were seen to occur in simulations, it also became a concern from the standpoint of electrical resistance. Figures 3.2.13(a) and 3.2.13(b) depict results of the first calculations to show the effect of tether heating with and without an emissive coating.

Bare tether current collection compared to sphere of equal area.

Ratio of current collected by a bare tether (orbital motion limited) to that collected by a sphere of equal area (assuming Parker-Murphy limit) for 5 km tethers of 0.7 mm and 2.0 mm diameter. Cu tether assumed. End-to-end motional emf is 750 V. The 0.7 mm diameter is what we have been using for ProSEDS calculations. Magnetic field of 0.3 G and electron temperature of 0.1 eV assumed in sphere calculations.

Note that Parker-Murphy limit assumes a static collector, and TSS-1R found current collected exceeded this limit by a factor of two or more.

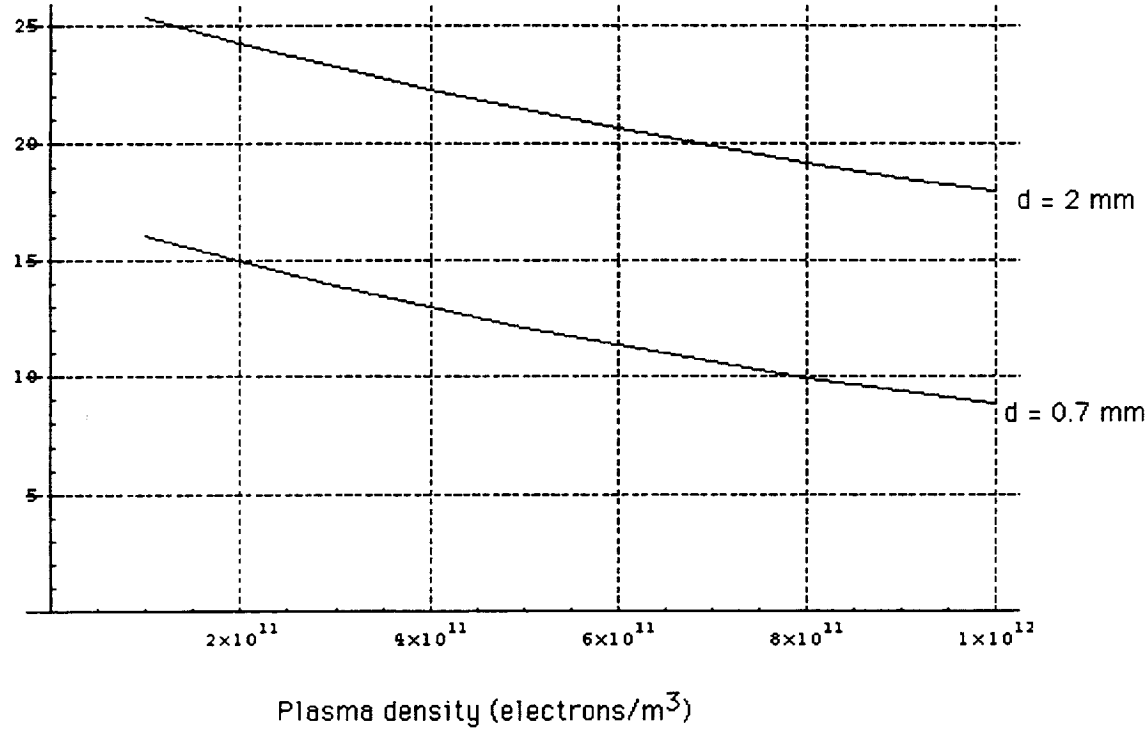

Bob Estes, SAO
8/7/97

Fig. 3.2.10. Bare tether current collection compared to sphere of equal area.

Maximum wire radius (relative to electron Debye length) for which orbital-motion-limited (OML) current collection applies is displayed here as a function of normalized bias voltage for different ratios of electron temperature to ion temperature. Magnetic field absent.

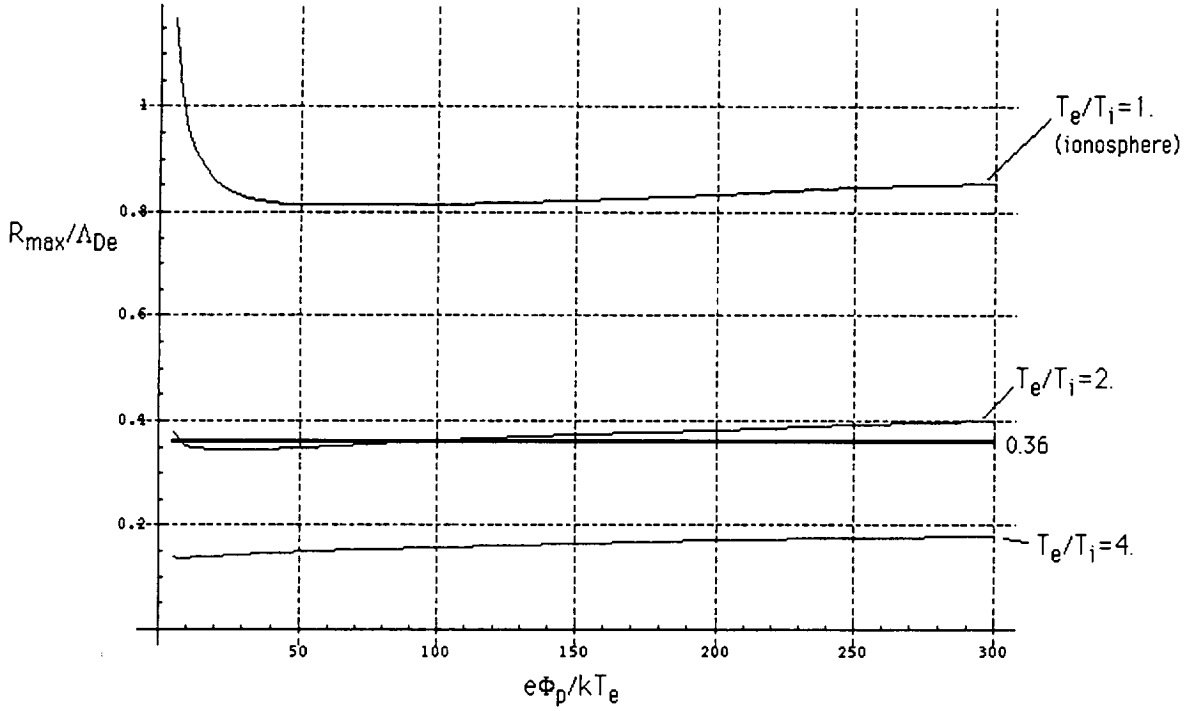

The wire radius for which OML collection applies is seen to drop with increasing T_e/T_i. The results are relevant to the last (April) plasma chamber tests conducted by MSFC on bare wire collection. In those tests, the temperature ratio was something like 10., while the ratio of the wire radius to the electron Debye length was about 0.36. Thus the wire radius substantially exceeded the maximum for which OML collection could be expected. Even so, the current collected was roughly 64% of OML with no applied magnetic field. Details of the calculation will be presented at the upcoming TIM in September.

Juan Sanmartin, UPM/SAO
Bob Estes, SAO
8/19/97

Fig. 3.2.11. Maximum wire radius for which the OML current collection applies.

Comparison of current collection of two 5 km wires:

(1)Aluminum wire (in red) with diameter 0.9 mm. R = 225 ohms, M = 8.6 kg.
(2) Copper wire with diameter 0.714 mm. R = 208 ohms, M = 17.9 kg.

Current (A) measured at Delta plotted versus electron density in electrons/m^3 for two end-to-end emf values (500 V and 1000 V).

Conclusions: We can get comparable current from Al wire of somewhat larger diameter than the previously considered Cu wire, while saving 9.3 kg (20.5 lbs). Increased collecting surface roughly compensates for slight increase in resistance.

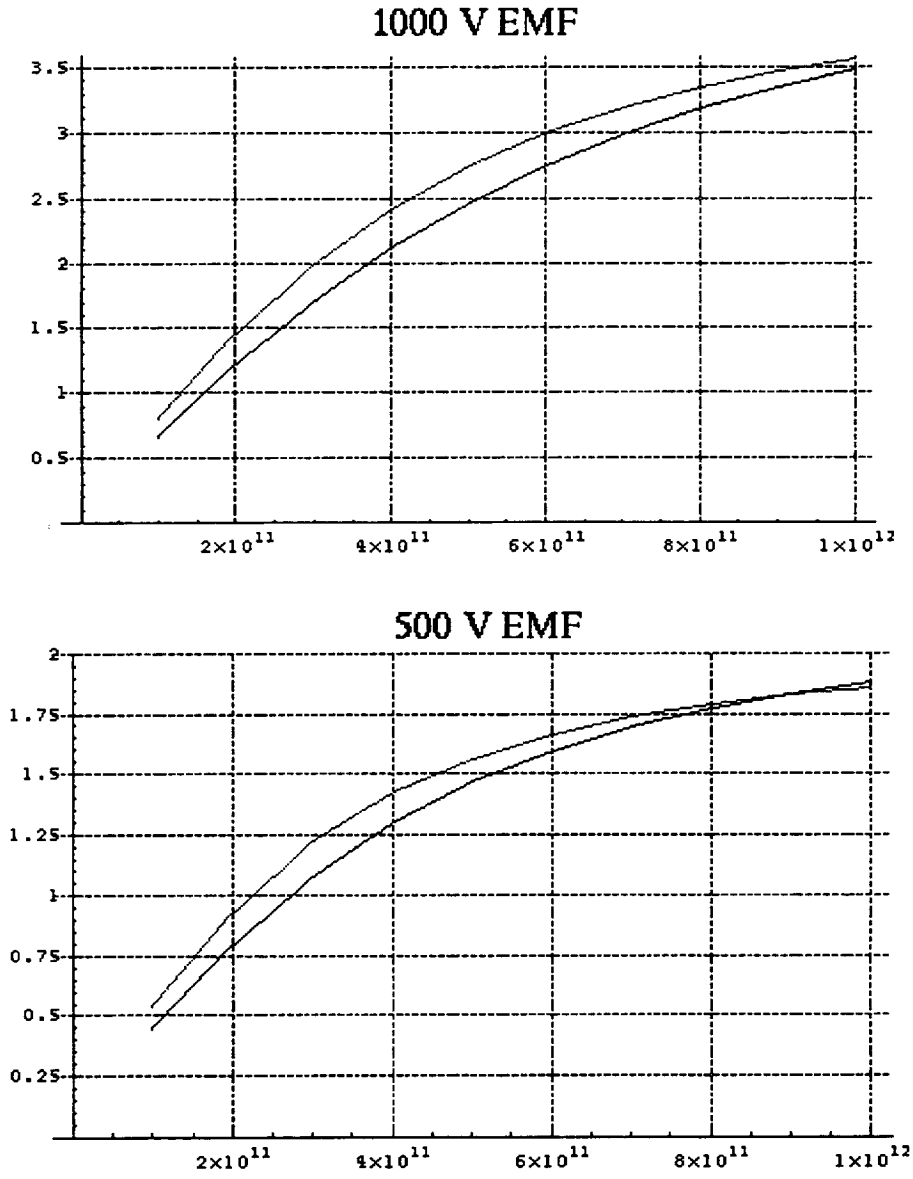

Bob Estes, SAO
8/20/97

Fig. 3.2.12. Comparison of current collection of two 5-km wires of different materials.

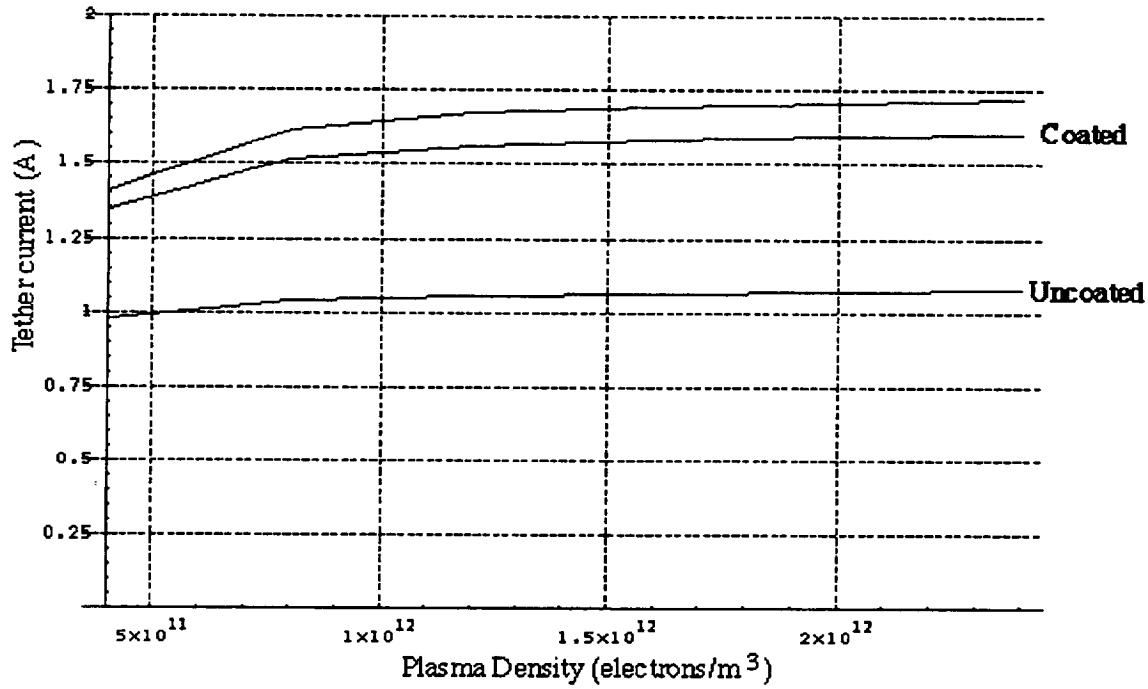

Fig. 3.2.13(a). Tether current vs. plasma density for coated and uncoated Al wires for EMF = 500 Volt (the top curve is the benchmark case of a 265-ohm constant resistance wire).

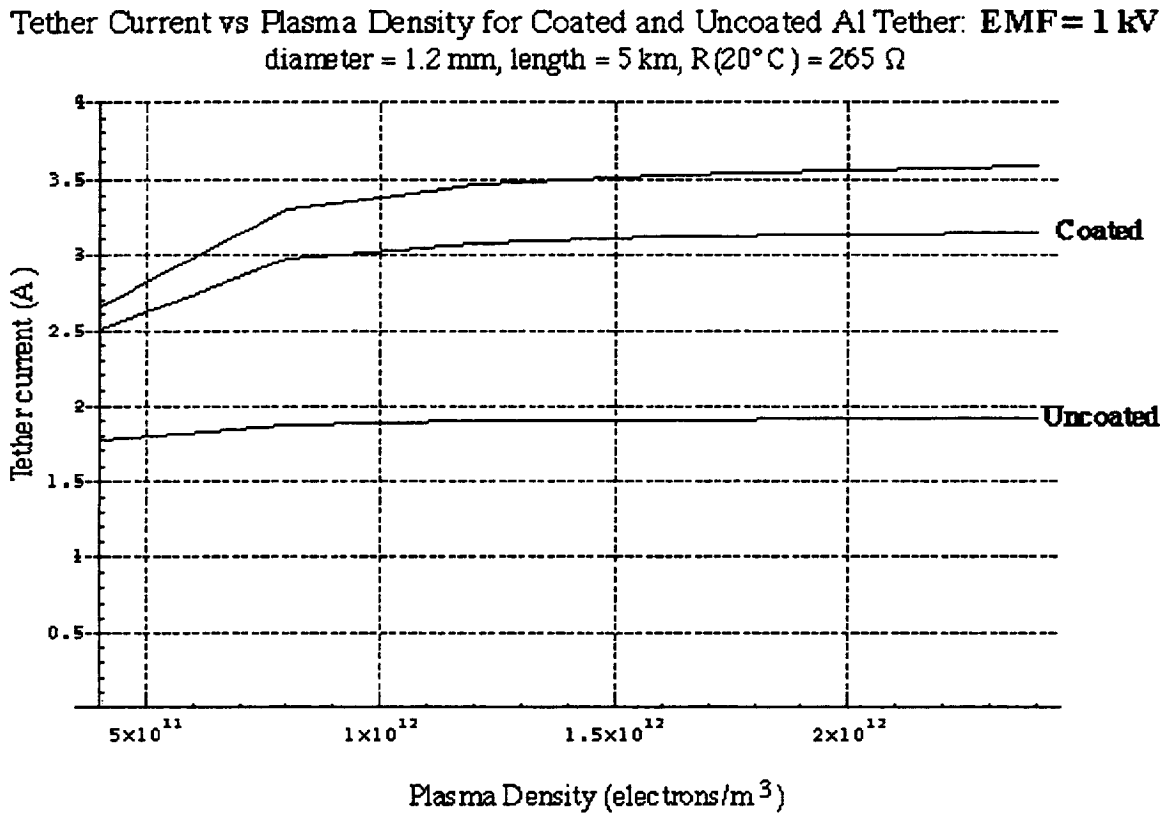

Coated tether: $\alpha = 0.95$, $\varepsilon = 0.8$; T = 52-61° C; R = 294-302 Ω
Uncoated tether: $\alpha = 0.14$, $\varepsilon = 0.03$; T = 263-279° C; R = 485-499 Ω
Solar flux = 1350 W/m^2

Bob Estes, SAO
4/27/98

Fig. 3.2.13(b). Tether current vs. plasma density for coated and uncoated Al wires for EMF = 1000 Volt (the top curve is the benchmark case of a 265-ohm constant resistance wire).

3.3. ProSEDS Dynamics

Introductory Remarks

ProSEDS exhibits features that are unlike any other space vehicle for what concerns the strong coupling among dynamics, electrodynamics and thermodynamics of the system. In fact, the tether temperature changes significantly the electrical conductivity of the wire that, in turn, affects the tether current and, consequently, the dynamic of the system. The dynamics itself couples into the current collection ability through changes in the tip-to-tip EMF acting on the tether and, through the Joule heating, into the tether temperature.

Consequently, the accurate simulation of ProSEDS requires a computer code that combines dynamics, electrodynamics and thermodynamics of the system. Our tether system simulation code at SAO has all these features. It combines an electron collection model in the orbital-motion-limited (OML) regime with a lumped-mass dynamic model of the system and a thermal model of the tether. It also has an IRI95 model of the ionosphere, a MSIS86 model of the atmosphere, an IGRF model of the magnetosphere and a $J_0 + J_2$ model of the Earth's gravity field. The thermal model of the tether takes into account all the relevant thermal flows in and out of the tether as follows: Sun's solar illumination (with eclipses), Earth's albedo and IR radiation, ohmic heating and emitted radiation. Once the tether temperature is computed along the tether, the temperature at the tether attachment to the Delta stage (where the current is maximum) is utilized to determine the wire effective resistance and compute the current collected from the ionosphere.

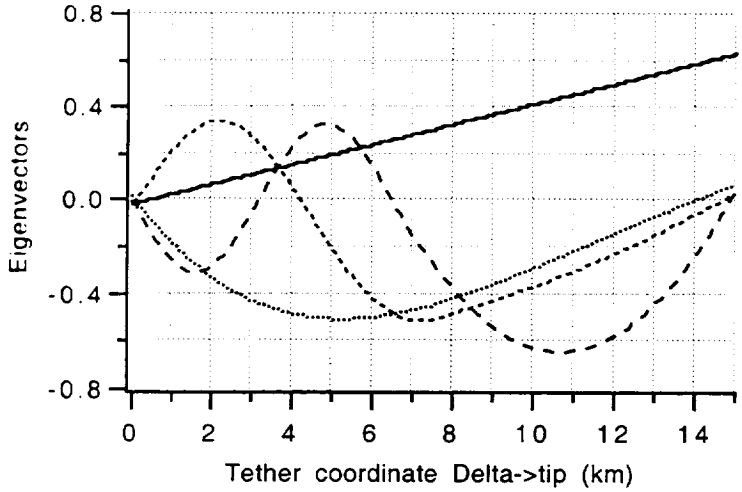

Fig. 3.3.1. Shape of first 4 eigenvectors (lateral dynamics).

Table 3.3.1. First 12 eigenvalues of ProSEDS (linearized system).

No.	Freq. (mHz)	Freq. (f=orb. freq)	Period (s)	Type
1	0.317	$\sqrt{3}$f	3156	In-plane librat.
2	1.32	7.2f	759	1st in-plane lat.
3	2.99	16.3f	335	2nd in-plane lat.
4	3.82	20.9f	262	3rd in-plane lat.
5	0.366	2f	2732	Out-plane librat.
6	1.33	7.3f	752	1st out-plane lat.
7	2.99	16.3f	335	2nd out-plane lat.
8	3.82	20.9f	262	3rd out-plane lat.
9	20.0	109f	50	1st longitudinal
10	81.3	455f	12.3	2nd longitudinal
11	185.1	1012f	5.4	3rd longitudinal
12	238.1	1301f	4.2	4th longitudinal

The first 12 eigenfrequencies of ProSEDS (linearized system) are shown in Table 3.3.1. Figure 3.3.1 shows the shape of the first 4 eigenvectors for the lateral dynamics. In-plane and out-of-plane eigenvectors have the same general shape that is dictated by the different linear densities of the aluminum wire and the spectra tether. The librational eigenvectros are rectilinear and independent of the tether density distribution. The 1st and 2nd lateral (string-like) modes play an important role in ProSEDS dynamics as shown later on in this report.

Current operating modes[1]

The current is controlled according to duty cycles that repeat themselves throughout the mission duration. Two duty cycles are adopted during the mission. The first one is the primary battery duty cycle that is utilized only during the first 3 orbits when the system is powered by the primary batteries. The second one is the secondary battery duty cycle that is utilized after the first 3 orbits till the end of the mission. The battery duty cycles are shown in Figs. 3.3.2(a) and 3.3.2(b):

[1] Contributed by NASA/MSFC.

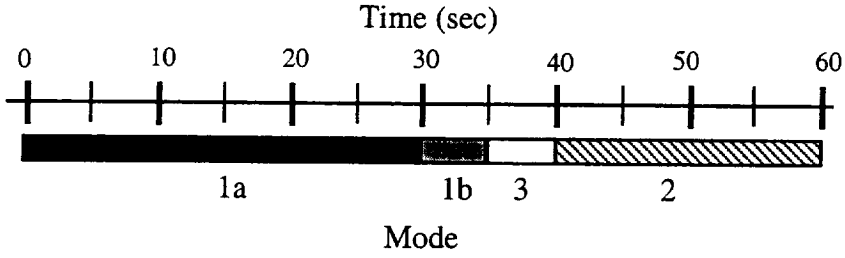

Fig. 3.3.2(a). EPT Sequence 1 (60-sec cycle) - Operation on Primary Battery.

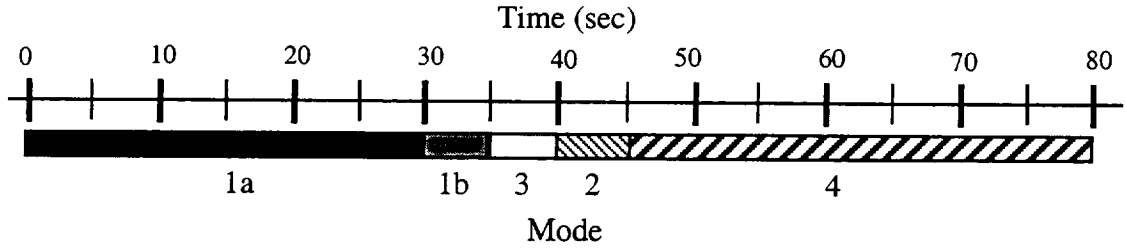

Fig. 3.3.2(b). EPT Sequence 2 (80-sec cycle) - Operation on Secondary Battery.

Mode 1a is open circuit, plasma contactor OFF
Mode 1b is open circuit, plasma contactor ON
Mode 2 is SHUNT mode
Mode 3 is RESISTOR mode
Mode 4 is BATTERY CHARGE mode

EPT Sequence 1 is for primary battery use only (first 3 orbits).

Numerical Results

A number of simulations have been carried out to analyze the response of ProSEDS under different conditions and assumptions. The changes in the system dynamics as a function of the tether electrical resistance and also depending on whether or not the resistance is assumed constant or varying with the temperature is of particular interest. Figures 3.3.3(a)-3.3.3(d) show the response of a bare (without any coating) aluminum wire with an electrical resistance of 265 ohm at 20 °C. The wire is actually made of 7x28 AWG aluminum strands wrapped around a kevlar core according to the present tether configuration (see next section of this report). The ballast tether in these simulations is assumed to be spectra-2000.

The following simulations were run with the current controlled by the secondary-battery duty cycle throughout the duration of the simulation.

One more comment, in the simulations shown here the current along the tether is modeled as follows: the value of the current at each lump location is assigned to the lump. Another option is to assign the average value of the current in the tether segment to each tether lump. The former discretization provides a more accurate estimate of the tether current at the Delta stage but it leads to a slight overestimate of the average current along the wire that, in turn, determines the system decay rate. Decay rates obtained by using the tether current point values (as used in the following simulations) are overestimated by about 14%. We will utilize either discretization in future work depending whether more accuracy is required in the current estimate at the Delta stage or in the decay rate.

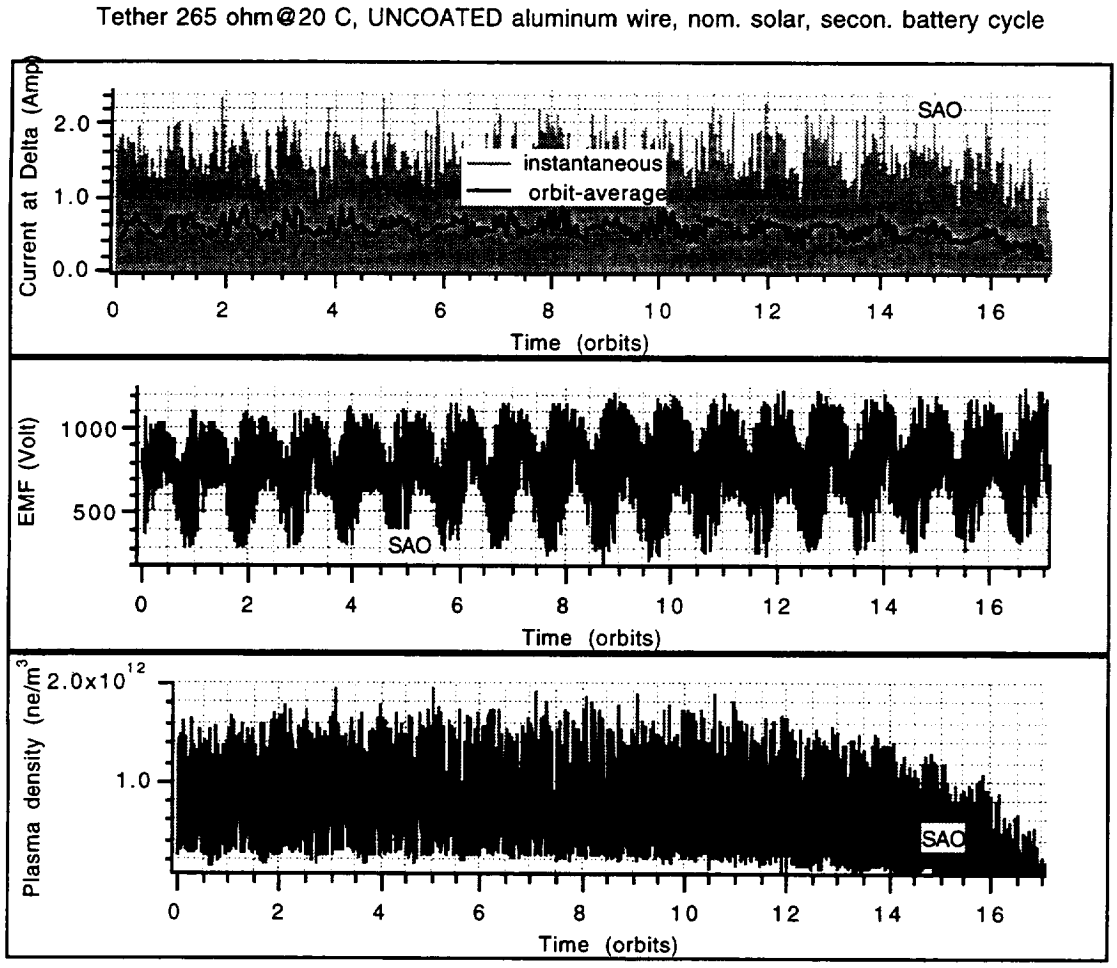

Fig. 3.3.3(a). Simulation of ProSEDS with 265-ohm (at 20°C) bare aluminum tether.

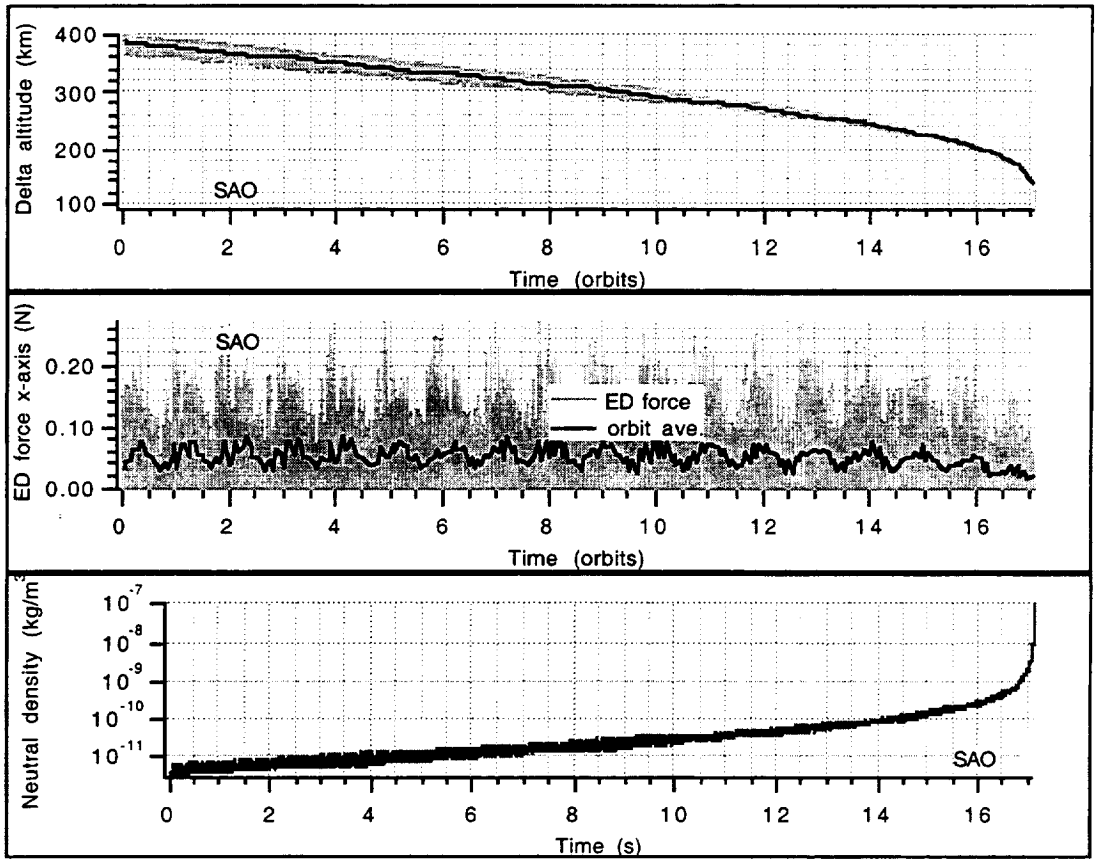

Fig. 3.3.3(b). Simulation of ProSEDS with 265-ohm (at 20°C) bare aluminum tether.

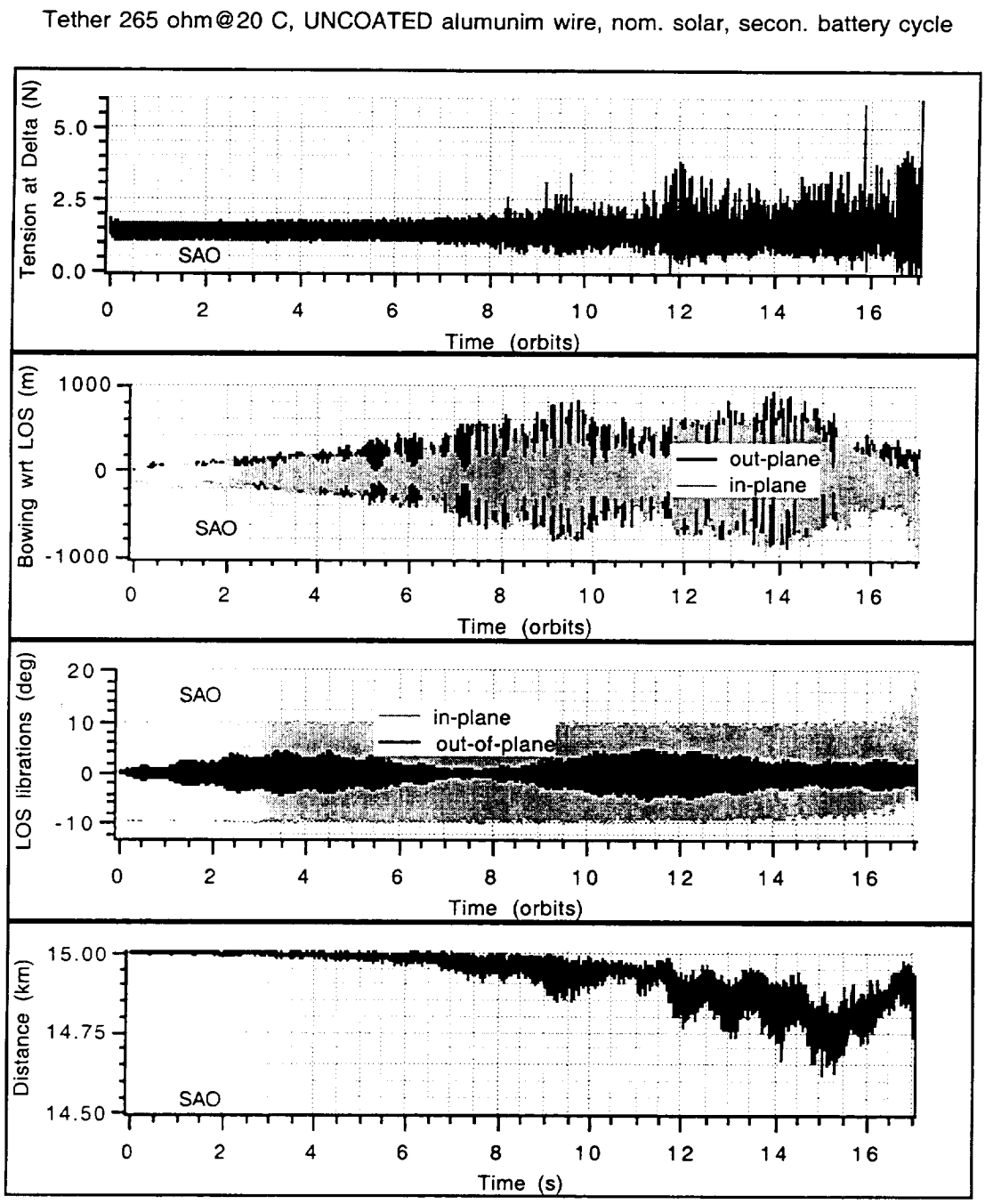

Fig. 3.3.3 (c). Simulation of ProSEDS with 265-ohm (at 20°C) bare aluminum tether.

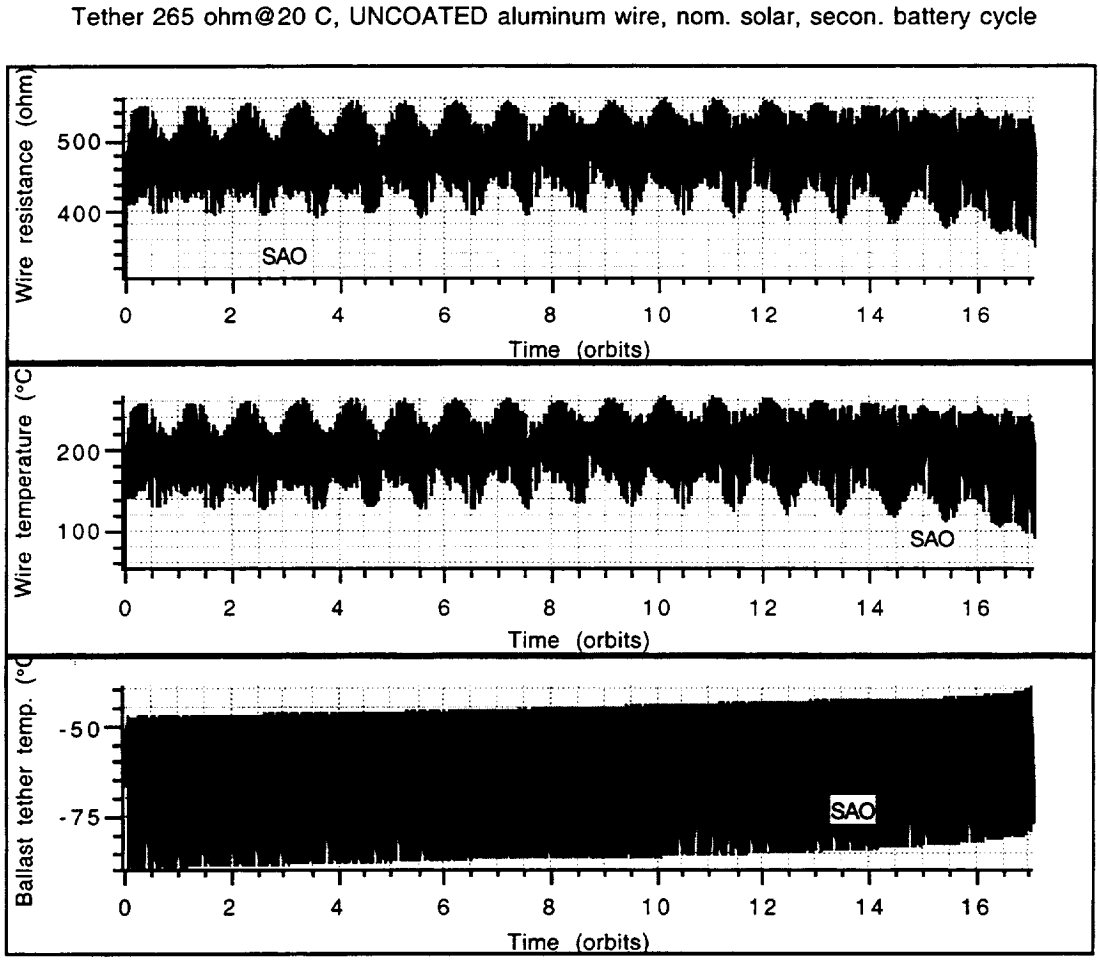

Fig. 3.3.3(d). Simulation of ProSEDS with 265-ohm (at 20°C) bare aluminum tether.

Table 3.3.2. Thermal optical properties of candidate tether materials[2]

Sample Description	Initial Solar Absorptance (α)	Initial Infrared Emittance (ε)	α/ε
Copper Foil-99.998% Pure	0.298	0.033	9.03
Aluminum Foil (1856 Alloy) Dull Side	0.115	0.034	3.38
Aluminum Foil (1856 Alloy) Shiny Side	0.140	0.018	7.78
Alodined Aluminum Foil (1856 Alloy) Dull Side	0.346	0.040	8.65
Alodined Aluminum Foil (1856 Alloy) Shiny Side	0.351	0.030	11.70
Aluminum Foil w/ C-COR (87%/13% PANi)	0.91	0.8	1.14
Aluminum Foil w/ 100% PANi	0.91	0.41	2.22

The relatively high tether temperature is a result of the high absorptivity/emissivity ratio (α/ε) of bare metals like aluminum and copper. In order to mitigate this problem, techniques were investigated for reducing the α/ε ratio of bare metals while preserving the ability to collect electrons. Various surface treatments and coatings were explored and the optical characteristics measured by Jason Vaughn at the EL Laboratory of NASA/MSFC as shown in Table 3.3.2.

As shown in the table, the alodine treatment worsened the optical ratio while the best results from the optical (and thermal) point of view were obtained with a polymer-based coating (developed by Triton Systems) doped with polyaniline (PANi) to give the coating electrical conductivity. The results are shown in the table at the entries C-COR/13%-PANi and 100%-PANi.

Figure 3.3.3(d) clearly shows that the wire temperature is relatively high ranging between 130 °C and 270 °C. The high temperature has two undesirable effects: (1) it

[2] Contributed by Jason Vaughn of NASA/MSFC

weakens the aluminum and the load-carrying kevlar core and (2) it increases the electrical resistance (that depends on the temperature) and, consequently, reduces the tether current.

Figures 3.3.3(a)-3.3.4(d) show the results of a simulation in which the conductive tether was coated with the 100% PANi (see previous table for the optical properties of the coating). The 100% PANi is attractive from the point of view of electron collection because it is perfectly transparent to the electrons (i.e., no voltage losses across the coating thickness). However, it is not very durable which may create problems during deployment. For this reason, other coating mixtures with less dopants will be developed by the coating manufacturer for use in ProSEDS.

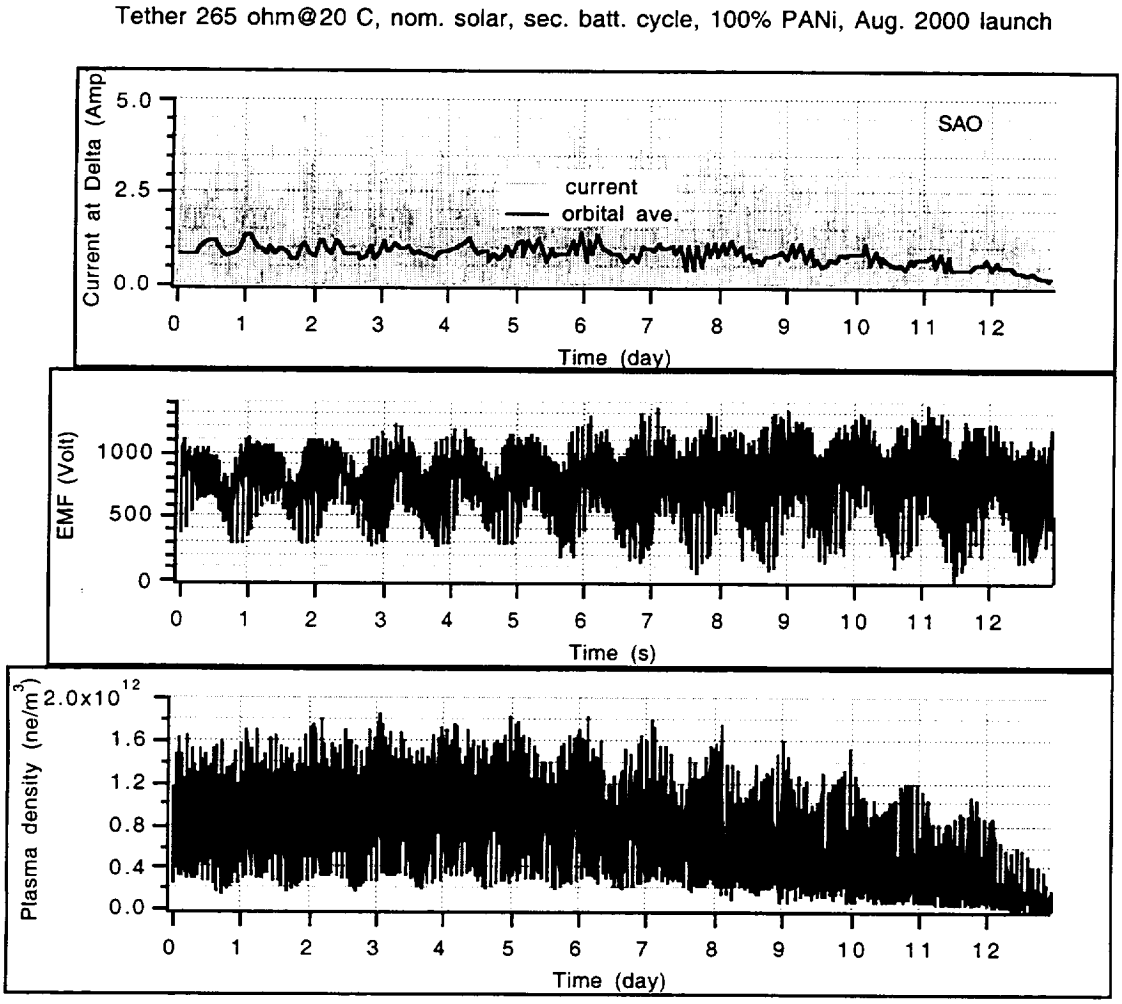

Fig. 3.3.4(a). Simulation of ProSEDS with 265-ohm (at 20°C) aluminum tether coated with a 100% PANi without collection losses.

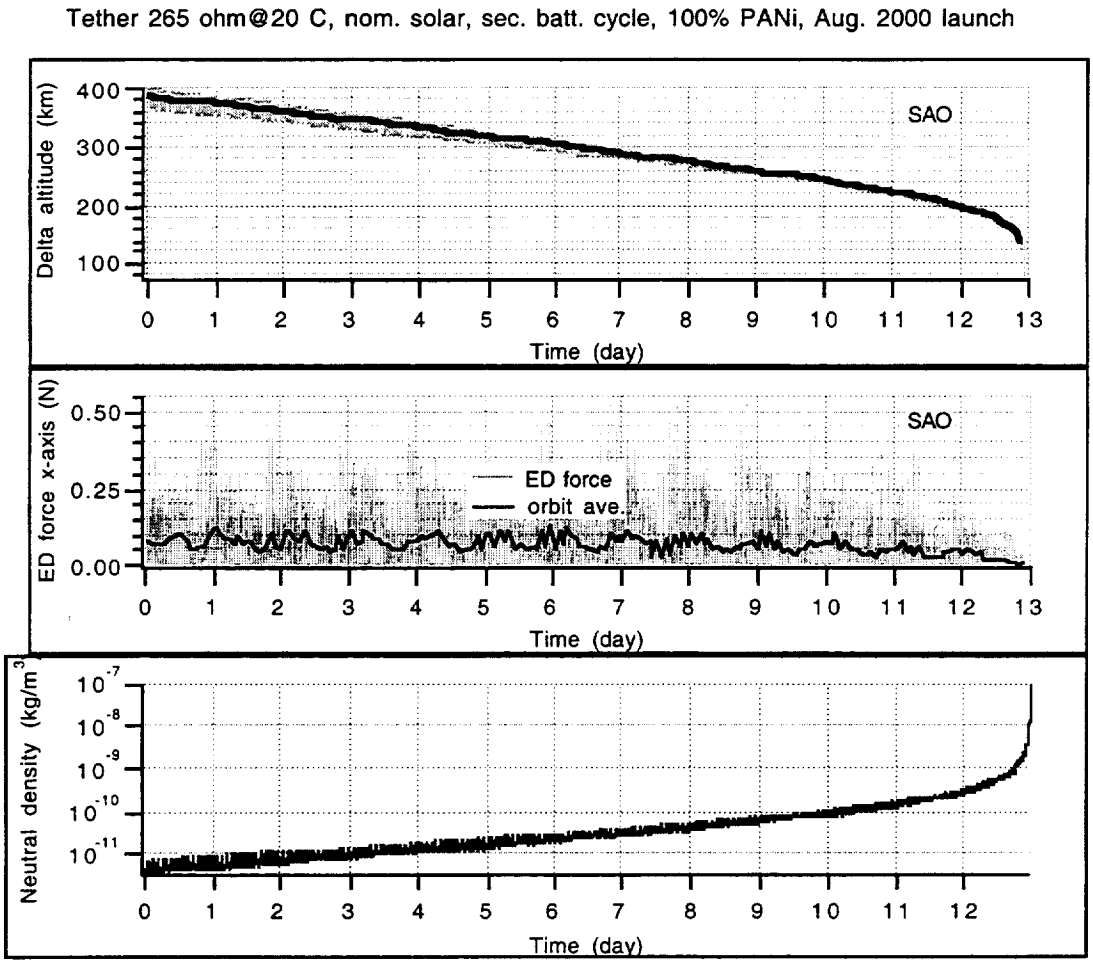

Fig. 3.3.4(b). Simulation of ProSEDS with 265-ohm (at 20°C) aluminum tether coated with a 100% PANi without collection losses.

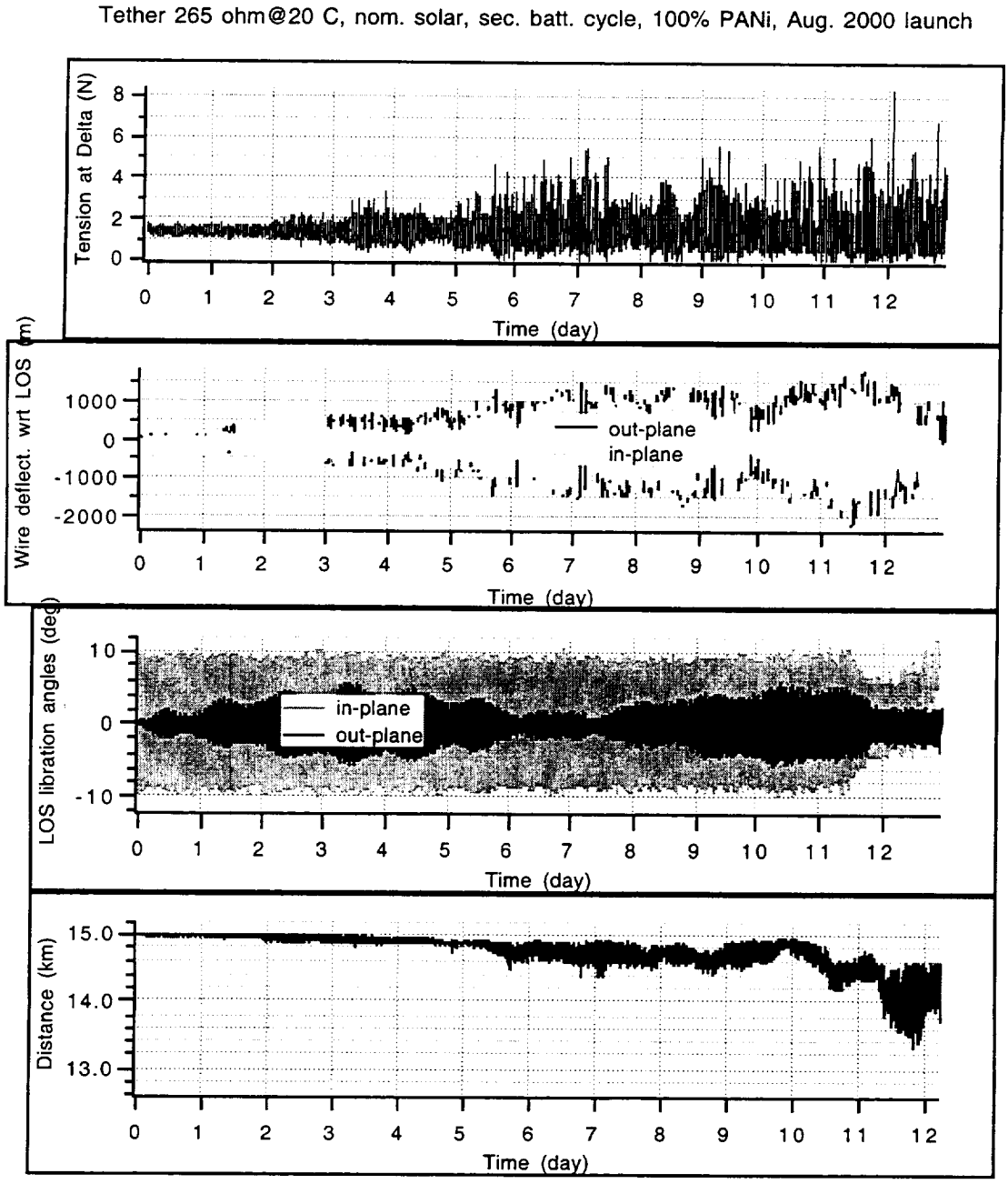

Fig. 3.3.4(c). Simulation of ProSEDS with 265-ohm (at 20°C) aluminum tether coated with a 100% PANi without collection losses.

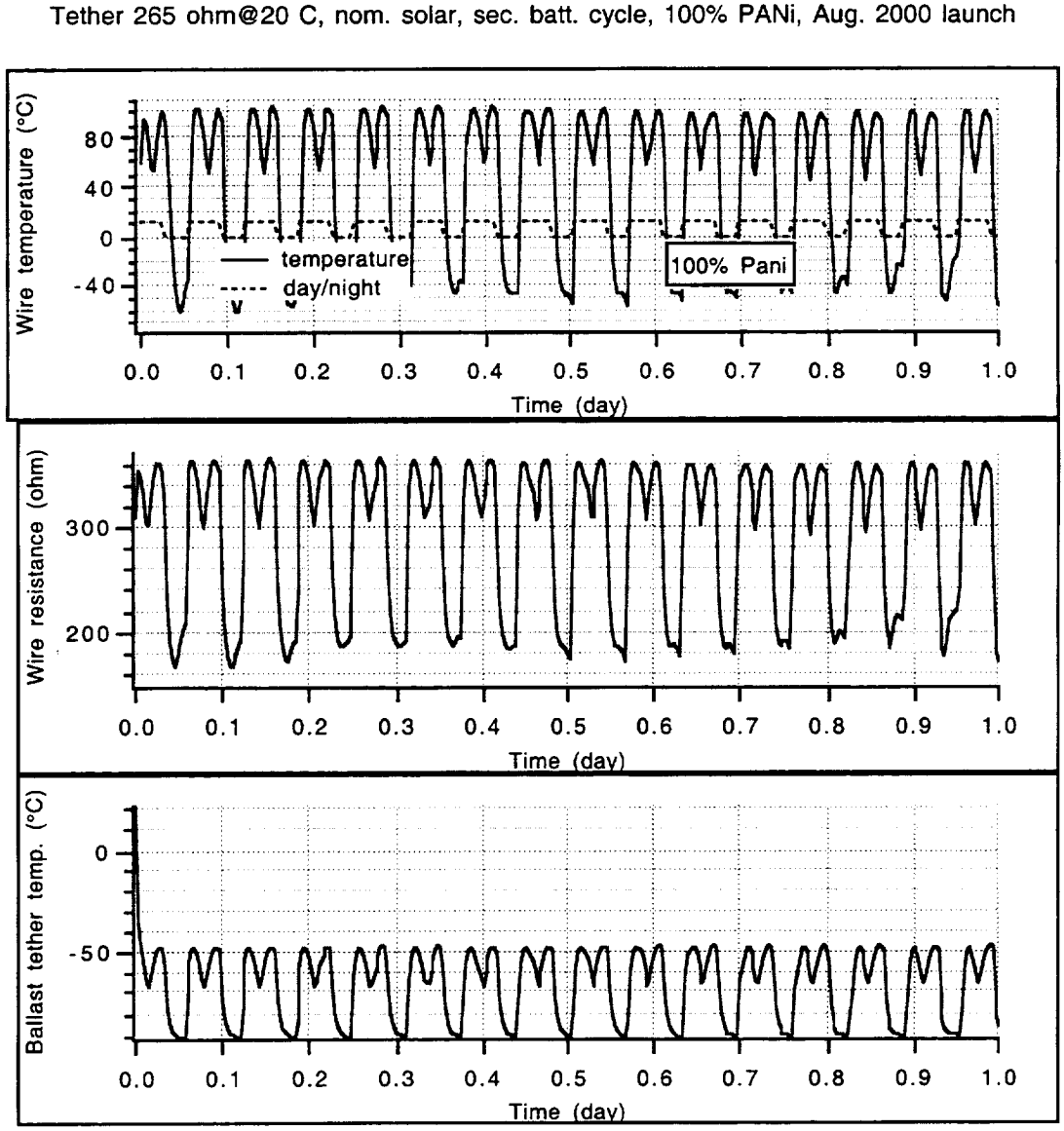

Fig. 3.3.4(d). Simulation of ProSEDS with 265-ohm (at 20°C) aluminum tether coated with a 100% PANi without collection losses.

At this point, it is interesting to isolate the effect of the changing tether temperature upon the tether current and the system dynamics. To this aim, we ran a simulation with the same system parameters adopted to derive Figures 3.3.4 but assuming (unrealistically) that the tether temperature stays constant at 20 °C. Key results of this simulation are shown in Figure 3.3.5.

We can now conclude that the system thermodynamics and its interaction with the current can not be neglected in the analysis of ProSEDS. The inclusion of the thermal model of the tether has actually a beneficial effect on the system dynamics. The tether current, in fact, becomes more uniform during the day/night cycles thanks to the decrease of temperature and electrical resistance during the night that compensates for the decrease in plasma density. Consequently, the 1-Ω (with Ω = orbital rate) spectral component of the tether current (related to the plasma density variation in the day/night cycle) is reduced and the dynamic stability of the system increases. This effect is apparent after comparing the relevant plots of the tether tension and the tip-to-tip distance shown in Figure 3.3.5. A strong reduction of the tip-to-tip distance (of the order of a km or more) is a clear indication of a significant tether skip-rope which can produce sizable tension spikes when it grows too large forcing a series of tether slacks and rebounds.

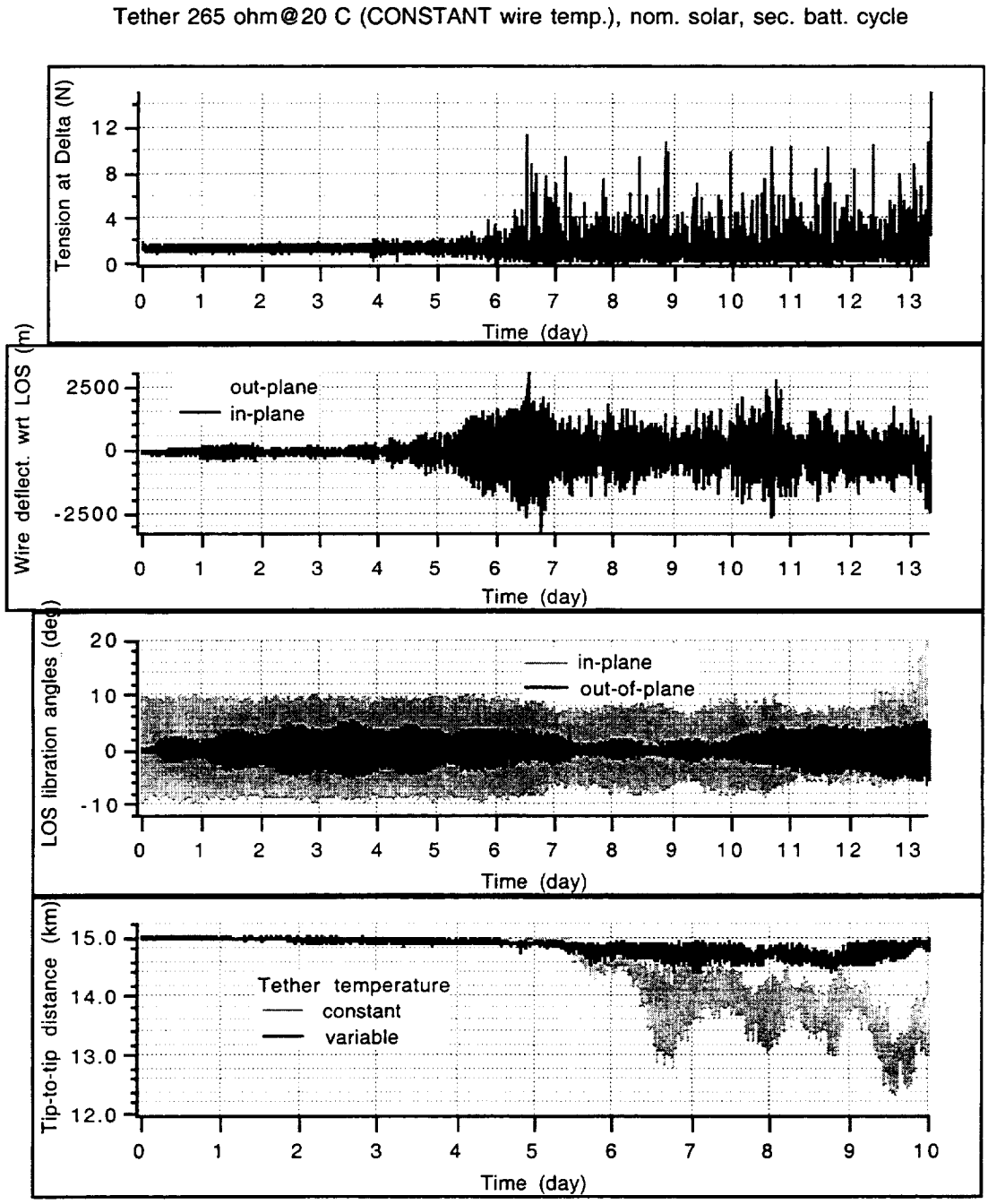

Fig. 3.3.5. Simulation of ProSEDS with a CONSTANT 265-ohm aluminum tether coated with a 100% PANi without collection losses. The last plot shows also the tip-to-tip distance for variable tether temperature.

The thermal balance of the tether plays a significant role in the dynamics of the system and its performance. Bare aluminum and copper have very high absortivity/emissivity (α/ε) ratios. Typical values are α/ε = 7-9 which would force the bare tether to run at a temperature ranging between 270 °C in daylight and 130 °C in eclipse conditions. Because of the dependency of electrical resistance on temperature, a purely bare tether would be subjected to strong current variations as the system moves around the orbit. In addition, the increase of electrical resistance during day conditions causes increased ohmnic losses and decreased performance.

The actual ProSEDS tether is a composite of a kevlar core for mechanical strength and 7x28AWG aluminum wires for electrical conductivity. The aluminum wires are coated with a newly developed conductive coating which provides a ratio α/ε ranging between 1-2 while maintaining good electrical contact with the plasma. The optical properties (absortivity and emissivity) of the wires play an important role in the performance of the system. Figure 3.3.6 shows the decay rate (over a week) for purely bare aluminum wires (α/ε = 8), coated aluminum (α/ε = 2) and an imaginary coating that mimics the optical properties of spectra (α/ε = 0.2).

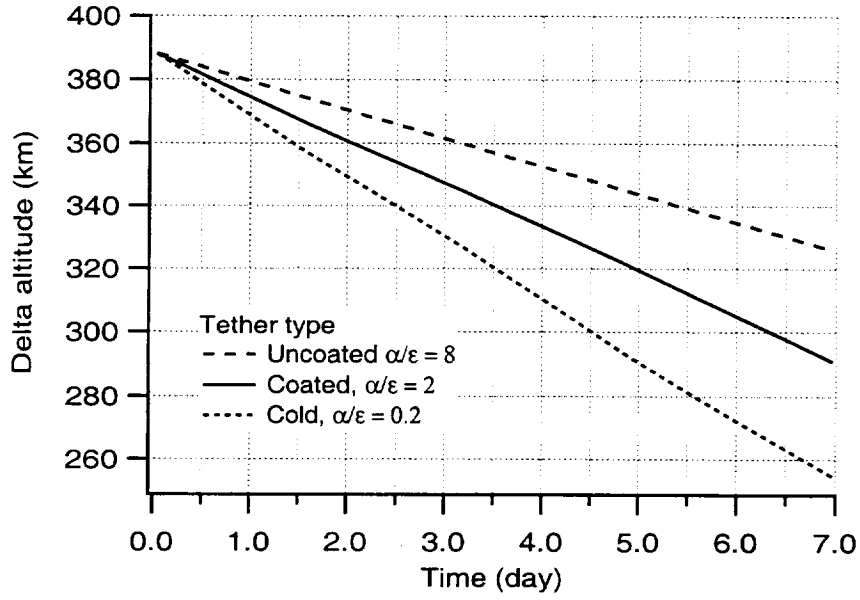

Fig. 3.3.6. Altitude vs. time during 1 week for tethers with various optical ratios.

Figure 3.3.7 shows the frequency spectrum of the electrodynamic force for two cases with constant and variable tether temperatures. The electrodynamic force is the dominant driving term of the system dynamics and its frequency content is analogous to that of the tether current (on which it depends). The spectrum shows a daily component, due to the rotation of the magnetic field, and a group of strong low-frequency components between f and 3f. There are no significant components at the frequency of the 1st and 2nd lateral modes (7.2f and 16.3f, respectively).

The variable temperature smoothes out in part the low-frequency components of the current (see Fig. 3.3.7). Figure 3.3.8 shows the spectrum of the out-of-plane lateral dynamics of the tether, measured at the mid point of the tether where the eigenvectors of interest have large displacements, with respect to the local vertical for constant tether temperature (when the skip rope is stronger). The in-plane dynamics has a similar spectrum except for a component $\sqrt{3}$f replacing the 2f component. Clearly, it can be concluded from Fig. 3.3.8 that a large portion of the energy ends up into the the higher-frequency modes even if the external excitation is at low frquency.

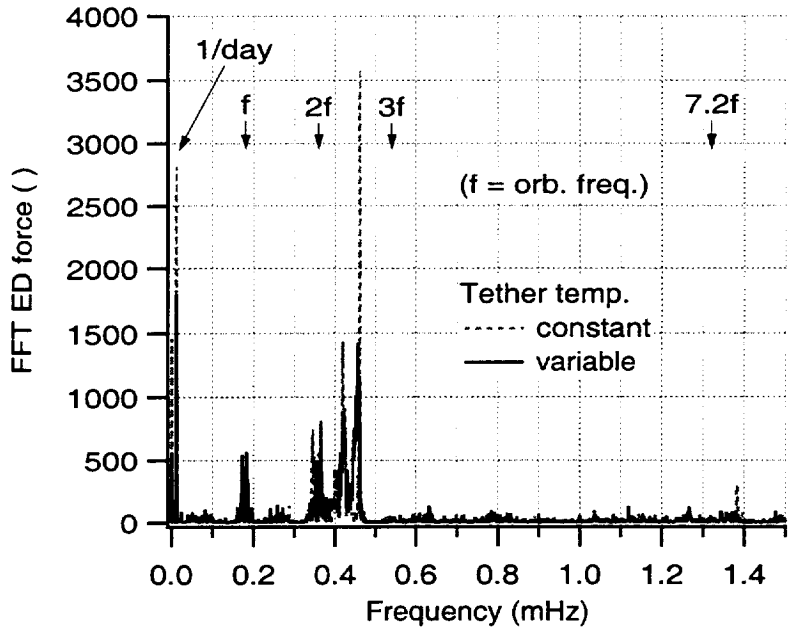

Fig. 3.3.7. FFT of electrodynamic force for constant and variable tether temperature.

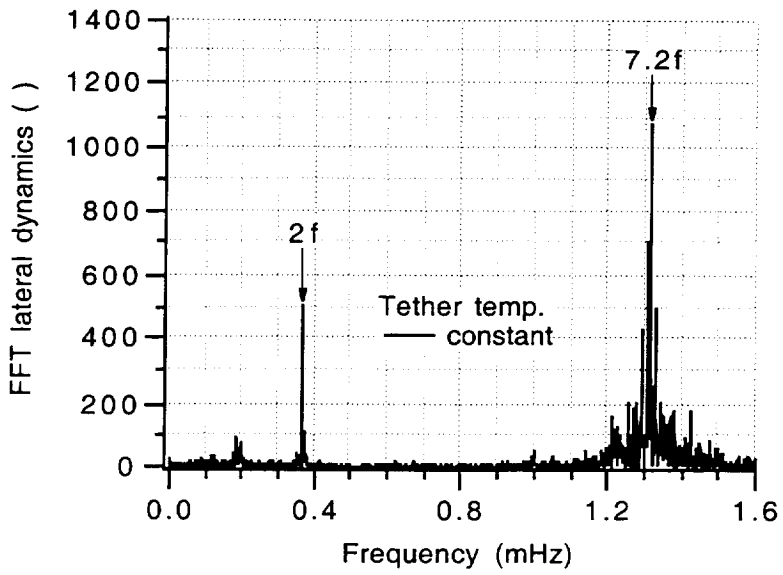

Fig. 3.3.8. FFT of lateral dynamics (mid-tether) with respect to LV.

The 1st and 2nd lateral mode frequencies in ProSEDS are roughly one order of magnitude higher (7.2f and 16.3f) than the orbital frequency and, consequently, force components between the orbital and three times the orbital frequency do not resonate with its natural frequency. The mechanism that connects the low-frequency components of the electrodynamic force to the amplification of the tether skip rope (at much higher frequency) is not obvious and not yet fully understood by us. Further analyses with simplified models are underway to try to understand the basics of this destabilizing mechanism.

Concluding Remarks

The accurate simulation of ProSEDS requires the combination of dynamics, electrodynamics and thermal models of the tether. The interplay among dynamics, electrodynamics and thermodynamics is crucial in explaining the performance of a system like ProSEDS. The changing tether temperature and, consequently, electrical resistance of the wire has a positive effect on the current profile over the day/night cycles and ultimately on the dynamics stability of the system.

Another important conclusion of the analysis conducted above is that an uncoated metal wire would attain high maximum temperatures that are strongly undesirable from the points of view of system performance and mechanical strength of the tether. Consequently, the α/ε (absorptance/emittance) ratio of the metal wire must be decreased (while preserving its

ability to collect electrons) by using appropriate coatings or other suitable techniques with the final goal of keeping the temperature of the wire well below (roughly-speaking) 100 °C.

The present estimate of the orbital decay rate during the first week of the mission is about 12 km/day (after correcting for the overestimate due to the tether current discretization adopted) with the present wire configuration coated with the 100% PANi coating (no collection losses). Coatings with collection losses different from zero will produce decay rates smaller than indicated above. Coatings with α/ε ratios lower than 2 and negligible collection losses will produce higher decay rates than indicated above.

3.4 ProSEDS Deployment

In addition to collecting high currents, ProSEDS must first deploy successfully and then show an orbital decay rate much greater than a satellite without an ED tether.

Deployment control

The non-linear deployment control law that deployed successfully SEDS-II (see Refs. 2-4) was adopted for ProSEDS deployment. The control law developed for the SEDS deployer follows the strategy of input-output linearization in order to eliminate the strong non-linearities associated with the SEDS deployer and the system dynamics. A set of deployment profiles (solutions of the non-linear equations) were derived for the deployed length, length rate and brake actuation under reference conditions. These reference profiles are stored in the SEDS on board computer. The control law, then, adjusts the brake actuation with a locally-linear feedback law based on the deployed length and rate errors with respect to the respective reference profiles. In other word, the control law tries to keep the deployment on the established deployment schedule by controlling the brake. The result is a robust control law that is accurate and highly tolerant of the large uncertainties affecting the parameters that characterize the deployer friction model (see Ref. 4). The most important parameter in the deployer model is the deployer minimum tension T_{min} which is highly uncertain but it must be guaranteed to be below a critical value for mission success as explained later on.

Unlike in SEDS-II, in ProSEDS the control law is inactive during the deployment of the wire (i.e., the last 5-km of tether) when the brake is fully open. This is because of the worry that debris from the conductive wire may jam the delicate brake mechanism. The final performance, in terms of residual libration, of ProSEDS can not therefore match the flight performance of the SEDS-II control law with a residual libration amplitude smaller than 4°. ProSEDS final libration will likely be in the 10°-20° range but the feedback law will be able to provide an adequate level of robustness with respect to variations of the tether friction parameters.

It is important to remark that in the following simulations, the minimum tension for the non-conductive tether is equal to 20mN that was the flight value of the SEDS-II tether. Tethers different from the SEDS-II tether will most likely have a different value of the minimum tension. The control law can tolerate without a significant decay in performance a value of the non-conductive tether minimum tension as follows: $5\ mN < T_{min} \leq 30\ mN$.

For 30 mN < T_{min} < 50 mN, the libration at end of deployemnt increases rapidly from 20 deg to 40 deg. For $T_{min} \geq$ 50 mN, the deployment stops at a distance of about 500 m because of eccessive friction and without any role being played by the control law. The critical value of 50 mN for the minimum tension is determined by the ejection velocity which with the present ejection system is equal to 1.85 m/s. Higher ejection velocities would increase this critical value and also improve further the robustness of the control law for values of the minimum tension higher than 30 mN. It is, therefore, very important that any non-conductive tether of new design satisfies the critical constraint on the minimum deployment tension.

The parameters adopted in the following simulations are:

Orbital and ejection parameters
Orbit: 400x400 km
Orbital inclination: 35 deg
Ejection velocity = 1.85 m/s
Ejection angle = 5 deg (foreward of LV with an upward deployment)

System parameters
Satellite mass = 20.4 kg
Delta-II Mass = 911 kg (2008 lb)
Tether lengths: 10 km (non conductive) and 5 km (conductive)
Tether linear densities: 0.2 kg/km (Spectra portion) and 2 kg/km (Conductive portion)
Baseline minimum tensions:
Tmin = 20 mN (Spectra, SEDS-II flight value)
Tmin = 200 mN (Conductive wire)
Inertia multiplier = 4.1
Annulus solidity = 9.427
Area exponent = -0.6

See Refs. 2 and 3 for a description of the deployer tension model.

The reference profiles for ProSEDS reference #9 are shown in Fig.3.4.1. The in-plane angle, which is also shown in the figure, is not a feedback parameter due to the lack of observability. The control law, therefore, only uses a partial knowledge of the system state.

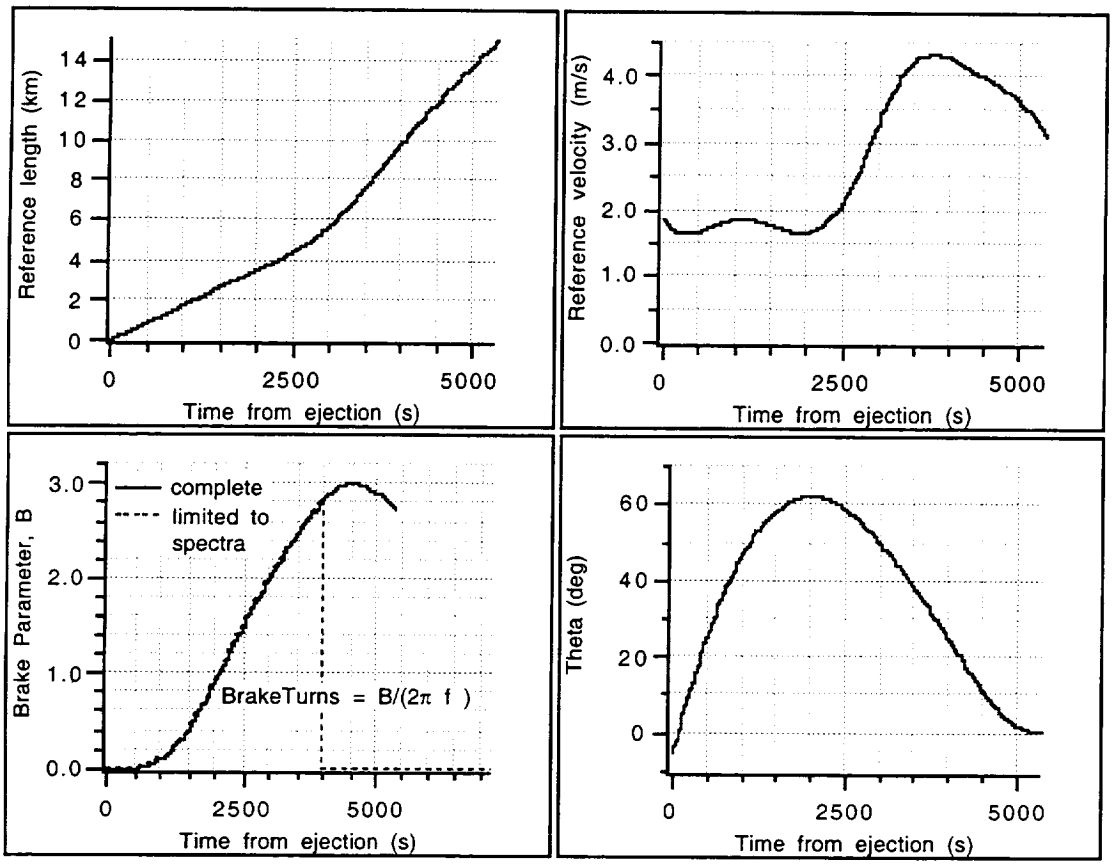

Fig. 3.4.1. Profiles for deployment Reference #9.

Simulation results of ProSEDS deployment for off-reference conditions are shown in Figures 3.4.2(a)-3.4.2(c). The final libration amplitude does depend on the spectra T_{min} but it is fairly insensitive to the value of the wire T_{min}. Values of T_{min} wire as high as 500 mN have been explored with satisfactory deployment dynamics. A summary plot of the final libration amplitude vs. the spectra T_{min} is shown in Fig. 3.4.3.

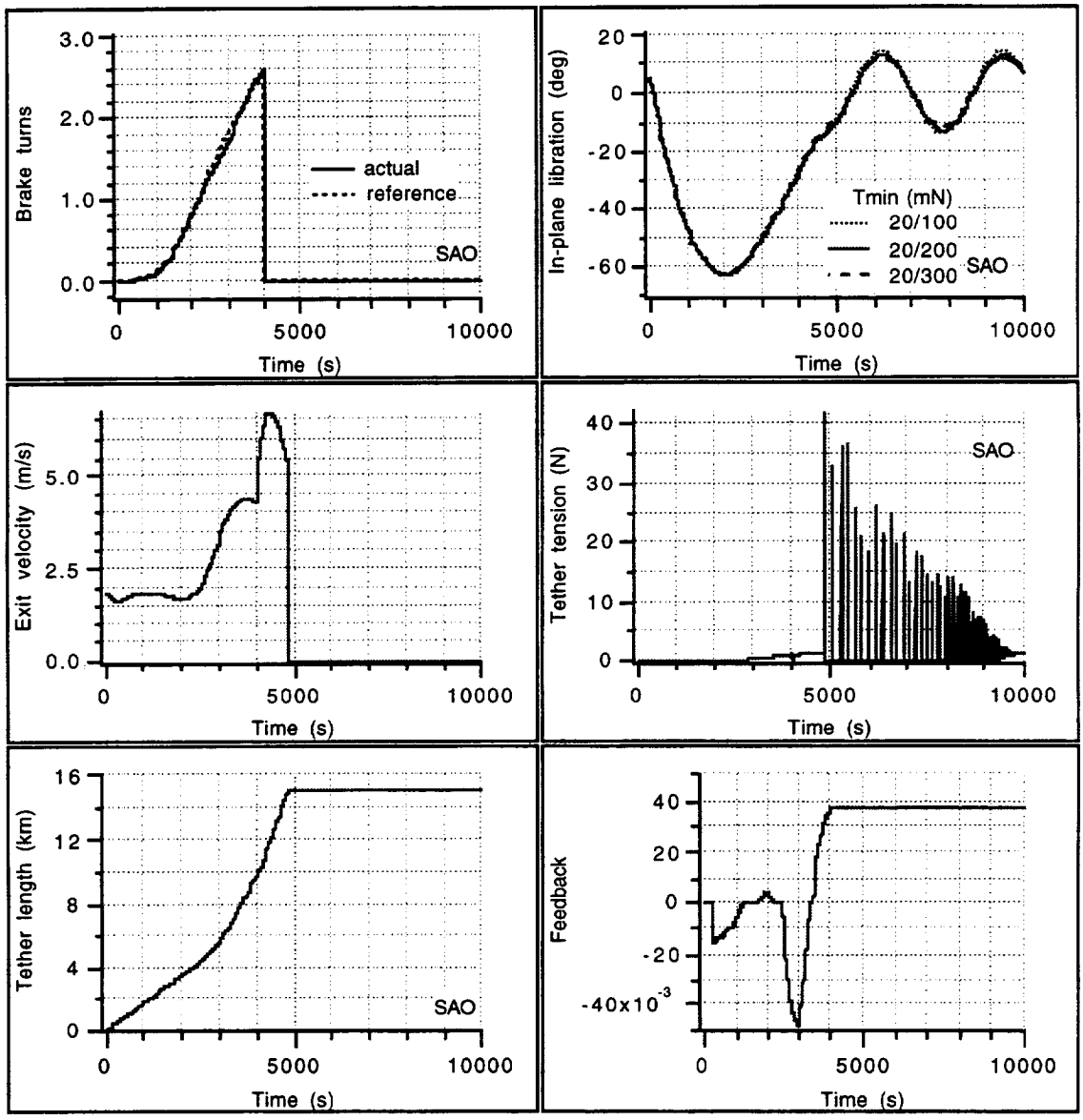

Fig. 3.4.2(a). Deployment Ref. #9; T_{min} (spectra) = 20mN, T_{min} (wire) = 100-300mN. A change in T_{min} wire has an almost negligible effect on the final libration amplitude.

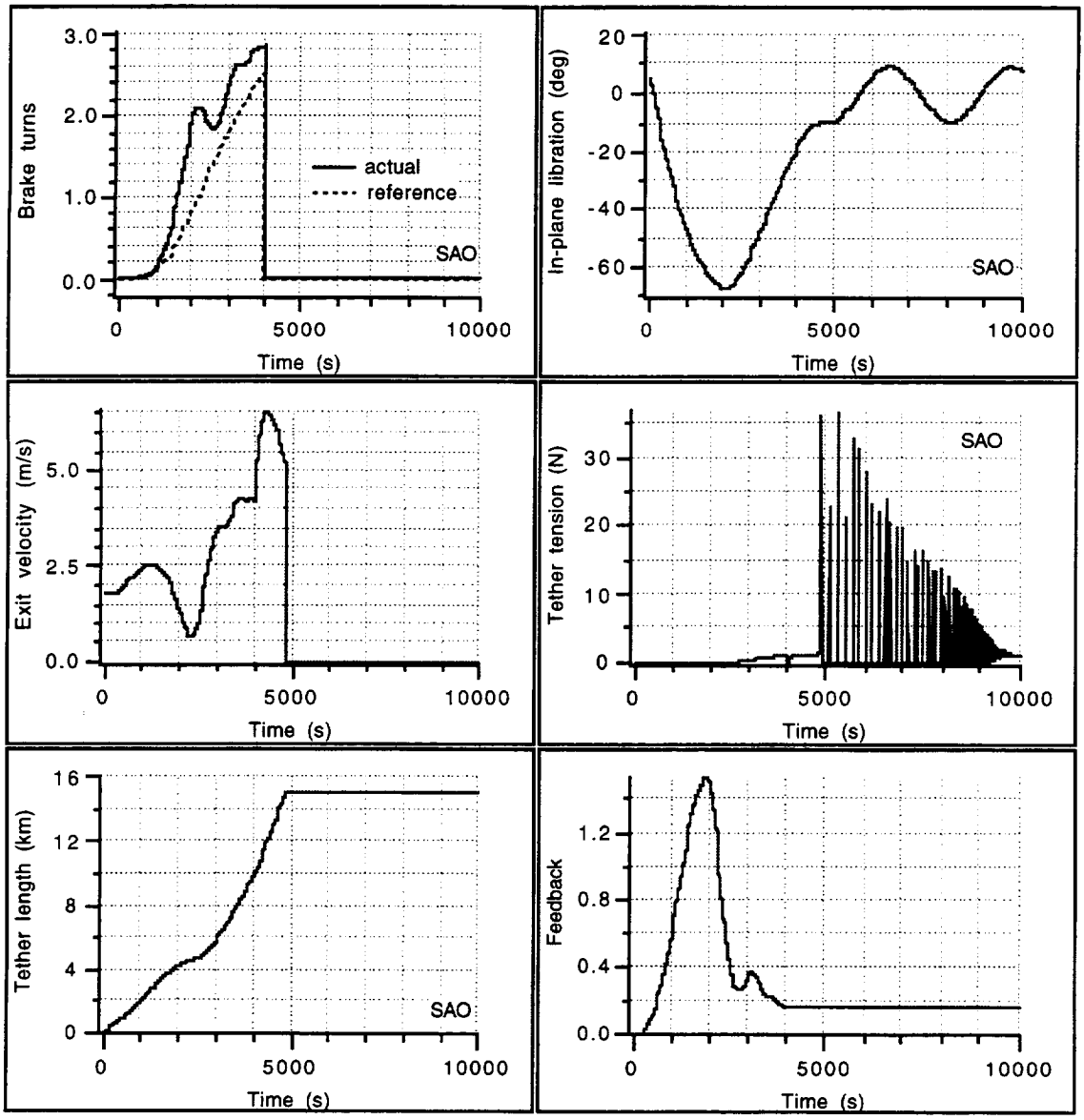

Fig. 3.4.2(b). Deployment Ref. #9, T_{min} (spectra) = 10mN, T_{min} (wire) = 200mN.

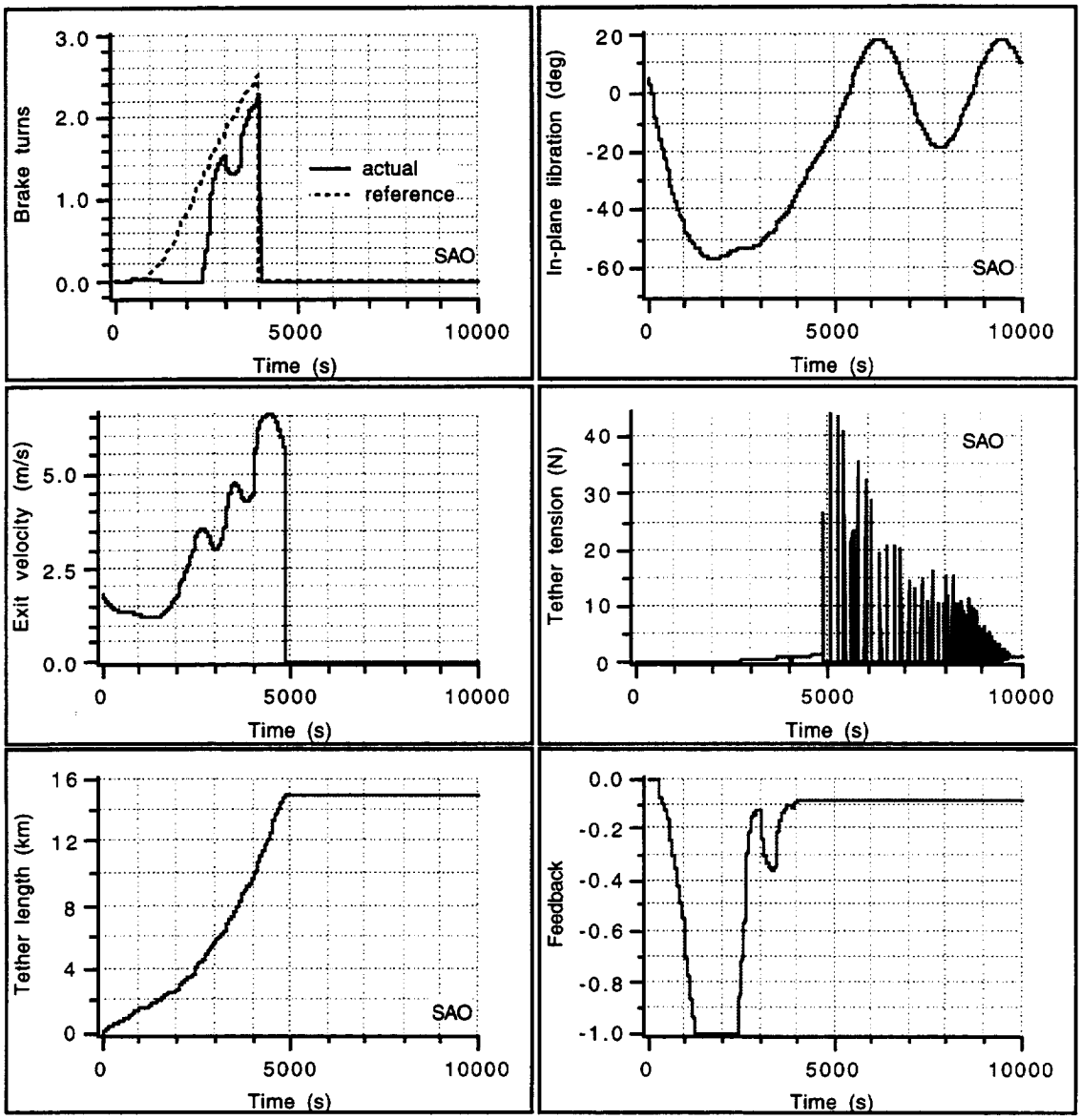

Fig. 3.4.2(c). Deployment Ref. #9, T_{min} (spectra) = 30mN, T_{min} (wire) = 200mN.

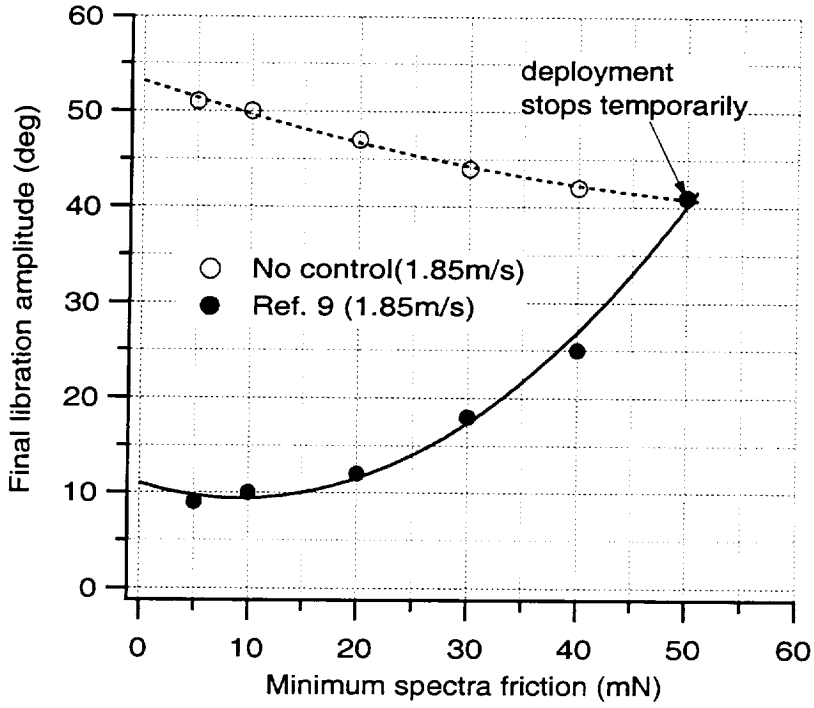

Fig. 3.4.3. Final libration amplitude vs. T_{min} (spectra) for deployment reference #9.

Preliminary conclusions on ProSEDS deployment

The deployment dynamics is well behaved up to a minimum tension Tmin = 500 mN for the conductive wire. It is important that the minimum tension (and associated friction coefficient) of the non-conductive tether satisfies the same constraint of the SEDS-II tether (i.e., T_{min} < 30 mN). This constraint is mandatory, given our current ejection velocity of 1.85 m/s, in order to obtain a final libration amplitude below 20 deg. A smooth transition (splice) between the non-conductive tether and the conductive wire must also be implemented. Some adjustments of the control law parameters should be considered. For example, the upper saturation value of the feedback (FeedSatur+ of the control law parameters) – should be increased from the baseline value of 1 to 1.5 in order to improve the control law insensitivity to changes in the tension model parameters.

3.5 ProSEDS Deboost Performance

ProSEDS Reentry Time

One of the primary objective of ProSEDS is to reenter the Delta stage at a strongly accelerated rate with respect to the natural reentry rate of the Delta second stage without an ED tether attached to it.

We have carried out a parametric analysis of the reentry time for different values of the average tether current and for different starting altitudes. Since the current distribution of a bare tether is not constant, "average" in our case means average along the tether (spacial average). The spacial average in a bare tether differs from the current measured at the Delta attachment point. The current collection model (predicated on the OML collection regime) relates the two quantities and make possible the scaling from the spacial average to the value measured at the Delta as explained in the previous chapter.

The parametric computations were carried out for ProSEDS present baseline and launch schedule as follows:

Launch in August 2000	-> F10.7 ≈ 155 (50% percentile probability)
	-> F10.7 ≈ 240 (98% percentile probability)
Tether	= 5-km wire + 10-km spectra
Delta mass	= 900 kg (≈2000lb)
ProSEDS mass	= 100 kg

The solar fluxes (F10.7) indicated above are in accordance with the NASA/MSFC predictions made in 1998. The 98% percentile probability is a conservative estimate which should be used as an upper limit for atmospheric density prediction and a lower limit for the reentry time estimates.

Moreover, a $C_D = 2.2$ was adopted throughout the orbital decay because the tether, that provides most of the drag area, is in free-molecular flow almost throughout the decay. The reentry time was also computed for zero current circulating in the tether and for a Delta stage without any tether attached to it. This last estimate, however, has a large error band because the Delta second stage is not stabilized and its drag area varies randomly during reentry. Also, the stage mass before reentry depends upon the residual propellant left in the stage after the depletion burn.

Figures 3.5.1(a) and 3.5.1(b) show the reentry time for the 50% percentile probability atmospheric density in the year 2000 vs. the tether average current for start altitudes of 400 km (the present baseline) and 500 km, respectively.

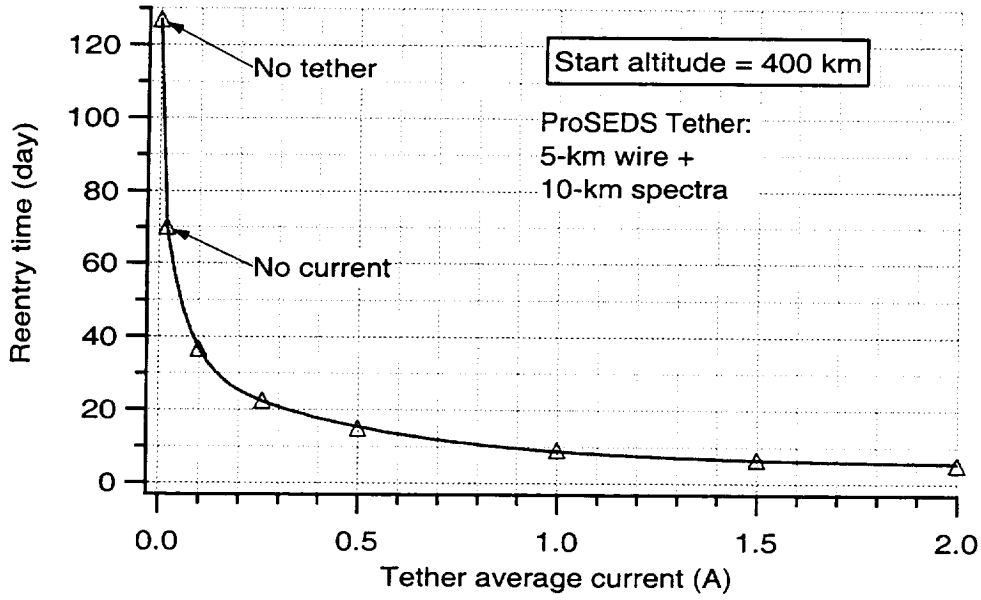

Fig. 3.5.1(a). Reentry time vs. average tether current for F10.7 with 50% percentile probability) in August 2000 and a starting altitude of 400 km.

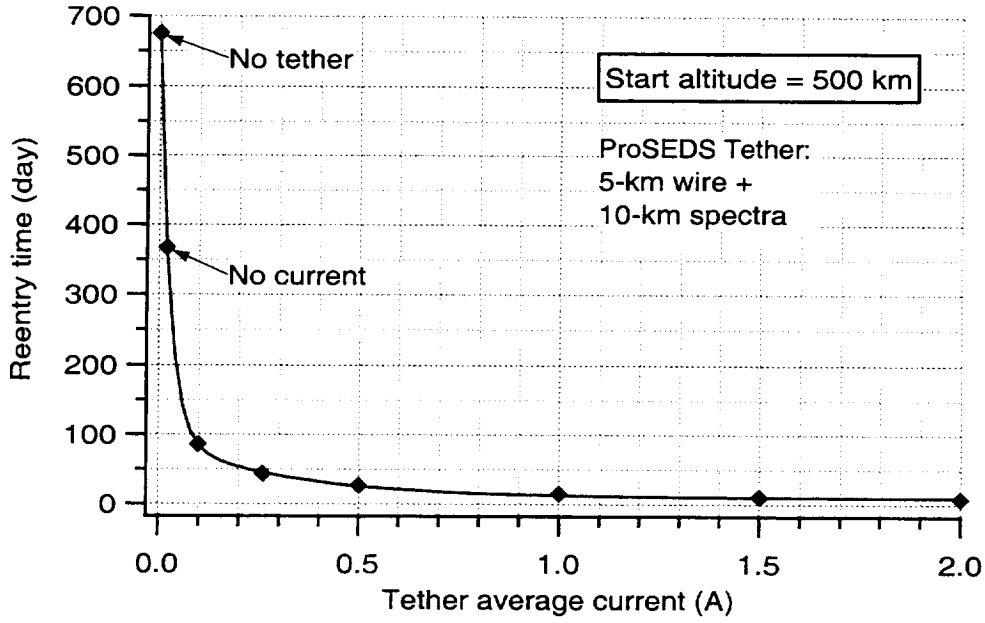

Fig. 3.5.1(b). Reentry time vs. average tether current for F10.7 with 50% percentile probability in the year 2000 and a starting altitude of 500 km.

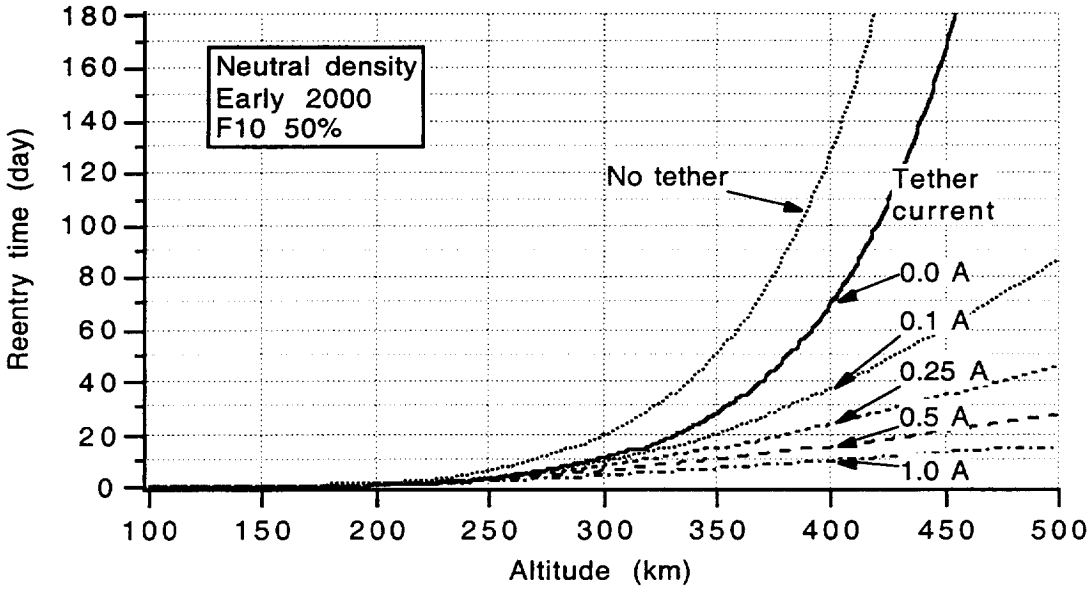

Fig. 3.5.2(a). Reentry time vs. starting altitude for different average tether currents for F10.7 with 50% percentile probability in the year 2000.

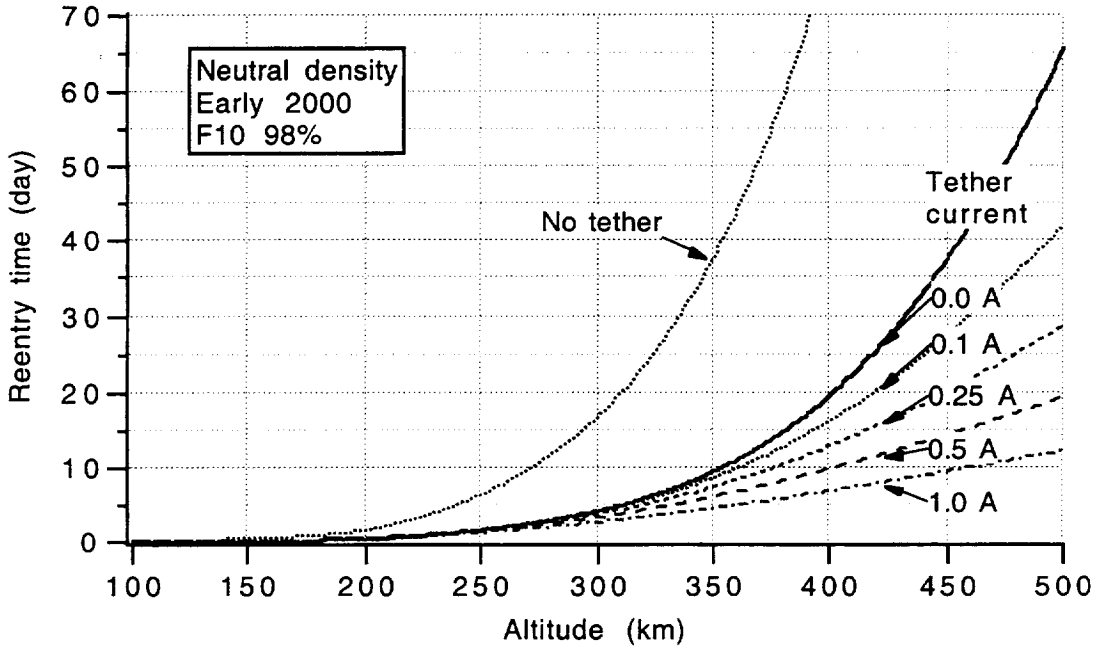

Fig. 3.5.2(b). Reentry time vs. starting altitude for different average tether currents for F10.7 with 98% percentile probability in the year 2000.

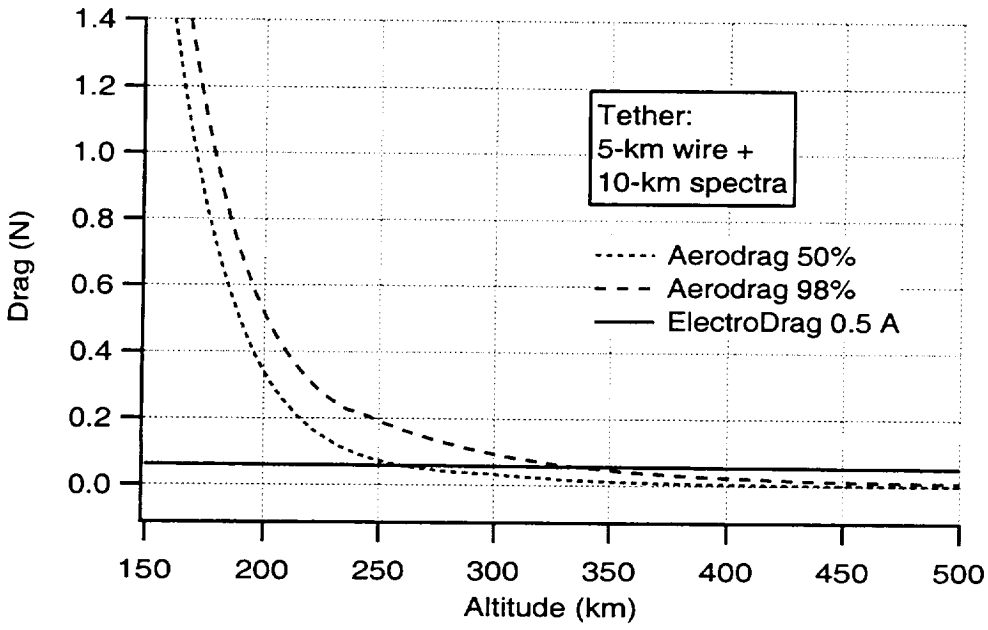

Fig. 3.5.3. Atmospheric and electrodynamic drag vs. altitude for 1-A average-along-tether current and F10.7 with 50% and 98% percentile probabilities in the year 2000.

Figures 3.5.2(a) and 3.5.2(b) show the reentry time vs. starting altitude for different values of the average tether current and solar fluxes with 50% and 98% percentile probabilities. In order to understand better the relative roles played by ED forces and atmospheric drag, we show the forces vs. altitude in Fig. 3.5.3.

Figure 3.5.3 clearly indicates that for the conditions under consideration, the ED force and atmospheric drag will be approximately equal at an altitude of about 250 km. For very conservative atmospheric predictions (98%), the cross over altitude moves higher.

As mentioned before, the average tether current along the tether differs from the current measured at the Delta which in turn is the current level being control by the operating duty cycle. For the current level and plasma conditions of interest to ProSEDS, the current measured at the Delta is roughly 30% higher than the average current along the tether. It is, therefore, important to specify which current is being considered when comparing reentry times of bare tethers. After taking into account the conversion factor from average tether current to Delta current, the results above are in full agreement with the result obtained by Ken Welzyn at NASA/MSFC for 0.5-A time-average current at the Delta end.

Table 3.5.1. ProSEDS reentry time for an average-along-tether current of 0.5 A.

Altitude (km)	Reentry time (day) F10.7 50%	Reentry time (day) F10.7 98%
400	**15**	**10**
450	**21**	**14**
500	**26**	**19**

Table 3.5.2. ProSEDS reentry time for an average-along-tether current of 1 A.

Altitude (km)	Reentry time (day) F10.7 50%	Reentry time (day) F10.7 98%
400	**9**	**7**
450	**12**	**9**
500	**15**	**12**

In summary, the reentry times are shown in Table 3.5.1 for an average-along-tether current of 0.5 A and in Table 3.5.2 for 1 A.

The present estimate of the average-along-tether current in ProSEDS is about 0.6 Amp (that corresponds to 0.85 Amp measured at the Delta), leading to a reentry time from a 400-km altitude of about 2 weeks.

Finally, Fig. 3.5.4 shows a comparison of the reentry profiles of the Delta 2nd stage with and without ProSEDS for an F10.7 ≈ 155, a Delta stage mass of 900 kg, a 100-kg ProSEDS mass and a tether coated with a 100% PANi coating without collection losses.

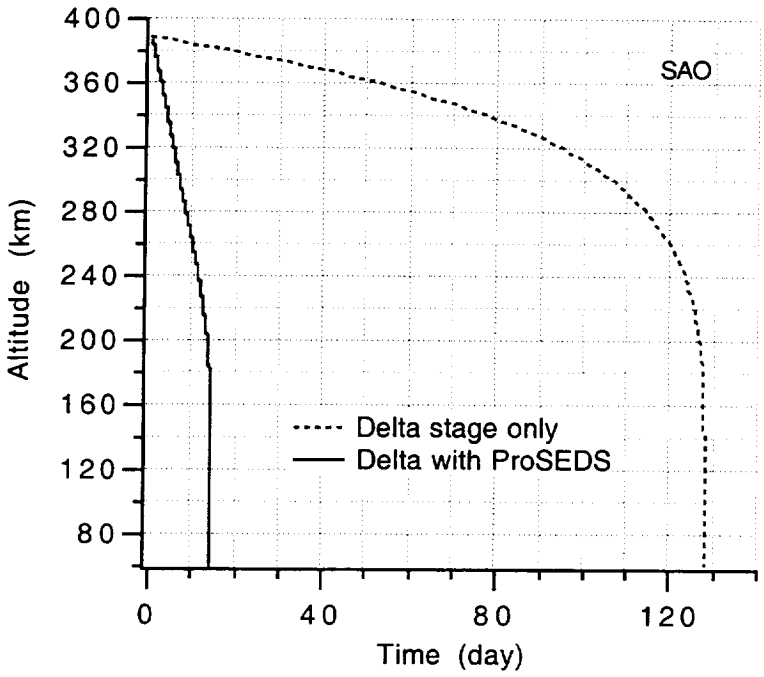

Fig. 3.5.4. Decay profiles for Delta stage with and without ProSEDS (F10.7 ≈ 155, Delta stage mass = 900 kg, 100-kg ProSEDS mass and 100%-PANi coated tether).

Conclusions

ProSEDS can strongly accelerate the reentry of the Delta 2nd stage. At the start altitude of 400 km, the electrodynamic force overpowers the atmospheric drag by a factor greater than 10. The electrodynamic forces will dominate the reentry down to an altitude of roughly 250 km. The presently estimated reentry time of the Delta stage with ProSEDS (if the system survives long enough) is about 2 weeks.

References to Section 3.0

1. Estes, R.D., E.C. Lorenzini, J.R. Sanmartin, M. Martinez-Sanchez and N.A. Savich, "New High-Current Tethers: A Viable Power Source for the Space Station?," Smithsonian Astrophysical Observatory, White Paper, December 1995.

2 E.C. Lorenzini (PI), et al., "Dynamics and Control of SEDS-II, Analyisis of SEDS-I Flight Data." NASA Quarterly Reports #33 and #34 on *Analytical Investigation of the Dynamics of Tethered Constellations in Earth Orbit (Phase II),* Contract NAS8-36606, pp. 1-118 and Appendices, March 1994.

3. E.C. Lorenzini (PI), et al., "Analytical Investigation of the Dynamics of Tethered Constellations in Earth Orbit (Phase II)", NASA Final Report, Contract NAS8-36606, pp. 1-160, May 1994.

4. E.C. Lorenzini, S.B. Bortolami, C.C. Rupp and F. Angrilli, "Control and Flight Performance of Tethered Satellite Small Expendable Deployment System-II," Journal of Guidance, Control, and Dynamics, Vol. 19, No. 4, 1148-1156, 1996.

4.0 STATIONARY TETHERS FOR POSITION CONTROL OF LARGE PLATFORMS

4.1 Tether-assisted station-keeping of a Solar Power Station in GEO

Introduction

This section describes the use of spaceborne tethers for the on-orbit management of a GEO platform. In the following, we will show how the east-west drifts can be compensated by deploying an electrodynamic tether, thus combining the effects of system's CM displacement with the Lorentz forces (e.g. $\underline{I} \times \underline{B}$).

The order of magnitude of the masses involved as well as the power needed to drive the system have been computed on very basic principles.

Moreover, tethers offer some additional advantages compared to more traditional systems like the built-in capability of stabilizing the satellite attitude around the pitch and roll axes.

Orbital Perturbations on a GEO platform

The orbital elements of an "ideal" geostationary satellite are:

a_0 = semimajor axis = 42,164 km; e_0 = eccentricity = 0; i_0 = inclination = 0°

The major perturbations affecting a satellite in GEO are the gravitational effects of the earth asphericity, solar pressure and third's body perturbations due to the Sun and the Moon. The effects of the external perturbations make the satellite drift both in latitude and longitude. If uncontrolled, the satellite longitude drifts about 180° in 2.5 years and the latitude drifts about 15° in 15 years. The longitudinal drift is caused mainly by a resonance with the C_{22} term of the Earth's gravity field and the latitudinal drift is caused by the sun and Moon's attraction. Therefore, a GEO satellite needs periodic stationkeeping maneuvers (e.g. ΔVs) to be kept at a desired location unless a position relocation is needed.

The longitudinal acceleration in GEO can be approximately written as [1,2]:

$$\ddot{\lambda} \approx [16.9 + 2.9 \sin(\lambda - 35^\circ)] \times [\sin(150^\circ - 2\lambda)] \times 10^{-4} \text{ (deg/day}^2\text{)} \quad (4.1a)$$

There are two stable longitudes at approximately 75° and 255° and two unstable longitudes at approximately 165° and 345° (East longitudes).

The longitudinal acceleration can be written also in a more simplified form as a function of the closest stable longitude λ_s as

$$\ddot{\lambda} \approx 16.8\,[\sin 2(\lambda - \lambda_s)] \times 10^{-4} \qquad (\text{deg/day}^2)\,(4.1b)$$

The perturbing acceleration caused by C_{22} can be computed as [2,3] with a_0 the semimajor axis:

$$A_{C22} \approx -\,a_0\,\frac{\ddot{\lambda}}{3} \qquad (4.2)$$

Figure 4.1.1 shows the longitudinal and the C_{22} perturbation accelerations in GEO as computed by equations 4.1b and 4.2, respectively.

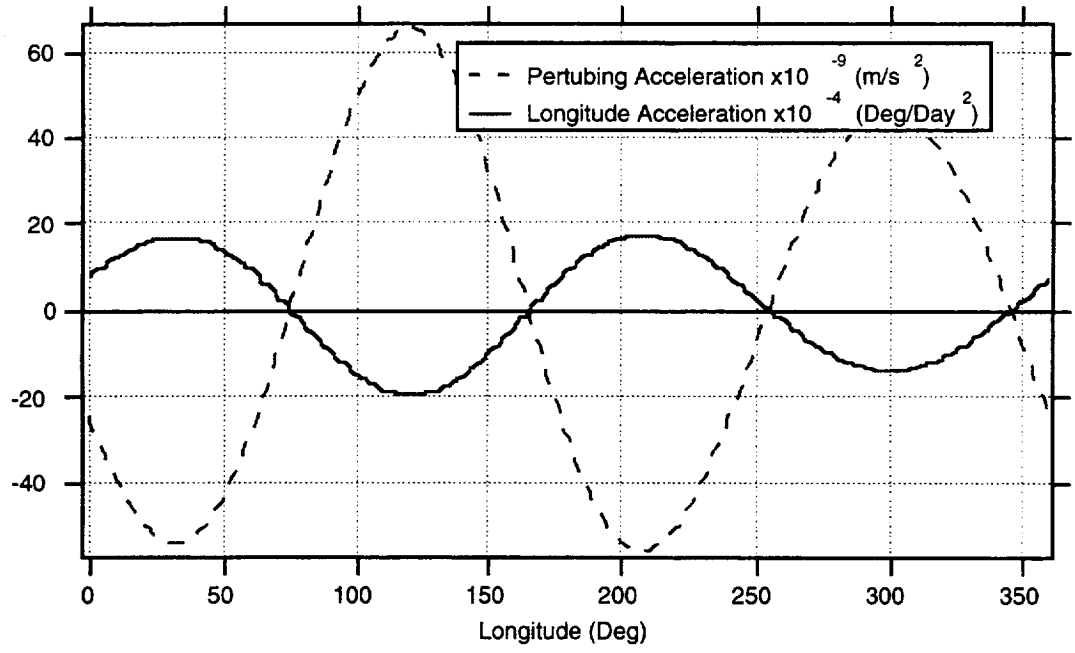

Figure 4.1.1. Longitudinal and C_{22} Acceleration in GEO vs. longitude

Figure 4.1.2 shows a one-cycle evolution of a free-drifting GEO satellite, initially displaced 45° from one of the stable longitudes (λ_s =75°). This situation corresponds to the maximum initial longitude acceleration (see equation 4.2).

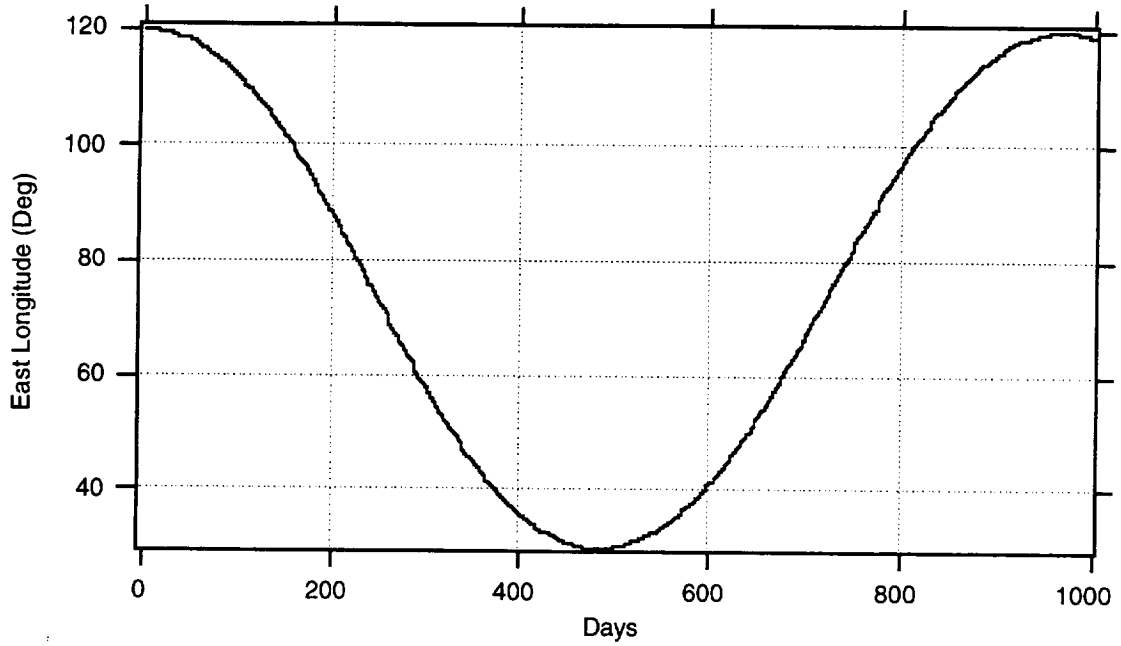

Figure 4.1.2. GEO Satellite Longitude Drift vs. Time.

The oscillation period is about 968 days which corresponds to about 2.5 years. The direction of the pendulation will reverse in the next cycle. Figure 4.1.3 shows a phase plot with the drift rate versus the distance from the closest stable longitude point.

The change in drift rate $\Delta\dot{\lambda}$ can be written as a function of the variation of semimajor axis Δa or in terms of ΔV necessary to correct it [3]:

$$\Delta\dot{\lambda} = -\frac{3}{2}\frac{\sqrt{\mu}}{a_o^{5/2}}\Delta a = -\frac{3}{a_o^{1/2}}\frac{V_o}{\sqrt{\mu}}\Delta V \qquad (4.3)$$

where the subscript "o" stands for the elements of the "ideal" GEO orbital elements, μ is the earth's gravitational constant and V_o is the orbital velocity of the "ideal" GEO orbit.

Thus, in order to correct for the drift, we need to apply a ΔV to counteract the action of the perturbing acceleration or change the orbital semimajor axis and, hence, the orbital period.

The ΔV required in a year to control the longitude of a GEO satellite can be written as [2,3]:

$$\Delta V = 1.74 \sin[2 (\lambda - \lambda_s)] \qquad \text{m/s/Year} \qquad (4.4)$$

where λ is the desired longitude and λ_s is the closest stable longitude.

Orbit Stationkeeping and Relocation of a freely drifting platform

A deployed tether can be used to displace the semimajor axis by the amount necessary to correct for $\Delta\dot{\lambda}$, as shown in equation 4.3.

During deployment the momentum of the system H is conserved and, neglecting the tether mass, we can write:

$$H_i = (M_1+M_2)\, \omega_0\, r_0^2 = H_f = (M_1\, r_1^2 + M_2\, r_2^2)\, \Omega \qquad (4.5)$$

where:

M_1 = Platform Mass
M_2 = Ballast Mass
r_0 = Geosynchronous Radius (= 42,164 Km)
r_1 = Radius of the satellite at the end of deployment
r_2 = Radius of the ballast at the end of deployment
ω_0 = Geosynchronous mean orbital rate
ω = Final mean orbital rate

In order for the system to be in circular orbit after deployment, we need also a balance between the gravitational and centrifugal forces on the end masses [4]:

$$\frac{\mu}{r_1^2} + \frac{\mu}{r_2^2} = m_1 r_1 \Omega^2 + m_2 r_2 \Omega^2 \qquad (4.6)$$

Since $r_1 = r_{cm} - L_1$ and $r_2 = r_{cm} + L_2$, by expanding the gravitational term to the second order and rearranging the above equations, we obtain:

$$P = P_o \left[1 - 9 \frac{M_{EQ}}{M_T} \left(\frac{L}{r_o} \right)^2 \right] \qquad (4.7a)$$

$$r_{CM} = r_o \left[1 - 5 \frac{M_{EQ}}{M_T} \left(\frac{L}{r_o} \right)^2 \right] \qquad (4.7b)$$

where $L = L_1 + L_2$, $M_T = M_1 + M_2$ and $M_{EQ} = M_1 M_2 / M_T$ and P is the orbital period.

Therefore the orbit of the GEO satellite/platform can be varied by deploying/retrieving the tether, thus raising/lowering the system CM and its orbital period. Equations 4.7 had been already derived for equal end-masses in [5].

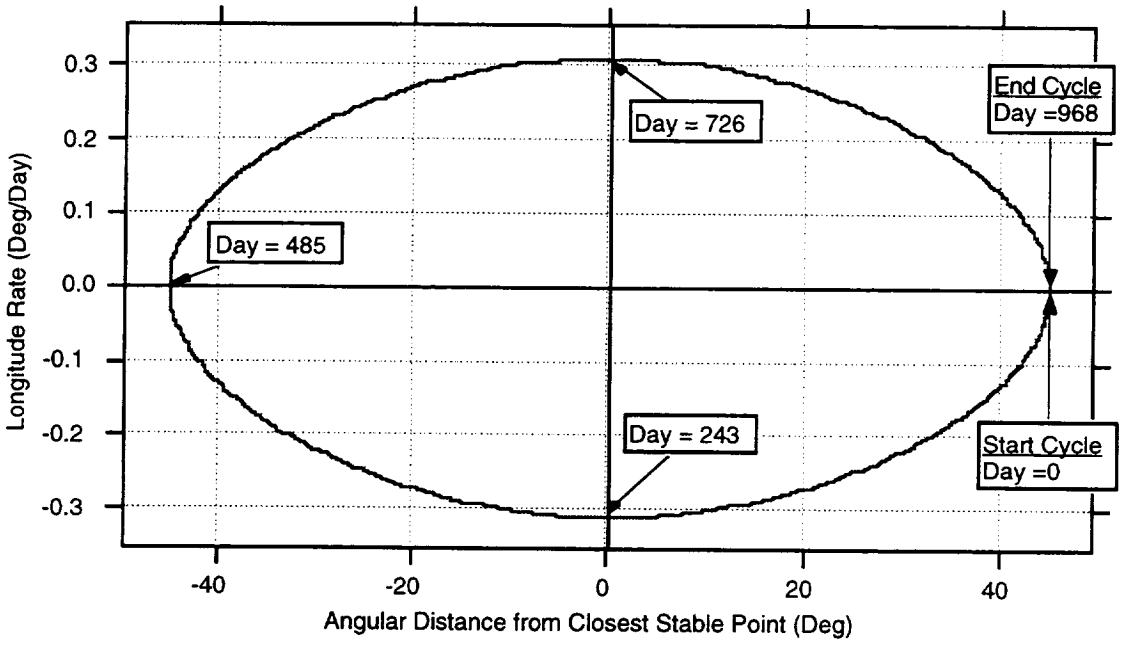

Fig. 4.1.3. GEO Satellite Longitude Rate vs. Distance from Closest Stable Longitude.

Figure 4.1.4 shows the overall longitude drift for different mass combinations. For our study we chose the following values:

- $M_{SAT} = M_{BAL} = 6000$ Kg (Equal Masses)
- $M_{SAT} = 6000$ Kg and $M_{BAL} = 2310$ Kg (Centaur Spent Stage)
- $M_{SAT} = 3440$ Kg and $M_{BAL} = 1140$ Kg (IUS Spent Stage)

Figure 4.1.4 shows that, in order to have zero longitudinal drift, we need a tether length of ~700 km. Slightly longer tether lengths are needed for different mass combinations. Figure 4.1.5 shows tether tension for different tether lengths.

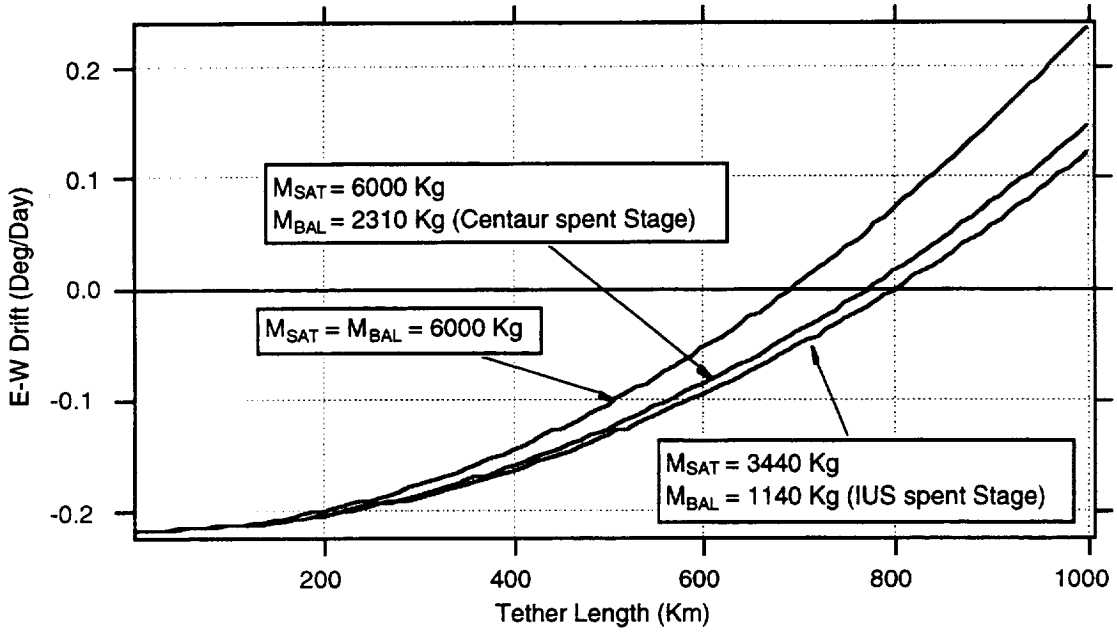

Figure 4.1.4. GEO Longitudinal drift vs. tether length for different mass combinations.

The tension values are very low and therefore the tether diameter should be chosen to minimize the micrometeroid risk.

By looking at the data from reference [6], the cross sectional flux Σ of micrometeroids of size a third of a tether diameter of 4.8 mm (e.g. twice TSS-1's) is 10^{-4} Impacts/m^2-yr.

Figure 4.1.6 shows that in the range of tether lengths of interest the probability of not being cut is not very high (~ 60-70% for a 1 year lifetime). New "fail-safe" tethers designs [7], currently under study, will eventually be tested in space.

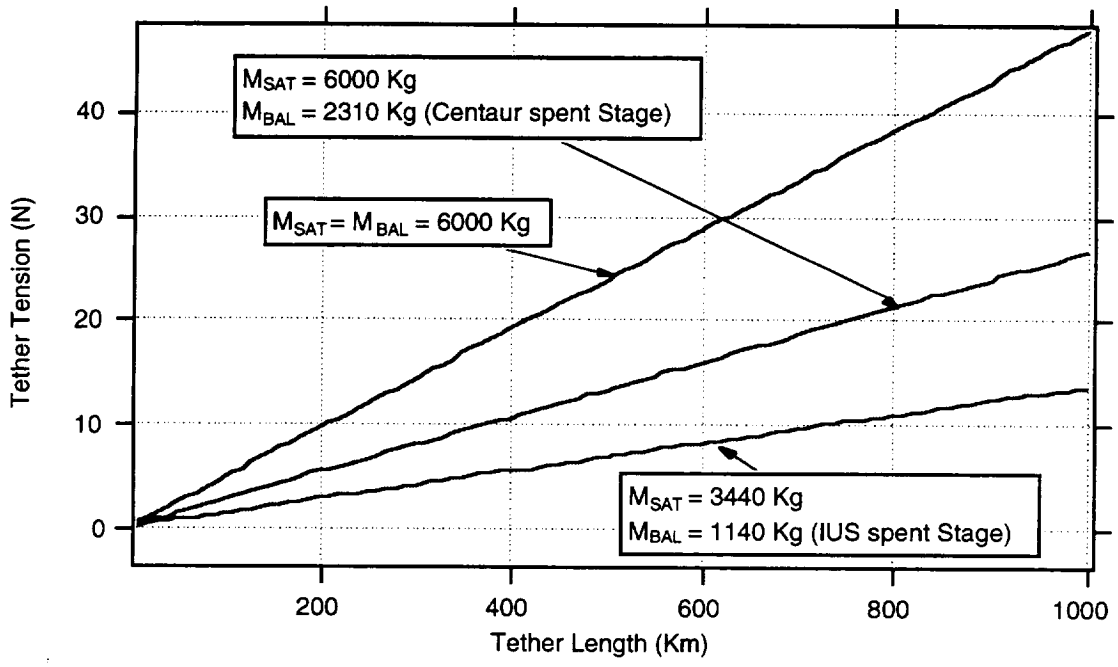

Figure 4.1.5. Tether tensions versus length for different mass combinations in GEO.

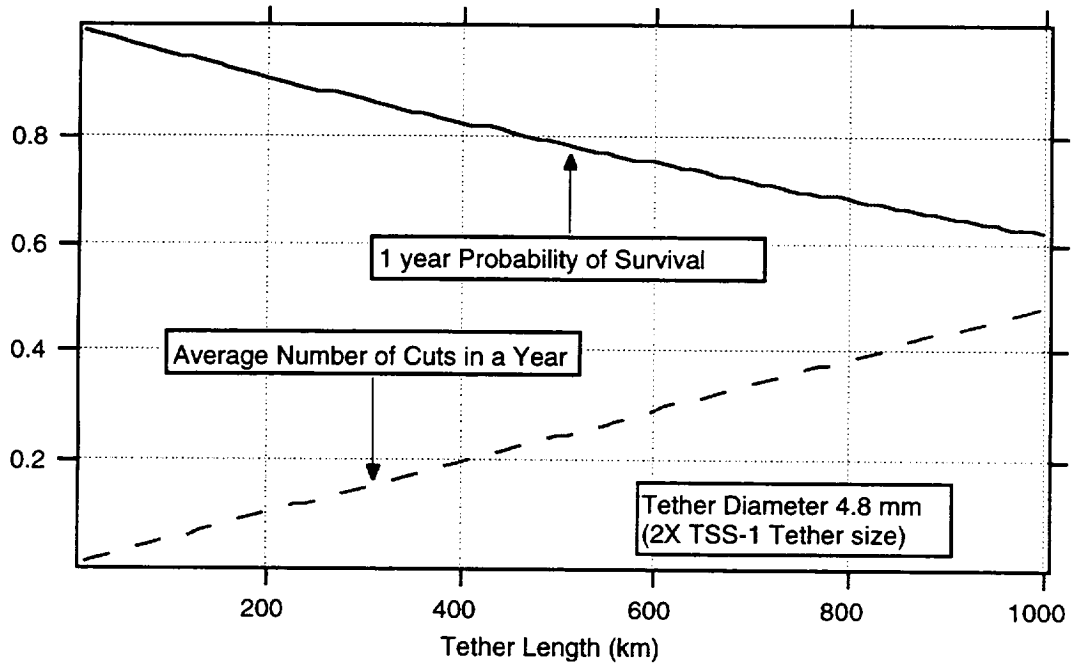

Fig. 4.1.6. Average number of cuts and probability in one year versus tether length.

An Electrodynamic Thruster for Orbit Stationkeeping

Regardless of the type of tether used, a decrease in tether length implies: (a) a lesser probability of being cut (see figure 4.1.6) ; (b) a reduction in the overall system mass which is always important in space applications. A way of reducing the length is by exploiting the thrusting capability of the electrodynamic tether.

In GEO, however, we do not have any motion-induced emf since the plasma is at rest with respect to the spacecraft. The voltage, therefore, must be completely supplied by the user. Fortunately, in our case our user is an orbiting generator and part of the power can be used to supply the electrodynamic tether for on-station management.

In first order of approximation, the tether current I can be written as function of the applied voltage V:

$$I = K\, n_e\, A\, V^{1/2} \qquad (4.8)$$

where n_e is the electrons' number density, A is the collection area and K is a constant extrapolated from the following TSS-1 data: $K = 3.16 \times 10^{-14}$ for I = 1 Amps, A = 10 m^2, V = 1 kV and $n = 10^{11}\ m^{-3}$.

The Lorentz force generated by a current I interacting at right angles with the geomagnetic field B can be written as:

$$F_{em} = I\, B\, L \qquad (4.9)$$

where L is the tether length.

By using the dipole model , the geomagnetic field in GEO is:

$$B \simeq B_o\, (R_{earth}/R_{geo})^3 = 3 \times 10^{-5}\, (R_{earth}/R_{geo})^3 = 1.03 \times 10^{-5} \ \text{Tesla} \qquad (4.10)$$

From the above formulas we can see that for a given orbit (e.g. B vector), the force is a function of the current and the tether length. We want to minimize both, since high currents need high power and longer tethers increase the probability of cuts.

For example, the voltage V and power P required to circulate 5 mA in GEO ($n_e \simeq 10^7$ m^{-3}) with a collection area of 50 m^2 , are approximately 77 kV (from equation 4.8) and 385 W, respectively.

The area of the solar panels A_{panel} and their mass M_{panel} needed to generate the required power P can be written as:

$$A_{panel} \simeq P/(\varepsilon_p S) \tag{4.11}$$

$$M_{panel} \simeq P \varepsilon_s \tag{4.12}$$

where S is the solar flux (1350 W/m^2), ε_p is the overall solar array efficiency (0.14x0.75x0.9) and ε_s is the mass per unit power ($\approx$0.02) of the solar panel. For a 1 mA tether current system, the solar panel area and the mass are 3 m^2 and 8 kg, respectively.

By using the force balance equation together with equations (4.3) and (4.9) we obtain:

$$(L\, I\, B_o)\frac{\Delta t}{M_{tot}} = \Delta V = -\frac{a_0^2 \Omega_o}{3V_o}\Delta\Omega \tag{4.13}$$

or

$$|L| = \frac{1}{I}\frac{M_{tot}}{\Delta t}\frac{1}{B_o}\frac{a_0^2\Omega_o}{3V_o}\Delta\Omega \tag{4.14}$$

So by entering the values with subscript "0" from the ideal GEO orbit and using the following values:

$\Delta\Omega$ = 0.3 °/Day (e.g. maximum free drift rate)

M_{TOT} = 1.2x10^4 Kg (equal masses cases neglecting tether mass)

Δt = 1 year

I = 10 mAmp

we obtain L = 315 Km which somehow has halved the original length and increased the probability of survival to almost 85%.

Since the longitudinal perturbation is not constant with respect to the longitude we run several numerical simulations (equal masses case) to find satisfactory tether lengths and current levels.

In order to simplify our preliminary analysis we integrated equation (4.1b) with the addition of the Lorentz force :

$$\ddot{\lambda} = A\,[\sin 2(\lambda - \lambda_s)]\ \times 10^{-4} - \frac{IB_o L}{M_{tot} a_0} \qquad (4.15)$$

Figure 4.1.7 shows the results from a run with the following values:

L = 295 Km

I = 60 mA

The time evolution is compared to the free drift case shown in Fig. 4.1.2. After one year the longitude has changed by only 2° compared to the natural 72°.

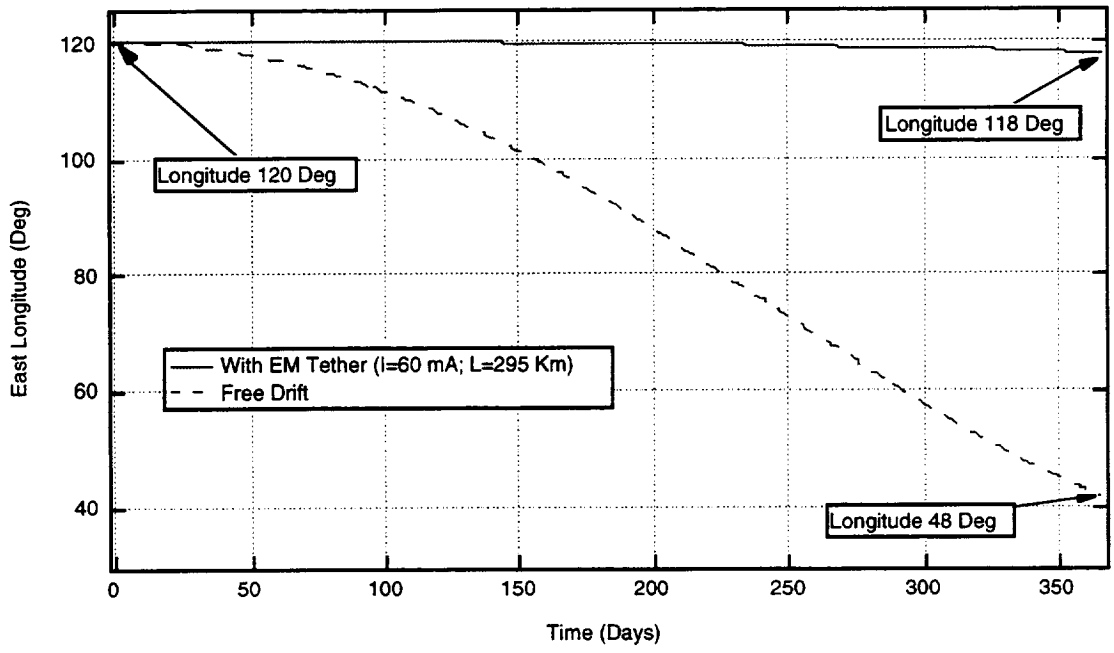

Fig. 4.1.7. Longitude Evolution over one year with an electrodynamic tether compared to a free drifting satellite.

Please note that equation (4.15) does not take into account that the system's semi-major axis, thus the drift rate, has been changed by the presence of a deployed tether. Further simulations with high-fidelity codes will take into account both effects. Therefore the tether length obtained by the numerical integration of equation (4.15) is partially correct.

Moreover, the above results can be optimized by either modulating the current in the tether with respect to the position or by using a "bang-bang" control law similar to the schemes currently used by chemical thrusters on GEO satellites. The efficacy of the method, however, is quite evident.

Additional Advantages of EM Tethers in GEO

Once that fail-safe tether designs will become a reality, thus minimizing the vulnerability, tethers offer additional advantages to the stationkeeping of GEO satellites/platforms over more traditional methods. To name just a few:

- End-masses Attitude stabilization along the pitch and roll axes [8]. For tether lengths of the order of 300 km the attitude steady state angles are about 2 arcseconds.

- Satellite relocation and deorbit. By using a combination of CM displacement and current flow.

- Inclination control [9]. By using the IxB effect and modulating the current as:

$$I = - I_o \cos(2\phi) \text{ where } \phi \text{ is the argument of latitude.}$$

The approximate change of inclination i over an orbit is then:

$$\Delta i = \frac{\pi}{2\Omega} \frac{B_o I_o L}{M V_o} \sin i \quad (rad/orbit)$$

Further Investigation

The work presented has shown the great promise of tethers for on-orbit stationkeeping of GEO satellites.

Nevertheless, a deeper investigation is needed to take into account the orbital perturbations acting on the system as a whole by using one of SAO's high-fidelity

numerical codes. The influence of the Sun-Moon attraction and solar radiation pressure should be included in the numerical simulations to study their effects on the system's drifts and the other orbital parameters.

Moreover, the current flow and the interaction of the system with the very rarefied plasma should also be included. A on-orbit thrusting system that modulates the current in an optimal fashion should be designed.

The system seems feasible and reliable and the use of fail-safe tethers should also be considered to increase the system's lifetime expectancy.

References to Section 4.0

1. Soop, E.M., "Handbook of Geostationary Orbits", Space Technology Library, Vol. 3, Kluwer Academic Publisher, 1994.

2. Berlin, P., "The Geostationary Application Satellite", Cambridge Univer. Press, 1988.

3. Pocha, J.J, "An Introduction to Mission Design for Geostationary Satellites", Kluwer Academic Publisher, 1987.

4. Arnold, D.A., "The Behavior of Long Tethers in Space", *The Journal of Astronautical Sciences*, Vol. 35, No.1, pp.3-18, 1987.

5. Landis, G.A., and F.J. Hrach, "Satellite Relocation by Tether Deployment", Journal of Guidance, Control and Dynamics, Vol. 14, No.1, pp. 214-216, 1991.

6. Anderson, J. (Ed.) , "Natural Orbital Environment Guidelines for Use in Aerospace Vehicle Development", NASA TM-4527, June 1994.

7. Forward, R.L., R.P. Hoyt, "Fail-safe Multiline Hoytether Lifetimes", AIAA paper 95-2890 31st AIAA/SAE/ASME/ASEE Joint Propulsion Conference, San Diego, CA, July 1995.

8. Lorenzini, E.C., C. Borgonovi, M.L. Cosmo, "Passive Attitude Stabilization of Small Satellites", *Space Technology*, Vol. 15, No. 4, pp.215-221, 1995.

9. Martinez-Sanchez, M., D.E.Hastings, "A System Study of a 100 kW Electrodynamic Tether", *The Journal of Astronautical Sciences*, Vol. 35, No.1, pp.75-96, 1987.

5.0 SPINNING TETHERS FOR EARTH AND PLANETARY TRANSPORTATION

5.1 LEO to GEO Tether Transport System

Introduction

The projected traffic to GEO is expected to increase during the next few decades and the cost of delivering payload from the Earth surface to LEO is projected to decrease thanks to the introduction of reusable launching vehicles (RLV). A comparable reduction in upper stages cost should take place in order to deliver payloads to GEO [1] at a fraction of today's cost.

Consequently, studies for alternatives means of transportation from LEO to GEO have been carried out with the aim at reducing substantially the cost per kilogram transferred to geostationary orbit. Tethers are possible candidates to accomplish this goal because spinning tethers are excellent storage devices for kinetic energy capable to provide very large ΔVs to the payload attached to the tether tip. A tethered system for transferring payload from LEO to GEO with a single stage was proposed some years ago by Bekey [2]. The present study is the first detail analysis of the original proposal, its extension to a two-stage system, and analyses on a possible operational system.

Concept Overview

Spinning tethers are used to impart the desired ΔV (or ΔVs) to the payload to be transferred. Each spinning system has a counter platform (or service module) on the opposite side of the tether. The spinning system acts as a giant momentum wheel, i.e., for each ΔV imparted to the payload there is a ΔV, proportional to the payload/platform mass ratio, imparted to the platform. After release, the payload is injected into a higher orbit and the platform is injected into a lower orbit which depends on the payload/platform mass ratio.

The transfer from LEO to geotransfer orbit (GTO) can be accomplished through a single ΔV of about 2.4 km/s (from a 300-km circular orbit) provided by a single stage tethered system or through two smaller ΔVs provided by a two-stage tethered system. This latter configuration is preferable with present day tether technology (as explained later on). A two-stage tethered system involves two facilities permanently in orbit: a spinning facility in LEO and another one in medium Earth orbit (MEO) with a perigee close to the LEO

facility. The payload is first boosted to MEO from the LEO facility, subsequently, it is captured (with zero relative velocity) at perigee by the MEO facility and later injected into GTO. In this study, the circularization ΔV from GTO to GEO is considered to be provided by the kick motor of the payload. However, a tethered system capable of delivering the payload to GEO could also be designed. This option is recommended for further analysis at the end of this report.

After payload delivery the two orbital platforms are reboosted by high-specific impulse electrical thrusters. The masses of the payloads to be handled by the tethered transfer system are assumed in the range 907 kg - 4082 kg (2000 lb - 9000 lb which according to present projections will constitute almost 80% of the traffic to GEO in the future. A time for platform reboosting of 10 weeks is assumed which, relates to a payload frequency transfer of 5 per year (more on this point later on in this report).

Orbital Transfers with Spinning Tethers

Tethers can provide ΔVs to the vehicles attached to their tips. If we refer the system dynamics to a local vertical - local horizontal (LV-LH) reference frame attached to the system CM, then tethers can be classified according to their motion with respect to LV-LH as hanging, swinging or spinning in much the same way as a pendulum in a gravity field (a tethered system in orbit is in fact a gravity-gradient pendulum). Clearly, for a given tether length, spinning tethers can impart the highest ΔV to the payload. If we call ΔH the separation between the two tip masses half an orbit after release and L the tether length, the following simple rules apply (see Fig. 5.1.1):

$$\begin{aligned} &\Delta H \approx 7L && \text{Hanging tethers} \\ &7L < \Delta H < 14L && \text{Swinging tethers} \\ &\Delta H > 14L && \text{Spinning tethers} \end{aligned} \qquad (5.1)$$

Given the fact that the required ΔHs (or alternatively ΔVs) are very high for a transfer from LEO to GTO, spinning tethers are the only practical solution for achieving the desired goal with tethers of moderate lengths.

Tether types

Tethers can have a constant cross section (cylindrical tethers) or a varying cross section (tapered tethers). The maximum velocity that a cylindrical spinning tether can sustain (the

critical velocity), without any payload attached to its end, is limited by its material properties and can be written as:

$$Vc = \sqrt{\frac{2\sigma}{\rho}} \tag{5.2}$$

where σ is the ultimate strength of the tether material and ρ is its mass density. A more realistic approach is to adopt a ratio $\sigma^* = \sigma / f$ where $f > 1$ is the stress safety factor. Eqn. (5.2) states that the ΔV that a cylindrical tether can provide is bounded. For example Spectra 2000 has a V_c = 2.6 km/s ($\sigma = 3.25 \times 10^9$ N/m^2 and ρ = 970 kg/m^3) with a safety factor of 1 (no safety margin) and V_c = 1.96 km/s with a safety factor of 1.75 as recommended for fail safe tethers [6].

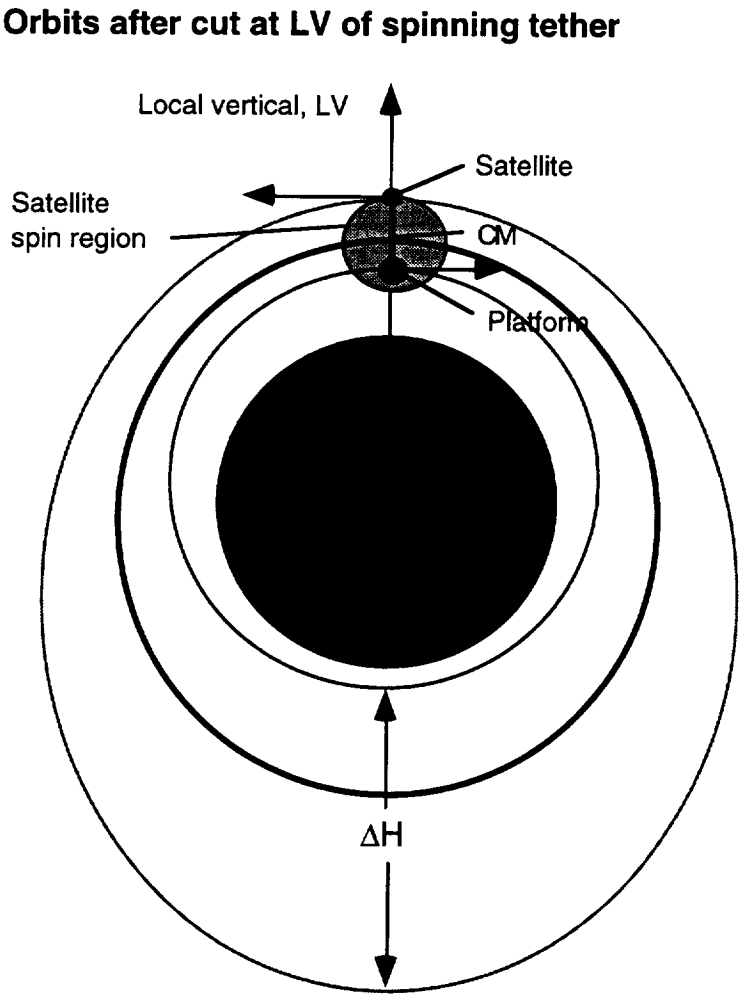

Fig. 5.1.1. Orbits after cut at LV of a spinning tether

Since the maximum load is at the hub of a spinning tether, the tether can be tapered thus saving tether mass and removing the limitation on the maximum sustainable ΔV. The mass of an optimally (i.e., with a constant stress distribution) tapered tether can be written as a function of the tip mass (payload) m_{PL} as follows:

$$M_{tether} = M_{PL}\sqrt{\pi}\frac{V}{V_c}\exp\left(\frac{V^2}{V_c^2}\right)erf\left(\frac{V}{V_c}\right) \tag{5.3}$$

where V is the tip velocity and erf() is the error function [3-4]. Figure 5.1.2 shows the tether/payload mass ratio for a cylindrical and a tapered tether of the same material (Spectra 2000) and a safety factor equal to 1.75.

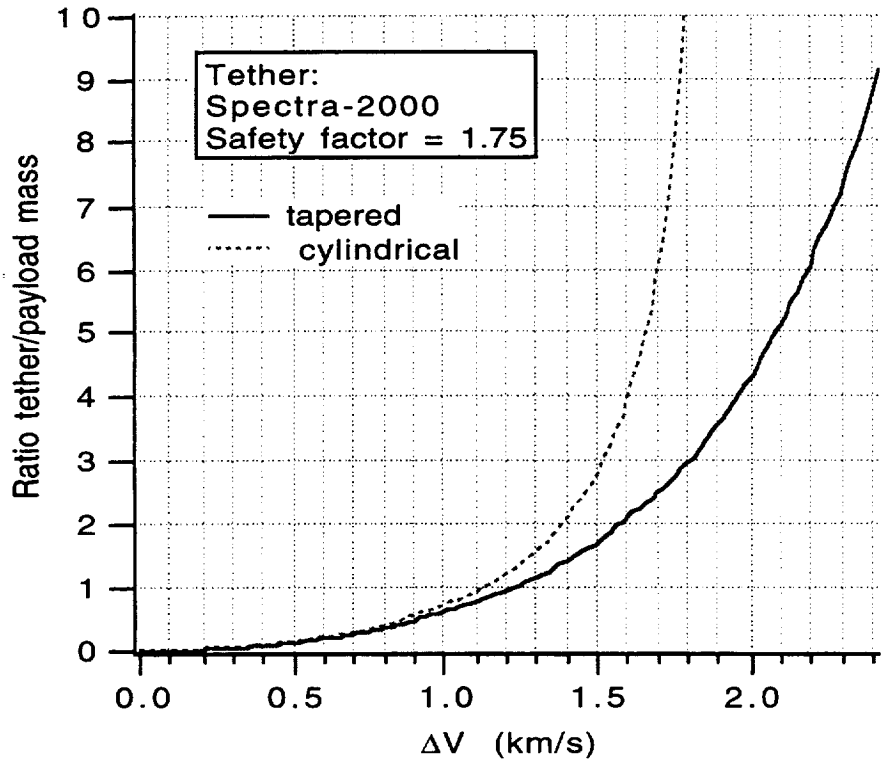

Fig. 5.1.2. Tether/payload mass ratio for cylindrical and tapered tethers.

In conclusion, a tapered tether is lighter than a cylindrical tether especially for ΔV > 1 km/s and more importantly the ΔV that a tapered tether can impart is not bounded by the strength to density ratio of the material.

Tether vs. rockets

Roughly speaking, a spinning tether can be compared to a rocket by comparing the tether mass needed to provide the desired ΔV to a payload and the propellant mass required to accomplish the same task [4]. We first introduce a performance index that relates the critical velocity of the tether to the ejection velocity of the propellant from the rocket nozzle, i.e., $n = V_c/(I_{sp}\, g)$ where I_{sp} is the specific impulse and g is the gravity acceleration on the Earth's surface (for a hydrazine system and several solid propellants, the product $I_{sp}g$ is ≈3 km/s). The ratio M_{prop}/M_{PL} where M_{prop} is the propellant needed for the transfer is [4]:

$$M_{prop} = M_{PL}\left[\exp\left(\frac{V^2}{I_{sp}g}\right)-1\right] = M_{PL}\left[\exp\left(n\frac{V}{V_c}\right)-1\right] \tag{5.4}$$

As shown in Figs. 5.1.3(a)-5.1.3(b) for different values of the tether material safety factor, the ratios M_{tether}/M_{PL} and M_{prop}/M_{PL} determine the relative mass of the tether vs. the propellant mass of an equivalent chemical system. Clearly, many other considerations apply to comparing a tether system vs. chemical propulsion among which the most important one is that a tethered system is reusable while a chemical system is not. Nevertheless, the plot of Fig. 5.1.3(b) gives a good indication of the ΔV range in which a spinning tether transportation system should operate with present day materials.

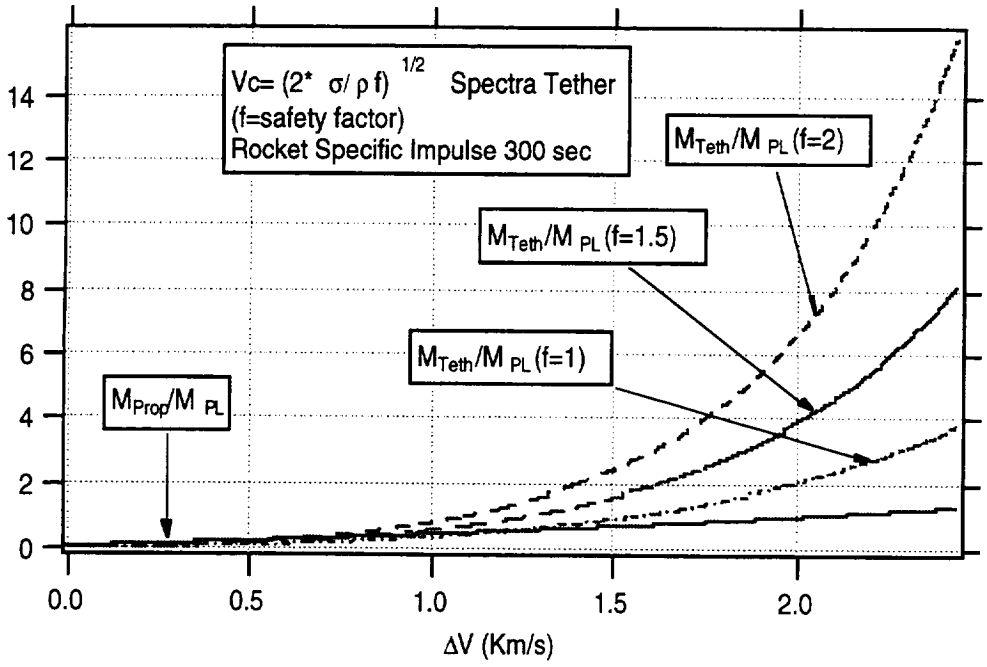

Fig. 5.1.3(a). Ratios of tether and propellant mass to payload mass vs. ΔV.

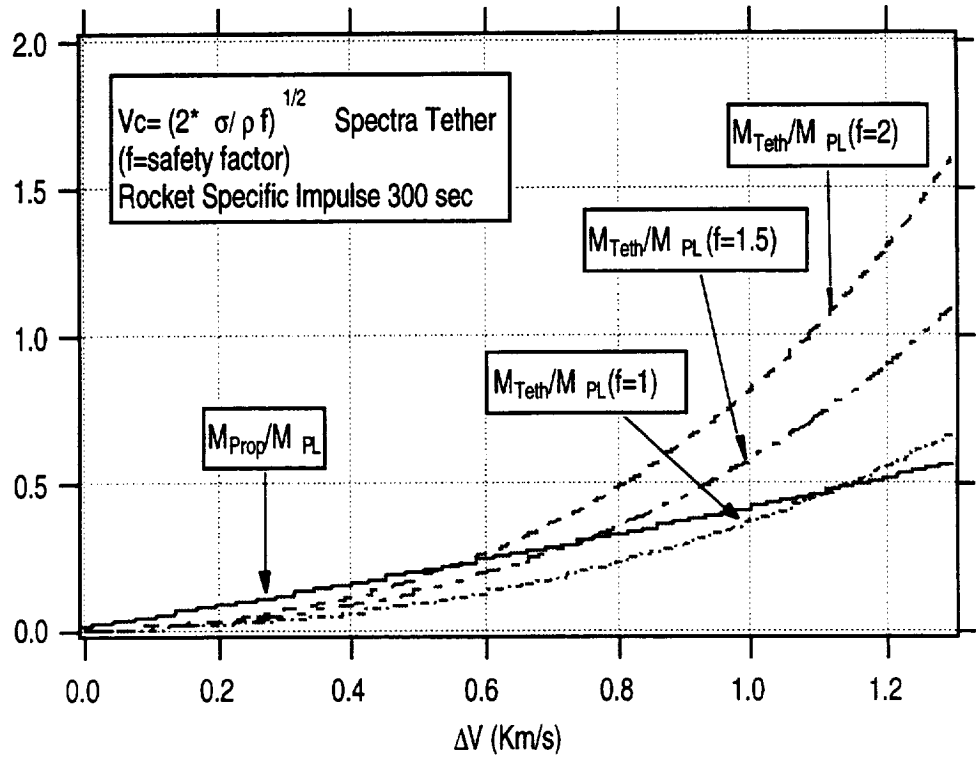

Fig. 5.1.3(b). Enlargement of previous figure for $\Delta V < 1.25$ km/s.

Let us look now at the ΔV required for transferring a satellite from LEO to GEO. The required injection velocity to transfer a payload (with a Hohmann transfer) to a higher orbit is shown in Fig. 5.1.4.

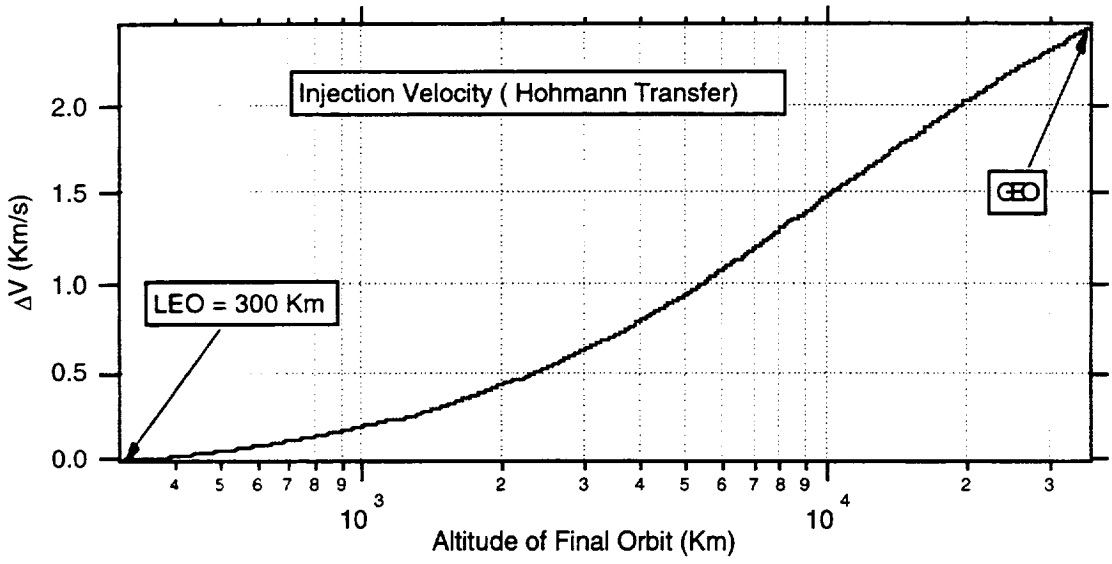

Fig. 5.1.4. Injection velocity required to transfer a payload from LEO to a given apogee.

The system must impart a ΔV of 2.4 Km/s to inject a payload into GTO (apogee height = 35,786 Km) while an additional 1.4 km/s is needed to circularize the orbit.

Consequently, if a single stage tethered system (with present day technology) were to be used to transfer a payload from LEO to GTO, the mass of the tether would be about 9x the payload mass while from Fig. 5.1.3(a) it can be concluded that the propellant (Hydrazine) mass would be less than 2x the payload mass. In other words, it would take about 5 launches for a single stage tethered system to become competitive. This is already an encouraging conclusion which however can be improved dramatically by looking into: (1) the trend in tether material improvement through the years in order to estimate possible values of the tether critical velocity 10-15 years from now; and (2) a two-stage system that by splitting the ΔV into two components utilizes the tethers at their best with present day technology.

It will be shown later on in this report that a two stage tethered system from LEO to GEO is more competitive, on a mass basis, than a present-day upper stage after only two launches.

Tether materials and future trends

The tether characteristic velocity depends on the material strength to density ratio. The change of this ratio through the years gives an indication of the future trend and the possible values of the tether characteristic velocity in the near future (see Fig. 5.1.5).

Figure 5.1.5 shows that the strength to density ratio of tether materials had two distinct eras during this century: (a) the metal era before 1960 with a very slow increase of the strength to weight ratio, and (b) the fiber era with a dramatic increase of the ratio after the year 1960.

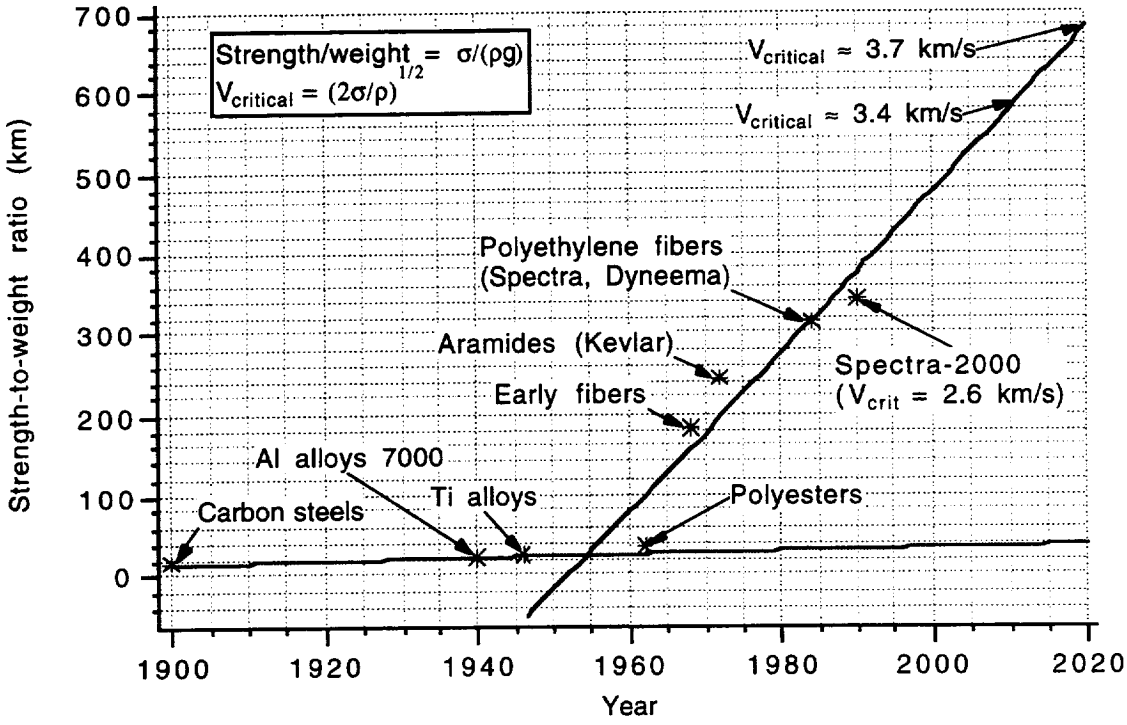

Fig. 5.1.5. Strength to density ratio of tether materials through this century and beyond.

If we believe in the linear regression analysis shown in Fig. 5.1.5, the strength to density ratio should be expected to increase by about 70% in the year 2010 with respect to the present value of Spectra 2000. Conversely, the tether critical velocity should increase by about 30% in the year 2010 with respect to the present value of Spectra 2000. Consequently, the tether in the year 2010 could be a factor 3 lighter than at present for a single stage tethered transportation system from LEO to GTO.

These improvements might seem dramatic but they would be completely eclipsed if experimental materials like Fullerenes come on line for the construction of long tethers. Fullerenes have demonstrated in the laboratory a strength to density ratio almost two orders of magnitude higher than Spectra 2000. At present, however, the samples being produced are only a few micron long [5] but several attempts are underway at making this new material suitable for forming tethers.

Mission Strategy

An alternative solution to reducing the mass of the tethered system (with present day technology) is by designing a two stage system. The first stage spinning in LEO injects the payload into a higher orbit where it is captured by the second stage spinning in MEO. After

the capture, the payload is released at a perigee passage into GTO. The 1st stage provides a velocity increase $\Delta V_1 = V_{tip\text{-}1}$ where the latter is the tip velocity of the stage. The second stage captures the payload at the bottom of the spin, during its retrograde rotation, and releases it at the top of the spin, during its posigrade rotation. Consequently, it accelerate the payload (with respect to the speed of its CM) from $-V_{tip\text{-}2}$ to $+V_{tip\text{-}2}$ thereby providing a total velocity increase of $\Delta V_2 = 2V_{tip\text{-}2}$. Since the masses of the first and second stages are determined by their tip velocities, we would expect that minimal tether mass configurations for a two stage system should be found for $\Delta V_2 > \Delta V_1$.

The optimal partition of ΔVs (or equivalently V_{tip}) between the two stages has been computed and the results are shown in Fig. 5.1.6. This figure shows the ratio between the total tether mass of the two stages and the payload mass vs. the ratio between the tip velocities of the two stages.

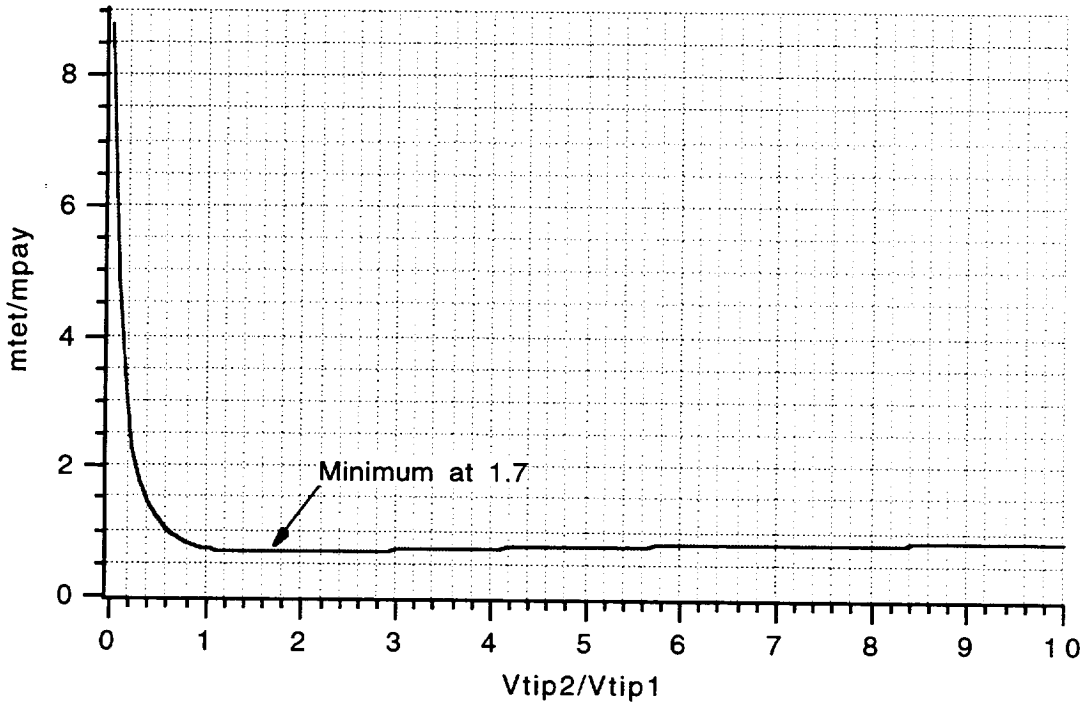

Fig. 5.1.6. Total tether mass over payload mass for a two-stage tethered system vs. the tether tip velocities ratio.

The minimum is for a tip velocity ratio $V_{tip\text{-}2}/V_{tip\text{-}1} \approx 1.7$. The tether/payload mass ratio increases strongly for ratios $V_{tip\text{-}2}/V_{tip\text{-}1} < 0.8$, and it reaches a value of 9 (consistent with a single stage tether system) for $V_{tip\text{-}2}/V_{tip\text{-}1} = 0$. On the contrary, the tether/payload mass ratio changes only slightly for $V_{tip\text{-}2}/V_{tip\text{-}1} > 0.8$. Consequently, the partition of the ΔVs

between the stages is rather free so long as $\Delta V_2 \geq 1.6\Delta V_1$ (remember that $\Delta V_2/\Delta V_1 = 2V_{tip\text{-}2}/V_{tip\text{-}1}$). It is worth noting that the optimum for a tether spinning system is for $\Delta V_2 > \Delta V_1$ unlike a conventional staging where the optimum is at $\Delta V_2 \approx \Delta V_1$.

Mission Analysis

Orbital Mechanics of a Two-stage Tethered System

In a two-stage tethered system, the 1st stage tether rotates with angular rate ω_1 and, in general, orbits in a LEO orbit $r_{p1} \times r_{a1}$ defined by its perigee and apogee radii. The 2nd stage, which rotates with an angular rate ω_2, is at an intermediate orbit (MEO) between LEO and GEO. This orbit is also elliptical in order to provide a velocity match at perigee, at the capture of the satellite released from the first stage, between the tether tip velocity and the incoming satellite that follows the transfer orbit (TO). For best efficiency, ΔVs are imparted at perigee where the energy produced by a given ΔV is maximum because the orbital velocity is maximum.

An important consideration to keep in mind is the synchronicity [6] between the LEO orbit, the transfer orbit (TO) after release from the 1st stage and the MEO orbit of the 2nd stage. Synchronicity between the orbits (also called orbital resonance) of the first and the second stage provides periodic encounters between the two stages. We must consider, however, the role played by the Earth oblateness on the differential precession of the orbits of the stages. The two orbits lie on the equatorial plane where the nodal regression and the apsidal precession add up. Consequently, the apsidal realignment rate of the two orbits determines the conjunction frequency of the two stages and, ultimately, the maximum frequency for transfer opportunities. In the two-stage configurations analyzed here, the period of orbit realignment for the two stages is about 70 days which corresponds to a maximum transfer frequency of about 5 per year. This transfer frequency can be doubled (to 10 transfers per year) by adding another 2^{nd} stage with a line of apses rotated by 90° with respect to the other 2^{nd} stage.

Synchronicity between the orbit of the second stage (MEO) and the transfer orbit of the payload (TO) provides multiple recapture opportunities if the first capture attempt is missed, i.e., there will be periodic encounters at the perigees of the two orbits after a miscapture.

The orbital periods of the TO orbit and of the MEO orbit can be expressed as follows:

$$P_{TO} = MP_1 \tag{5.5.a}$$

$$P_2 = NP_1 \tag{5.5.b}$$

where P stands for orbital period, the subscript 1 stands for 1st stage in LEO and 2 stands for 2nd stage in MEO. M and N do not have to be necessarily integer numbers for having periodic encounters but rather rational numbers. That is, M and N must satisfy the following equation in order to provide periodic encounters at perigee passages:

$$\frac{N}{M} = \frac{J}{K} \qquad \text{with J and K integer numbers} \tag{5.6}$$

The satellite is first released by the 1st stage at perigee, which must have the same orbital anomaly of the perigee of the 2nd stage. If the satellite is released when the tether crosses the local vertical (LV), the perigee of TO is also at the point of release. After a time $T_{rev} = NKP_1$ (revisit time) the satellite passes through the perigee of TO when the 2nd stage passes through the perigee of MEO (i.e., multiple recapture opportunities). The relative position and velocity of the satellite with respect to the tether tip of the 2nd stage dictate that:

$$r_{pTO} = r_{tip2} \;\rightarrow\; r_{p1} + L_{12} = r_{p2} - L_2 \tag{5.7.a}$$

$$v_{tip1} = v_{tip2} \;\rightarrow\; v_{p1} + \omega_1 L_{12} = v_{p2} - \omega_2 L_2 \tag{5.7.b}$$

in which 1 stands for 1st stage and 2 for 2nd stage and $L_1 = L_{11} + L_{12}$, $L_2 = L_{21} + L_{22}$ are the overall lengths of the 1st and 2nd stage tethers, ω_1 and ω_2 are the rotational rates of the two tethers. After defining $\chi_1 = m_{sat}/m_{plat1}$ and $\chi_2 = m_{sat}/m_{plat2}$, we have:

$$L_{11} = \frac{\chi_1}{1 + \chi_1} L_1$$

$$L_{12} = \frac{1}{1 + \chi_1} L_1$$

$$L_{21} = \frac{\chi_2}{1 + \chi_2} L_2 \tag{5.8}$$

$$L_{22} = \frac{1}{1 + \chi_2} L_2$$

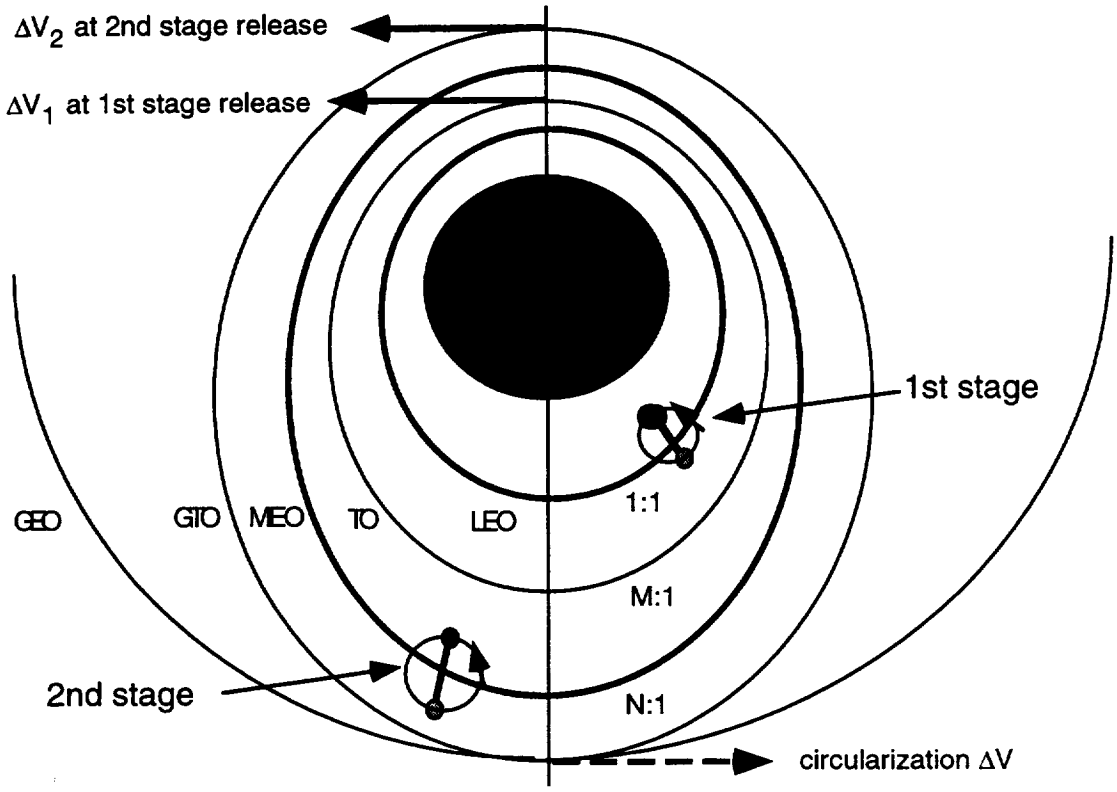

Fig. 5.1.7. Skematic of 2-stage tether system for LEO to GEO payload transfers.

In the following, we summarize the formulas for the computation of the orbital characteristics of satellite and platforms before release and after release for the general case of a first stage in an elliptical initial orbit. After defining μ the Earth's gravitational constant, the orbital velocity of the center of mass (CM) of the 1st stage at perigee is:

$$V_{p1} = \sqrt{\frac{\mu}{r_{p1}}}\sqrt{1 + e_1} \tag{5.9.a}$$

where r_{p1} is the perigee radius and e_1 is the orbital eccentricity. The velocities at perigee of the second stage before release and of the satellite on its transfer orbit TO are:

$$V_{p2} = \sqrt{\frac{\mu}{r_{p1}}}\sqrt{\frac{2}{(L_{12} + L_2)/r_{p1} + 1} - (1 - e_1)N^{(-2/3)}} \tag{5.9.b}$$

$$V_{pTO} = \sqrt{\frac{\mu}{r_{p1}}}\sqrt{\frac{2}{L_{12}/r_{p1} + 1} - (1 - e_1)M^{(-2/3)}} \tag{5.9.c}$$

Since $\omega_1 = \frac{1}{L_{12}}(V_{pTO} - V_{p1})$ and $\omega_2 = \frac{1}{L_2}(V_{p2} - V_{pTO})$, the rotational rates of the two stages are as follows:

$$\omega_1 = \frac{1}{L_{12}}\sqrt{\frac{\mu}{r_{p1}}}\left(\sqrt{\frac{2}{L_{12}/r_{p1}+1} - (1-e_1)M^{(-2/3)}} - \sqrt{1+e_1}\right) \qquad (5.10.a)$$

$$\omega_2 = \frac{1}{L_2}\sqrt{\frac{\mu}{r_{p1}}} \cdot \qquad (5.10.b)$$

$$\left(\sqrt{\frac{2}{(L_{12}+L_2)/r_{p1}+1} - (1-e_1)N^{(-2/3)}} - \sqrt{\frac{2}{L_{12}/r_{p1}+1} - (1-e_1)M^{(-2/3)}}\right)$$

The velocity increments ΔV_1 and ΔV_2 imparted by the first and second stage and the perigee velocity of TO are:

$$\Delta V_1 = \omega_1 L_{12} \qquad (5.11.a)$$

$$\Delta V_2 = 2\omega_2 L_{22} \qquad (5.11.b)$$

$$V_{pTO} = V_{p1} + \Delta V_1 \qquad (5.11.c)$$

The second stage captures the incoming satellite at a velocity equal to $V_{CM-2} - \omega_2 L_{22}$ and accelerates it to a velocity $V_{CM-2} + \omega_2 L_{22}$, thereby producing a velocity increment $\Delta V_2 = 2\omega_2 L_{22}$. However, the tip velocities and not the ΔVs determine the structural strength of the stages. The first stage tether must be designed to withstand a tip velocity $V_{tip-1} = \Delta V_1$ and the second stage a tip velocity $V_{tip-2} = 1/2\Delta V_2$.

The perigee radius and velocity of the satellite in GTO after release (with the tether along LV) from the second stage are:

$$r_{pGTO} = r_{p1} + L_{12} + 2L_{22} \qquad (5.12.a)$$

$$V_{pGTO} = V_{pTO} + \Delta V_2 \qquad (5.12.b)$$

From conservation of energy and angular momentum we can readily obtain the apogee radius and velocity of the satellite after release as follows:

$$r_{aGTO} = \frac{r_{pGTO}}{\frac{2\mu}{r_{pGTO}V^2_{pGTO}} - 1} \qquad (5.13.a)$$

$$V_{aGTO} = V_{pGTO} \frac{r_{pGTO}}{r_{aGTO}} \tag{5.13.b}$$

At the apogee of the geotransfer transfer orbit, the orbit must be circularized with an additional velocity increment ΔV_c as follows:

$$\Delta V_c = \sqrt{\frac{\mu}{r_{aGTO}}} - V_{aGTO} \tag{5.14}$$

In this study, the circularization ΔV is assumed to be supplied by the kick motor of the satellite. The overall ΔV_{Tot} for the transfer from LEO to GEO is:

$$\Delta V_{Tot} = \Delta V_1 + \Delta V_2 + \Delta V_c \tag{5.15}$$

At this point it is necessary to establish a procedure for computing the orbital period ratios M and N (for different tether lengths and mass ratios) which satisfy eqn. (5.6) and produces the desired apogee altitude of the satellite after release from the second stage. This search could be conducted by trial and error but it would be very time consuming. A faster procedure is by utilizing eqn. (5.13.a). After substitution of the relevant expressions and assuming that L_1 and $L_2 << r_1$, eqn. (5.13.a) yields:

$$(1+\chi_2)^2\left(1 - \frac{1-e_1}{2}N^{(-2/3)} + \frac{1-e_1}{4}M^{(-2/3)} + \chi_2\left(1 - \frac{1-e_1}{4}M^{(-2/3)}\right)\right)^{-2} - \frac{r_{p1}}{r_{aGTO}} - 1 \approx 0 \tag{5.16}$$

Equation (5.16) can be solved numerically to find N and M.

Figure 5.1.8 shows solutions for three relevant pairs of orbital period ratios i.e., (a) M = 2, N = 4, (b) M = 1.5, N = 4.5, (c) M = 1.2, N = 3.6, and for two eccentricities of the LEO orbit. It is worth reminding that M is the ratio between the TO and LEO orbital periods while N is the ratio between the MEO and LEO orbital periods. From eqn (5.12) we can also see that the mass ratio χ_1 does not play any role in the orbit synchronicity while the ratio χ_2 plays an important role. Since $1/\chi_2$ is the platform_2/satellite mass ratio, the lower its value the lighter the platform of the second stage. The lightest platform of the second stage, among the cases of interest, is obtained for case (b) and its mass is about 1.3x the mass of the payload.

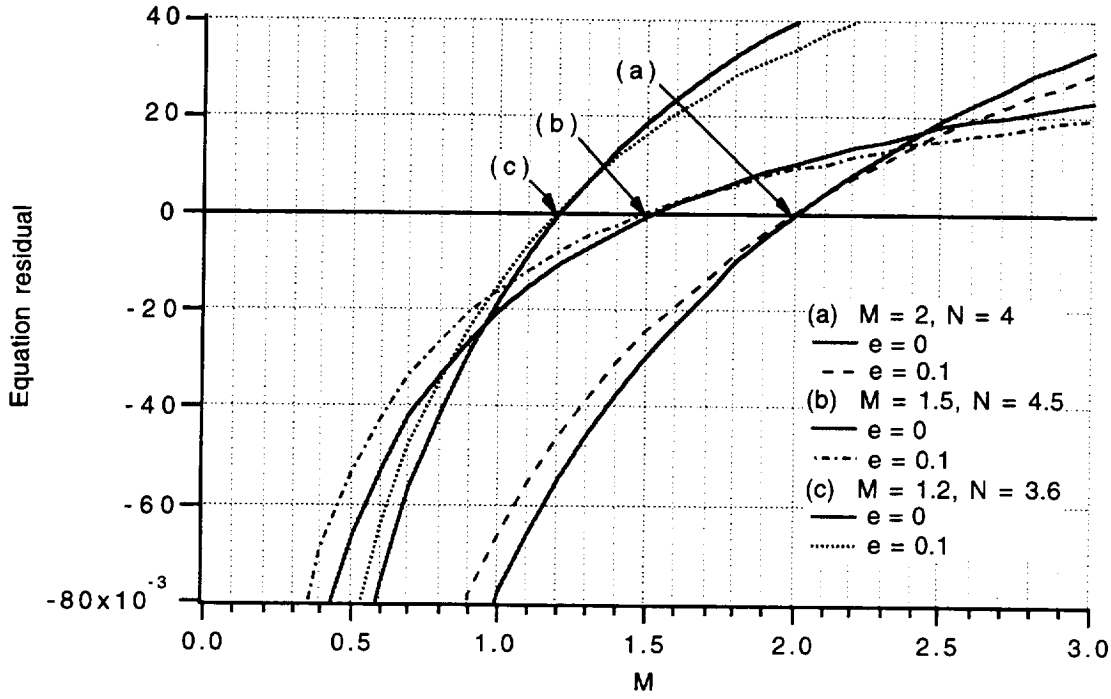

Fig. 5.1.8. Possible roots of the synchronicity equation.

Platform Orbits after Release

Tethers (whether spinning or not) simply exchange angular momentum between the end bodies once they are cut. For this reason, if the satellite is propelled upward after release, the platform is propelled downward. The satellite altitude gain and the platform altitude loss depend upon the satellite over platform mass ratio. The orbital characteristics of the platform after release can be computed from conservation of energy and angular momentum.

The orbit of the platform of the 2nd stage after release is not critical because the MEO orbit is a high-energy orbit. Consequently, the mass of the 2nd stage platform is solely determined by the synchronicity equation as pointed out before. On the contrary, the mass of the 1st stage platform is determined by the characteristics of the LEO orbit and the velocity increment ΔV_1 imparted by the 1st stage. The first stage must be prevented from reentering the atmosphere after releasing the payload. From this point of view initial elliptical orbits are advantageous when compared to an equal-energy circular orbit because the ΔV (at perigee) causes a decrease of the apogee height after release in the former case and a (dangerous) decrease of the perigee height after release in the latter case.

The geocentric radius of the platform absidal point (that can either be a perigee or an apogee depending on the magnitude of the ΔV) opposite to the release point can be computed from conservation of energy and angular momentum, as follows:

$$r_{pl,s} = \frac{r_{pl,r}}{\frac{2\mu}{r_{pl,r}\ V_{pl,r}^2} - 1} \tag{5.17.a}$$

$$V_{pl,s} = V_{pl,r}\, r_{pl,r}/r_{pl,s} \tag{5.17.b}$$

and the platform velocity at release $V_{pl,r}$ is given by

$$V_{pl,r} = V_{CM} + \Delta V_{pl} \tag{5.17.c}$$

$$\Delta V_{pl} = -\chi \Delta V \tag{5.17.d}$$

In eqns. (5.17), the subscript pl stands for platform, r identifies the point at release and s the opposite absidal point, χ is the mass ratio and ΔV is the velocity increment of the payload. These equations can be applied either to the platform of the 1st or 2nd stage.

Tethers masses

The tether mass for an optimally-tapered tether is proportional to the tip mass (satellite) according to the following formula:

$$m_{Tet} = m_{tip}\ \sqrt{\pi}\frac{V_{tip}}{V^*}\exp\left(\frac{V_{tip}^2}{V^{*2}}\right)\mathrm{erf}\left(\frac{V_{tip}}{V^*}\right) \tag{5.18}$$

where m_{tip} is the tip mass and $V^* = \sqrt{2\sigma/(\rho f)}$, σ is the ultimate stress, ρ the material density and f the safety factor. The tether material adopted for this study is Spectra-2000 with a density $\rho = 970$ kg/m^3 and an ultimate strength $\sigma = 3.25 \times 10^9$ N/m^2. The tether safety factor is 1.75 as recommended for fail-safe tethers in Ref. 6.

The tether has its maximum cross section at the system CM and tapers toward the satellite and the platform. The cross section at the tether tip is given by (see Ref. 4)

$$A_{tip} = \frac{m_{tip} V_{tip}^2}{\sigma^* L_d} \tag{5.19}$$

where $\sigma^* = \sigma/f$ and L_d is distance from CM to the tip mass (either payload or platform). The tether cross section at CM is readily obtained as follows:

$$A_{CM} = A_{tip} \exp\left(\frac{V_{tip}^2}{V^{*2}}\right) \tag{5.20}$$

where the ratio A_{CM}/A_{tip} is called the tapering ratio.

Accelerations

The maximum acceleration on the payload attached to a stage is simply:

$$a_{max} = V_{tip}^2/L_d \tag{5.21}$$

The relative acceleration (between the incoming payload and the rotating tip mass of the 2nd stage) can also be readily computed with respect to the LV-LH reference frame. From symmetry considerations, the LH component of the relative acceleration at capture is zero. In fact, the horizontal component of the orbital velocity is symmetric with respect to perigee and the horizontal component of the rotational velocity profile is also symmetric with respect to LV. The symmetry is preserved when we take the difference of the two velocities in order to compute the relative velocity. Consequently, the point of capture is a stationary point in the horizontal relative velocity profile which means that the horizontal acceleration at capture is zero.

On the contrary, the vertical orbital and rotational components are antisymmetric and, consequently, the vertical component of the relative acceleration is different from zero. Its numerical value can be simply computed by considering that the vertical component of the orbital acceleration at perigee is zero leaving only the non-zero vertical component of the rotational acceleration (at capture) at the crossing of LV. The vertical relative component of the acceleration at capture, therefore, is:

$$a_{LV}^{rel} = V_{tip}^2 / L_2 \tag{5.22}$$

where L_2 is the tether length of the 2nd stage. The total tether length is used here because, if we assume for simplicity that the capture device has negligible mass with respect to the platform, the CM of the 2nd stage *before capture* coincides approximately with the platform.

From eqns. (5.21-5.22), longer tethers imply smaller accelerations when the satellite is attached to a stage and, more importantly, at capture. In the design of the system, we have limited the maximum tether lengths to $\leq$ 100 km which sets the lower limit of the accelerations as shown later on.

Numerical Cases

By using the equations derived above, several cases have been analyzed for different orbital eccentricities and synchronicity factors. The cases presented in this chapter were derived for the heaviest payloads predicted in the traffic model, that is, telecommunication satellites of the 9000-lb class (4082 kg) which are heavier than an Intelsat VII.

In order to perform a meaningful comparison, initial orbits with approximately the same energy were adopted. Equal energies of the initial orbits imply same semimajor axes and, for this reason, similar semimajor axis were adopted for the initial orbits. Also a minimum perigee altitude of 400 km (r_p = 6778 km) was assumed.

The numbering of the cases (from 5a to 6d) presented in the Tables 5.1.1-5.1.5 may seem odd but it reflects the original numbering of the cases. We must preserve it in this report because the original numbering appears in several related plots and analyses.

System Mass

Tables 5.1.1 through 5.1.5 clearly show that, with present day technology, a single stage tethered system from LEO to GEO would be about 4 times more massive than the best results obtained here with a two stage system (cases 6b, 6c and 6d).

The masses shown in the tables are end-of-life (EOL) masses. At the beginning-of-life (BOL) the system must include all the propellant needed for reboosting the stages after each transfer for the number of missions planned between propellant resupplies. The trade off among various thrust systems, carried out by D.J. Vonderwell at Boeing, Huntsville, AL [7], favors high specific impulse (e.g., I_{sp} = 3000 s) ion thrusters. After assuming a 70-day reboost time, the propellant per launch, the power required and the EOL masses of the systems for the various cases of interest are shown in Table 5.1.6. Propellant mass for reboosting can be traded in for lower power by utilizing lower-specific-impulse thrusters.

For the sake of clarity, the masses of the various components are expressed in term of multiplication factors of the maximum payload mass (4082 kg) in Table 5.1.7 for case 6d.

Table 5.1.1. Key parameters of a two-stage tethered system for transferring a 4082-kg (9000 lb) satellite from LEO to GEO with orbital ratios M = 2 and N = 4 and for a single stage tethered system. Here the initial LEO orbits are circular.

	Two stage	Single stage
Dimensions: All distances (km) All masses (kg)	$L_1 = L_2 = 20$ km $\chi_1 = 0.191$; $\chi_2 = 0.454$ $e_1 = 0$	$L_1 = 60$ km $\chi_1 = 0.107$ $e_1 = 0$
1st stage CM orbit (km) Altitudes (km) Semimajor axis (km)	7588 x 7588 1210 x 1210 7588	7588 x 7588 1210 x 1210 7588
2nd stage CM orbit	7624.8 x 30616	n/a
Satellite orbit after 1st stage release	7604.8 x 16486	7642.2 x 42165
Platform-1 orbit after 1st stage release Altitudes	6675.5 x 7584.8 298 x 1207	6681 x 7582.2 303 km
Satellite orbit after 2nd stage release	7632.3 x 42165	n/a
Platform-2 orbit after 2nd stage release	7612.3 x 20260	n/a
Rotational rate ω_1 (rad/s)	0.07277	0.04
Rotational rate ω_2 (rad/s)	0.03397	n/a
$\Delta V_1 = V_{tip\text{-}1}$ (km/s)	1.222	2.149
$\Delta V_2 = 2V_{tip\text{-}2}$ (km/s)	0.934	n/a
$\Delta V_{circularize}$ (km/s)	1.372	1.371
ΔV_{Tot} (km/s)	3.528	3.520
Platform-1 mass (kg)	21370	38150
Tether-1 mass (kg)	4720	23890
Platform-2 mass (kg)	8990	n/a
Tether-2 mass (kg)	700	n/a
1st stage mass (kg) 2nd stage mass (kg)	26090 9690	62040 n/a
EOL Mass Grand Total (kg)	35780	62040

Table 5.1.2. Key parameters of two-stage tethered system from LEO to GEO with elliptical initial orbits. For all cases $L_1 = L_2 = 20$ km, M = 2, N =4.

	Case 5a	Case 5b	Case 5c	Case 5d
Dimensions All distances (km) All masses (kg)	$\chi_1 = 0.352$ $\chi_2 = 0.473$ $e_1 = 0.1$	$\chi_1 = 0.15$ $\chi_2 = 0.462$ $e_1 = 0.05$	$\chi_1 = 0.275$ $\chi_2 = 0.462$ $e_1 = 0.05$	$\chi_1 = 0.26$ $\chi_2 = 0.462$ $e_1 = 0.04$
1st stage CM orbit Altitudes Semimajor axis	6778 x 8397.2 400 x 2019 7588	7208 x 7966.7 830 x 1589 7588	7208 x 7966.7 830 x 1589 7588	7288 x 7895.3 910 x 1517 7588
2nd stage CM orbit	6812.8 x 31426	7245.4 x 30993	7243.7 x 30994	7323.9 x 30936
Satellite orbit after 1st stage release	6792.8 x 17296	7225.4 x 16863	7223.7 x 16865	7303.9 x 16798
Plat-1 orbit after 1st stage release Altitudes	6772.8 x 6788 395 x 410	7205.4 x 7232.6 827 x 855	6684.6 x 7203.7 307 x 826	6677.5 x 7284 300 x 906
Satellite orbit after 2nd stage release	6819.9 x 42165	7252.8 x 42165	7251 x 42165	7331.2 x 42165
Plat-2 orbit after 2nd stage release	6799.9 x 20878	7232.8 x 20556	7231 x 20558	7311.2 x 20492
Rot. rate ω_1 (rad/s)	0.07519	0.0672	0.0746	0.0743
Rot. rate ω_2 (rad/s)	0.03134	0.0327	0.0327	0.033
ΔV_1 (km/s)	1.112	1.17	1.17	1.18
ΔV_2 (km/s)	0.851	0.896	0.896	0.9
ΔV_{circ} (km/s)	1.452	1.41	1.41	1.4
ΔV_{Tot} (km/s)	3.415	3.476	3.476	3.48
Platform-1 mass	11600	27210	14850	15700
Tether-1 mass	4100	4100	4490	4530
Platform-2 mass	8630	8840	8840	8840
Tether-2 mass	600	650	650	650
1st stage mass 2nd stage mass	15700 9230	31310 9490	19340 9490	20230 9490
EOL Mass Grand Total	24930	40800	28830	29720

Table 5.1.3. Key parameters of two-stage tethered system from LEO to GEO for orbital ratios M = 2 and N = 4 and different tether lengths.

Dimensions Distances (km), Masses (kg)	Case 5d (repeated)	Case 5e	**Case 5f**
1st stage mass ratio	$\chi_1 = 0.26$	$\chi_1 = 0.26$	**$\chi_1 = 0.26$**
2nd stage mass ratio	$\chi_2 = 0.462$	$\chi_2 = 0.462$	**$\chi_2 = 0.462$**
LEO eccentricity	$e_1 = 0.04$	$e_1 = 0.04$	**$e_1 = 0.04$**
Capture revisit time (hr:min)	7:18	7:19	**7:20**
LEO-GEO transfer time (hr:min)	16:21	16:23	**16:25**
1st stage tether length (km)	$L_1 = 20$	$L_1 = 60$	**$L_1 = 100$**
2nd stage tether length (km)	$L_2 = 20$	$L_2 = 20$	**$L_2 = 30$**
1st stage CM orbit	7288 x 7895.3	7298 x 7906.2	**7308 x 7917**
Altitudes	910 x 1517	920 x 1528	**930 x 1539**
Semimajor axis	7588	7602	**7612**
2nd stage CM orbit	7323.9 x 30936	7365.6 x 30946	**7417.4 x 30947**
Sat. orbit after 1st stage release	7303.9 x 16798	7345.6 x 16789	**7387.4 x 16781**
Plat-1 orbit after 1st stage release	6677.5 x 7284	6689.5 x 7285.6	**6701.3 x 7287.4**
Altitudes	300 x 906	311 x 908	**323 x 909**
Sat. orbit after 2nd stage release	7331.2 x 42165	7373 x 42165	**7428.4 x 42165**
Plat-2 orbit after 2nd stage release	7311.2 x 20492	7353 x 20488	**7398.4 x 20482**
Rot. rate ω_1 (rad/s)	0.0743	0.0242	**0.0142**
Rot. rate ω_2 (rad/s)	0.0331	0.0331	**0.0218**
$\Delta V_1 = V_{tip1}$ (km/s)	1.18	1.15	**1.12**
$\Delta V_2 = 2V_{tip2}$ (km/s)	0.9	0.9	**0.9**
ΔV_{circ} (km/s)	1.4	1.4	**1.39**
ΔV_{Tot} (km/s)	3.48	3.45	**3.41**
Sat. acceleration on 1st stage	8.9	2.8	**1.6**
LV acceleration at capture (g)	2.2	2.2	**1.4**
LH acceleration at capture (g)	0	0	**0**
1st stage mass	20230	20230	**20230**
2nd stage mass	9490	9490	**9490**
EOL Mass Grand Total	29720	29720	**29720**

Table 5.1.4. Key parameters of two-stage tethered system from LEO to GEO. For all cases $L_1 = L_2 = 20$ km, M = 1.5, N = 4.5.

	Case 6a	Case 6b
Dimensions All distances (km) All masses (kg)	$\chi_1 = 0.4$ $\chi_2 = 0.75$ $e_1 = 0.04$	$\chi_1 = 0.54$ $\chi_2 = 0.753$ $e_1 = 0.1$
1st stage CM orbit Altitudes Semimajor axis	7268 x 7873.7 890 x 1496 7571	6778 x 8284.2 400 x 1906 7531
2nd stage CM orbit	7302.3 x 33969	6811 x 34244
Sat. orbit after release	7282.4 x 12559	6791 x 12946
Plat-1 orbit after release Altitudes	6677 x 7262 299 x 884	6683 x 6771 305 x 393
Sat. orbit after release	7305.2 x 42165	6813.8 x 42165
Plat-2 orbit after release	7285 x 14052	6793.8 x 14417
Rot. rate ω_1 (rad/s)	0.053641	0.0564
Rot. rate ω_2 (rad/s)	0.057751	0.0553
$\Delta V_1 = V_{tip1}$ (km/s)	0.77	0.73
$\Delta V_2 = 2V_{tip2}$ (km/s)	1.32	1.26
ΔV_{circ} (km/s)	1.40	1.45
ΔV_{Tot} (km/s)	3.49	3.44
Platform-1 mass	10470	7560
Tether-1 mass	1900	1900
Platform-2 mass	5440	5420
Tether-2 mass	1700	1550
1st stage mass 2nd stage mass	12370 7140	9460 6970
EOL Mass Grand Total	19510	16430

Table 5.1.5. Key parameters of two-stage tethered system from LEO to GEO for orbital ratios M = 1.5 and N = 4.5 and different tether lengths.

Dimensions Distances (km), Masses (kg)	Case 6b (repeated)	Case 6c	**Case 6d**
1st stage mass ratio	$\chi_1 = 0.54$	$\chi_1 = 0.54$	**$\chi_1 = 0.54$**
2nd stage mass ratio	$\chi_2 = 0.753$	$\chi_2 = 0.753$	**$\chi_2 = 0.753$**
LEO eccentricity	$e_1 = 0.1$	$e_1 = 0.1$	**$e_1 = 0.1$**
Capture revisit time (hr:min)	8:08	8:08	**8:10**
LEO-GEO transfer time (hr:min)	16:08	16:08	16:12
1st stage tether length (km)	$L_1 = 20$	$L_1 = 40$	**$L_1 = 60$**
2nd stage tether length (km)	$L_2 = 20$	$L_2 = 40$	**$L_2 = 80$**
1st stage CM orbit	6778 x 8284.2	6778 x 8284.2	**6798 x 8308.7**
Altitudes	400 x 1906	400 x 1906	**420 x 1931**
Semimajor axis	7531	7531	**7551**
2nd stage CM orbit	6811 x 34244	6844 x 34211	**6917 x 34259**
Sat. orbit after 1st stage release	6791 x 12946	6804 x 12933	**6837 x 12958**
Plat-1 orbit after 1st stage release	6683 x 6771	6687 x 6764	**6709.7 x 6777**
Altitudes	305 x 393	309 x 386	**332 x 399**
Sat. orbit after 2nd stage release	6813.8 x 42165	6849.6 x 42165	**6928.2 x 42165**
Plat-2 orbit after 2nd stage release	6793.8 x 14417	6809.6 x 14404	**6848.2 x 14434**
Rot. rate ω_1 (rad/s)	0.0564	0.0277	**0.0181**
Rot. rate ω_2 (rad/s)	0.0553	0.0272	**0.0132**
$\Delta V_1 = V_{tip1}$ (km/s)	0.73	0.72	**0.71**
$\Delta V_2 = 2V_{tip2}$ (km/s)	1.26	1.24	**1.2**
ΔV_{circ} (km/s)	1.45	1.45	**1.44**
ΔV_{Tot} (km/s)	3.44	3.41	**3.35**
Sat. acceleration on 1st stage	4.2	2	**1.3**
LV acceleration at capture (g)	6.2	3	**1.4**
LH acceleration at capture (g)	0	0	**0**
1st stage mass	9460	9460	**9460**
2nd stage mass	6970	6970	**6970**
EOL Mass Grand Total	16430	16430	**16430**

70 day reboost time
tb/Period = 0.35

Isp = 3000 s (ion engine)
Efficiency = 0.75

	LEO Platform		MEO Platform			
Case	Prop Mass per launch (kg)	Power Required (kW)	Prop Mass per launch (kg)	Power Required (kW)	System Prop Mass per launch (kg)	*EOL system mass (kg)
5a	840	58.025	526	35.147	1366	24930
5b	773	51.629	554	37.121	1328	40800
5c	859	58.586	554	37.125	1413	28830
5d	858	58.386	558	37.389	1416	29720
5e	862	58.301	560	37.545	1422	29720
5f	867	58.236	557	37.332	1425	29720
6a	519	34.930	938	67.155	1457	19150
6b	520	35.445	886	62.910	1406	16430
6c	522	35.372	880	62.384	1402	16430
6d	523	35.232	872	61.791	1395	16430

* - EOL system mass does not include payload mass and propellant mass

Table 5.1.6. Power and propellant mass requirements for the LEO to GEO tethered system [adapted from Boeing]

Table 5.1.7. Masses of components expressed as mutiplication factors of the maximum payload mass of 4082 kg for case 6d. The propellant mass is for 1 mission at maximum payload capacity.

Component	Factorx satellite mass
1st stage platform	1.8x
1st stage tether	0.5x
2nd stage platform	1.3x
2nd stage tether	0.4x
1st stage propellant	0.13x
2nd stage propellant	0.21x
System (w/o payload)	4.3x

If we consider that the total mass of an IUS Upper Stage (which can transfer a 4.5-ton payload from LEO to GTO) is equal to 14800 kg [8], then it can be concluded that the tethered system becomes competitive, on a mass basis, after 2 missions.

Tether sizes

Fail-safe tethers will likely be the preferable candidates for spinning tethers. If we assume, for the sake of picturing the size, that the tethers have solid cross section, the tether diameters for the best-case system under consideration (case 6d) average about 0.64 cm for the 1st stage tether and 0.48 cm for the 2nd stage. The ratio between the cross section at the tether tip and at the CM (i.e., the tapering ratio) is 1.1. Since the tapering ratio is close to unity, we could for simplicity of construction utilize non-tapered tethers of maximum cross sections at the expense of a small mass increase.

This last conclusion stems from the fact that in a two-stage tethered system from LEO to GEO the ΔV provided by each stage is well below 1 km/s and, consequently, tapered tethers do not have a striking mass advantage over cylindrical tethers.

Accelerations

The maximum acceleration at capture is 1.4 g (that is all in the vertical component because the horizontal component is zero) for the most interesting case 6d. The maximum accelerations on the satellite when attached to the 1st and 2nd stages are 1.3 g and 0.8 g, respectively for case 6d. Accelerations can be reduced in accordance with eqns. (5.21) and (5.22) by adopting longer tethers.

Mission Sequence

Figures 5.1.9(a)-5.1.9(c) [9] show the mission sequence and orbits for case 6d. The satellite is first released from the 1st stage at the appropriate phase angle (that depends upon the M/N ratio) with respect to the perigee. For case 6d the satellite is released from the 1st stage when the 2nd stage is 2:43 hr:min before its perigee passage. After the satellite is captured by the second stage at perigee, the satellite is released one orbit later when the second stage passes again through perigee. The total transfer time from LEO to GEO in case the satellite is captured at the first attempt is 16:12 hr:min for case 6d (M = 1.5 and N = 4.5). For case 5f (M = 2 and N =4) the total transfer time is 16:25 hr:min.

Revisit and Transfer Times

The time $T_{rev} = NKP_1$ is the periodic revisit time between the 2nd stage and the satellite released from the 1st stage in case of miscapture. Cases with M = 2, N = 4 have a slightly shorter revisit time than cases with M = 1.5, N = 4.5. In fact, in the former case N = 4 and K = 1 (see eqn. 5.6) while in the latter case N = 4.5 and K = 1. The revisit time is equal to 7:20 hr:min for case 5f with M = 2 and N = 4 and 8:10 hr:min for case 6d with M = 1.5 and N = 4.5.

Mission sequence, Snapshot #1

- Time = 0
  Satellite release from stage 1

  Orbits (altitudes kmxkm)
  – Before release
  • stage-1 CM (LEO) 420x1931
    orbital period 1:1 1:49 hr:min

  • stage-2 CM (MEO) 539x27881
    orbital period 4.5:1 8:10 hr:min

  – After release
  • sat. transfer orbit (TO) 459x6580
    orbital period 1.5:1 2:43 hr:min

  • platform-1 orbit 332x399

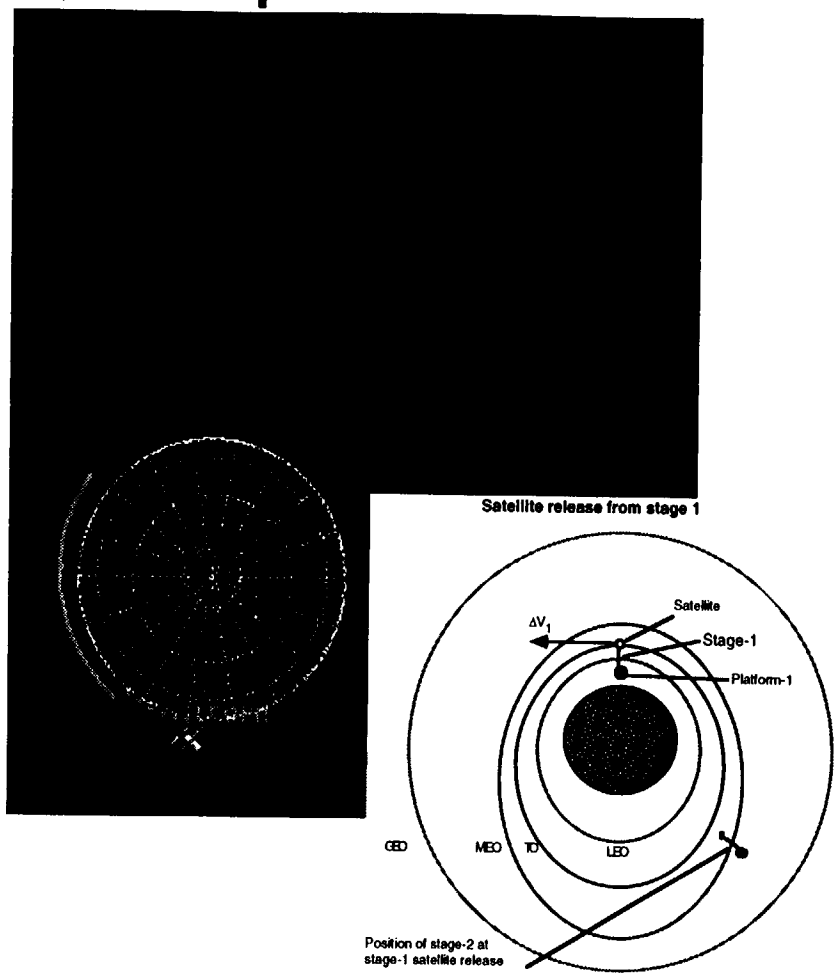

Fig. 5.1.9(a). Mission sequence for case 6d. Snapshot #1: satellite release from 1st stage [from Boeing].

Mission sequence, Snapshot #2

- Time = 2:43 hr:min
  Satellite capture by stage 2

  Orbits (altitudes kmxkm)
  – Before capture
  • sat. transfer orbit (TO) 459x6580

  – After capture
  • stage-2 orbit in MEO

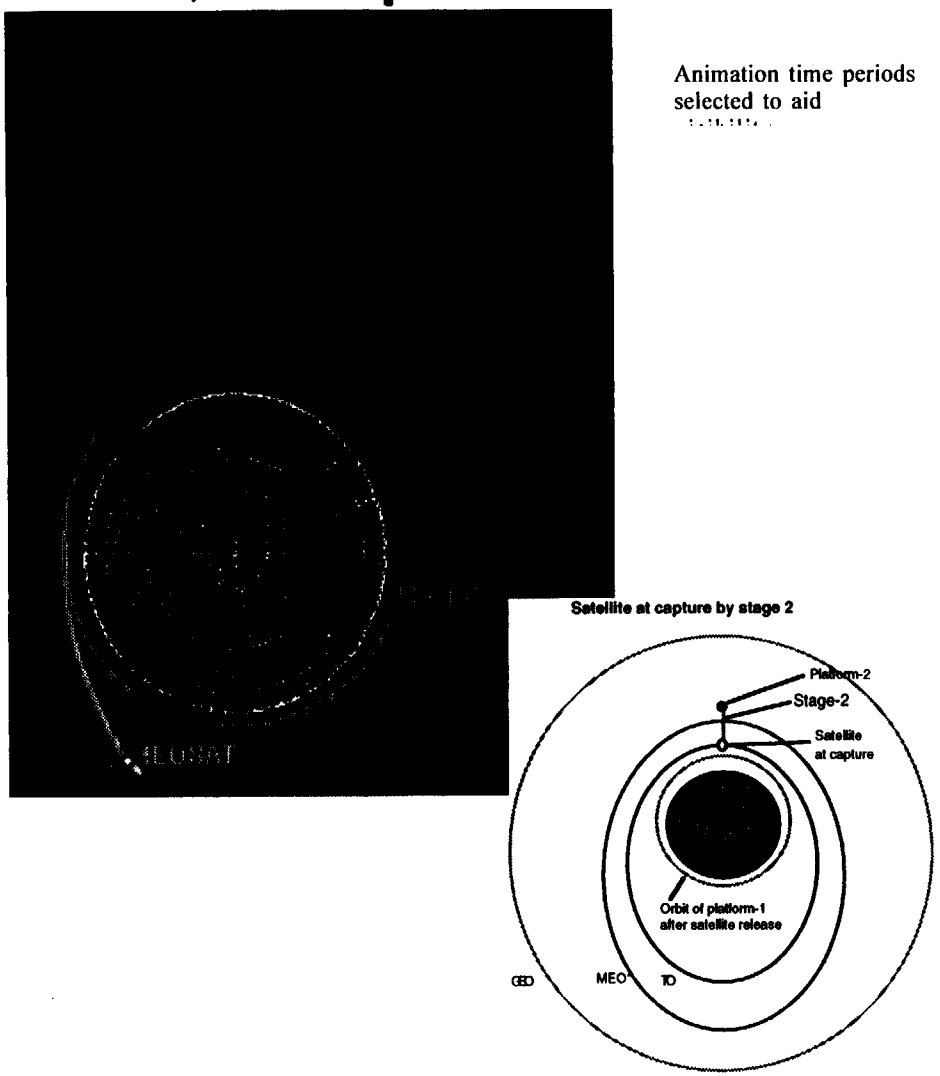

Fig. 5.1.9(b). Mission sequence for case 6d. Snapshot #2: satellitecapture by 2nd stage [from Boeing].

Mission sequence, Snapshot #3

- Time = 10:53 hr:min
  Satellite release from stage 2

  Orbits (altitudes kmxkm)
  – Before release
  • stage-2 in MEO

  – After release
  • satellite in GTO 550x35787
    orbital period 10:38 hr:min

- Time = 16:12 hr:min
  Arrival of satellite at apogee of GTO

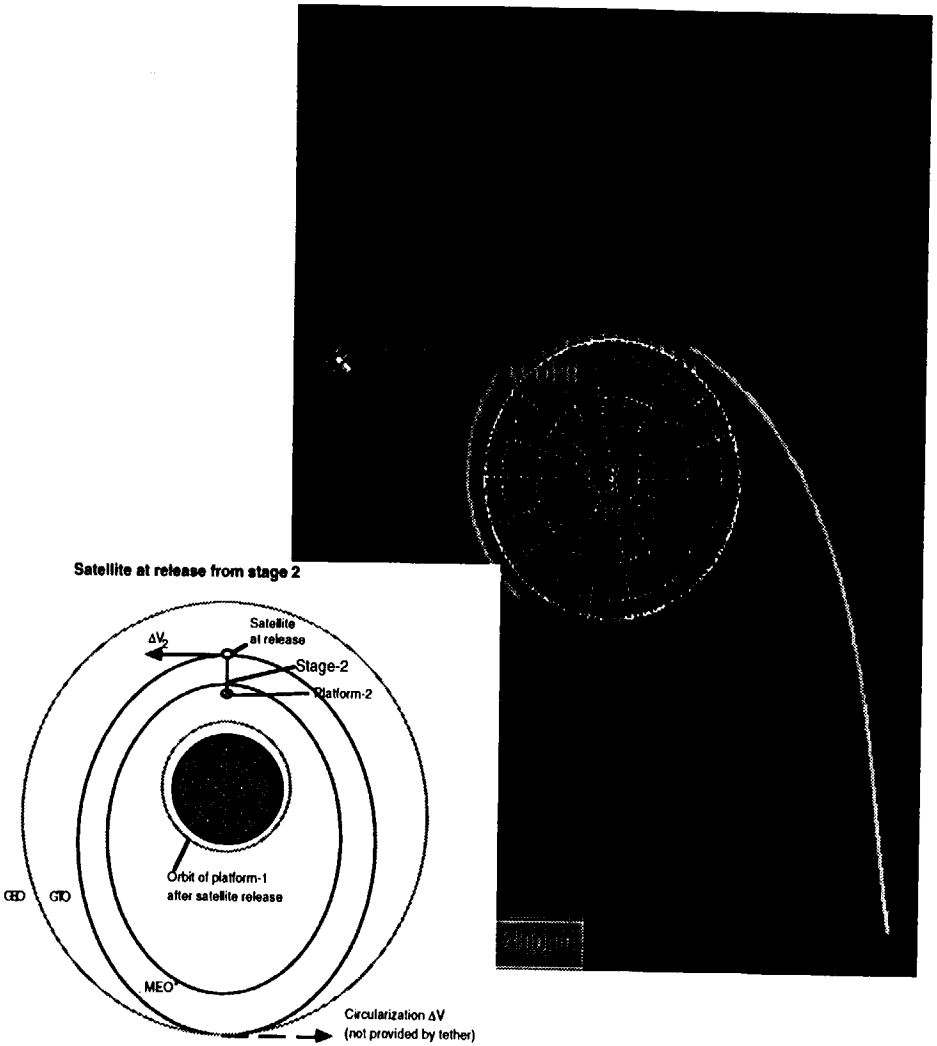

Fig. 5.1.9(c). Mission sequence for case 6d. Snapshot #3: satellite release from 2nd stage [from Boeing].

Payloads with different masses

The cases analyzed previously were all for the heaviest payloads of 4082 kg (9000 lb). The system however can handle any lighter payload with ease. Lighter payloads in fact only require adjustments of the rotational rates of the two stages. The adjustments of the orbits of the two stages are almost negligible. The orbit adjustments, in fact, are only of a few kilometers in order to compensate for the fact that the CMs of the two stages have shifted somewhat because of the lighter payload. The orbital adjustment are therefore very minor and they can be simply implemented during the reboost phases of the stages.

In the 9000-lb cases analyzed before, the rotational rates of the second stage at capture and at release of the payload were the same and equal to ω_2. This implies that the second stage does not need to be spun up or down after the capture of a 9000-lb payload. For payloads lighter than 9000 lb, the rotational rate at release from the 2nd stage ω_{2b} is lower than at the rate at capture ω_{2a}. Consequently, the second stage must be spun down after capture. This can be accomplished by either lengthening the tether (i.e., because of the conservation of angular momentum, the tip speed changes inversely with the tether length) or by using electrical thrusters or a combination of the two techniques.

Table 5.1.8 shows the orbital characteristics and other relevant parameters of case 6d for payloads of 9000 lb (repeated), 5000 lb and 2000 lb. In the table, ω_1 is the rotational rate of the 1st stage and ω_{2a} and ω_{2b} are the rotational rates of the 2nd stage at capture and at release, respectively. It should be pointed out that the synchronicity of the orbits and the zero distance at capture is preserved for all payload masses thanks to the minor orbit adjustments indicated in the table.

Figure 5.1.10 shows the rotational rates ω_1, ω_{2a} and ω_{2b} vs. the payload mass for case 6d. After inspection of Table 5.1.8 and Fig. 5.1.10, it appears that a possible design option is to choose an equi-ratio value for the payload mass as a nominal case (4243 lb is for example a factor 2.12 greater than 2000 lb and a factor 2.12 smaller than 9000 lb). By following this option, the rotational speed of the 2nd stage must be increased after capture for payloads > 4243 lb and decreased for payloads < 4243 lb. The advantage of this option is that the required rotational speed increases and decreases could be handled by a 2.12 increase or decrease of the 2nd stage tether length. Consequently, the tether length of the 2nd stage could be 17.8 km for 2000-lb payloads, 37.7 km for the design-point payloads of 4243 lb and 80 km for 9000-lb payloads.

Table 5.1.8. Key parameters of LEO to GEO system for case 6d for different payload masses. For all cases M = 1.5, N = 4.5, $e_1 = 0.1$.

Dimensions Distances (km), Masses (kg)	Case 6d_1 9000-lb payload	Case 6d_2 4500-lb payload	Case 6d_3 2000-lb payload
Capture revisit time (hr:min)	8:10	8:10	8:10
Transfer time to GEO (hr:min)	16:50	16:50	16:50
1st stage tether length (km) 2nd stage tether length (km)	$L_1 = 60$ $L_2 = 80$	$L_1 = 60$ $L_2 = 80$	$L_1 = 60$ $L_2 = 80$
1st stage CM orbit Altitudes Semimajor axis	6798 x 8308.7 420 x 1931 7551	6798 x 8308.7 420 x 1931 7551	6798 x 8308.7 420 x 1931 7551
2nd stage CM orbit	6917 x 34259	6925.2 x 34251	6931.6 x 34244
Sat. orbit after 1st stage release	6837 x 12958	6845.2 x 12950	6851.6 x 12944
Plat-1 orbit after 1st stage release Altitudes	6709.7 x 6777 332 x 399	6785.2 x 7455.2 407 x 1077	6791.6 x 7914.7 414 x 1537
Sat. orbit after 2nd stage release	6928.2 x 42165	6961.4 x 42165	6988.7 x 42165
Plat-2 orbit after 2nd stage release	6848.2 x 14434	6881.4 x 20953	6908.7 x 26980
Rot. rate ω_1 (rad/s)	0.0181	0.0148	0.0129
Rot. rate ω_{2a} (rad/s)	0.0132	0.0132	0.0132
Rot. rate ω_{2b} (rad/s)	0.0132	0.0072	0.00384
Sat. acceleration on 1st stage	1.3	1.1	0.9
LV acceleration at capture (g)	1.4	1.4	1.4
LH acceleration at capture (g)	0	0	0
1st stage mass 2nd stage mass	9460 6970	9460 6970	9460 6970
EOL Mass Grand Total	16430	16430	16430

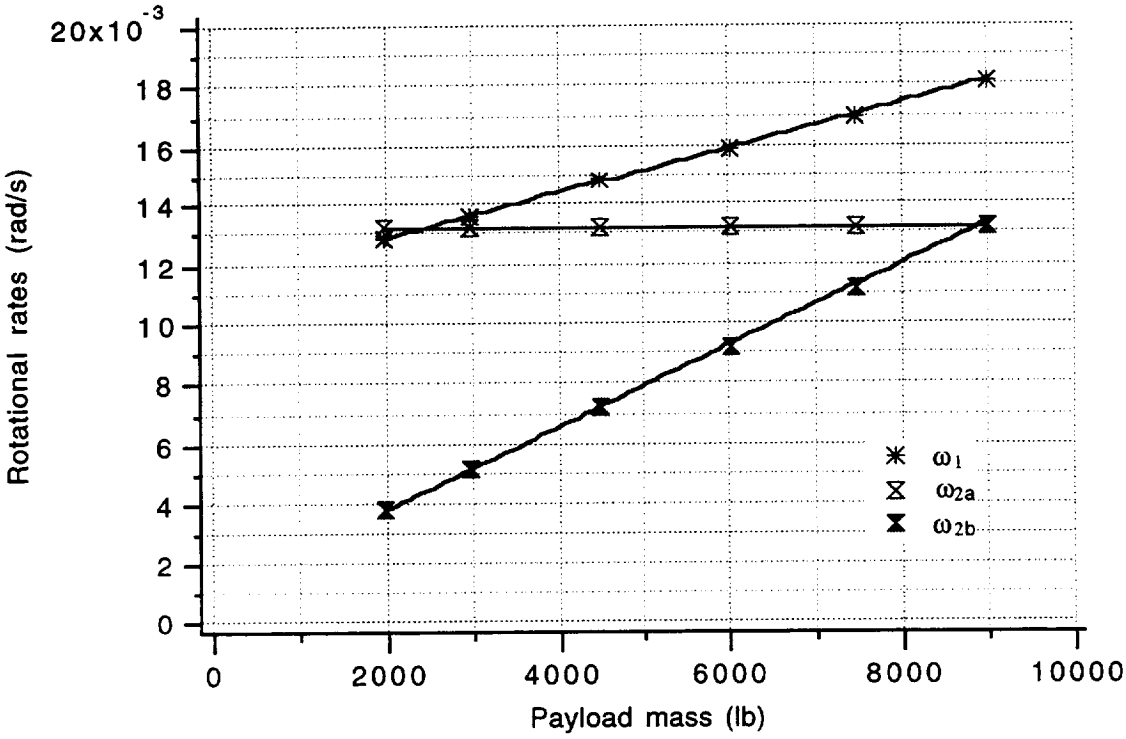

Fig.5.1.10. Rotational rates of the two stages vs. payload mass. The rotational rates are: ω_1 for the 1st stage, ω_{2a} and ω_{2b} for the 2nd stage at capture and release, respectively.

Rendezvous and Capture

One of the important aspect of a two-stage tethered system is the capture of the satellite by the second stage. A few important points must be stressed regarding this particular rendezvous and capture, as follows: (a) the relative velocity at capture is zero; (b) the horizontal component of the relative acceleration is zero; (c) the vertical component of the relative acceleration is about 1.4 g for our cases 6d and 5f; and (d) the timing of the rendezvous maneuver is faster than a conventional rendezvous.

Considering that the vertical acceleration is the only non-zero component at capture, the capture maneuver is fairly similar to capturing an object, thrown in the air from the ground, at the top of its parabolic trajectory with the hand moving at the same horizontal velocity of the object. The only non-zero component at capture is, in both cases, the vertical acceleration that is equal 1 g on the ground and 1.4 (cases 6d and 5f) for the tethered system in space.

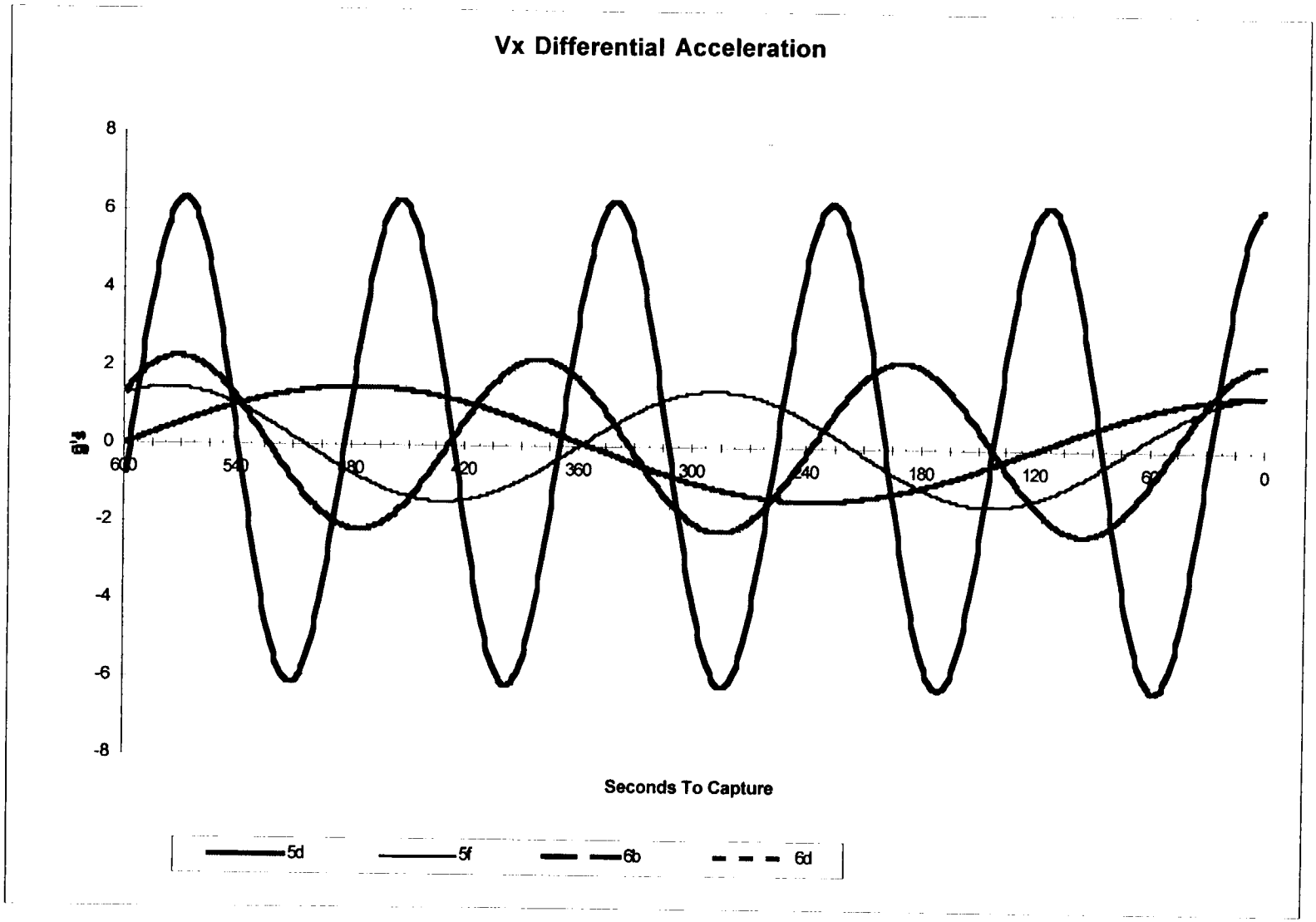

Fig. 5.1.11(a). LV relative acceleration at capture of satellite by 2nd stage [courtesy of Boeing]

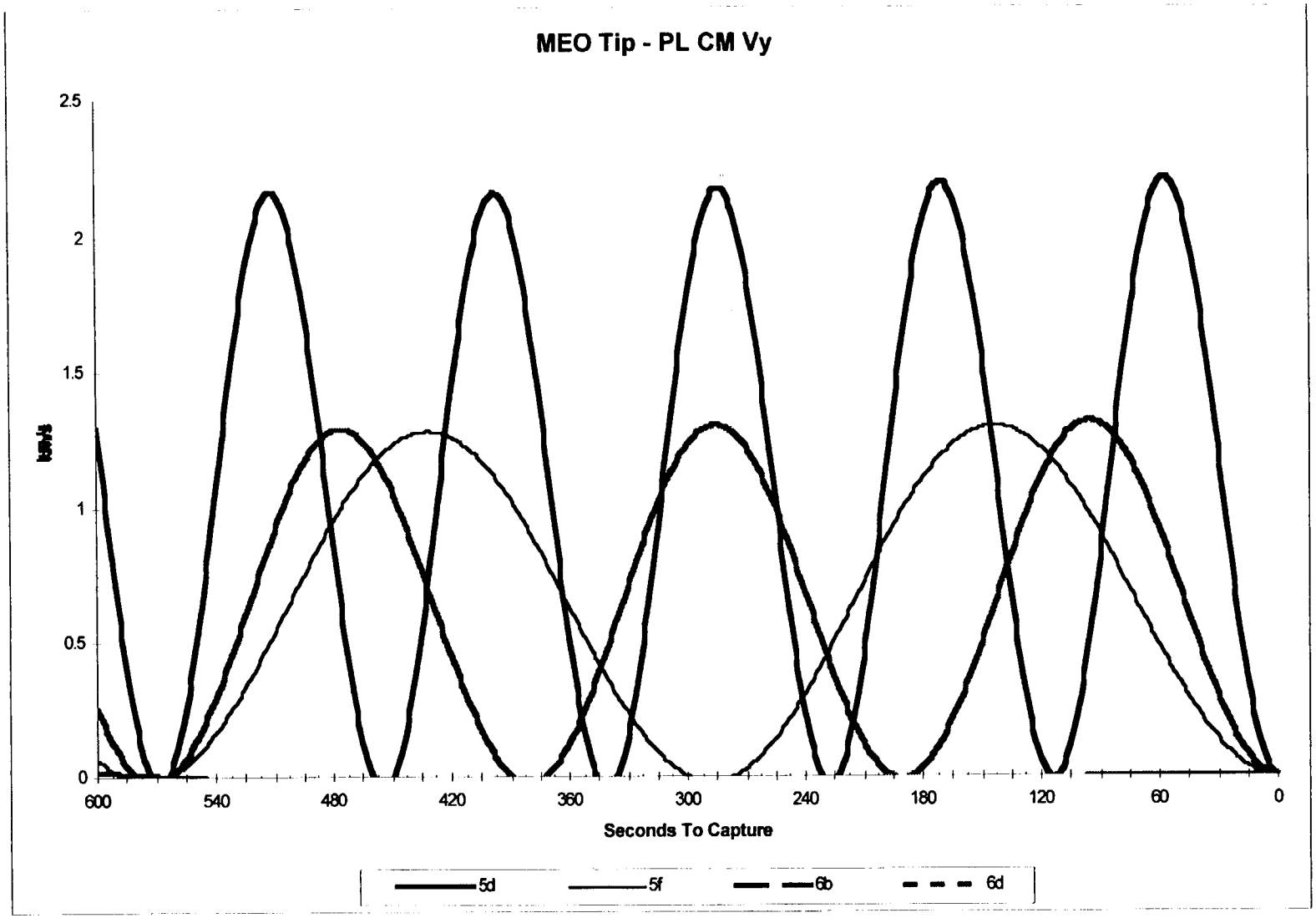

Fig. 5.1.11(b). LH relative velocity at capture of satellite by 2nd stage [courtesy of Boeing]

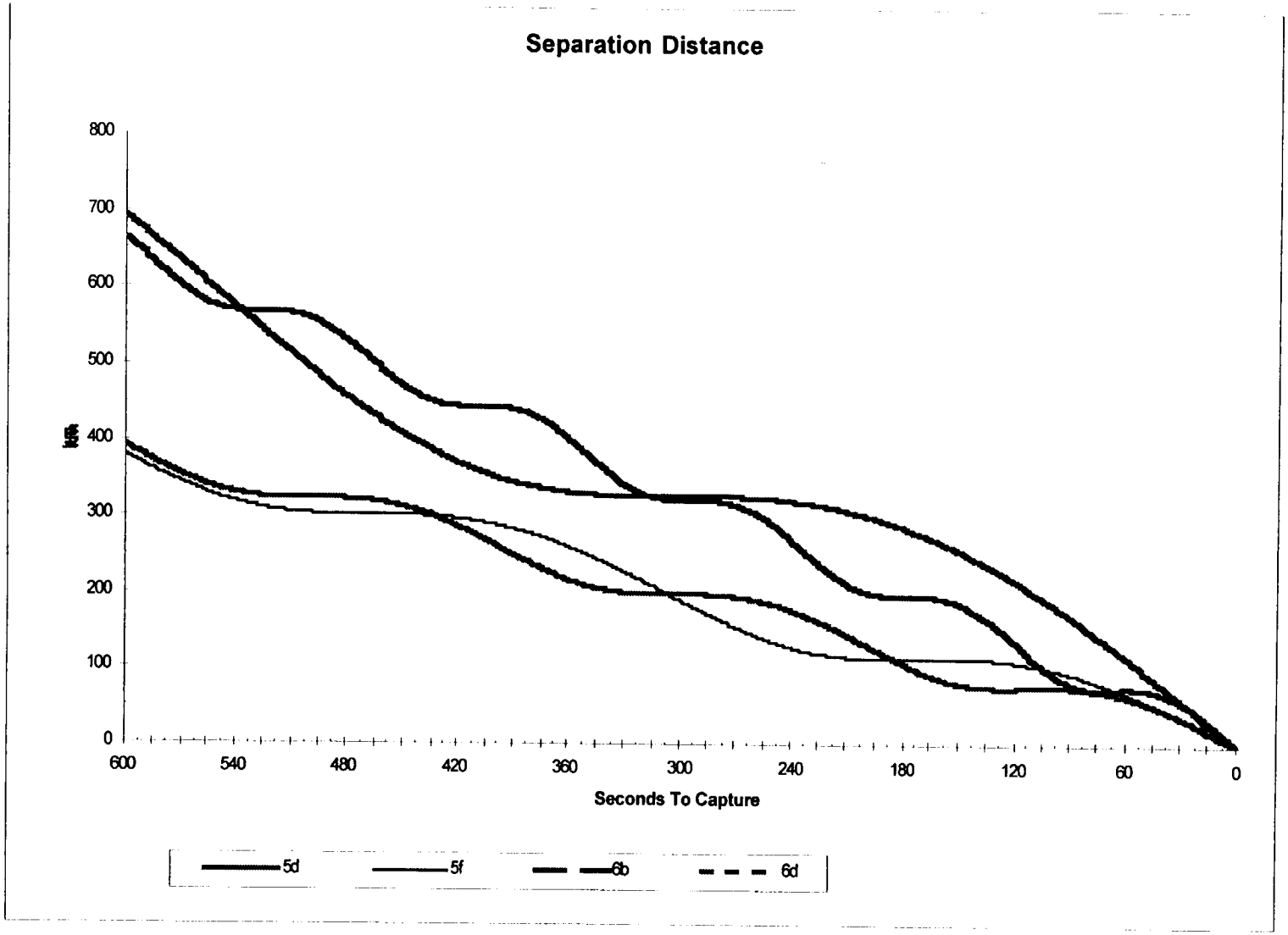

Fig. 5.1.11(c). Separation distance at capture of satellite by 2nd stage [courtesy of Boeing]

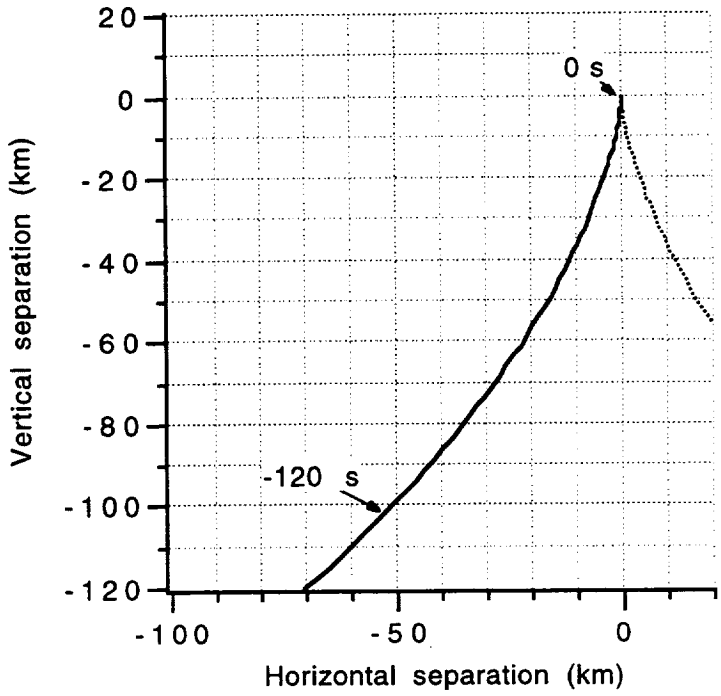

Fig. 5.1.12. Example of relative trajectory of satellite at rendez-vous with 2nd stage. Dashed line indicates trajectory of satellite in case of miscapture.

Accurate simulations of the rendez-vous have been carried out by H. Dionne at Boeing, Huntsville, AL [10]. The relative distance, velocity and acceleration profiles are shown in Figs. 5.1.11(a)-5.1.11(c) for the cases of greatest interest. In the figures, the x-axis is along LV and the y-axis is along LH. Figure 5.1.12 shows the relative trajectory of the satellite with respect to the rotating tip of the 2nd stage for one of the cases analyzed. The previous figures show clearly the important points about this rendezvous and capture that were previously highlighted.

Additional Considerations

The tethered system discussed here is reversible: it can be used to transport spent satellites from GEO to LEO. In this case the 2nd stage would capture the satellite at the top of its spin and release it at the bottom of its spin to rendezvous later with the 1st stage. Another interesting feature is as follows: thanks to the conservation of angular momentum, if a satellite is transferred to GEO and an equal-mass satellite is retrieved from GEO at the next available opportunity, then no propellant is required for reboosting the stages. Clearly, in a realistic situation the return traffic will be different from the outgoing traffic

and some propellant will be necessary for making up the deficit of angular momentum. In summary, the return traffic besides being important in itself can also provide sizable savings to the propellant budget of the system.

Conclusions

A two-stage tethered system of reasonable size and relatively small mass can be designed for transferring satellites with a mass up to 9000 lb from LEO to GEO (with the circularization ΔV provided by the kick motor of the satellite). The transfer times from LEO to GEO for the two-stage systems examined here are between 16:12 hr:min and 16:25 hr:min (5:30 hr:min are needed from LEO to GEO with a conventional upper stage).

The best estimate of the end-of-life system mass is about 16500 kg for the two stages without propellant. If we assume that the systemis used to transfer the heaviest payloads of 4082 kg (9000-lb), about 1400 kg propellant per transfer is required for reboosting. The tethered system, therefore would become competitive with respect to a present upper stage of similar payload capacity (e.g., Inertial Upper Stage), on a mass basis, after 2 launches.

The orbital mechanics of the system is designed with resonant orbits so that there are periodic conjunctions (or visits) between the 1st and 2nd stage and there are multiple opportunities for capture of the satellite in case of miscapture by the 2nd stage (the revisit time after miscapture ranges between 7:18 hr:min and 8:10 hr:min for the cases analyzed).

A single stage tether system from LEO to GEO would be >3 times more massive than a two stage system with present day tether technology. However, an increase of the strength-to-weight ratio of 70% (which is conceivable over the next 15 from the current trend) would reduce the tether mass by a factor three and consequently make the single stage tether system much more attractive than at present. Moreover, the transfer rate of a single-stage system is not dependent upon the realignment frequency (due to the Earth's oblateness) of the orbits of the two stages.

The tethered system can not only be used to deliver payloads to GEO but also to return satellites from GEO to LEO. In a future scenario, not analyzed in this report, the return traffic could be used to offset a portion of the propellant used for reboosting the stages.

In summary, the tether system combines the efficiency of electrical propulsion (high specific impulse) and the delivery speed to GEO of a chemical system.

Recommendations

From the results obtained in this study, the tether system from LEO to GEO appears to be competitive from a mass standpoint vs. the present chemical upper stages. This tether system is well worth further analyses of its key aspects as follows:

1) the influence of environmental perturbations over time and the necessary adjustments to the orbital design;
2) the guidance and control during rendezvous and docking;
3) the capturing of payloads incoming from the Earth's surface by the 1st stage, with consequent propellant savings for the launcher;
4) the flow of angular momentum and the use of return traffic to restore the momentum;
5) the use of the spinning tethers for storing electrical energy and reduce the requirement on batteries;
6) the investigation of alternative orbital scenarios which enable the 2nd stage to provide also the circularization ΔV at apogee;
7) the detail analysis of the system architecture and the identification of the most favorable configuration.

Acknowledgement

We would like to thank the contributors to the LEO to GEO mission analysis. They are as follows: Mike Bangham, Heather Dionne and Dan Vonderwell from the Boeing Company; and Markus Kaiser on visit to SAO as student of the Technische Universität München in Munich, Germany.

References

1. I. Bekey and P. Penzo, "Tether Propulsion." *Aerospace America,* Vol. 24, No. 7, 40-43, 1986.

2. P.N. Fuller, "Commercial Spacecraft Mission Model Update." Report of the COMSTAC Technology & Innovation Working Group, US Department of Transportation, July 1995.

3. H. Moravec, "A Non-Synchronous Orbital Skyhook." *The Journal of the Astronautical Sciences,* Vol. 25, No. 4, 307-322, 1977.

4. J. Puig-Suari, J.M. Longuski and S.G. Tragesser, "A Tether Sling for Lunar and Interplanetary Exploration." Proceedings of the IAA International Conference on Low-Cost Planetary Missions, Paper IAA-L-0701P, Laurel, MD, April 1994.

5. B.I. Yakobson and R.E. Smalley, "Fullerene Nanotubes: $C_{1,000,000}$ and Beyond." American Scientist, Vol. 85, 324-337, July-August 1997.

6. R.P. Hoyt and R.L. Forward, "LEO-Lunar Tether Transport System Study." Final Report to Smithsonian Astrophysical Observatory, April 1997.

7. D. Vonderwell, Unpublished Report, Boeing, Huntsville, AL, August 1997.

8. J.R. Wertz and W.J. Larson, "Space Mission Analysis and Design." p. 614, Kluwer Academic Publishers, 1991.

9. L. Johnson, M. Bangham and E.C. Lorenzini, "LEO to GEO Tether Transportation System Study." Interim Review Presentation to NASA/MSFC, May 16th, 1997.

10. H. Dionne, Unbublished Report, Boeing, Huntsville, AL, July 1997.

5.2 LEO-Lunar Tether Transport System Study

FINAL REPORT

LEO-LUNAR TETHER TRANSPORT SYSTEM STUDY

SAO Purchase Order S06-34444

subcontract on
NASA Grant NAG8-1303 to the
Smithsonian Institution Astrophysical Observatory
entitled
"In-Space Transportation with Tethers"

Report submitted by

Tethers Unlimited
Dr. Robert P. Hoyt and Dr. Robert L. Forward, Partners
8114 Pebble Court, Clinton, WA 98236
Phone: 206-306-0400; Fax: 206-306-0537; Email: TU@tethers.com
www.tethers.com

Report dated:
April 28, 1997

Period of Performance:
23 September 1996 to 23 April 1997

SUMMARY

Systems composed of several rotating tethers in orbit can provide a means of exchanging payloads between low Earth orbit and the lunar surface with little or no propellant required. The underlying concept is to use long rotating tethers to throw payloads to the Moon and to catch return payloads sent from the Moon. By transporting equal masses to and from the Moon, the total energy and momentum of the system can be conserved, minimizing or even eliminating the need to use propellant for round-trip travel between LEO and the lunar surface. By reducing the need to lift propellant into orbit, such a LEO to Lunar Surface Tether Transport System could greatly reduce the cost of transportation in the Earth-Moon system.

In this research effort, we have investigated the design of tether systems for LEO to Lunar transport, focusing on four issues critical to the viability of such a system: the orbital mechanics of multi-tether systems, high-strength tether materials, high strength-per-weight survivable tether designs, and propellantless spin-up and orbital maintenance of LEO tether facilities.

We have found that because the mass of a rotating tether increases dramatically with the ΔV the tether is required to impart to a payload, splitting the lunar transfer boost operation up into two or more stages can reduce the required tether mass to very reasonable levels. We have developed mathematical tools for calculating orbital parameters and tether configurations for staged tether systems capable of repeatedly exchanging payloads between low Earth orbits and bases on the lunar surface. In addition, we have developed a numerical software tool for simulating the 3D orbital mechanics of staged tether systems. Using these tools, we have found that by properly choosing the orbital design of the system, the total tether and facility masses required for the system can be reduced by an order of magnitude compared to previous studies, with the whole system requiring an initial mass of less than thirty times the mass of the payload the system can take from a sub-Earth-orbit trajectory and transport to the lunar surface.

We have developed designs for high strength tether structures capable of reliably performing for periods of decades or more. *Using currently available materials*, the tethers for the Earth-orbit facilities used to throw payloads to the Moon can be built with a total tether mass less than the mass of the payload they can transport.

In addition, we have developed a concept for combining the principle of propellantless electrodynamic tether propulsion with that of rotating momentum-exchange tethers to create a LEO tether facility capable of repeatedly boosting payloads to higher orbits, requiring neither propellant nor return traffic to maintain its orbital momentum.

Combining these results, we have formed a development plan for a LEO to Lunar Tether Transport System that can be built incrementally, beginning with a near-term, low cost demonstration mission based upon the proven SEDS tether system.

Nomenclature

a	semimajor axis
e	ellipse eccentricity
E	orbital energy
L	tether arm length
r	radius
r_p	perigee radius
V	velocity
ω	angular velocity
γ	phase angle
ϕ	flight path angle
μ_e	Earth's gravitational parameter = GM_e
μ_m	Moon's gravitational parameter = GM_m

subscripts:

$\blacksquare_a$	apogee
$\blacksquare_p$	perigee

TLA's (three-letter-acronyms):

LEO Low-Earth Orbit
IPO Initial Payload Orbit
EEO Elliptical Earth Orbit
PEO Payload Elliptical Orbit
GEO Geostationary Orbit
SEO Sub-Earth Orbit
SSO Space Station Orbit
LLO Low-Lunar Orbit
LTO Lunar Transfer Orbit
RLV Reusable Launch Vehicle
SOI Gravitational Sphere of Influence
TTF Tether Transport Facility
EDBT Electrodynamic Bolo Tether

INTRODUCTION

If mankind is to develop a sustained and prosperous presence in space, the cost of in-space transportation must be greatly reduced. Presently, the cost of in-space transportation is dominated by the expense of launching propellant into orbit. Systems composed of several rotating tether facilities in orbit can significantly reduce the cost of in-space transportation by exchanging payloads between suborbital trajectories, LEO, MEO, and GEO orbits, and even the surface of the Moon, with little or no propellant required. By reducing the amount of propellant needed for transporting supplies between Earth orbits and the Moon, and by reducing the propellant required for delivering lunar resources to facilities in Earth orbit, a tether transport system may make the development of both lunar bases and Earth-orbit facilities more economically viable.

A space tether is a long, thin cable used to connect two or more objects in space to one another. There are many applications of space tether technologies, many of which have already been demonstrated in flight. At least sixteen tether missions have already flown, beginning with short tether experiments on Gemini 11 and 12 in 1967 and continuing through the highly successful series of SEDS (Small Expendable-tether Deployer System) experiments over the past several years. In fact, as of this writing, a SEDS-based tether system called the Tether Physics and Survivability (TiPS) experiment is currently in orbit, and has demonstrated tether survivability for over 300 days.

Among the numerous applications of space tethers is "momentum-exchange" between masses in orbit. By physically connecting two objects together, a tether provides a means of transferring orbital energy and momentum from one object to another. Consequently, a tether can be used to perform in-space propulsion by enabling one spacecraft to "throw" another spacecraft into a different orbit.

This study has investigated the concept of using a system composed of several tether facilities in orbit around the Earth and the Moon to pick up payloads from low-Earth-orbit (LEO) and transfer them to bases on the lunar surface. Once a lunar base has been established, the tether system can also pick up resources from the lunar surface and transfer them down to facilities in Earth orbit. This "LEO-Lunar Surface Tether Transport System" was originally proposed by Forward,[1] who combined the tether designs of Moravec,[2] Carroll,[3] and the UCSD Space Institute[4] to form a system that could exchange payloads between LEO and the Moon. In his paper, Forward showed that if the flow of mass to and from the Moon is balanced, the potential energy of lunar resources dropped down to LEO can provide the "fuel" needed to move payloads up to the Moon. A tether transport system could thus minimize or even eliminate the need for propellant for round-trip travel between LEO and the lunar surface.

In this document, we will first review the results of several prior studies of tether transport systems, and then discuss the motivation behind the present study. We will then report the results of our efforts to advance the design of tether systems for transportation between LEO and the Moon. Our efforts have focused on four areas critical to the viability of the system:

First, we investigated the orbital mechanics of tether transport in the Earth-Moon system, and have developed analytical method for studying multi-tether systems. Using these tools, we have developed several preliminary designs for staged tether transport systems capable of exchanging payloads between low Earth orbits and bases on the lunar surface. In addition, we have developed a numerical software package for simulating the 3D orbital mechanics of multi-tether systems. Using these tools, we have found that with proper choice of the orbital parameters of the tether facilities, the total tether and facility mass required for the system can be reduced by an order of magnitude compared to previous estimates, bringing the system mass down into the realm of economic feasibility. Moreover, with proper scheduling of transfer operations, these systems can provide round-trip travel opportunities roughly once a month, enabling frequent low-cost travel between LEO and the Moon.

The second issue we investigated was the current state-of-the-art and probable near-term future of high strength tether materials. We have found that high strength fibers have improved steadily since the previous tether studies were performed, and these improvements have significantly reduced the total mass required for the tethers in these transport systems. Moreover, realistic projections for advances in high strength fibers expected in the next 5 to 10 years will further reduce the required tether masses, making tether transport systems even more competitive.

The third issue we investigated is the optimization of the failsafe multiline Hoytether design to achieve both long life and high strength-per-weight performance. Using numerical simulation tools, we have identified designs that can provide reliable high-strength performance for decades-long lifetimes.

In the fourth part of this effort, we developed and analyzed a concept for combining electrodynamic tether propulsion with the rotating momentum-exchange tether concept to form an "Electrodynamic Bolo Tether" facility capable of repeatedly boosting payloads from LEO to higher orbits without requiring propellant or return traffic.

Finally, we have assembled the results of these four investigations to form a development plan for a LEO to Lunar-Surface Tether Transport System that can be built incrementally, with each stage performing useful in-space transportation missions to earn revenue to pay for the next stage. We conclude by proposing a plan to pave the way for this ambitious endeavor by demonstrating the principles and technology required for tether transport to the Moon in a near-term, low-cost flight experiment based upon proven tether technology.

REVIEW OF PREVIOUS WORK

The concept of using long, rotating tethers in space to move payloads from low Earth orbit to the Moon has evolved from investigations of the applications of momentum-exchange tethers carried out by a number of researchers over the past several decades. For an overview of the basic principles of momentum-exchange tethers, the *Tethers in Space Handbook* provides summaries of many applications of tethers and an extensive list of references.[5] This LEO to Lunar Tether Transport System design effort resulted in particular from a previous study performed by Robert L. Forward, who proposed to combine three tether facilities designed by Joe Carroll, the UCSD Space Institute, and Hans Moravec to form a system capable of exchanging payloads between low Earth orbit and the surface of the Moon without requiring propellant.

Carroll Tether Transfer Facility

In 1991, Carroll presented a detailed design of a rotating tether transport facility for lifting payloads from a sub-Earth-orbital trajectory into a stable low Earth orbit.[3,6] The Carroll tether facility design, illustrated in Figure 1, consists of a slowly-spinning, 290 km long high strength tether deployed from a massive facility in a 420 km altitude circular orbit. The rotating tether swings down and, at its lowest point, catches a payload traveling 1.2 km/s slower than the facility at the apogee of a suborbital trajectory. The tether facility can then either reel in the tether and then deploy the payload into a circular orbit, or it can throw the payload at the top of its swing, providing it an additional ΔV of 1.1 km/s.

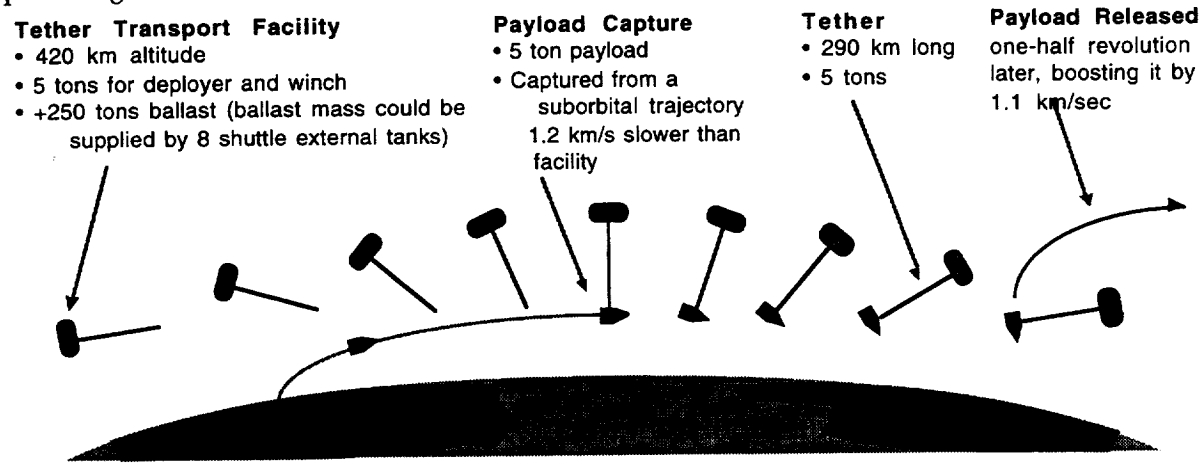

Figure 1. Schematic of the Carroll Tether Transport Facility.

Because the orbital momentum gained by the payload is taken out of the orbital momentum of the facility, the Carroll design requires a facility with a mass greater than 50 times the payload mass to prevent the facility and tether from falling into the atmosphere after boosting the payload. The orbital momentum taken from the facility can be replaced by de-orbiting an equal mass of return traffic. During periods when there is no return traffic, reboost would be accomplished using high-Isp electric propulsion. Using electric propulsion to reboost the facility would enable payloads to be boosted into orbit with the fuel efficiency of electric propulsion but without the long orbital transfer times usually associated with electric propulsion; essentially, the tether facility would act as a momentum "bank," where electric thrusters could be used to slowly and efficiently build up momentum which could then be "withdrawn" by the payloads in a short period of time.

Carroll's reference design was a facility sized to handle payloads massing 5,000 kg. The facility would require a ballast mass of approximately 250 metric tons, which could be supplied by 8 shuttle external tanks. Using Spectra 1000 fiber, with a density of 0.97 g/cc and a design tensile strength of 2 GPa, the tether would mass approximately 4,700 kg. The tether

would thus mass roughly the same as the intended payload, enabling the tether facility to lift its own replacement tethers.

UCSD Tether Transfer Facility

In 1988, Stern, Arnold, and Thompson at the UCSD Space Institute proposed several variations of a rotating tether as components of a Low Earth Orbit to Low Lunar Orbit transport system.[4] The first part of the system was a rotating tether in circular LEO orbit similar to the design Carroll developed in more detail several years later. The second part of the system was a hanging tether in low lunar orbit. The third part of the system, illustrated in Figure 2, was a 100 km long tether facility in an elliptical Earth orbit (EEO) with a perigee at 600 km altitude, eccentricity $\varepsilon_1 = 0.3$, and a perigee velocity of 8.6 km/s. The EEO tether would rotate with a tip speed of 1 km/s, enabling it to rendezvous with and catch a payload in a 7.6 km/s, 500 km circular LEO orbit on its downswing. This EEO tether would then throw the payload on its upswing into a elliptical orbit with a perigee altitude of 700 km, orbit eccentricity of $\varepsilon_2 = 0.64$, and perigee velocity of 9.6 km/s. A chemical or electric propulsion orbital transfer vehicle would then be used to insert the payload

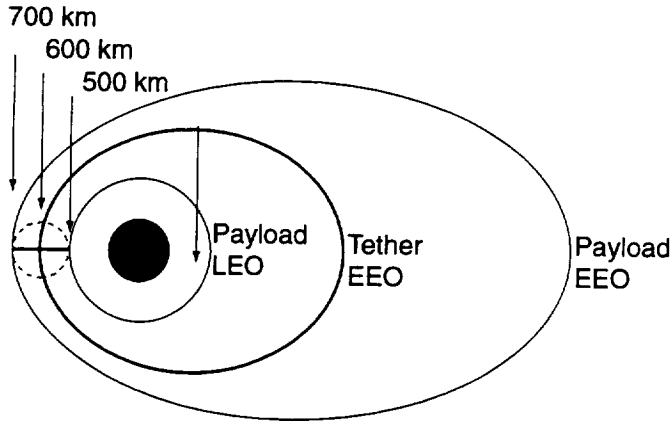

Figure 2. Schematic of the tether in Elliptical Earth Orbit (EEO) proposed by the UCSD Space Institute.

into a lunar transfer orbit.

The UCSD group estimated that the mass of the EEO facility would have to be approximately 20 times the payload mass to prevent deorbit of the facility after payload boost operations. Using material data for Kevlar, the best fiber available at the time, they estimated that the tether would have to mass 1.4 times the payload mass.

Moravec Lunar Rotovator

In 1978, Moravec found that it would be possible to use existing material such as Kevlar to construct a tether rotating around the Moon that would periodically touch down on the lunar surface.[2,7] The Moravec lunar rotovator, or "Lunavator," is illustrated in Figure 3. Moravec found that the mass of the tether would be minimized if the tether had an arm length equal to one-sixth of the diameter of the Moon. The tether would rotate in the same direction as the orbit so that the two tips would touch down on the surface a total of six times per orbit. At touchdown, the relative velocity between the tether tip and the surface would be zero (to visualize this, imagine the tether as a spoke on a giant bicycle wheel rolling around the Moon).

Using data for Kevlar, which has a density of 1.44 g/cc and a tensile strength of 2.8 GPa, Moravec found that a two-arm Lunavator with a design safety factor of two would have to weigh approximately 13 times the payload mass. Each arm of the tether would be 580 km long, for a total length of 1160 km, and the tether would orbit the Moon every 2.78 hours in a circular orbit with radius of 2,320 km.

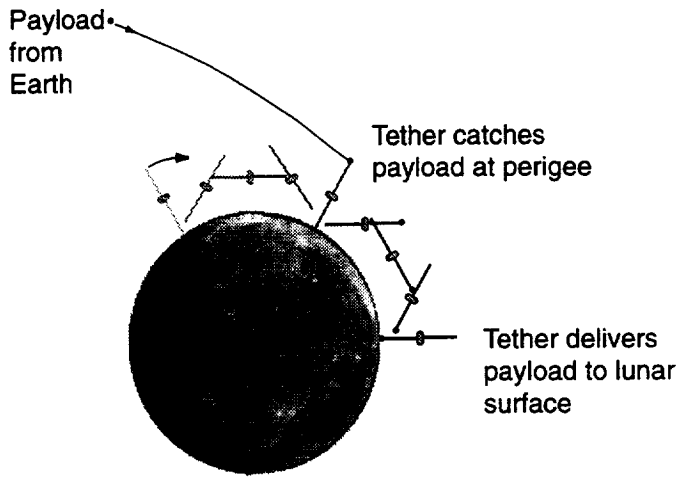

Figure 3. Time-lapse schematic of a double-arm Moravec Lunavator capturing a payload from Earth and depositing it on the lunar surface.

Forward LEO-Lunar Surface Design

In 1991, Forward proposed to combine the tether designs of Carroll, Moravec, and the California Space Institute to form a tether transport system capable of exchanging payloads between LEO and the lunar surface without the use of propellant.[1] The LEO-Lunar system proposed by Forward, illustrated in Figure 4, was composed of three tether facilities, one in low Earth orbit (LEO), one in an elliptical Earth orbit (EEO), and one in lunar orbit. The LEO tether facility would be placed in a circular orbit with altitude 400 km. It would have two tether arms, each 150 km long, and rotate with a tip velocity of approximately 1.3 km/s. On its downswing, it would catch a payload launched into a suborbital trajectory with an apogee altitude of 150 km. At the top of the LEO tether's swing, it would throw the payload into an elliptical orbit with a period twice that of the LEO facility's period, from which it could be picked up by the EEO tether facility. The EEO tether facility would have an orbital period 4 times the period of the LEO tether facility so that there would be frequent opportunities for payload transfer. The EEO tether would then throw the payload into a lunar transfer orbit. When the payload arrives at the Moon, it would be caught by a lunar rotovator, which would transfer it to the lunar surface.

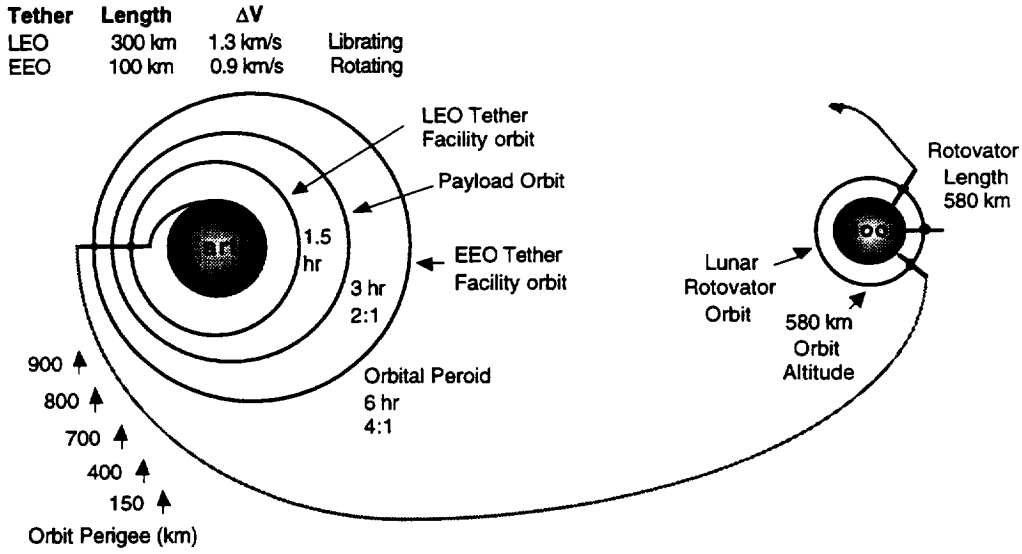

Figure 4. LEO-Lunar Tether Transport system proposed in 1991 by Forward.

In his study, Forward did not perform any trajectory analyses of this concept. He did, however, demonstrate that by balancing the mass of the payloads sent from LEO to the Moon with mass of materials or lunar dirt brought back down from the Moon through the system, the total energy of the system could be conserved. Thus, bags of lunar dirt moving down the tether system into the Earth's gravity well would be the "fuel" needed to move payloads from LEO to the surface of the Moon. If a manufacturing facility is established on the lunar surface, materials such as oxygen and water processed from lunar resources could be dropped down to LEO space stations, providing energy to boost additional supplies to the Moon.

MOTIVATION

If a tether transport system such as Forward proposed could be developed, it could significantly reduce the cost of transporting payloads to and from the Moon. Moving a payload from low Earth orbit to the lunar surface and back to LEO requires a total ΔV of approximately 10 km/s. With storable chemical rockets, which have exhaust velocities around u = 3.5 km/s, the ratio of propellant mass to payload mass, given by the rocket equation,

$$\frac{M_{propellant}}{M_{payload}} = e^{\Delta V/u} - 1, \tag{1}$$

is roughly 16. Currently, the cost to place 1 kg in LEO is approximately $20,000. Transporting 1 kg to the Moon and back to LEO would thus cost $320,000 in propellant alone. A tether system, on the other hand, could transport mass to the lunar surface and back with little or no recurring propellant costs. As a result, if a tether transport system could be developed to handle frequent traffic between LEO and the lunar surface, and if the total mass of this tether system is not too large a multiple of the mass of the payload it can handle, the tether system could greatly reduce the cost of travel to and from the Moon. Moreover, such a tether system could, in principle, use orbital energy and momentum gained by dropping lunar materials into the Earth's gravity well to throw payloads to Mars and other planets, greatly reducing the cost of interplanetary travel as well.

As Forward and Carroll have pointed out, it is one thing for a concept to be technically feasible, but it is another thing entirely for it to be credible. Consequently, this study has focused on improving the credibility of the LEO-Lunar Surface Tether Transport System concept by investigating and refining the aspects of the design that are most critical to its credibility. As pointed out in Forward's paper, these issues include the questions of whether the orbital mechanics of the system can be designed to enable payloads to be exchanged between tethers and delivered to the lunar surface, and whether the masses of the tethers and facilities required can be reduced to reasonable levels.

RESEARCH RESULTS

This study has focused on advancing the credibility of using tethers to transport payloads between low-Earth-orbit and the lunar surface by addressing four issues critical to the viability of the concept: orbital mechanics, tether mass, tether survivability, and tether spin and orbit maintenance.

The first issue is the orbital mechanics of staged tether systems. In a staged tether systems, the ΔV operations required to throw a payload to the Moon is broken up into several smaller ΔV operations by two or more tethers. Staging the tether boosts has a large advantage in that it reduces the tether mass required for the boost operation. However, it requires careful design of the facility orbits to ensure frequent opportunities for payload transfer between tethers. We have developed analytical methods for designing preliminary configurations of multiple tethers in orbit around the Earth and the Moon that will enable frequent opportunities for payloads to be exchanged between low-Earth-orbit and the lunar surface. Using these analytical methods, we have designed three similar but distinct systems for Earth-Moon payload exchange, one for payloads beginning in sub-Earth-orbit trajectories, one for payloads beginning on a LEO space station such as the International Space Station, and one for payloads beginning in low Earth orbit. These three designs, and the methods used to develop them, are summarized in Sections 0.0.0-0 and described in detail in Appendices A, B, and C.

To improve upon these preliminary designs, we have also developed a numerical tool called "OrbitSim" to simulate systems of rotating tethers and payloads in the Earth-Moon system. This numerical simulation is described in Section 0.0, and animations of LEO-Lunar tether transport systems generated using this program are included on the diskette and/or videotape accompanying this report. It should be emphasized that the animations are not just for show. They are graphical output of the accurate numerical calculations carried out by OrbitSim that predict the rotational motion and orbital trajectories that actual tethers and payloads would follow. The animations are also available for viewing on the Tethers Unlimited web site, *www.tethers.com.*

The second issue is the required mass of the tethers used to throw the payloads from one orbit to another. The designs proposed by Forward, Carroll, the UCSD Group, and Moravec required tether and facility masses that, while technically feasible, were probably too large to be economically viable. In the years since those reports were completed, however, there has been significant improvement in the specific strength of commercially available high-strength fibers. Consequently, a portion of this effort was expended in assessing the current state-of-the-art in high-strength fibers and in determining reasonable predictions for the specific strengths of advanced materials expected to be commercially available within the next decade. Using these new data for currently available materials, we have found that the required tether masses can be reduced to very reasonable levels.

The third issue is that of tether survivability. For a tether transport system to be economically viable, the tethers in the system must be able to survive and perform their duties for periods of many years. Impacts by orbital debris and meteorites, however, limit single-line tether lifetimes to periods of days or weeks. This issue has been solved by the development of the Hoytether, a multiline tether structure with redundant load-bearing paths that allow it to withstand many cuts due to impactors and still survive and complete its mission for periods of years or decades. In addition, because the Hoytether structure provides link redundancy, it can be loaded to very near its maximum capacity and still operate reliably. In this study, we have investigated the upper limits of the strength-to-weight performance of Hoytether structures, and identified structures that can be safely loaded to safety factors as low as 1.75. Using these structures, tethers for the LEO-Lunar Surface transport systems can be designed with masses less than the payload mass for the Earth-orbit facilities and as low as 3.2 times the payload mass for the lunar orbit tether, yet still achieve lifetimes of decades or more. The results of this investigation are summarized in Section 0.0 below.

The fourth issue is the need to spin-up the tether facilities and maintain their orbital energy when there is no return traffic to balance the flow of orbital energy and momentum. For the first stage of this system, the LEO tether, it may be possible to combine the principles of momentum-exchange tethers with the principles of electrodynamic tether propulsion to create a LEO tether facility which can repeatedly throw outbound payloads and use electrodynamic torques and propulsion to replenish the orbital energy and momentum of the facility. An analysis of this concept, called the electrodynamic bolo tether (EDBT), is summarized in Section 0.0.

By combining the results of our investigations of these issues, we have developed a conceptual roadmap for building a tether transport system for LEO to Lunar Surface payload transport. This development plan is described in Section 0. In Section 0, we present recommendations for future research directed at developing the technology necessary for this tether transport system, including a low-cost, near-term flight experiment based upon the successful SEDS tether system.

Orbital Mechanics of Staged Tether Systems for LEO⇔Lunar Surface Transport

In his paper "Tether Transport from LEO to the Lunar Surface," Forward showed that it is conceptually possible to construct a system of rotating tethers in Low-Earth Orbit (LEO), Elliptical Earth Orbit (EEO), and Low-Lunar Orbit (LLO) which can move payloads from LEO to the lunar surface while simultaneously dropping lunar resources down to LEO, without requiring propellant.[1]

For such a system to be economically viable, it must be capable of handling a significant flow of two-way traffic. This means that the orbital mechanics and facility designs of the tether system must be chosen so that there will be frequent opportunities for payloads to be transferred between tethers in Earth orbit as well as frequent opportunities for payloads to be exchanged between tethers in Earth orbit and tethers in orbit around the Moon. Moreover, while in theory such a system could exchange payloads without requiring propellant, in reality the system will require some propulsion capability both on-board the payloads and on the tether facilities to optimize trajectories and facilitate rendezvous. Thus, minimizing the propellant needed is also critical to enabling the system to achieve its potential in cost reductions for traffic between Earth and the Moon. In this portion of the research effort, we developed methods for planning orbital parameters for multi-tether systems that will not only permit frequent opportunities for payload exchange between LEO and the lunar surface but also minimize the propellant mass required for payload and facility propulsion. Using these analytical methods, we developed three candidate tether systems, one where the payload begins in a sub-orbital trajectory, one where the payload begins on a LEO space station, and one where the payload begins in a low-Earth-orbit.

Tether Staging

While it is possible to design a single tether in LEO to throw payloads to the Moon, the large ΔV requirements make a single tether for this task very massive. However, the scaling of tether mass with ΔV makes it possible to greatly reduce the necessary tether mass by splitting the ΔV operations up between two or more tethers.

The mass of a tapered rotating tether depends upon the ratio of its design tip speed V_t to the "characteristic" tip speed V_c of the tether material, which is the design tip speed of an untapered tether constructed of that material:

$$V_c = \sqrt{\frac{2T}{Fd}}, \tag{2}$$

where T is the tensile strength of the material, F is the design safety factor, and d is the material density. For Spectra 2000, the best fiber presently available on the commercial market, T = 3.25 GPa, d = 0.97 g/cc, and thus V_c = 1.83 km/s for a safety factor of F = 2. Moravec found that a tapered tether capable of giving a payload with mass M_p a velocity increment ΔV has a mass M_T given by[8]

$$M_T = M_p \sqrt{\pi} \frac{\Delta V}{V_c} e^{\frac{\Delta V^2}{V_c^2}} erf\left\{\frac{\Delta V}{V_c}\right\}, \tag{3}$$

where *erf{x}* is the error function of x; The error function varies from 0.68 for $\Delta V/V_c$ = 1 to 1.0 for $\Delta V/V_c$ = 3. The mass of the tether thus depends upon the *exponential* of the *square* of the ratio $\Delta V/V_c$. As a result, if the ΔV operation can be split up into several operations of smaller ΔV's that add up to the total required ΔV, the sum of the staged tether masses can be significantly less than the mass of a single tether designed for the entire ΔV operation.

A spacecraft in LEO orbit requires an injection speed of approximately 11 km/s to reach the Moon. For a tether in a circular orbit at 300 km altitude, a tip speed of approximately 3.3 km/s is required to throw a payload into a lunar transfer orbit (LTO). To accomplish this ΔV in one "throw" operation with a tether constructed of Spectra 2000 at a safety factor of 2 would require a tether massing more than 80 times the payload mass! If, however, this ΔV

operation is instead accomplished using two rotating tethers which impart ΔV to a payload through both "catch" and "throw" operations, the total tether mass required can be greatly reduced. For instance, a facility moving with a speed 0.825 km/s faster than the payload could use a tether rotating with a tip speed of 0.825 km/s to pick up the payload at the bottom of the tether's swing and then throw it into a temporary elliptical orbit, imparting two 0.825 km/s boosts to the payload. The payload could then be caught and boosted by a second rotating tether facility. If that second facility is moving 0.825 km/s faster than the payload, and if its tether has a tip speed of 0.825 km/s, it could capture the payload with zero relative velocity on its downward swing and throw the payload on its upward swing, providing it a total ΔV of 1.65 km/s for that second stage. The total ΔV would be the required 3.3 km/s, and the staged tether system would require a total tether mass approximately the same as the payload mass. Consequently, until advances in the state of the art of high-strength fibers increases the strength-per-weight of tethers substantially, a multi-stage tether system will have great advantages for reducing the required tether mass.

Analytical Method and Simplifying Assumptions

While staging the tether transport system can significantly reduce the tether mass required, it adds the complication of the requirement to carefully select the tether lengths, rotation rates, and orbital parameters to enable payloads to be transferred from one tether to another and tossed into a lunar transfer trajectory that will permit rendezvous with a tether in lunar orbit. Moreover, the system design must be chosen so that transfer opportunities occur frequently.

The three system designs we pursued followed the general structure of the Forward LEO-Lunar tether transport system, with two tether facilities in Earth orbit and one in orbit around the Moon. The orbital parameters of the Earth-orbit facilities were selected so that the orbits of the tether facilities were resonant; this resonance enables the tethers to rendezvous periodically, permitting frequent opportunities for the tethers to exchange payloads. The tether lengths and rotation rates were chosen so that when a tether catches a payload, the tether tip rendezvous with the payload with zero relative velocity. In addition, these design parameters were also chosen so that the orbits of the payloads would be resonant with the tether facilities' orbits; this additional requirement enables a tether to have several opportunities to rendezvous with a payload, reducing the risk associated with an unsuccessful capture attempt.

To begin to design tether transport systems that can achieve these requirements, we developed a set of analytical equations for determining a first approximation for the preferred system configuration. Initially, we used several simplifying assumptions to make the mathematics tractable. These assumptions were:

1. *Elliptical Low-Earth Orbits.* We ignored the perturbative effects of the Sun, the Moon, and other bodies on the orbits of the LEO and EEO tethers, and assumed that their orbits are described by Keplerian orbital mechanics (i.e.- their orbits are ellipses).
2. *Ignore Nodal Regression.* The oblateness of the Earth causes nodal regression (rotation of the orbital plane) of satellites in orbits that have inclinations other than equatorial or polar. The regression rate depends upon the inclination and altitude of the orbit, and thus will be different for tether facilities in different orbits. For the initial analysis we assumed that the LEO and EEO tethers orbit in the Earth's equatorial plane and thus do not suffer nodal regression.
3. *Co-Planar , Circular Lunar Orbit.* An additional and very significant complication is that the orbit of the Moon is inclined by an average of 5°8' to the ecliptic, while the Earth's axis of rotation is inclined to the ecliptic by 23°27'. Thus even an equatorial tether transport system will require either careful scheduling or some propulsion capability on the payload to permit intercept with the Moon. For these preliminary analyses, the tether facilities and the Moon were assumed to be in co-planar equatorial orbits. We also ignored the slight eccentricity of the lunar orbit ($e_m \approx 0.0549$), and assumed that the Moon travels in a circle with radius of 384,400 km with a velocity of 1.018 km/sec.
4. *Large Tether Terminal Ballast Mass.* The transfer of momentum from the tether transfer terminal to a payload will significantly alter the orbit of the tether terminal. For these initial

analytical analyses, we assumed that the payload mass is small compared to the central terminal mass so that changes in the terminal orbit are negligible.

5. *Patched Conic Approximation for Lunar Transfer Trajectory* We utilized the methods of 2-body orbital mechanics by assuming that a payload in a Lunar Transfer Orbit moves under the influence of Earth's gravity alone until it enters the gravitational "sphere of influence" (SOI) of the Moon. Thus, the payload trajectory from LEO to the SOI is described by a conic section. Inside the lunar SOI, the gravitational effects of the Earth were assumed to affect the payload and Moon orbits equally, and so the payload was assumed to move relative to the Moon under the influence of only the gravitational field of the Moon; the payload trajectory in the Moon's reference frame thus was hyperbolic. In addition, we assumed that the lunar sphere of influence is perfectly spherical with a radius of 66,300 km.

It should be emphasized that these assumptions were used only in the initial analytical calculations to make the mathematics tractable. After the approximate tether transport system design parameters had been found using the analytical equations, we refined the designs further using a numerical simulation of the 3D orbital mechanics of multi-tether systems to begin removing the simplifying assumptions. This program, called OrbitSim, is described in Section 0.0.

Using the initial simplifying assumptions listed above, we have used our set of analytical equations to produce three candidate tether system designs for similar but distinct missions. The analytical methods are described in detail in Appendices A, B, and C, and the resulting tether transport system designs are summarized below.

SEO⇔Lunar Tether Transport System *(Appendix A)*

The first system concept we investigated was a staged tether system which can capture payloads in a sub-Earth-orbit (SEO) trajectory and transfer them to the lunar surface. This "Sub-Earth-Orbit to Lunar Surface Tether Transport System," illustrated in Figure 5, uses three rotating tether facilities, two in Earth orbit and one in lunar orbit. The first stage of the system is a tether facility in low Earth orbit (LEO). Whereas Forward[1] proposed that the LEO stage would be in a circular orbit, we chose a slightly elliptical orbit to reduce the required facility mass, as will be explained below. This first stage will, on its downward swing, catch a payload launched into a suborbital trajectory. One orbit later, it will transfer the payload to the second stage. The second stage is a tether facility in a higher elliptical Earth orbit (EEO), which acquires the payload, carries it for one orbit, and then throws it into a lunar transfer orbit (LTO). The length and spin of the two tethers are chosen so that the tips have zero relative velocity when they rendezvous, facilitating transfer of the payload. When the payload reaches the Moon, a Lunavator in a circular low-lunar orbit catches the payload and swings it down to the surface. The Lunavator's length, orbit, and spin are chosen so that the tip touches down on the lunar surface with zero velocity relative to the surface (like a spoke on a bicycle wheel). Thus, when the Lunavator's tip touches down, the payload can be delivered to a lunar base.

Note that whereas Forward suggested a lunar transfer trajectory that would be roughly elliptical, with the payload approaching the Moon from behind in its orbit (see Figure 4), in the current designs we have chosen the lunar transfer trajectory to be one that approaches the leading face of the Moon, so that the round trip orbit would look like the "figure-8" trajectory used by the Apollo missions. This change was made because the figure-8 trajectory requires a lower ΔV for insertion into a trajectory that can rendezvous with a tether in orbit around the Moon.

Using the analytical methods described in Appendix A, we developed a preliminary design for a sub-Earth-Orbit to Lunar surface tether transport system. The stages of this system are illustrated in Figure 6 to Figure 9. The operation of this system is also illustrated by the QuickTime animation "SEO-Lunar.QT" on the diskette and/or video tape accompanying this report. A round trip from the surface of the Earth to a lunar base and back would be accomplished in several steps:

Suborbital Launch Trajectory:

First, a reusable launch vehicle would lift the payload into a suborbital trajectory with an apogee altitude of 150 km and an apogee velocity of 7.381 km/s. This first stage is the only one

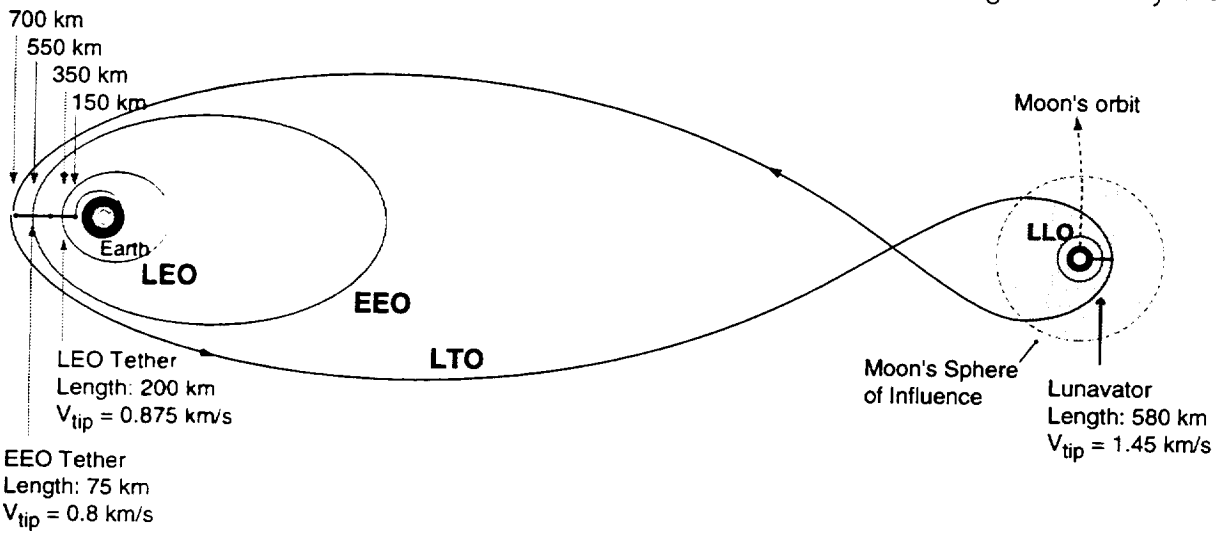

Figure 5. Idealized schematic of the orbital configuration of a SEO⇔Lunar Tether Transport System where the payload begins in a suborbital trajectory. (Not to scale)

that requires expenditure of large quantities of propellant.

LEO Tether:

When the payload reaches the apogee of its suborbital trajectory, it rendezvous with the tip of a 200 km long tether attached to a facility in an elliptical orbit with perigee at 350 km altitude. The orbit of this LEO facility has a semimajor axis of 7,915.92 km, an eccentricity of 0.15, and a period of 116.77 minutes. At its perigee, it is traveling at 8.257 km/s. The tether rotates around the facility in the prograde direction with an angular velocity of 0.00438 rad/sec, giving it a tip speed of 0.876 km/s. Thus, at the bottom of its swing, the tether tip has a velocity of 7.381 km/s with respect to the Earth, and thus will rendezvous with the payload with a relative velocity that is momentarily zero. At that time payload will dock with the tether tip, and the tether will carry the payload as it swings around the facility. At the tether tip, the centripetal acceleration on the payload is 0.4 g,

Rendezvous Issues: In practice, trajectory errors will require orbital maneuvering on the part of the payload and/or the tether facility to accomplish docking between the tether and the payload. To facilitate rendezvous, the system will use a "grapple" vehicle equipped with small thrusters and a tether reel. Previous investigations have estimated the grapple vehicle mass at approximately 0.2 times the payload mass.[3] Stuart[9] has investigated the problem of tether rendezvous and has found that the propellant required for matching position and velocity can be minimized by combining reeling operations by the grapple vehicle with thruster maneuvers by the launch vehicle and/or the grapple vehicle.

Tether Mass: Using the best strength-per-weight material presently available on the commercial market, Spectra 2000 fiber,* a tapered tether with a design safety factor of 2.4† would mass 0.66 times the tip mass. If the tip mass includes the payload and a grapple vehicle massing 0.2 times the payload, the required tether mass would be (1+0.2)x0.66 = 0.8 times the payload mass. Using advanced materials currently under development, such as PBO/Zylon or next-generation Spectra fibers, the required tether mass could be reduced even further. Note that the mass of the tether plus grapple vehicle is *less* than the payload mass; thus the LEO tether facility could lift its own replacement tethers.

Transfer to EEO Tether

After capturing the payload, the LEO tether facility will carry it for one orbit. By reeling the tether in or out, the angular velocity of the tether can be adjusted so that, when the tether facility returns to perigee, the tether will be at the top of its swing. At that time it can hand the payload off to the EEO tether, as illustrated in Figure 6. Note that if that transfer is unsuccessful the payload will *not* be stranded. The tether facility orbits, lengths, and rotation rates have been chosen so that, if the EEO tether does not capture the payload on the first opportunity, the payload will continue in a temporary "payload elliptical orbit" (PEO) with a period exactly two times the LEO tether period and one third of the EEO tether period. Thus there will be multiple opportunities for either the LEO or EEO tethers to capture the payload.

EEO Tether

The second tether facility is in a highly elliptic orbit with a semimajor axis of 26138 km, eccentricity of 0.732, and perigee altitude of 625 km. It orbits with a period of 700.64 minutes, six times the period of the LEO facility. Connected to it is a 75 km long tether rotating with a tip speed of 0.8 km/s. At perigee, the tether swings down and docks with the payload. As with the LEO tether, the relative velocity between the tether tip and the payload at the time of rendezvous is momentarily zero. The centripetal acceleration at the tip is 0.86 g.

Note that whereas the design Forward proposed used an EEO:LEO orbital resonance of 4:1,[1] we have found it necessary to increase the ratio to 6:1. When the tether spin rates are matched to enable transfers at perigee, an EEO orbit with period 4 times that of the LEO orbit

---

* Material characteristics of Spectra 2000 and other high strength fibers are given in Section IV.0.

† The choice of a safety factor of 2.4 will be explained in Section IV.0.

does not have sufficient perigee velocity to throw a payload to the Moon. A 5:1 ratio is sufficient to throw to an elliptical transfer orbit, but this trajectory will result in a perilune velocity too slow to rendezvous properly with a tether rotating around the Moon. A ratio of 6:1, which results in a hyperbolic transfer trajectory, provides sufficient ΔV to rendezvous with the a lunar rotovator.

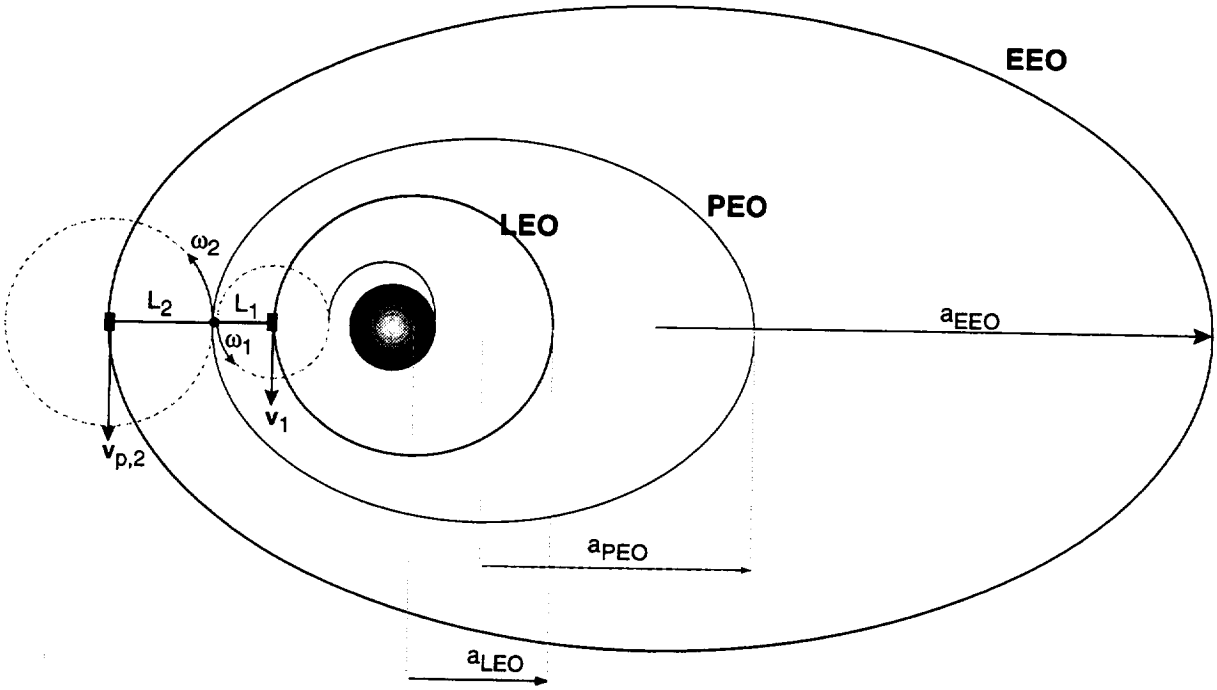

Figure 6. Schematic of the orbits and rotation of the LEO and EEO tether facilities for the SEO⇔Lunar Tether Transport System.

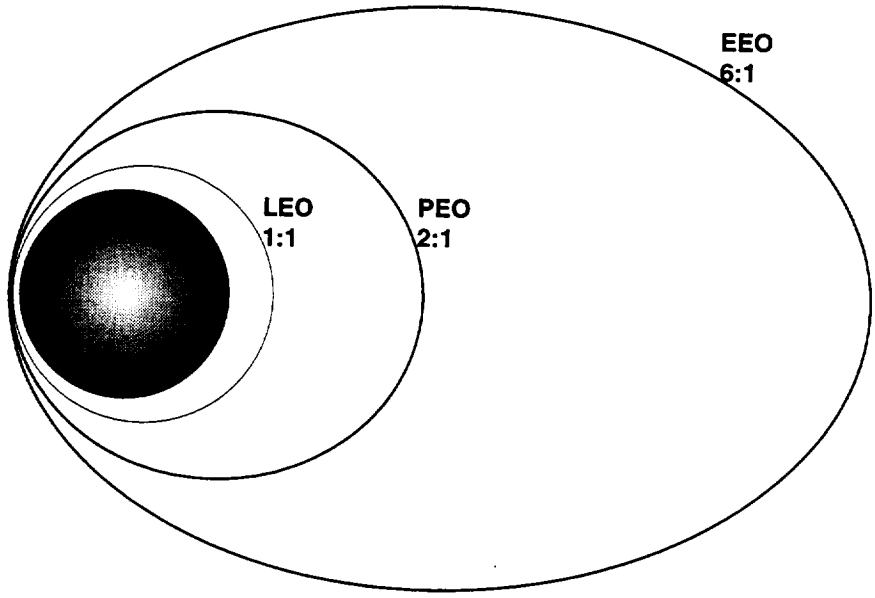

Figure 7. Orbits of the LEO tether, the payload in temporary elliptical orbit (PEO), and the EEO tether for the suborbital to lunar surface transport system, shown to scale.

EEO Tether Mass: Using Spectra 2000 fiber at a design safety factor of 2.4, the required tether mass given by the Moravec formula is 0.54 times the tip mass. If the EEO facility has a grapple vehicle massing 0.2 times the payload mass, the required mass of the tether plus grapple vehicle is (1+0.2)x0.54 = 0.65 times the payload mass. As with the LEO Tether facility, the mass of the tether and grapple vehicle is less than the payload mass, so the facility can lift its own replacement tethers.

Lunar Transfer Orbit

The EEO tether injects the payload into a lunar transfer trajectory with a perigee altitude of 700 km and a velocity of 10.73 km/s. The lunar transfer orbit is illustrated in Figure 8. As mentioned above, the transfer trajectory is hyperbolic, with a time-of flight from perigee to the lunar sphere of influence of only 31 hours. The transfer trajectory has a semimajor axis of -161,119 km, and an eccentricity of 1.044. If the insertion into the transfer trajectory is timed so that the angle between the perigee and the Moon, γ_o, is 135.24 degrees, the payload reaches the Moon's gravitational sphere of influence with a velocity of 2.28 km/s relative to the Moon at an approach angle λ_s of 83.9 degrees.

Lunavator

Once inside the lunar sphere of influence, the payload travels in a hyperbolic orbit under the influence of the Moon's gravity. It reaches perilune at an altitude of 1160 km with a velocity of 2.9 km/s relative to the Moon. When it reaches perilune, it can be caught by the tip of a 580 km long Moravec "Lunavator" tether in orbit around the Moon. The Lunavator facility would orbit around the Moon at an altitude of 580 km. The Lunavator tether would rotate prograde to its orbit with a tip speed of 1.45 km/s, equal to the orbital velocity of the facility. Thus, at the top of its swing it could rendezvous with the payload with zero relative velocity between the tether tip and the payload, and at the bottom of its swing it can deliver the payload to a lunar base with zero velocity relative to the Moon's surface.

It should be noted that because the trajectory of the payload in both the Earth and Lunar frame is hyperbolic, if the payload and Lunavator do not successfully rendezvous, the payload will be left in a trajectory that has sufficient energy to leave the Earth-Moon system. The payload, therefore, should have some propulsion capability to change its trajectory into one that will return to either the Earth or the Moon.

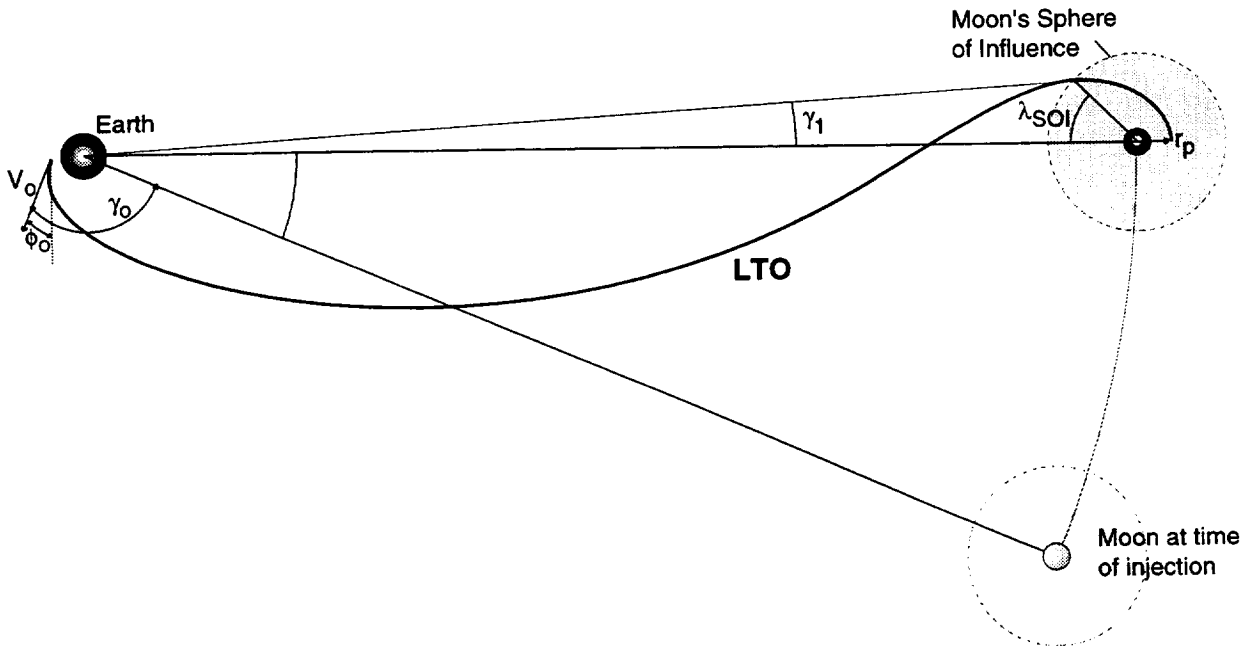

Figure 8. Schematic of the lunar transfer orbit (LTO).

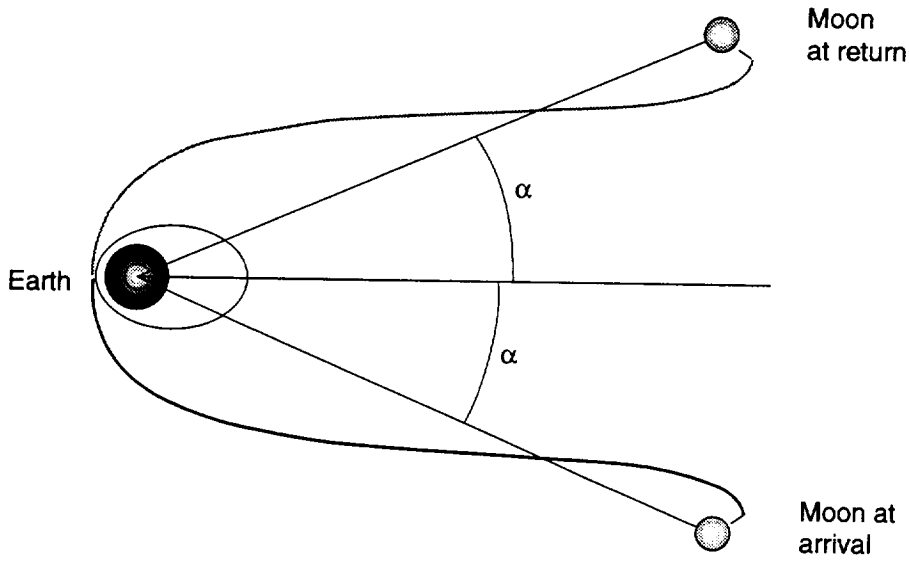

Figure 9. Schematic of outbound and inbound trajectories (not to scale).

Lunavator Tether Mass: Since Moravec performed his analysis of the Lunavator concept, available material strengths have improved significantly, greatly reducing the tether mass required. Moreover, although Moravec envisioned a two-arm tether that would touch down on the lunar surface six times per orbit, only one arm is really necessary. Using PBO fiber at a safety factor of 2.4, the Lunavator tether mass required would be 2.5 times the tip mass. If the Lunavator has a grapple vehicle 0.2 times as massive as the payload, the required total tether mass is approximately 2.9 times the payload mass.

Return Traffic

Using this system for outbound traffic only would save propellant and time over other methods by allowing high-Isp propulsion to be used to boost payloads to the Moon without requiring the long transfer times normally associated with electric propulsion. However, the key to making this SEO-Lunar transport system worthwhile is to have return traffic to balance the flow of orbital momentum and energy in the system. By balancing outbound and inbound mass flow, the system can reduce the amount of propellant required to move mass between Earth and the Moon to the small amounts required for trajectory corrections. By properly scheduling payload departures and returns, the lunar transfer trajectories can be selected to allow rendezvous with the tether facilities in Earth orbit.

The outbound and inbound payload trajectories are illustrated in Figure 9. At the time of arrival of the payload at the upper tip of the Lunavator, the angle between the Earth-Moon radius vector and the centerline of the LTO hyperbola is $\alpha = 23.43°$. After depositing the payload on the surface of the Moon and picking up a return payload, the orbit and rotation rate of the Lunavator are adjusted slightly so that 3 days, 13 hours, and 43 minutes later, when the Moon is at an angle α above the hyperbola centerline, the Lunavator is in position to throw the return payload back down to Earth in a transfer trajectory that is essentially the mirror image of the outbound trajectory. The perigee of the transfer trajectory will thus be at the same point as the perigee of the outbound trajectory, enabling the return payload to rendezvous with the EEO tether.

Opportunities for these ideal trajectories will occur once every 27.3 days. It should be possible to exchange payloads at other times by throwing and catching payloads at positions other than perigee, and by using propulsion onboard the payload to alter the transfer trajectory. However, unless the tether facilities are very massive, the alterations to the facility orbits caused by non-perigee maneuvers will make trajectory planning quite complicated. For the

near future, the 13+ opportunities per year to exchange payload between Earth and the lunar surface that can be provided by perigee-only maneuvers would seem to be more than sufficient.

Facility Masses

In previous studies of tether transfer facilities,[3,1] the LEO facility orbit was chosen to be circular. As mentioned above, in this sub-LEO to Lunar surface transport system design the LEO facility orbit was chosen to be elliptical rather than circular. This choice was driven by the desire to minimize the facility mass required to keep the tether facility in orbit after a boost operation.

The LEO tether boosts the payload by a total $\Delta V_{payload} = 2V_{tip}$ Because total momentum must be conserved, the LEO facility will be decelerated by approximately

$$\Delta V \cong 2V_{tip}\frac{1}{\chi_{LEO}}, \tag{4}$$

where χ_{LEO} is the ratio of LEO facility mass to payload mass and V_{tip} is the tether tip velocity. Therefore, if the LEO facility began in a circular orbit, immediately after the LEO facility releases the payload the facility would be placed into a new orbit with an apogee roughly equal to its original circular orbit radius and a perigee that depends upon the mass ratio. For an orbit altitude of 400 km and a tip speed of 1 km/s, a mass ratio of $\chi_{LEO} > 75$ is required to keep the facility perigee above 300 km of altitude, and the tether must be retracted rapidly to prevent it from burning up in the atmosphere. While it may be feasible to use on-orbit waste (spent booster rockets, main shuttle tanks, ISS waste materials) to provide this ballast mass, this large mass requirement appears to make a circular orbit impractical for the LEO facility.

If the LEO orbit is chosen to have a significant eccentricity, however, its perigee velocity will be significantly above the circular orbit velocity at that altitude. Thus, with a sufficient mass ratio χ_{LEO}, the post-boost facility velocity can still be greater than or equal to circular orbit velocity. The facility orbit will have essentially the same perigee altitude, and thus the facility and tether will not be de-orbited. For the design given above, a facility mass of 5 times the payload mass would be adequate to keep the reduction in facility perigee to less than 30 km.

Because the EEO tether facility is in a highly elliptical orbit, its total mass can also be low while still maintaining the perigee altitude. In fact, a EEO facility mass of approximately 2 times the payload mass would have an interesting benefit in that after the boost operation, the facility would be placed into an orbit nearly the same as the payload orbit (PEO), where it could periodically rendezvous with the tip of the LEO tether. The EEO tether could therefore be captured, serviced, or refueled by the LEO tether facility.

Note, however, that with such low mass ratios, the orbits of the facilities will be significantly changed by boost operations, making orbit planning for rendezvous more complicated. The equations used to calculate these system designs, describe in Appendix A, will require modification to account for small facility masses. Nonetheless, it may be possible to start the system with a relatively low initial ballast mass and increase the ballast mass over time using lunar dirt that has been exchanged with payloads from Earth. With initial mass ratios as low as 5 a possibility, a LEO facility that starts out with a total mass of 5 tons could move 1000 kg payloads to begin with and increase its capacity over time.

The mass ratio required for the Lunavator facility is higher, but still within the limits of reason. Unlike the case of LEO and EEO tether facilities, the required Lunavator facility mass is driven not by the need to keep the facility from deorbiting into the Moon, but rather to keep the payload from pulling the facility too far away from the Moon after capture. The Lunavator rotates in the same direction as it orbits the Moon; consequently, when it captures the payload sent from the Earth-orbit tethers, the payload is traveling faster than the Lunavator center of mass. After payload capture the facility and payload center of mass will be in an elliptical orbit with radius always equal to or greater than the facility's initial orbit radius. A facility mass of 20 times the payload mass will keep the post-capture orbit eccentricity below 0.1. The orbit will also be altered when a payload is deposited on the surface of the Moon. Because the tether decreases the orbital momentum of the payload when it deposits it on the surface, the orbital

momentum of the facility will again be increased. Alterations to the orbit can most effectively be minimized or eliminated by picking up a return payload at the same time a payload is delivered to the surface.

As with the LEO and EEO tether facilities, it may be most economical to build a relatively low mass Lunavator facility to begin with and build its mass up over time using material lifted from the lunar surface. Oldson and Carroll have found that, with proper timing, a slowly spinning tether can pick up a payload and release it into an orbit that will rendezvous with the tether facility with a low relative velocity.[6] Thus a Lunavator could possibly build up its ballast mass by picking up bags of lunar dirt and tossing the bags to itself like an elephant tossing peanuts into its mouth.

Summary

By properly choosing the orbital parameters of the tether facilities, a staged tether transport system for frequent round-trip travel between sub-Earth-orbit and lunar bases can be developed with very reasonable mass requirements. The total tether and facility masses required in Earth orbit can be less than ten times the payload mass. The lunar stage of the system will require a tether mass of approximately 3 times the payload mass. The lunar orbit facility will require the largest mass, roughly 20 times the payload mass as a minimum, but deployment costs for this facility can be reduced by utilizing lunar resources for ballast mass. Moreover, because a round-trip from LEO to the Moon and back requires a propellant mass of approximately 16 times the payload mass using conventional rockets, once a lunar base is developed, a tether transport system that can handle one payload per month could "pay for itself" in less than a year.

ISS-Lunar Tether Transport System *(Appendix B)*

The largest potential market for a LEO to Lunar tether transport system will likely be in exchanging supplies and materials between LEO facilities and lunar bases. It may, therefore, be possible to simplify the LEO to Lunar tether transport system by eliminating one of the rotating tether facilities and replacing it with a hanging tether extended upwards from a LEO space station such as the International Space Station (ISS).

A schematic of a tether system for LEO station to lunar surface transport is shown in Figure 10. A payload is assembled onboard the station and then deployed at the end of a long upward-hanging tether. When the tether is fully deployed, the payload is released, injecting it into perigee of a "payload elliptical orbit" (PEO). Half an orbit later, when it is at apogee, it is caught by a rotating tether in elliptical earth orbit (EEO), which carries it around one orbit and then throws it into a lunar transfer orbit (LTO). At the Moon, a Lunavator catches the payload and swings it down to a base on the lunar surface.

It should be noted that the hanging tether in this system provides a relatively small fraction of the total ΔV. This places the lion's share of the ΔV requirement on the rotating tether, necessitating a higher mass for the rotating tether than if the ΔV were equally distributed between the two tethers. The choice of a hanging tether for the first stage thus is not optimum from the standpoint of minimizing the total tether mass. However, the main purpose of the hanging tether on the space station is not to provide ΔV to the payload. Rather, its purpose is to provide a propellantless means of deploying the payload a large distance upwards from the station so that there will be no concern of collision between the station and the second-stage tether. Moreover, this system will utilize the existing mass of the space station as ballast mass for one of the tethers, thereby keeping the total mass required by the tether transport system low.

Alternatively, the first stage of this system could be a hanging tether extended upwards from a reusable launch vehicle in LEO in a manner similar to that proposed by Bekey.[10,11] Thus one tether system could handle lunar traffic originating both at the Earth's surface and at LEO facilities.

Using the analytical method described in Appendix B, we have developed a preliminary design for a staged tether system for exchanging payloads between LEO space stations and lunar bases. The stages of this system are illustrated in Figure 10. The operation of this system is also illustrated by the QuickTime animation "ISS-Lunar.QT" on the diskette and/or video tape accompanying this report. A round trip from the surface of the Earth to a lunar base and

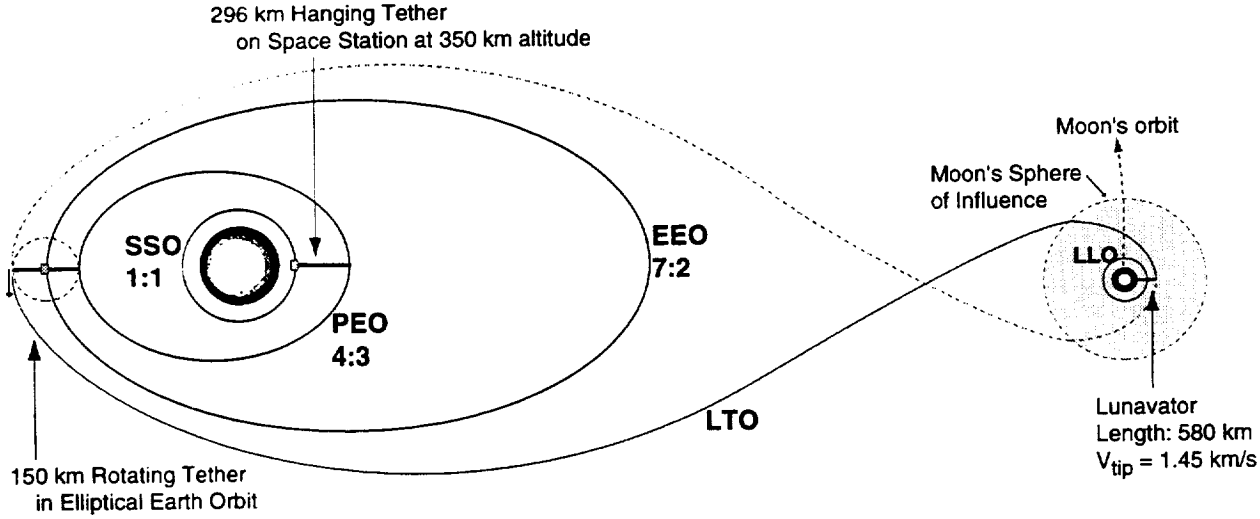

Figure 10. Idealized schematic of the orbital configuration of a Tether Transport system for exchanging payloads between a LEO space station and a lunar base. (not to scale).

back would be accomplished in several steps:

Space Station

First, a payload would be assembled onboard a LEO space station such as the ISS. In this analysis, the station is assumed to have a circular orbit with an altitude of 350 km and an orbital period of 91.5 minutes. The payload is then deployed at the end of a 296.4 km long tether and deployed upwards from the station. Because the load on the tether is quite small, the tether mass required is very low, approximately 1/200 times the payload mass.

Payload Elliptical Orbit

The hanging tether releases the payload, injecting it into the perigee of an elliptical orbit with a semimajor axis of 8151 km and an eccentricity of 0.138. This orbit has a period of 122 minutes, 4/3 times the period of the space station; thus the station could retrieve the payload 3 orbits later if necessary.

EEO Tether

Half an orbit later, when the payload is at apogee with an of altitude 2,897 km and a velocity of 6.09 km/s, the payload will be caught by a 150 km long rotating tether in elliptical Earth orbit. The tether facility will be in an elliptical orbit with a semimajor axis of 15511 km and an eccentricity 0.39. This orbit has a period of 320.25 minutes, 7/2 times the period of the space station, so there are frequent opportunities for transfer of the payload from the station to the EEO tether. The facility's orbit will be timed so that, when the payload is at apogee, the facility is at perigee with a velocity of 7.67 km/s. Thus if the tether rotates prograde to its orbit with a tip velocity of 1.58 km/s, the tether tip can rendezvous with the payload with zero relative velocity. Once the tether has caught the payload, the payload will experience a centripetal force of 1.7 g. The EEO facility carries the payload for one orbit. When it returns to perigee, it throws the payload into a lunar transfer trajectory.

Tether Mass: This system places a larger ΔV requirement on the EEO tether than the SEO-Lunar design, and, as a consequence, the EEO tether must be more massive. Using Spectra 2000 fiber with a design safety factor of 2.4, the required tether mass is approximately 3.3 times the tip mass. With a tip vehicle massing 0.2 times the payload mass, the required tether mass is (1+0.2)x3.3 = 4 times the payload mass.

Facility Mass: Because the facility is in a highly elliptic orbit, the facility mass can be as small as two times the payload mass and the facility will not de-orbit after a boost operation. It may be possible to initiate the system with a small ballast mass and build the ballast up over time using lunar material sent down to LEO as return traffic.

Lunar Transfer Orbit

The EEO tether injects the payload into a lunar transfer trajectory with a perigee altitude of 3197 km and a velocity of 9.26 km/s. The lunar transfer orbit is illustrated in Figure 8. As with the SEO-Lunar system, the transfer trajectory is hyperbolic, with a time-of flight from perigee to the lunar sphere of influence of only 31 hours. The transfer trajectory has a semimajor axis of -158,708 km, and an eccentricity of 1.06. If the insertion into the transfer trajectory is timed so that the angle between the perigee and the Moon, γ_o, is 131.4 degrees, the payload reaches the Moon's gravitational sphere of influence with a velocity of 2.23 km/s relative to the Moon at an approach angle λ_s of 82.9 degrees.

Lunavator

Once the payload reaches the Moon, it is caught and delivered to a lunar base by a Moravec Lunavator. The design for the Lunavator is described in Section IV.0.

Return Traffic

The key to making a space station to Lunar base system viable would be to have outbound mass flow balanced by mass flow from the Moon to the station. Such a system could allow supplies such as oxygen and metals processed from lunar resources to be delivered to LEO at a much lower cost than equivalent supplies could be launched from the Earth. As with the SEO-Lunar transport

system described in the previous section, optimum opportunities for outbound trips will occur roughly once a month, and the trajectories for the return trip will line up three days after arrival at the Moon.

Summary

By properly choosing the orbital design, a staged tether system for frequent round-trip traffic between a station in low Earth orbit and lunar bases can be developed with very reasonable total mass requirements. By leveraging the system upon the mass of an existing space station, the total required mass of the two tethers and one facility required for throwing payloads to the Moon could be less than ten times the payload mass.

LEO-Lunar Tether Transport System *(Appendix C)*

In constructing a tether system for round-trip traffic to lunar bases, it may be preferable to design the system to handle payloads that begin in low Earth orbits rather than in suborbital trajectories or on a station. Having the payload begin in a free orbit would reduce the criticality of arranging for a rendezvous with a launch vehicle in a suborbital trajectory and ameliorate the issue of tether proximity to a space station.

A candidate design for a LEO-Lunar tether transport system is illustrated in Figure 11 and Figure 12. The payload would originate in a slightly elliptical "initial payload orbit" (IPO). At the apogee of its orbit, it would be caught by a rotating tether facility in an elliptical LEO orbit. The orbits would be arranged so that capture occurs when the facility is at perigee. One orbit later, the LEO tether would transfer the payload to a second tether in a highly elliptical Earth orbit (EEO). This EEO tether would carry the payload for one orbit and then throw it into a lunar transfer orbit. At the Moon, a Lunavator would catch the payload and deliver it to a lunar base.

The analytical methods used to design the candidate LEO-Lunar system are developed in Appendix C. In this system, round trip travel between LEO and the lunar surface would be accomplished in the following steps:

Initial Payload Orbit

First, a payload would be placed in a slightly elliptical free orbit by either a launch vehicle or by release from a space station. For this case, the IPO was chosen to have a perigee altitude of 250 km and an eccentricity of 0.1. This orbit has a period of 104.8 minutes, an apogee altitude of 1723 km, and an apogee velocity of 6.65 km/s. Capture of the payload by the first stage is timed to occur when the payload is at apogee so that the payload will be traveling slower than the tether facility.

LEO Tether

The LEO tether facility would be placed in an orbit with a semimajor axis of 10695 km and an eccentricity of 0.212. The facility will have a perigee altitude of 2050 km and a perigee velocity of 7.57 km/s. It orbits once every 183.4 minutes, 7/4 of the initial payload orbit period; thus opportunities for rendezvous occur once every four orbits of the facility. A 323 km long tether will be deployed from the facility, rotating prograde to the facility orbit with a tip speed of 0.92 km/s. When the payload is at apogee and the LEO tether facility is at perigee, the tether tip can

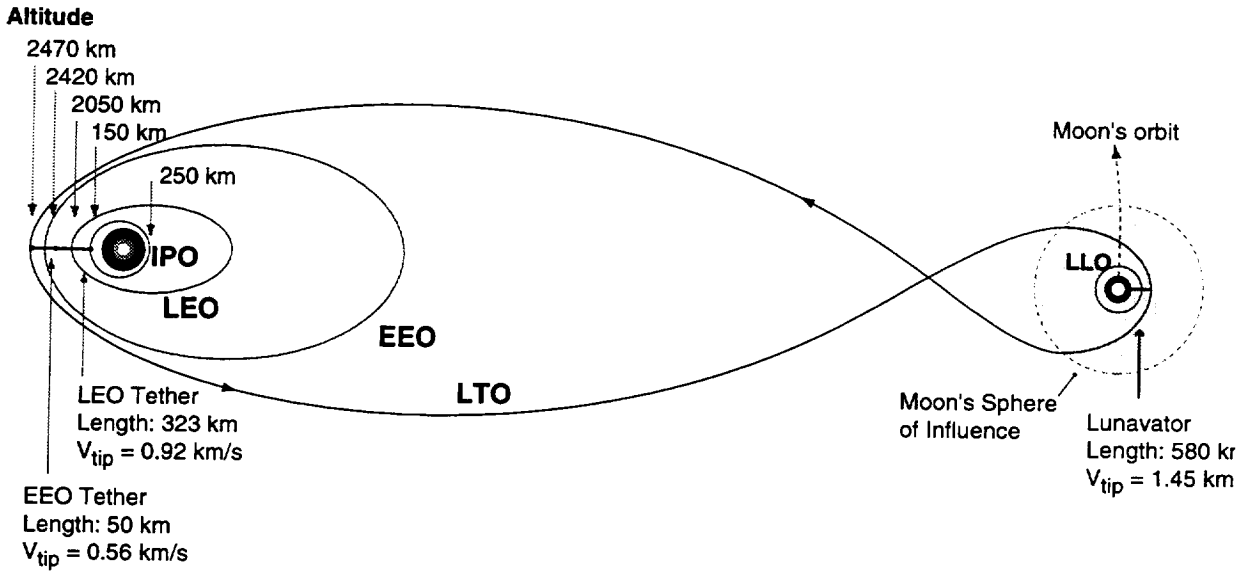

Figure 11. Schematic of a tether system for exchanging payloads between LEO and the lunar surface (not to scale).

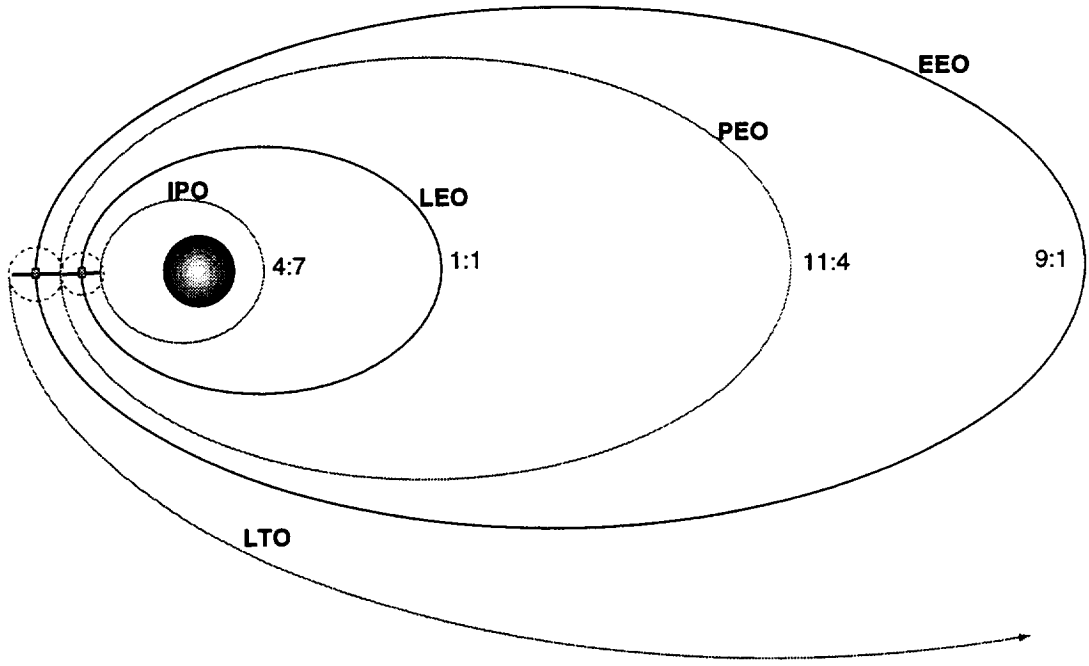

Figure 12. Schematic of the Earth-orbit portion of a LEO to Lunar Surface Tether Transport System. Shown are the initial payload orbit (IPO), the LEO tether facility orbit, the temporary payload elliptical orbit (PEO), and the EEO facility orbit (not to scale).

rendezvous with the payload with zero relative velocity. The tether will then capture the payload and carry it for one orbit, adjusting the tether rotation so that the tether will be at the top of its swing when it returns to perigee. The acceleration at the tether tip will be 0.26 g.

Tether Mass: Using Spectra 2000 with a design safety factor of 2.4, the required tether mass is 0.66 times the tip mass. With a grapple vehicle massing 20% of the payload mass, the total tether mass required is approximately (1+0.2)x0.75 = 0.9 times the payload mass.

Facility Mass: As in the SEO-Lunar design, placing the facility in an elliptic orbit and performing boost operations at perigee enables small ballast masses to be used. Facility masses of less than 5 times the payload mass are possible for the LEO stage.

EEO Tether

When the LEO tether facility returns to perigee, it will hand the payload off to a 50 km long tether attached to a facility in a higher, more elliptic orbit. This EEO facility will be in an orbit with semimajor axis of 46,276 km and an eccentricity of 0.583, with perigee altitude of 2420 km and perigee velocity of 9.06 km/s. The tether will rotate with a tip speed of 0.56 km/s, enabling the transfer to occur with zero relative velocity between the tether tips. The tether lengths and rotation speeds are chosen so that if the transfer is unsuccessful, the payload will enter an orbit with a period of 504.35 minutes, 11/4 times the LEO facility orbit period, so that the LEO tether can recapture the payload after 11 orbits.

Tether Mass: Using Spectra 2000 with a design safety factor of 2.4, the required tether mass is 0.25 times the tip mass. With a grapple vehicle massing 20% of the payload mass, the total tether mass required is approximately 0.3 times the payload mass.

Facility Mass: As in the SEO-Lunar design, placing the facility in a highly elliptic orbit and performing boost operations at perigee enables small ballast masses to be used. Facility masses as small as 2 times the payload mass are possible for the EEO stage.

Lunar Transfer Orbit

After carrying the payload for one orbit, the EEO tether injects the payload into a lunar transfer trajectory with a perigee altitude of 2470 km and a velocity of 9.62 km/s. The lunar

transfer orbit is illustrated in Figure 8. The transfer trajectory is hyperbolic, with a time-of flight from perigee to the lunar sphere of influence of only 31 hours. The transfer trajectory has a semimajor axis of -165,699 km, and an eccentricity of 1.053. If the insertion into the transfer trajectory is timed so that the angle between the perigee and the Moon, γ_o, is 132.56 degrees, the payload reaches the Moon's gravitational sphere of influence with a velocity of 2.21 km/s relative to the Moon at an approach angle λ_s of 83.14 degrees.

Lunavator

Once the payload reaches the Moon, it is caught and delivered to a lunar base by a Moravec Lunavator. The design for the Lunavator is described in Section IV.0.

Return Traffic

As with the tether transport systems described in the previous two sections, optimum opportunities for outbound trips will occur roughly once a month, and the trajectories for the return trip will line up three days after arrival at the Moon.

Summary

By properly choosing the orbital design, a staged tether system for frequent round-trip traffic between low Earth orbit and lunar bases can be developed with very reasonable total mass requirements. The total required mass of the two tethers and two facilities required for throwing payloads to the Moon could be less than ten times the payload mass.

Numerical Simulation of Staged Tether Systems: OrbitSim

In order to further refine the design of LEO-Lunar tether transport systems by removing the assumptions of co-planar orbits, patched-conic trajectories, and the other simplifying assumptions listed in Section 0.0.0, we have developed a software tool for numerical simulation of staged tether systems in the Earth-Moon system. This program, called "OrbitSim," models the 3-D orbital dynamics of rotating tethers, payloads, and other satellites.

Numerical Method:

OrbitSim uses a 4th order Runge-Kutte algorithm to integrate the equations of motion in the Earth-Moon system according to Cowell's method.[12] In the current implementation of the code, tethers are treated as rigid-rotators, ignoring tether dynamics; more detailed handling of tether dynamics could be included in the future. The code provides controls for scheduling captures and releases of payloads by the tether facilities. In addition, the code provides controls for directing a tether facility to adjust its tether length to control its spin rate, as well as for directing a facility to perform impulsive course corrections. Currently, the code uses first-order approximations to the geo- and lunar gravitational potentials. In future efforts, these models will be improved to account for higher order perturbations.

Output

The OrbitSim code has provisions for outputting the positions and velocities of the payloads and tether facilities at any time during a simulation. However, due to the complexity of the system, the primary form of output is in the form of computer animations. The code generates QuickTime movies of the simulation which can be used to visualize the operation of the tether systems.

Results

To date, the OrbitSim program has been used to simulate and refine two tether systems, one for the sub-Earth-orbit to Lunar surface transport system described in Section 0.0.0, and the other for the LEO Space Station to Lunar Surface transport system described in Section 0.0.0. QuickTime movies of these two systems can be found on the diskette with the electronic version of this report. Alternatively, the movies can be downloaded from the Tethers Unlimited web page, *www.tethers.com*.

These two animations show system designs which have been refined from the first-order designs of Section 0.0 by removing the assumption of patched-conic trajectories. Outside of the lunar sphere of influence, the objects move under the influence of the Earth as the primary gravitational body with the Moon's gravity as second order perturbation. Within the Moon's sphere of influence, the Moon is taken as the primary and the Earth's gravity is treated as a perturbation. The other simplifying assumptions listed in Section 0.0.0 have not yet been removed; specifically the facility masses are very large compared to the payload masses, and the orbits of the Moon and the satellites are taken to be in the equatorial plane. In the future, OrbitSim will be used to investigate these other effects on the design of the system.

High Strength Materials

As discussed in Section 0.0.0, the mass required for a rotating tether depends strongly on the ratio of the tip speed to the characteristic velocity of the tether material. Consequently, the economic viability of the rotating tether as a method of in-space propulsion depends upon whether materials are available with sufficiently large strength-to-weight ratios to make the tether masses practical. When several of the prior analyses of rotating tether systems were performed, the required tether masses were determined using the best material available at the time, Kevlar. Since that time, there has been steady improvement in the field of high-strength fibers,[13] particularly in the development of Spectra fibers. Because of the strong dependence of the required tether mass on the tip speed to characteristic velocity ratio, even a small increase in the characteristic velocity of tether materials can greatly reduce the tether mass, and thus the launch cost of the tether system. To determine the effects of improved fiber strengths on the viability of the LEO-Lunar tether transport concept, a portion of this effort was directed at assessing the current state-of-the-art in high strength fibers and in obtaining reasonable predictions for the performance of fibers expected to become available within the next decade.

Current Technology:

Spectra 2000

Currently, the material with the best strength to weight ratio commercially available in large quantities is Spectra 2000, a form of highly oriented polyethylene fabricated by AlliedSignal. Spectra 2000 fiber has a density of 0.97 g/cc and a tenacity of 37.3±1 g/denier, about 8% better than Spectra 1000.[14] A similar fiber called Dyneema 66 is available in Europe from DSM High Performance fibers. It also is highly oriented polyethylene, but it is made by a slightly different process. Dyneema 66 is advertised as having a tenacity of 37 g/denier. Word-of-mouth has it that some of the fiber sold in the US by AlliedSignal as Spectra 2000 is, in fact, Dyneema 66. Spectra 2000's tenacity of 37.3 g/denier translates to a tensile strength of 3.25 GPa. Using Eqn. (1) with a safety factor of 1 (ie- no safety margin), the maximum characteristic velocity of Spectra 2000 is 2.59 km/s. With a more reasonable safety factor of 2, the characteristic velocity of Spectra 2000 is 1.83 km/s.

One disadvantage to Spectra is that it has a relatively low melting temperature. It is not useful for applications where it will reach temperatures over about 423 K (150 C).

Low Temperature Spectra

Spectra fiber has a very low absorption coefficient for solar spectrum light. As a result, clean Spectra tethers in Earth orbit will have rather low temperatures, on the order of 180-200 K.[15] Joe Carroll of Tether Applications has found that when Spectra is cooled to 190 K, its strength increases by 21%. If it is placed under a load of approximately 1% of the breaking strength before and during the cooling, the strength increase improves to 41%.[16]

A 41% increase in tenacity translates to a tensile strength of 4.58 GPa. With a safety factor of 2, the low temperature characteristic velocity of Spectra 2000 in Earth orbit should be approximately 2.17 km/s.

PBO/Zylon

Poly(p-phenylene-2,6-benzobisoxazole) (PBO) is a rigid-rod isotropic crystal polymer marketed under the brand name Zylon by the Toyobo company in Japan. PBO has a tenacity of 42 g/denier (5.8 GPa) and a density of 1.56 g/cc. With a safety factor of 2, the characteristic velocity of PBO is 1.93 km/s. PBO also has excellent temperature resistance properties, maintaining nearly full strength to temperatures near 500 C.[17] Using Eqn. (1) with a safety factor of 2, the characteristic velocity of PBO is 1.93 km/s.

Near-Future Technology

Spectra X000

We have discussed the potential for further improvements in Spectra fiber strengths with Allied Signal High Strength Fiber engineers. They have informed us that they are "targeting" a

tenacity of 45 g/denier (3.8 GPa) Spectra for development within the next 5 years. We will refer to this next-generation fiber as "Spectra 3000." These engineers have indicated to us that tenacities approaching 60 g/denier (5.24 GPa) are theoretically possible for the Spectra material, and that single-fibers with strengths of 50 g/denier have been produced in the laboratory. According to the Allied engineers, fiber with such strengths approaching 60 g/denier could be produced in usable quantities, but the cost of producing such fibers would be astronomical using current technologies. However, they believe that fibers with 45 g/denier tenacities can be produced at a reasonable cost, and are currently building the production line to fabricate these fibers.

With a safety factor of 2, a 45 g/denier Spectra 3000 will have a characteristic velocity of 1.98 km/s. If the low-temperature improvement in Spectra strength holds true for this next-generation fiber, characteristic velocities of 2.35 km/s may be possible.

Possible Future Technology

Nanotube Fibers

Recently, there have been some very encouraging advances in the production of nanotube fiber "ropes."[18] Nanotubes are a form of fullerene in which carbon atoms form perfect hexagonal bonds to create tubular structures composed of a single layer of carbon atoms. Nanotubes have the theoretical potential to offer strength-to weight ratios one or two magnitudes of order greater than currently available materials. In fact, the theoretical upper limit on the strength of a fullerene rope is 1.5 times the strength of a hypothetical diamond cable.[19] Small quantities of "10-100 micrometer long" nanotube ropes have been produced with surprisingly high (>70%) yield efficiencies. Moreover, the research has indicated that it may be possible to fabricate nanotubes with much longer lengths. Even if this material falls far short of its theoretical strength in actual production, a nanotube rope with only 1/10 of its theoretical strength could make the concept of using tethers to throw payloads to the outer planets a real possibility. While this technology is still in the nascent phase, and real-world application is likely decades off, it appears to have the potential to greatly improve the benefits of tether technology, and bears further observation.

Tether Mass Requirements

To examine the viability of developing rotating tether concepts with materials that are currently available or expected to be available in the near future, we have calculated the tether mass ratios required for several candidate tether facility designs using the tensile strength data for Spectra 2000 (presently available) and Spectra 3000 (targeted for market in 5-10 years). To calculate these mass ratios, we used Moravec's equation for the mass of a tapered tether, given in Eqn. (3). For these calculations, we have chosen to use a design safety factor of F=2.4. This is a conservative safety number appropriate for a high-strength, long-life Hoytether design, as will be discussed in Section 0.0; this safety number also includes an extra safety margin to account for the shock loads that are expected due to capture dynamics.

The tether mass ratios for the LEO, EEO, and Lunavator tethers in the Sub-Earth-Orbit to Lunar Surface Tether Transport System described in Section 0.0.0 are presented in Table 1. In addition, the table presents mass ratio requirements for a 1.7 km/s single-stage tether capable of catching a payload in LEO and throwing it to the Moon on a low-energy trajectory. The table shows that, with currently available fibers, the required masses for the LEO and EEO tethers are lower than the payload mass. Moreover, if the low-temperature improvement in Spectra strength proves to be reliable, and if the expected near-future improvements in Spectra strength are realized, the tether mass ratio for both of these tethers can be reduced to less than half of the payload mass. The mass of a Moravec Lunavator using Spectra 2000 would be about 2.5 times the tip mass, and this number could be reduced to about 1.25 in the future. The single-stage LEO-Lunar tether requires a larger mass ratio of 4.3 with current fibers. Nonetheless, if low-temperature improvements in Spectra strength prove to be true, and if Spectra 3000 or a better material becomes commercially available, the mass ratio could be reduced to about two, and single-stage tether systems could become feasible for LEO-Lunar transport.

Summary

Because launch costs to place mass in orbit are so high, the competitiveness of an in-space propulsion system is measured largely by the mass required for the system. Our analyses have shown that by using *currently available materials* such as Spectra 2000 and PBO, tethers for significant propulsion missions such as LEO to Lunar transport will require total masses of less than 5 times the payload mass. Moreover, fiber strengths have improved steadily over the past several decades, and near term improvements in fiber strength will reduce the tether mass even further.

Table 1. TETHER MASS RATIO (TETHER MASS/TIP MASS) FOR CURRENT AND NEAR-FUTURE MATERIALS

	CURRENT		*NEAR FUTURE*		
Material	Spectra 2000 300 K	Spectra 2000 190K	PBO/Zylon	Spectra 3000 300 K	Spectra 3000 190 K
Tensile Strength (g/denier)	37.3	52	42	45.0	63
Tensile Strength (GPa)	3.25	4.58	5.8	3.8	5.35
Density (g/cc)	0.97	0.97	1.56	0.97	0.97
Characteristic Velocity, km/s with Safety Factor F = 2.4	1.67	1.98	1.76	1.8	2.14
LEO Tether V_{tip} = 0.876 km/s Safety Factor F = 2.4	0.66	0.44	0.57	0.55	0.375
EEO Tether V_{tip} = 0.8 km/s Safety Factor F = 2.4	0.54	0.36	0.48	0.44	0.3
Lunavator V_{tip} = 1.45 km/s, Safety Factor F = 2.4	2.53	1.54*	2.2	2.0	1.25*
Single-Stage LEO-Lunar Tether V_{tip} = 1.7 km/s, Safety Factor F = 2.4	4.3	2.44	3.6	3.3	1.93

* The temperature of the portion of the tether near the sun-facing surface of the Moon will probably be closer to 300 K due to radiation by the Moon's surface. Thus the required lunavator mass will probably be in between the 300 K and the 190 K number.

High-Strength Survivable Tethers

Motivation

For a tether transport system to be economically advantageous, it must be capable of handling frequent traffic for a period of at least a decade. Consequently, a tether transport system will require the use of tethers designed to remain fully functional for many years despite degradation due to impacts by meteorites and space debris. An additional requirement for this system is that the tether mass be minimized to reduce the cost of fabricating and launching the tethers. These two requirements present conflicting demands upon the tether design that make conventional single-line tethers impractical for this application. For a single-line tether to achieve a high probability of survival for many years, it would have to be very thick and massive. Fortunately, a survivable tether design, called the Hoytether, exists which can balance the requirements of low weight and long life, enabling tether transport facilities to become feasible.

The Hoytether is a multiline, failsafe tether design that is capable of surviving for periods of decades.[20,21] The Hoytether is an open net structure where primary load bearing lines are interlinked by redundant secondary lines. The secondary lines are designed to be slack initially, so that the structure will not collapse under load. If a primary line breaks, however, the secondary lines become engaged and take up the load. This redundant linkage enables the structure to redistribute loads around primary links that fail due to meteorite strikes or material failure, as illustrated in Figure 13. Consequently, the Hoytether structure can be loaded at high stress levels yet achieve a high margin of safety.

Because minimizing the tether mass is critical to the viability of tether systems for LEO-Lunar or LEO-GEO transport, we have sought to optimize the design of the Hoytether structure so as to maximize the strength-to-weight ratio of the tether while achieving high probability of survival for periods of years.

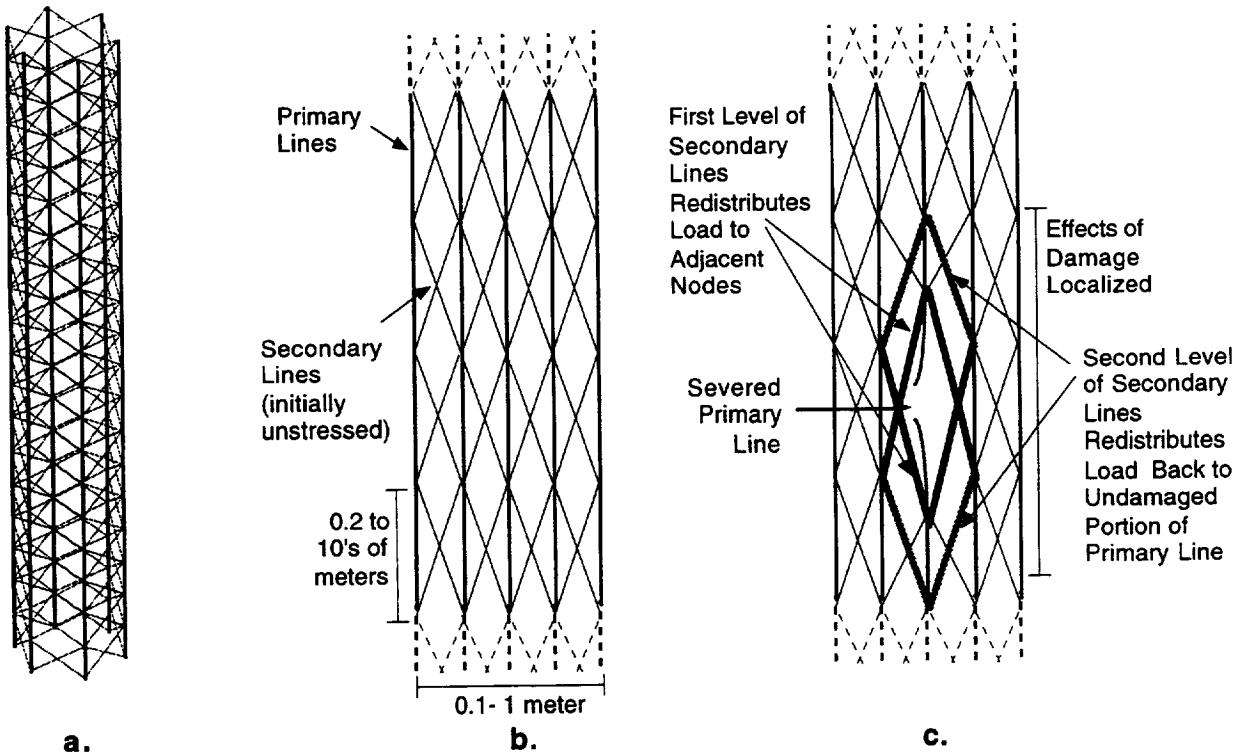

Figure 13 a) Section of a tubular Hoytether ("Hoytube"). b) Schematic of undisturbed Hoytether. c) Secondary lines redistribute load around a failed primary line without collapsing structure. *Note*: the horizontal scale is expanded relative to the vertical scale; in reality the secondary lines are nearly parallel to the primary lines.

Minimizing the "Safety Factor" While Maintaining Reliability

When a tension member such as a tether is developed, it is normally designed to operate at a load level somewhat lower than the maximum it could support without breaking. This derating provides margin of error in case of imperfections in the material or the construction. Typically, a tether is designed to carry a maximum load that is 50% of its breaking limit; this tether would have a "design safety factor" of $F = 1/50\% = 2.0$. For rotating tether systems, it is necessary to operate at the minimum acceptable safety factor so as to minimize the required tether mass. For conventional single-line tethers, however, reducing the safety factor causes a corresponding increase in the likelihood of failure.

For the Hoytether, we define the safety factor as the ratio of the maximum load capacity *of both primary and secondary lines* to the design load. The safety factor thus provides the same measure of the strength-to-weight ratio of the Hoytether structure as it does for a single-line tether. However, this definition of the safety factor does not accurately represent the margin of safety for the Hoytether. Because the Hoytether has redundant links that can reroute loads around parts of the tether that have failed, it is possible to load the Hoytether at a large fraction of the capacity of the primary lines (ie.- small "safety factor") and still have a large margin of safety. Consequently, using the Hoytether structure allows us to design the tether with a low "safety factor" to minimize the tether mass and yet still have a very reliable structure. In this effort we have sought to optimize the Hoytether by finding a design that minimizes the safety factor and thus minimizes the required mass while still providing the ability to withstand many cuts due to meteorite strikes.

It should be noted that the manner in which we calculate the Hoytether safety factor below is not obvious. Typically, we refer to Hoytether designs by the level of stress on the *primary lines*. Thus, if each secondary can support 1/2 as much tension as a single primary line can support (ie- each secondary has half the cross-sectional area of a primary line), and if it is loaded at 50% of the capacity of the primary lines, it will be loaded at a design safety factor of

$$F = \frac{[(\#\ of\ primaries)(primary\ line\ area)+(\#\ of\ secondaries)(secondary\ line\ area)]}{(\#\ of\ primaries)(primary\ line\ area)} \frac{1}{(primary\ stress\ level)} \qquad (5)$$

$$F = [1+2(1/2)]/50\% = 4.$$

Method: Simulation with the SpaceNet Program

To study the optimization of the Hoytether structure for high-load applications, we performed a series of simulations of variations of the structure using the SpaceNet program.[22] The SpaceNet program uses a combination of finite-element methods with a structural relaxation scheme to calculate the effects of damage to complex 3-D net structures such as the Hoytether.

Results

We began by studying multi-line Hoytethers with secondary lines having 1/4 the cross-sectional area of the primary lines; the secondary lines thus have a total mass of 1/2 of the mass of the primary lines (there are two secondary lines per primary line). In addition, the secondary line length was chosen so that they would be slack under design load. We found that if this tether is loaded at 90% of capacity of the primary lines, giving it a design safety factor of 1.67, it can survive a cut to one of the primary lines. Moreover, the tether can survive an additional cut on the same level. However, if the second cut is on a primary line immediately adjacent to the first cut, the structure will fail. While the probability of two adjacent primary lines being cut by two separate meteoroid impacts is very small, it is possible that two lines could be cut by one impactor if it is large enough. Consequently, it is necessary to design the tether to withstand several localized cuts. Therefore, a larger safety factor is required.

The results of our subsequent analyses indicate that the design of an optimal Hoytether depends upon how much of its mission duration will be spent under high load. Consequently, there are two classes of Hoytether designs, one for tethers that are always under high load, and one for tethers that are heavily loaded for brief periods only.

Continuous-High Load Tether

If the tether will be under high load for most of its mission, then it should be designed with secondary lines slack at the expected load level. This will enable the tether lines to remain spread apart at all times, minimizing the chances of a single impactor cutting several lines. For this case, a near-optimal tether design would be a cylindrical Hoytether with a large number of primary lines (~20) stressed at 75% of their maximum load and with initially-slack secondary lines that each have a cross-sectional area 0.4 times that of a primary line. Splitting the tether up into a large number of primary lines is necessary. From Eqn. (5), such a tether will have a design safety factor of 2.4. However, the redundant nature of the structure will make the Hoytether far more reliable than a single line tether with the same safety factor. Simulations with the SpaceNet program have shown that this tether design can withstand multiple cuts on a single level. In fact, even if all of the primary lines on one level are cut, the secondary lines will support the load.

Intermittent High-Load Tether

A tether transfer facility, however, would likely be loaded at high levels for only a few hours every month. Therefore, it is possible to reduce the tether weight by designing it to have slack secondaries at the load level experienced during its long "off-duty" periods, but to have the secondaries bear a significant portion of the load during a brief high-stress operation such as a payload catch-and-throw operation. During the high-stress period, the loading of the secondaries will cause the structure to collapse to a cylindrical tube. Once a payload is released and the stress is reduced, however, the tether lines will spread back apart. If this high-load period is brief, it will only slightly increase the chances of tether failure due to impact by a large object. Because the secondaries bear a significant fraction of the stress at high load levels, the tether can safely be loaded to higher levels. Simulations indicate that a 20-primary line Hoytether with secondary lines having cross-sectional area 1/4 of that of the primary line area can be loaded to more than 100% of the primary line capacity and still survive cuts to two adjacent primary line segments. A reliable design for this class of tether would be a cylindrical Hoytether with primary lines sized so that they will be loaded at 85% of their capacity during peak stress operations, and secondary lines with cross-sectional areas 1/4 of the primary lines. The secondary line lengths would be chosen so that they would be slightly slack during off-duty periods. Eqn. (5) above gives the design safety factor of this tether as 1.75.

Lifetimes of High-Strength Hoytethers for a SEO-Lunar Tether Transport System.

The three tethers in the SEO-Lunar transportation system will be subject to continuous bombardment by micrometeorites and small space debris particles. If the tethers were made of a single thick line, there is always the chance, at any time, that a sufficiently large particle can damage the line enough that it will part under the high stresses experienced by the tethers in this transport system, causing a catastrophic failure. The proposed transportation system will use tethers constructed using the failsafe interconnected multiline Hoytether design.[21] The design assumed for each tether will use 20 straight load-bearing primary lines arranged in a circle that run in parallel along the length of the tether, as described in Section 0.0.0. The diameter of the circle will be roughly 30-60 cm, so the spacing between adjacent primary lines will be 5-10 cm. At 50-100 cm intervals long each primary line, two secondary lines will be connected to the primary line by a knotless, slipless interconnection. The two secondary lines then cross over to the two adjacent primary lines and are interconnected there at the next level up and down. There are 40 secondary lines interconnecting the 20 primary lines, 20 spiraling clockwise and 20 spiraling counterclockwise. In the proposed high-strength Hoytether design, the cross-sectional area of the secondary lines will be 0.40 times the cross-sectional area of the primary lines, so that the diameter of the secondary lines is 0.632 time the diameter of the primary lines. Since the ratio of the length of the secondary line segments to the spacing between the primary lines is so small (1:10), the effective length of each of the secondary lines is essentially the same (1.005) as the length of the primary lines. With these assumptions, it is easy to calculate the diameter D of the primary lines in each tether as a function of the tether mass M, length L, and line density ρ as:

$$D = \left[\frac{4M}{(20+40\{0.40\})\pi\rho L}\right]^{1/2} = \left[\frac{M}{9\pi\rho L}\right]^{1/2} \quad (6)$$

Because of the high speed of the impacting particles, typically ranging from Earth escape velocity (12 km/s) up to Earth orbital velocity (30 km/s) for the meteorites, and up to twice orbital velocity (7-15 km/s) for the debris particles, the kinetic energy of the particles is so high that the particles essentially explode when they impact the line, creating a ball of high temperature plasma that melts a hemispherical hole with a radius typically three times larger than the radius of the impactor particle. Since the primary lines of the tethers in the proposed transportation system are under high stress, typically 75% of their ultimate strength, they will fail if more than 25% of their cross-sectional area is destroyed by an impactor. From the limited experience gained by operation of tethers in space, it is usually assumed[23] that the "lethality coefficient" of an incoming impactor is K=1/3, or that a line will be cut by an impactor with a diameter 1/3rd the diameter of the line. To be conservative, we will assume a "lethality coefficient" of less than half of that, or K=0.15. (For a discussion of the survivability of high-stress tether lines, see Appendix D)

Once the diameter of the "cutting" impactor is known, the cross-sectional flux of all particles with a diameter greater than the cutting diameter can be obtained from NASA cumulative models for the meteorites[24] and the space debris particles.[25] The two fluxes are combined into a single flux number and then multiplied by the cross-sectional area DL of the tether to obtain the number of cuts per year of a line of length L. For a single long tether of length L of many kilometers, the average cut rate is predicted to be many cuts per year, leading to a estimated 1/e lifetime measured in only a few weeks. Because the primary load-bearing lines on a Hoytether are interconnected at intervals to produce "line segments" that are only a number of centimeters long, the average cut rate on these line segments is quite low. On top of that, in order for tether failure to occur, cuts must be made on a large number of the many line segments at the same level and the probability of that occurring is quite low.

In addition to individual line segment cuts, there is the possibility that all the lines can be cut at the same time by a single large object, like a very large meteoroid (very unlikely) or by a large derelict spacecraft. These large objects are known and tracked, and we will assume, that since the tethers in this transportation system have considerable communication, radar, and self-propulsion capability, that they and their operational system will be designed to avoid these large hazards.

The probability of survival S of an interconnected multiline Hoytether from cuts by small space impactors can be shown[21] to be:

$$S = [1-(1-e^{-\frac{C}{n}t})^x]^n \quad (7)$$

where C is the cut rate of the entire length of a primary load-bearing line and n is the number of segments in the line, so that C/n is the cut rate for a single line segment, while x is the number of line segments that must be cut at the same level before the tether as a whole will fail. This survival probability equation does not display a 1/e exponential decay curve. Instead it describes what can be called a "bingo" curve. No failures will occur until at least x line segments have been cut, and even then, it would be very unlikely that all those cuts will have occurred at the same level. Thus, the survival probability S stays very high (>99%) for a long time, then a point is reached where a number of the levels have x-1 lines cut, then shortly after that, "Bingo!", and one of those levels has x lines cut and the tether fails. The high-strength Hoytethers designed for this transportation system can survive having all 20 of the primary line segments cut at the same level because the secondary line segments can still carry the load. In reality, however, some of the secondary line segments will have been cut before all 20 of the primary line segments are cut at the same level, so we will make the conservative assumption that the tether can no longer be considered safe if more than x=10 primary line segments have

Table 2. Survival probabilities of the tethers in the SEO-Lunar Tether transport System

TETHER TYPE	LENGTH (km)	MASS (kg)	LINE D (mm)	LEVELS n	CUT RATE (per line yr.)	SURVIVAL (10 yr.)	PROB. (20 yr.)
LEO	200	800	0.38	400,000	6000	0.998900	0.572
EEO	75	650	0.56	75,000	840	0.999980	0.991
Lunavator	580	2900	0.47	580,000	5000	0.999991	0.994

been cut at the same level. Under these assumptions, the calculated survival probabilities of the three tethers in the transportation system are:
The survival probabilities of the three tethers are graphed in Figure 14. We can thus see that we should plan to replace the LEO tether, which is subject to the heaviest bombardment, once every 10 years, while the EEO tether and the Lunavator tether can be expected to operate without replacement during their technological lifetime of 20+ years, by which they will have been replaced by much stronger and more massive tethers capable of handing much larger payloads.

In comparison to these decade-long, 0.99+ survival probability lifetimes of the Hoytether, if the same mass were placed in a single line tether of the same mass and length, the calculated 1/e (0.37 survival probability) "lifetimes" would be 3 weeks for the LEO tether, 21 weeks for the EEO tether, and 2 weeks for the Lunavator.

Conclusion

Using numerical simulations, we have shown that multiline failsafe tethers can be built with safety factors as low as 2.4 if continuously loaded and 1.75 if loaded only infrequently. The tethers in the LEO-Lunar transport systems will likely be loaded for only several hours every month; as a result, the lower safety factor could chosen to minimize the tether weight. However, the LEO and EEO tethers in these systems already have masses lower than the payload mass. Therefore, in our analyses above we have chosen to use the higher safety factor of 2.4 to allow for higher shock loads during payload capture and to provide an extra margin of safety; because the tether tip speeds in these designs are lower than the characteristic velocity of the tether, the mass penalty of the higher safety factor is minor. Our analytical survival modeling has shown that even with these low safety factors, these tethers will be capable of surviving the orbital debris environment and performing their missions for periods of decades. Consequently, a Hoytether optimized for high-load operation can minimize the tether mass and provide the long tether lifetimes necessary

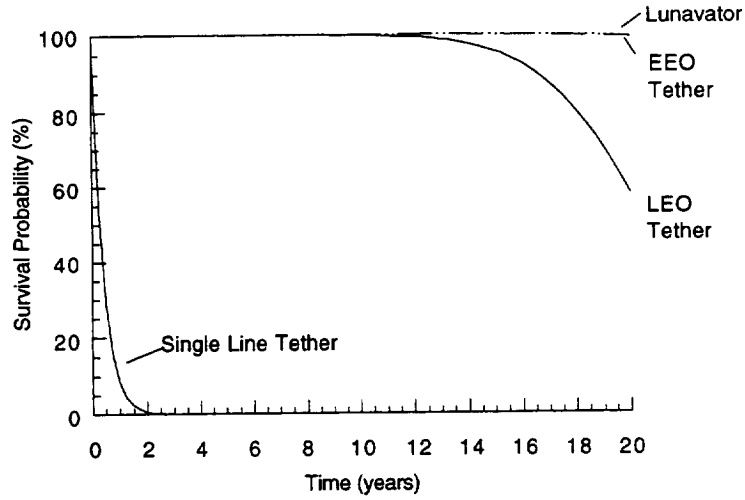

Figure 14. Survival probabilities of the Hoytether designs for the tethers in the SEO-Lunar Transport System. Also shown is the survival probability for a comparable mass single line tether.

for the LEO-Lunar tether system to be economically viable.

Electrodynamic Bolo Tether

In this research effort we have also investigated the possibility of combining the principles of momentum-exchange tethers with the concept of electrodynamic tether propulsion. This combination could form a system capable of repeatedly throwing payloads to higher orbits without requiring propellant for reboost or return traffic.

For a tether system to greatly reduce the cost of in-space transportation, the orbital energy and momentum of the system must be conserved to minimize the need for reboost propellant. Once a LEO-Lunar system has been set up and frequent lunar traffic develops, momentum and energy can be conserved by balancing the flow of mass to and from the Moon. However, such a system will most likely be built incrementally. While the system is under construction, return traffic may not be available to balance the flow of mass through the system. Thus, an alternate means of maintaining the orbits of the tether facilities must be provided.

Prior studies have proposed to reboost tether facilities using high specific impulse electric propulsion.[3,6,4,1] A tether facility with electric propulsion reboost would be able to place payloads into operational orbits with the fuel efficiency of electric propulsion but without the long transit times normally associated with high-Isp propulsion. Long transit times are costly to many satellite users because of the lost revenue incurred in the interval between launch and the beginning of operation. Nonetheless, such a system will still require propellant for the electric thrusters. Moreover, elimination of the transit delay may not suffice to make a tether/electric propulsion system more competitive than an electric propulsion system without the tether.

It may be possible, however, to use electrodynamic tether propulsion to spin up and reboost a tether facility, eliminating the need for any propellant. A long conducting tether in low Earth orbit can generate thrust through Lorentz-force interactions between currents in the tether and the Earth's magnetic field. A current I passing through a wire of length $\boldsymbol{L}$ in a magnetic field $\boldsymbol{B}$ will generate a force $\boldsymbol{F} = I\ \boldsymbol{L}\times\boldsymbol{B}$. Thus if current is driven through a long conducting tether, thrust can be generated by pushing on the Earth's magnetic field. No propellant is required for this thrust, because the reaction mass is provided by the Earth itself, coupled through the geomagnetic field.

The recent flight of the TSS-1R mission demonstrated that electrodynamic tethers are a viable means of propelling spacecraft in low Earth orbit. The tether rupture ended the TSS-1R science mission prematurely. Before that mishap, however, the tethered satellite system demonstrated that not only could an electrodynamic tether generate significant levels of thrust (drag thrust, in this case), but it could do so with a much better efficiency than previously expected. In tests conducted during the five hours of tether operation, the tether generated thrusts of approximately 0.3 N at thrust efficiencies of 0.148 N/kW.[26]

Normally, application of electrodynamic tether propulsion is limited to LEO altitudes below 1,000 km because an ambient plasma is required for operation. The current "loop" in the tether system must be completed by drawing electrons from the plasma at one end of the tether and by emitting electrons into the plasma at the other end.[27] At low altitudes, this current closure can be provided by the ionospheric plasma. However, beyond an altitude of approximately 1,000 km, the ionosphere is too tenuous to carry a sufficient current. Nonetheless, propellantless electrodynamic propulsion can be used to move payloads beyond that range, perhaps even to the Moon or other planets, by using electrodynamic propulsion in a rotating tether system. The basic concept is to place a payload at the end of a long conducting tether and use electrodynamic "torque" to spin up the tether. In this manner, the payload can be accelerated at LEO altitudes and then thrown into a transfer trajectory beyond LEO.

Conceptual Design

To accomplish propellantless electrodynamic tether propulsion for in-space transportation missions, we propose a LEO electrodynamic bolo tether (EDBT) facility. The EDBT facility could serve as the first building block of a modular LEO-GEO or LEO-Lunar transport system. One possible configuration for this facility is illustrated in Figure 15.

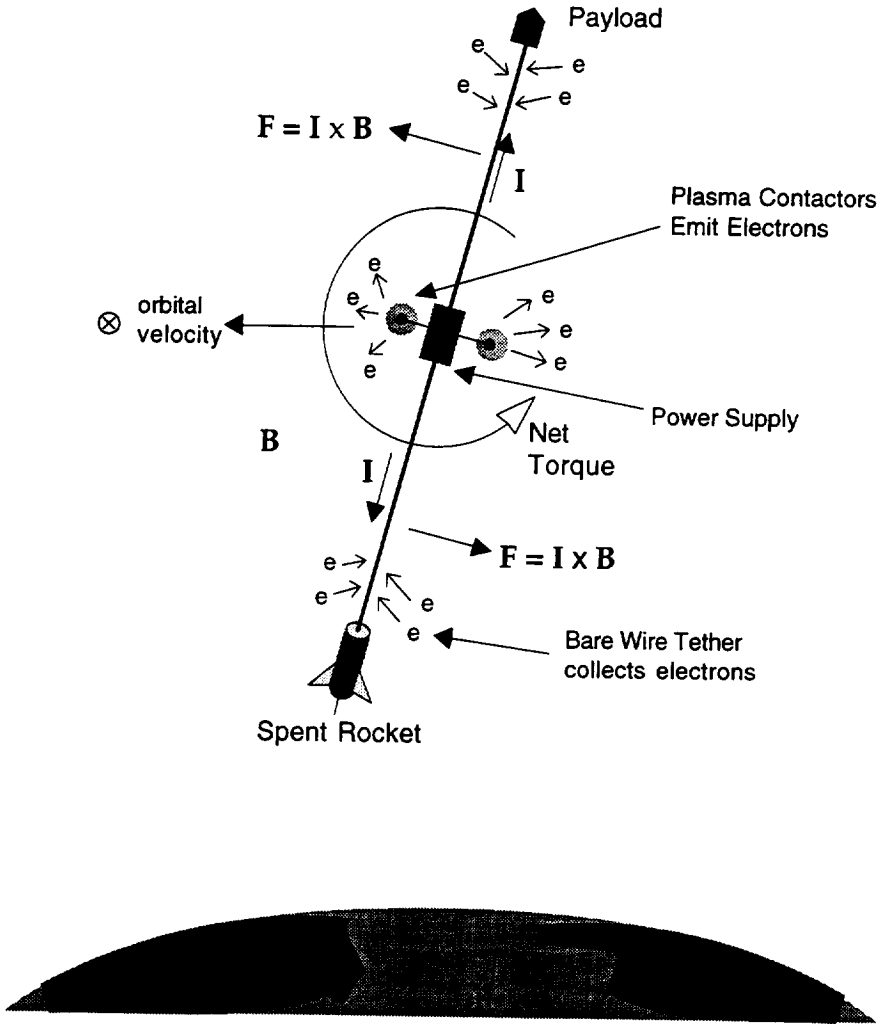

Figure 15. Electrodynamic Bolo Tether system.

The EDBT facility would be composed of two symmetric tethers with a small power system in the center. At the power station, plasma contactors would provide an electrical connection to the space plasma. Each of the tethers would be made of high-strength fibers with a core of conductor. At the end of the tethers, the conductor would be exposed to the space plasma. The payload would be placed at the end of one tether, and a ballast mass, such as the spent launch rocket, would be placed at the other. By using the power supply to apply a voltage between the contactors at the center and the two tether tips, current would be forced to flow radially outward through the two tethers. The exposed sections of bare conductor at the tether tips would collect electrons from the ionosphere through the bare-wire anode method,[28] and the plasma contactors at the central facility would emit the electrons into the space plasma. The current flow in the system is illustrated in Figure 16. The action of the radial current **I** flowing across the Earth's magnetic field **B** would create a Lorentz force **F** = **IxB** which would induce a net torque on the system. This torque would be used to spin-up the system until the payload achieves the desired velocity. The payload and rocket would then be released, throwing the payload into an elliptical transfer orbit (or possibly even to escape) and simultaneously deorbiting the spent rocket. With proper design, the system would loose no net orbital momentum or orbital energy. The tether spin could then be slowed by passive electrodynamic braking to prepare for another payload.

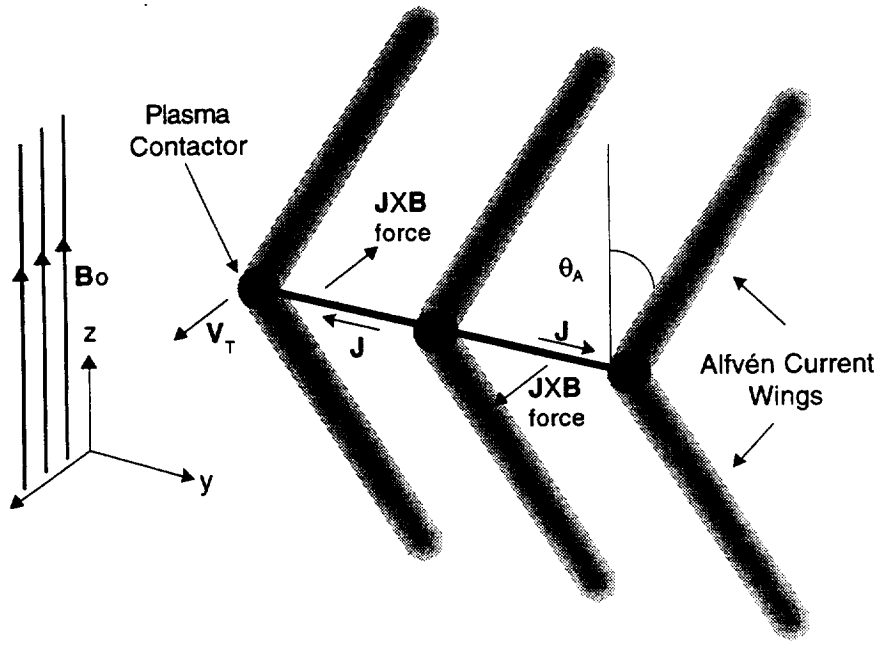

Figure 16. Schematic of current flow in an Electrodynamic Bolo Tether system with plasma contactors at the center and at the two tether tips.

Alternatively, the system could be constructed with just one tether arm. The system would thus appear similar to the Carroll tether transfer facility illustrated in Figure 1, except that the tether would have a conducting core, and plasma contactors would be installed at both ends of the tether to provide connection to the ambient plasma. The tether could be deployed vertically with a small swing and induced to spin by driving an alternating current phased with the swing of the tether. Once the tether begins to spin, driving current along the tether in the proper direction will induce a torque on the system in the same direction as its rotation, spinning up the tether to high speeds. If a waste mass such as a spent launch rocket is available, the momentum of the facility could be conserved by first spinning up the payload and rocket together. The rocket could then be released at the bottom of the tether swing, simultaneously deorbiting the rocket and boosting the tether and payload to a higher orbit. The payload would then be released at the top of the tether swing, throwing it into a transfer orbit and simultaneously returning the facility to its original orbit. If, however, a spent rocket is not available, the facility could throw a payload and then restore the momentum it transfers to the payload using electrodynamic thrust.

Analysis

To examine the feasibility and utility of an electrodynamic bolo tether system, we will calculate the power and time required for a EDBT system to accelerate a 1000 kg payload to 1 km/s. The example EDBT facility would be a two-arm tether system, as illustrated in Figure 15. Each arm would be $L = 50$ km long. If the tethers are constructed of PBO high strength fiber, with tenacity of 5.8 GPa and density of 1.56 g/cc, the required mass for each of the two tethers, given by Eqn. (2), is 0.8 times the payload mass, or 800 kg. In addition to the high strength fibers to bear the load, each tether will have a conductor running along its length. We will choose this conductor to be an aluminum wire massing 200 kg, so each tether masses a total of 1000 kg, the same as the payload. We will assume that the tether will simultaneously boost the payload and deorbit a spent rocket massing the same as the payload.

The rotational inertia of the payload and the rocket are

$$\Theta_p = m_p L^2 = 2.5\text{e}12 \text{ kg}\cdot\text{m}^2 , \qquad \text{(E-1a)}$$

$$\Theta_r = m_r L^2 = 2.5e12 \text{ kg•m}^2. \quad \text{(E-1b)}$$

The taper on these tethers is small, so the rotational inertia of each of the tether arms can be approximated by

$$\Theta_t \approx \frac{m_t}{L}\int_0^L x^2 dx = m_t \frac{L^2}{3} = 0.84e12 kg \bullet m^2 \quad \text{(E-1c)}$$

The rotational inertia of the facility can be ignored, since it is at the center of the rotational system. The total rotational inertia of the payload, spent rocket, and the two tethers is thus

$$\Theta_{tot} = 2\,\Theta_t + \Theta_r + \Theta_p = 6.7e12 \text{ kg•m}^2. \quad \text{(E-2)}$$

The resistance of the tether is

$$R = \frac{\rho \delta L^2}{m_{conductor}} = 925\ \Omega, \quad \text{(E-3)}$$

where $\rho = 27.4\text{x}10^{-9}$ is the resistivity of aluminum and $\delta = 2700$ kg/m^3 is its density.

The power supply is used to drive a current of $I = 1$ Amp radially outward through both tether arms (currents larger than this were observed in the TSS-1R experiment). The EDBT system will thus consume an ohmic power of

$$P_{ohm} = 2\,I\,R = 1.85 \text{ kW}. \quad \text{(E-4)}$$

For this analysis, we will assume that the current flows along the whole length of the tethers. The action of the current $\boldsymbol{I}$ flowing across the Earth's magnetic field $\boldsymbol{B}$ induces a Lorentz $\boldsymbol{I}\text{x}\boldsymbol{B}$ force on the tether. At 350 km altitude, $B \approx 3\text{x}10^{-5}$ T . The net torque on the system is

$$\tau = 2\int_0^L Fl\ dl = 2IB\frac{L^2}{2} = 7.5e4 \text{ N•m}^2. \quad \text{(E-5)}$$

To achieve a tip speed of 1 km/s at the end of the 50 km tethers, the EDBT facility must accelerate rotationally to an angular velocity of

$$\omega = V_{tip}/L = 0.02 \text{ rad/s}. \quad \text{(E-6)}$$

With a constant torque τ, the EDBT will spin up at a constant angular acceleration α and reach the desired angular velocity in a time

$$T = \omega/\alpha = \omega\Theta/t \approx 21 \text{ days}. \quad \text{(E-7)}$$

If the current is held constant, the power going into rotational energy will vary linearly with the angular momentum, increasing from zero to a maximum of $P_{rot} = \tau\omega = 1.5$ kW. Consequently, the "thrust efficiency" will increase from zero to approximately 44% as the facility spins up, with an average of around 22%. While this thrust efficiency is lower than the numbers usually quoted for some electric propulsion techniques, this measure of thrust efficiency is not a valid comparison. In electric propulsion, the propellant and power supply must be accelerated along with the payload; if one looks at the efficiency of thrust power going into the payload alone, the efficiency of standard electric propulsion techniques is very small. In the EDBT, there is no propellant required, and the power supply is at the center of the system, so the power required to spin up its mass is negligible. Thus nearly all of the thrust power goes into accelerating the payload.

The reader may wonder about the power required to overcome the voltage on the tether due to its orbital motion across the Earth's magnetic field. Fortunately, it turns out that the net power is zero, because while the voltage on one tether will oppose the desired current, on the other tether the voltage will be in the same direction as the desired current. The power supply

will require the ability to vary its voltage output as the facility rotates to properly balance the power going into each tether, but no net power will be required to overcome the motional-*emf*.

Because launch costs are so large, it is desirable to minimize the mass of an EDBT facility. If simultaneous payload boost/spent rocket deboost is performed, no ballast mass is required for the facility. The facility would require a power supply with a capability of approximately 5 kW for the electrodynamic tethers (includes margin for power processing inefficiencies). Using rule-of-thumb numbers for power supply mass of 15 kg/kW for solar cells and 9 kg/kW for power processing electronics, and adding 20% for structural mass, the power supply for the electrodynamic tethers would mass approximately 150 kg. The facility would also require two tether deployment systems capable of deploying the tethers and then slowly rewinding them after a throw operation in preparation for subsequent payloads. The facility, including both tethers, power supply, deployers, and guidance electronics, can probably be built with a total mass of approximately 3,000 kg.

Thus, from these simple calculations, it appears possible that an EDBT facility consisting of two 50 km high strength conducting tethers, massing approximately 3,000 kg, a 5 kW power supply massing 150 kg, and two tether deployers massing 500 kg each, could accelerate a 1,000 kg payload by 1 km/s within three weeks, and require no propellant to do so. If the facility de-orbits a launch vehicle of equal mass at the same time, the facility orbit will not be changed by the boost operation, so no return traffic or reboost propellant would be needed. The time to accelerate the payload will vary inversely with the total power, so shorter acceleration times would be possible with larger power supplies.

Conclusions

By combining propellantless electrodynamic tether propulsion with tether momentum-exchange techniques, it is possible to develop an Electrodynamic Bolo Tether system that can repeatedly boost payloads from LEO to higher orbits without requiring propellant. The EDBT system would have a number of advantages over conventional propulsion techniques:

- No propellant is needed for boosting the payload and deorbiting the spent rocket.
- The power supply *does not need to be accelerated.* Moreover, because most of the mass of the tapered tether is near the center of the rotating system, the rotational inertia of the tether facility is low. Consequently, the electrodynamic spin-up of the system can be very efficient. Our calculations indicate that a 3,000 kg system with only 5 kW of power could accelerate a 1,000 kg payload to a ΔV of 1 km/s in under three week.
- If a spent rocket massing the same as the payload is deorbited when the payload is boosted, the system looses no net orbital momentum or energy. Thus, no return traffic or electric propulsion is needed to maintain the system's orbital momentum. Moreover, if simultaneous boost and deorbit is performed, the system would not require a large ballast mass.
- The system is fully reusable.

DEVELOPMENT PLAN FOR A LEO⇔LUNAR TETHER TRANSPORT SYSTEM

A staged tether transport system has the potential to greatly reduce the cost of round-trip transport between low Earth orbit and the Moon. Its development will certainly require a significant expenditure of effort and resources, and its ultimate payoff, propellantless transport between LEO and the lunar surface, can only be fully realized once the entire system is in place. However, the full three-stage system need not be built all at once. It is possible to build the system incrementally. Moreover, it may be possible to use the first stages for commercial transportation applications, earning revenue to fund development of additional stages until the system is complete.

Recent projections of the growth of the commercial launch market predict that "*at least* three Big LEO (including MEO) and two Little LEO [telecommunication] systems will be deployed in" the 1996-2005 time frame.[29] These telecommunication systems are projected to require placement of nearly a hundred satellites per year into LEO and MEO orbits over the next ten years, and roughly 10-30 replacement satellites per year thereafter.

With this large market opportunity over the next decade, an incremental plan for a full LEO-Lunar tether transport system could begin with an electrodynamic bolo tether facility in low Earth orbit. This EDBT facility, after an initial period of testing and demonstration, could earn revenue by boosting LEO communications satellites from low-LEO parking orbits into their operational orbits. As described in Section 0.0, an EDBT facility massing approximately 3,000 kg, including two 50 km long tethers and a central power supply could boost 1,000 kg payloads by 1 km/s roughly once a month. Thus small launch vehicles could be used to boost the satellites up to the EDBT facility in low LEO, which would then toss the satellites up to their high LEO and MEO operational orbits. Because the EDBT uses the electrodynamic tether propulsion technique to accelerate the payloads, neither propellant nor return traffic would be required for this first stage.

The revenues and operational experience from this first stage could then be used to develop a second tether facility to be placed in a higher, elliptical orbit. Because the tether masses for the EEO facility are less than the payload mass, the LEO facility could be used to throw the EEO tether and facility components into its elliptical orbit. In conjunction with the LEO facility, the EEO facility could earn revenues by boosting satellites to geostationary orbits. In addition, the EEO tether could be used to throw spacecraft to lunar transfer orbits, facilitating the development of a lunar base. Because the EEO tether spends only a small fraction of its orbital period at altitudes where electrodynamic tether propulsion is useful, this facility will likely require solar-electric propulsion to maintain its orbit during the buildup period when return traffic from the Moon is not available to balance outbound mass flow. It will, therefore, require propellant during the initial build-up phase. Nonetheless, it can reduce the cost of transport to GEO and the Moon by providing high-Isp propulsion without the long transfer times normally associated with electric propulsion.

Once a lunar base has been established and the need for frequent Earth-Lunar traffic has developed, development of the third stage of the system, the Lunavator, would begin. This tether is the longest and most remote of the three facilities, and thus likely the most complex to build. Initially, the Lunavator could begin with a low mass facility and a relatively short tether that would be used to catch payloads sent from the Earth and drop them into lower lunar orbits. The tether could then be lengthened incrementally, and the facility mass built up using lunar materials, until the facility becomes a full-fledged Lunavator capable transferring payloads between lunar transfer trajectories, and bases on the lunar surface.

Once all three stages are complete, the LEO-Lunar tether transport system will be fully operational, capable of exchanging payloads between low Earth orbits and the lunar surface with little or no propellant requirements.

CONCLUSIONS AND RECOMMENDATIONS FOR FUTURE WORK

This research effort has addressed several of the issues concerning the utility of tether systems for transport to and from the Moon, including orbital dynamics, tether and facility mass, tether survivability, and high strength tether materials. We have succeeded in identifying methods of designing staged tether systems that will reduce the total required mass to levels that make these systems economically feasible. Given the potential of tether systems for greatly reducing the costs of in-space transportation, we believe that the results of this effort warrant further development of LEO-Lunar tether transport system concepts.

The basic principles of in-space transportation using tethers have already been demonstrated experimentally in space. In 1993, the SEDS-1 experiment demonstrated that a tether could de-orbit a payload from LEO, and in 1996, the TSS-1R flight demonstrated (albeit unintentionally) that a satellite could be deployed at the end of a tether and released into a higher orbit.

The next element of tether transport systems that must be demonstrated is the capability of a rotating tether to rendezvous with and capture a payload. To accomplish this task, we propose:

- The development of a simple experimental system to demonstrate that a small rotating LEO tether facility can capture a payload in a low Earth orbit and toss it into a higher orbit. An inexpensive method of performing this demonstration would be to follow in the successful footsteps of the SEDS tether experiments and design the tether system as a piggyback experiment on a satellite launch. For example, a small, simple tether deployer resembling the SEDS system could be attached to a Delta second stage; the tether system would use the second stage as a ballast mass. A small satellite would be deployed at the end of a tether, and the tether could be spun up through proper control of the deployment and use of leftover propellant on the Delta stage. At the bottom of its swing, the tether could drop the payload into a lower, elliptical orbit with a period resonant with the tether. Several orbits later, the tether would rendezvous with the payload and capture it. Half a revolution later, at the top of its swing, the tether would toss the satellite into a higher orbit. Most of the technology necessary to perform such an experiment has already been developed under the SEDS programs. The main new development that would be required would be a grapple vehicle capable of capturing the satellite.

In addition, we suggest that future work be performed to further refine the design of systems for tether-based transport. Issues that should be addressed include:

- Continuation of the development of analytical and numerical models of the orbital dynamics of the LEO-Lunar Surface Tether Transport Systems. Specifically, future work should examine the requirements imposed by the eccentricity and inclination of the Moon's orbit as well as the effects of finite facility ballast masses.
- Extension of the work by Stuart[9] and Carroll[3] on rendezvous with tethers to develop designs for a grapple vehicle and guidance systems for facilitating rendezvous between payloads and rotating tether facilities.
- Further investigation of the possibility of combining electrodynamic tether propulsion with rotating tether principles to create an Electrodynamic Bolo Tether facility capable of boosting multiple payloads from LEO to higher orbits without requiring propellant.

APPENDIX D

SURVIVABILITY OF HIGHLY STRESSED TETHERS

When a tether is designed to be stressed at a significant fraction of its maximum load-bearing capacity, calculations of its survival probability must take into account the effect of non-severing damage on the ability of the tether to sustain the design load.

If the tether is designed to bear a load of W_{design}, and its maximum load-bearing capacity is W_{max}, then its design safety factor is

$$F = W_{max} / W_{design} \qquad (1)$$

and its design stress level is

$$Z = W_{design} / W_{max}. \qquad (2)$$

When a tether with initial cross-sectional area A_T is partially damaged by a particle impact, its remaining cross-sectional area must be sufficient to carry the design load. That is, its undamaged area must be

$$A_{undamaged} \geq Z A_T \qquad (3)$$

If a particle with diameter d causes damage to an area $\Delta(d)$, then the criterion for survival is

$$A_T - \Delta(d) \geq Z A_T \qquad (4)$$

or, equivalently:

$$1 - \Delta(d)/A_T \geq Z$$

There is, unfortunately, a significant amount of uncertainty on the dependence of the damaged area Δ on the particle diameter d. Consequently, we will use available experimental data to extrapolate an approximate relationship. Hypervelocity tests on Spectra and Kevlar indicate that a tether line will be cut by a particle with a diameter smaller than the tether diameter by a factor of 0.2-0.5. This ratio is referred to as the "lethality coefficient," k_L. In addition, tests on aluminum plates have found that hypervelocity particles blast roughly hemispherical craters into the surface of a target plate. From these two observations, we will assume that a high velocity impactor will cause a hemispherical crater in a tether line with a maximum cross-sectional area $(1/k_L)^2$ times that of the impactor cross-sectional area. Thus, if the lethality coefficient is somewhere between 0.2 and 0.5, the damage area Δ is somewhere between 4-25 times the particle cross-sectional area. Choosing a mid-range value for k_L of 0.3, and assuming that the particles are roughly spherical, this results in a (very approximate) dependence of

$$\Delta(d) \approx 11\, d^2. \qquad (5)$$

If we further assume that the tether line has a cyllindrical cross-section with diameter d_T, then the criteria for tether survival becomes

$$1 - \frac{11 d_{crit}^2}{\pi d_T^2 / 4} \geq Z. \qquad (6)$$

For lines loaded at 50% of maximum capacity (F=2), this results in tethers failing when hit by particles with diameters $d_{crit} \approx 0.2\ d_T$. For 75% loading ($F$=1.33), $d_{crit} \approx 0.15\ d_T$.

For single-line tethers loaded at high levels, this new critical impactor diameter d_{crit} should be used in calculating cut rates. For multi-line tethers stressed at high fractions of the primary line capacity, this relationship for d_{crit} should be used in calculating both primary and secondary line cut rates from the debris and meteoroid flux models.

REFERENCES TO SECTION 5.0

1. Forward, R.L., "Tether Transport from LEO to the Lunar Surface," AIAA paper 91-2322, *27th AIAA/ASME/SAE/ASEE Joint Propulsion Conference*, July 1991.

2. H. Moravec, "A Non-Synchronous Orbital Skyhook," *J. Astro. Sci*, 25(4), pp 307-322, 1977

3. Carroll, J.A, *Preliminary Design of a 1 km/sec Tether Transport Facility*, March 1991, Tether Applications Final Report on NASA Contract NASW-4461 with NASA/HQ.

4. Stern, M.O., *Advanced Propulsion for LEO-Moon Transport*, NASA CR-172084, June 1988, California Space Institute Progress Report on NASA Grant NAG 9-186 with NASA/JSC.

5. Paul A. Penzo and Paul W. Ammann. *Tethers in Space Handbook -- Second Edition*. NASA Office of Space Flight, NASA Headquarters, Washington, DC 20546.

6. Oldson, J, Carroll, J.A., "Potential Launch Cost Savings of a Tether Transport Facility, " AIAA paper 95-2895, *31st AIAA/ASME/SAE/ASEE Joint Propulsion Conference*, July 1995.

7. H. Moravec, "Non-Synchronous Orbital Skyhooks for the Moon and Mars with Conventional Materials," unpublished paper, 1978.

8. Moravec, H, "Free Space Skyhooks," unpublished notes dated November 1978.

9. Stuart, D.G., "Guidance and Control for Cooperative Tether-Mediated Orbital Rendezvous," *J. Guidance*, 13(6), Nov-Dec 1990, pp. 1102-8.

10. Bekey, I., "Decreasing the Cost/Pound and Increasing the Performance of the Reusable Launch Vehicle by Using Tethered Payload Deployment, " NASA/HQ white paper, March 25, 1996.

11. Bekey,I., "Tethering: a new technique for payload deployment, " *Aerospace America*, March 1977, pp. 36-40.

12. Battin, R.H., *An Introduction to the Mathematics and Methods of Astrodynamics*, AIAA, 1987, p. 447.

13. Lorenzini, E.C., "Tethers for LEO to GEO: Materials and comparison data" Smithsonian Astrophysical Observatory Presentation, December 2, 1996.

14. Material Data Sheets provided by Spectra Performance Materials, AlliedSignal Inc., High Performance Fibers Division, P.O. Box 31, Petersburg, VA 23804, 10/24/96.

15. Carroll, J.A., personal communication, 1/11/95.

16. Carroll, J.A., personal communication, email 4/8/97.

17. Information on PBO is available on the web at http://www.toyobo.co.jp/e/seihin/kc/pbo/index.htm

18. Thess, A., et al., "Crystalline Ropes of Metallic Carbon Nanotubes," *Science* 273, 483 (1996). Available on the web at http://cnst.rice.edu/reshome.html.

[19]. Smalley, R.E., *From Balls to Tubes to Ropes: New Materials from Carbon,* presentation to the AICE, Jan 4, 1996. Text available at http://cnst.rice.edu/aiche96.html.

[20]. Forward, R.L., "Failsafe Multistrand Tether Structures for Space Propulsion," AIAA paper 92-3214, *28th AIAA/ASME/SAE/ASEE Joint Propulsion Conference,* Nashville, TN, July 1992.

[21]. Forward, R.L., Hoyt, R.P., "Failsafe Multiline Hoytether Lifetimes," AIAA Paper 95-2890, *31st AIAA/ASME/SAE/ASEE Joint Propulsion Conference,* San Diego CA, July 1995.

[22]. "Simulation of Complex Multiline Space Tether Structures: SpaceNet" Appendix N in *Failsafe Multistrand Hoytether SEDS Technology Demonstration,* Tethers Unlimited Final Report on NASA SBIR contract NAS8-40545, June 1995.

[23]. Pavelitz, Steven, personal communication, 1/97.

[24]. Anderson, B.J., Editor and Smith, R.E., Compiler, *Natural Orbital Environment Guidelines for Use in Aerospace Vehicle Development,* Section 7 "Meteoroids and Orbital Debris", Don Kessler and Herb Zook, NASA TM-4527, June 1994.

[25]. D.J. Kessler, et al., *A Computer Based Orbital Debris Environment Model for Spacecraft Design and Observations in Low Earth Orbit,* NASA TM (to be released). [Beta test copies of the program can be obtained by contacting Christine O'Neill at JSC at 713-483-5057 or oneill@snmail.jsc. nasa.gov]

[26]. Nobie Stone, personal communication, NASA/MSFC, 29 August 1996.

[27]. R.D. Moore, "The Geomagnetic Thrustor- A High Performance 'Alfvén Wave' Propulsion System Utilizing Plasma Contacts," *AIAA Fifth Electric Propulsion Conference,* AIAA paper 66-257.

[28]. Sanmartin, J.R., Martínez-Sánchez, M., Ahedo, E., "Bare Wire Anodes for Electrodynamic Tethers", *J. Propulsion and Power,* 7(3), pp. 353-360, 1993.

[29]. *LEO Commercial Market Projections,* Department of Transportation, Federal Aviation Administration, April 5, 1996.

6.0 Papers in the open literature produced by this NASA grant

Papers in peer-reviewed journals

1. M.E. Bangham, E. Lorenzini and L. Vestal, "Tether Transportation System Study." NASA Technical Publication, NASA/TP-1998-206959, March 1998.

2. E.C. Lorenzini, M.L. Cosmo, M. Kaiser, M. Bangham, D. Vonderwell and L. Johnson, "Mission Analysis of a Tethered System for LEO to GEO Orbital Transfers." Journal of Spacecraft and Rockets, Vol. 36, No. 6 (in press), Nov-Dec 1999.

3. R.D. Estes, E.C. Lorenzini, J. Sanmartin, M. Martinez-Sanchez, J. Pelaez, L. Johnson, and I. Vas, "Bare Tethers for Electrodynamic Spacecraft Propulsion." Journal of Spacecraft and Rockets, Vol. 36, No. 6 (in press), Nov-Dec 1999.

Papers in conference proceedings

4. L. Johnson, J. Carroll, R.D. Estes, E.C. Lorenzini, B. Gilchrist, M. Martinez-Sanchez, J. Sanmartin and I. Vas, "Electrodynamic Tethers for Reboost of the International Space Station and Spacecraft Propulsion." Proceedings of the AIAA Space programs and Technologies Conference and Exhibit, Huntsville , Alabama, 24-26 September 1996, Paper AIAA 96-4250, AIAA, Washington, DC, 1996.

5. Hoyt, R.P. and R.L. Forward, "Tether Transport from Sub-Earth-Orbit to the Lunar Surface – and Back!" Procs. of the 1997 International Space Development Conference, Orlando, Florida , May 22-26, 1997.

6. Hoyt, R.P., "Tether System for Exchanging Payloads between the International Space Station and the Lunar Surface." Procs. of the 48th International Astronautical Federation Congress, October 6-10, 1997,

7. Hoyt, R.P., "Tether System for Exchanging Payloads between Low Earth Orbit and the Lunar Surface." Procs. of the 33rd AIAA/ASME/SAE/ASEE Joint Propulsion Conference, Seattle, Washington, July 7, 1997.

8. E.C. Lorenzini, M.L. Cosmo, M. Kaiser, M. Bangham, H. Dionne, D. Vonderwell and L. Johnson, "Mission Analysis of a Tethered System for LEO to GEO Orbital Transfers." Advances in the Astronautical Sciences, Vol. 99, *Spaceflight Mechanics 1998*, pp. 3-20, AAS Publications, San Diego, CA, 1998.

9. Les Johnson, Brian Gilchrist, Robert Estes, Enrico Lorenzini and Judy Ballance, "Propulsive Small Expendable Deployer System (ProSEDS) Space Experiment." Procs. of the Joint Propulsion Conference, Cleveland, Ohio, 13-16 July 1998.

10. L. Johnson, R.D. Estes, E.C. Lorenzini, M. Martinez-Sanchez, J. Sanmartin and I. Vas, "Electrodynamic Tethers for Spacecraft Propulsion." Procs. of the AIAA 36th Aerospace Sciences and Exhibit, Paper AIAA 98-0983, Reno, Nevada, 12-15 January 1998.

11. Les Johnson, Brian Gilchrist, Robert Estes, Enrico Lorenzini, Manuel Martinez-Sanchez and Juan Sanmartin, "Electrodynamic Tether Propulsion for Spacecraft and Upper Stages." Procs.of the Joint Propulsion Conference, Cleveland, Ohio, 13-16 July 1998.

12. E.C. Lorenzini, R.D. Estes, M.L. Cosmo and J. Pelaez "Dynamical, Electrical, and Thermal Coupling in a New Class of Electrodynamic Tethered Satellites." Advances in the Astronautical Sciences, Vol. 102, , pp. 1333-1344, *Spaceflight Mechanics 1999*, AAS/AIAA Space Flight Mechanics Meeting, Brekenridge, Colorado, 7-10 February 1999.

13. J. Pelaez, O. Lopez-Rebollal, M. Ruiz, E.C. Lorenzini and M.L. Cosmo, "On the radial oscillation of an electrodynamic tether." Advances in the Astronautical Sciences, Vol. 102, 1361-1380, *Spaceflight Mechanics 1999*, AAS/AIAA Space Flight Mechanics Meeting, Brekenridge, Colorado, 7-10 February 1999.